

**EXPANSION OF HEMATOPOIETIC STEM CELLS
AND ITS APPLICATION IN WOUND HEALING**

Kamonnaree Chotinantakul

**A Thesis Submitted in Partial Fulfillment of the Requirements for the
Degree of Doctor of Philosophy in Microbiology
Suranaree University of Technology
Academic Year 2011**

การเพิ่มจำนวนเซลล์ต้นกำเนิดเม็ดเลือดและ
การประยุกต์ใช้ในการรักษาบาดแผล

นางสาวกมลนารี โชตินันท์กุล

วิทยานิพนธ์นี้เป็นส่วนหนึ่งของการศึกษาตามหลักสูตรปริญญาวิทยาศาสตรดุษฎีบัณฑิต
สาขาวิชาจุลชีววิทยา
มหาวิทยาลัยเทคโนโลยีสุรนารี
ปีการศึกษา 2554

**EXPANSION OF HEMATOPOIETIC STEM CELLS
AND ITS APPLICATION IN WOUND HEALING**

Suranaree University of Technology has approved this thesis submitted in partial fulfillment of the requirements for the Degree of Doctor of Philosophy.

Thesis Examining Committee

(Assoc. Prof. Dr. Yupaporn Chaiseha)

Chairperson

(Asst. Prof. Dr. Wilairat Leeanansaksiri)

Member (Thesis Advisor)

(Prof. Dr. Kovit Pattanapanyasat)

Member

(Dr. Chavaboon Dechsukhum)

Member

(Assoc. Prof. Dr. Patcharee Jearanaikoon)

Member

(Assoc. Prof. Dr. Tassanee Saovana)

Member

(Prof. Dr. Sukit Limpijumnong)

Vice Rector for Academic Affairs

(Assoc. Prof. Dr. Prapun Manyum)

Dean of Institute of Science

กมลนารี โชตินันท์กุล : การเพิ่มจำนวนเซลล์ต้นกำเนิดเม็ดเลือดและการประยุกต์ใช้ในการรักษาบาดแผล (EXPANSION OF HEMATOPOIETIC STEM CELLS AND ITS APPLICATION IN WOUND HEALING) อาจารย์ที่ปรึกษา : ผู้ช่วยศาสตราจารย์ เทคนิคการแพทย์หญิง ดร.วิไลรัตน์ ลือนันต์ศักดิ์ศิริ, 217 หน้า.

งานนี้มีวัตถุประสงค์เพื่อเปรียบเทียบความสามารถในการเพิ่มจำนวนเซลล์ต้นกำเนิดเม็ดเลือด (CD34⁺ cells) จากเลือดสายสะดือที่เลี้ยงในอาหารเลี้ยงเซลล์ที่มีส่วนผสมของสารอาหารไซโตไคน์ชนิดที่ประกอบด้วย 4 ไซโตไคน์ (4F; Flt3L SCF TPO และ IL-6) เทียบกับ 4 ไซโตไคน์ร่วมกับ Wnt1 (4FW) เปรียบเทียบระหว่างการเลี้ยงในอาหารที่มีซีรัมและไม่มีซีรัมสัตว์เป็นส่วนผสม นอกจากนี้ยังเปรียบเทียบความสามารถในการเพิ่มจำนวนเซลล์ต้นกำเนิดเม็ดเลือดในอาหารเลี้ยงเซลล์ที่ประกอบด้วยส่วนผสมของไซโตไคน์ชนิดใหม่จำนวน 6 ชนิดเทียบกับไซโตไคน์ 4F ซึ่งไม่มีซีรัม และทำการทดลองศึกษาผลการรักษาบาดแผลในหนูทดลองที่ถูกเหนี่ยวนำให้เป็นเบาหวานจากสารสเตรปโตโซโตซินด้วยเซลล์ต้นกำเนิดเม็ดเลือดชนิด CD34⁺ เปรียบเทียบกับเซลล์ต้นกำเนิดเม็ดเลือดชนิด CD34⁺ ที่เลี้ยงในอาหารเลี้ยงเซลล์ที่มีส่วนผสมของ 4FW ที่ไม่มีส่วนผสมของซีรัมเป็นเวลา 5 วัน จากการทดลองแรกพบว่า อาหารที่ไม่มีส่วนผสมของซีรัมประกอบด้วย 4F และ 4FW เพิ่มจำนวนเซลล์ CD34⁺CD38⁻ (~18.5 และ ~24.3 เท่า ตามลำดับ) ได้ดีกว่าอาหารที่มีส่วนผสมของซีรัม (~4.2 และ ~6.6 เท่า ตามลำดับ) เมื่อเลี้ยงไปได้ 7 วัน และเป็นที่น่าสนใจอย่างยิ่งที่อาหารที่ไม่มีส่วนผสมของซีรัมเพิ่มจำนวนเซลล์ CD133⁺CD38⁻ และยับยั้งการเพิ่มจำนวน CD34⁺CD38⁺ ได้ดีกว่าการเลี้ยงในอาหารที่มีซีรัม การทดลองที่สองในการเปรียบเทียบทั้ง 7 ชนิดของส่วนผสมของไซโตไคน์ต่างๆในอาหารที่ไม่มีส่วนผสมของซีรัมพบว่า กลุ่มที่มีส่วนผสมของไซโตไคน์ 4FW และ P0 สามารถเพิ่มจำนวนเซลล์ CD34⁺CD38⁻ (~24.3 เท่า) และ CD133⁺CD38⁻ (~18.2 เท่า) ได้สูงสุดตามลำดับ เมื่อเลี้ยงได้ 7 วัน อาหารทุกกลุ่มของไซโตไคน์รวมชนิดต่างๆ ที่ทำการเลี้ยงเพื่อเพิ่มจำนวนเซลล์ต้นกำเนิดสามารถรักษาความเป็นเซลล์ต้นกำเนิดของเซลล์ได้ โดยทำการศึกษาจากระดับเซลล์ด้วยวิธีการดูการสร้างโคโลนีของเซลล์โปรเจเนเตอร์ต่างๆ และการเลี้ยงในสื่อน้ำชนิดต่างๆ เพื่อดูการพัฒนาไปเป็นเม็ดเลือดเต็มวัยสายต่างๆ และศึกษาในระดับโมเลกุลด้วยการดูการแสดงออกของยีน *Oct3/4* และ *Nanog* ที่เกี่ยวข้องในการรักษาความเป็นพลูริโพเทนท์ของเซลล์ ซึ่งผลการทดลองที่ได้ให้ผลที่ใกล้เคียงกับผลจากเซลล์ต้นกำเนิดเม็ดเลือดที่สกัดใหม่ซึ่งเป็นกลุ่มควบคุม สำหรับการทดลองสุดท้ายในการรักษาบาดแผลในหนูที่เป็นเบาหวานพบว่า เซลล์ต้นกำเนิดเม็ดเลือดและเซลล์ที่เพิ่มจำนวนในอาหาร 4FW ที่ไม่มีส่วนผสมของซีรัมสามารถช่วยรักษาบาดแผลได้ดีขึ้น โดยไปเพิ่มการเดินทางและเพิ่มจำนวนของเซลล์แมโครฟาจที่

แสดง CD68 โมเลกุล และเซลล์เอนโดทีเลียมที่แสดง CD31 โมเลกุลบนผิวเซลล์โดยการวิเคราะห์ด้วยเทคนิคอิมมูโนฮิสโตเคมีสทรี ผลการทดลองทั้งหมดสามารถสรุปได้ว่าการใช้อาหารที่ไม่มีซีรัมและมีส่วนผสมของไซโตไคน์ชนิดต่างๆ ที่คิดค้นใหม่นี้ สามารถช่วยลดการปนเปื้อนส่วนผสมจากสัตว์ และเพิ่มจำนวนเซลล์ที่แสดงโมเลกุล CD34 บนผิวเซลล์ได้ภายนอกร่างกาย โดยเฉพาะการทดลองครั้งนี้แสดงให้เห็นเป็นครั้งแรกว่าการเพิ่มไซโตไคน์ Wnt1 มีบทบาทในการเพิ่มจำนวนของเซลล์ และประโยชน์จากการใช้เซลล์ชนิด $CD34^+$ จากเลือดสายสะดือและเซลล์ที่เพิ่มจำนวนในอาหารที่มีส่วนประกอบของ Wnt1 เป็นเวลา 5 วันช่วยรักษาบาดแผลในหนูทดลองที่เหนียวน่าให้เป็นเบาหวานด้วยสารสเตโรปโตไซโตซินได้อีกอย่างมีนัยสำคัญ



สาขาวิชาจุลชีววิทยา

ปีการศึกษา 2554

ลายมือชื่อนักศึกษา _____

ลายมือชื่ออาจารย์ที่ปรึกษา _____

ลายมือชื่ออาจารย์ที่ปรึกษาร่วม _____

ลายมือชื่ออาจารย์ที่ปรึกษาร่วม _____

KAMONNAREE CHOTINANTAKUL : EXPANSION OF
HEMATOPOIETIC STEM CELLS AND ITS APPLICATION IN WOUND
HEALING. THESIS ADVISOR : ASST. PROF. WILAIRAT
LEEANANSAKSIRI, Ph.D. 217 PP.

HEMATOPOIETIC STEM CELLS/CORD BLOOD/CD34⁺ CELLS/ EXPANSION/
WOUND HEALING

The aims of this study were to compare the ability of *ex vivo* expansion of human cord blood (CB) CD34⁺ cells cultured in cytokine factors; 4F (Flt3L, SCF, TPO, and IL-6) and 4F containing Wnt1 (4FW) in serum and serum-free medium and to compare newly six combinations of cytokine cocktails with 4F in serum-free medium in supporting proliferation. In the present study, the capacity of expanded CD34⁺ cells in serum-free medium in wound healing was also investigated and compared with freshly isolated CD34⁺ cells in streptozotocin (STZ)-induced diabetic mice. Firstly, the culture of CB-CD34⁺ cells in serum-free medium with 4F and 4FW showed superior *ex vivo* expansion of CD34⁺CD38⁻ cells (~18.5- and ~24.3-folds, respectively) than those of serum containing medium (~4.2- and ~6.6-folds, respectively) significantly at day 7. Interestingly, in the serum-free medium exhibited the increase in CD133⁺CD38⁻ cells and preserved the expansion of CD34⁻CD38⁺ cells (more committed cells) than those of serum containing medium. Secondly, among the seven combinations of cytokine cocktails in serum-free medium investigated in this study, cultivation in 4FW and P0 medium showed the highest expansion of CD34⁺CD38⁻ cells (~24.3 fold) and CD133⁺CD38⁻ cells (~18.2 fold), respectively, at

day 7. All cocktails could maintain stemness of expanded cells in which the cellular level as determined by colony forming cell and liquid culture assay, and the molecular level as analyzed from the expression pluripotency genes (*Oct3/4* and *Nanog*) displayed the comparative results compared to freshly isolated CD34⁺ cells. Finally, fresh and day 5-expanded CD34⁺ cells obtained from 4FW in serum-free culture could accelerate wound healing in diabetic mice by improved proliferation and migration of CD68⁺ macrophages and CD31⁺ endothelial cells as identified by immunohistochemistry analysis. In conclusion, these data demonstrate the benefits of using serum-free medium with new cytokine cocktails as an effective choice to eliminate the contamination of animal product and enhance CB-CD34⁺ cells expansion *ex vivo*. Particularly, this study is the first research that confirms the addition of Wnt1 plays an essential role in promoting the proliferation. In addition, our findings also indicate for the first time that significantly improvement of wound healing in STZ-induced diabetic mice can be succeeded by the use of freshly isolated and day 5-expanded CB-CD34⁺ cells from 4FW medium.

School of Microbiology

Academic Year 2011

Student's Signature_____

Advisor's Signature_____

Co-advisor's Signature_____

Co-advisor's Signature_____

ACKNOWLEDGEMENTS

The completion of this thesis work would not be possible without the inspiration, support patience, and guidance received in so many ways.

Firstly, I would like to express my deepest gratitude and respect to my thesis advisor Asst. Prof. Dr. Wilairat Leeanansaksiri. I always have benefit from her expertise supervision and valuable advice throughout the entire Ph.D. study.

I would like to express my gratitude to my thesis co-advisors, Dr. Chavaboon Dechsukhum and Prof. Dr. Kovit Pattanapanyasat for their guidance.

My appreciation is also to committee members, Assoc. Prof. Dr. Yupaporn Chaiseha, Assoc. Prof. Dr. Patcharee Jearanaikoon and Assoc. Prof. Dr. Tassanee Saovana for their valuable suggestions.

Many thanks go to Suranaree University of Technology (SUT), for Ph.D. scholarship awarded to me. I am very grateful for all lecturers and staffs in the School of Microbiology/Biology and The Center for Scientific and Technology Equipment at SUT. I would like to thanks all physicians, nurses and medical staffs from Por Pat Hospital, St. Mary Hospital, and Fort Suranari Hospital for their kindness and warm assistance for years.

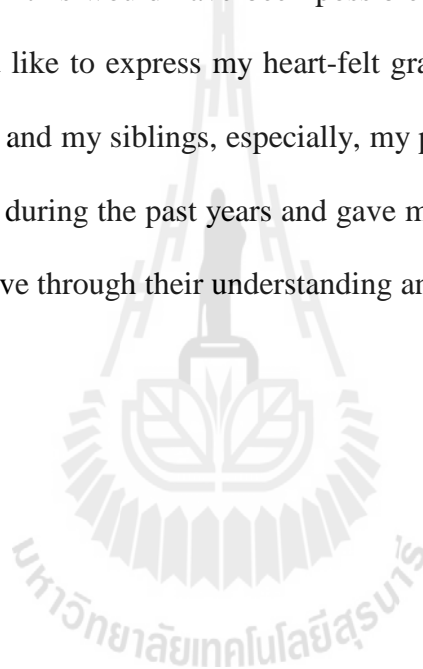
A very special thanks to members past and present of the Stem Cell Therapy and Transplantation Research Group at Institute of Science, SUT, friends at Mahidol University and friends at SUT, especially Ms. Patcharee Prasjak and Ms. Duangnapa Dejjuy for their help. Many thanks to whom it may concern for their contribution to

my studies during this work. All warm friendships are most appreciated. My deepest appreciation also goes to Mr. Kampanat Sriprasert for his warm wishes and always cheering me up.

I gratefully acknowledge Prof. Dr. Seiji Okada and Dr. Panida Khunkaewla for their thoughtful comments, some troubleshooting lab experiments and inspired suggestions on my thesis work.

Finally, none of this would have been possible without the love and patience of my family. I would like to express my heart-felt gratitude to Phra Maha Suthinun Suthiyano, my parents and my siblings, especially, my parents who shared my joy and experiences in my life during the past years and gave me great support, good care and a constant source of love through their understanding and encouragement.

Kamonnaree Chotinantakul



CONTENTS

| | Page |
|---|-------------|
| ABSTRACT IN THAI..... | I |
| ABSTRACT IN ENGLISH | III |
| ACKNOWLEDGEMENTS | V |
| CONTENTS..... | VII |
| LIST OF TABLES | XII |
| LIST OF FIGURES | XIII |
| LIST OF ABBREVIATIONS..... | XXIV |
| CHAPTER | |
| I INTRODUCTION..... | 1 |
| 1.1 Introduction..... | 1 |
| 1.2 Objectives..... | 4 |
| II LITERATURE REVIEW..... | 5 |
| 2.1 Hematopoietic stem cells origin and development | 5 |
| 2.2 HSC niches..... | 13 |
| 2.3 Hierarchy of human hematopoiesis..... | 17 |
| 2.4 Molecular niche in self-renewal and maintenance of HSCs | 20 |
| 2.5 <i>Ex vivo</i> HSCs expansion | 29 |
| 2.5.1 Cytokine-based culture..... | 29 |
| 2.5.2 Viral-based culture | 31 |

CONTENTS (Continued)

| | Page |
|---|-------------|
| 2.5.3 Stromal cell-based culture | 32 |
| 2.6 Flt3-Ligand..... | 33 |
| 2.6.1 Structure and expression pattern | 33 |
| 2.6.2 Biological function | 36 |
| 2.7 Interleukin-6..... | 37 |
| 2.7.1 Structure and expression pattern | 37 |
| 2.7.2 Biological function | 39 |
| 2.8 Stem cell factor | 40 |
| 2.8.1 Structure and expression pattern | 40 |
| 2.8.2 Biological function | 41 |
| 2.9 Thrombopoietin..... | 42 |
| 2.9.1 Structure and expression pattern | 42 |
| 2.9.2 Biological function | 44 |
| 2.10 Wnt1 | 45 |
| 2.10.1 Structure and expression pattern | 45 |
| 2.10.2 Biological function..... | 46 |
| 2.11 Wound healing in diabetes mellitus by stem cells | 49 |
| III MATERIALS AND METHODS | 51 |
| 3.1 Materials and Methods..... | 51 |
| 3.1.1 Human cord blood collection and separation..... | 51 |

CONTENTS (Continued)

| | Page |
|--|-------------|
| 3.1.2 CD34 ⁺ cell purification | 51 |
| 3.1.3 Expansion of enriched CD34 ⁺ cells <i>in vitro</i> | 53 |
| 3.1.3.1 Cytokines and plant extract | 53 |
| 3.1.3.2 <i>Ex vivo</i> expansion | 53 |
| 3.1.4 Liquid differentiation assay | 54 |
| 3.1.4.1 Feeder cell preparation for lymphoid differentiation | 54 |
| 3.1.4.2 <i>In vitro</i> liquid differentiation | 55 |
| 3.1.5 Colony forming cell assay | 56 |
| 3.1.6 Flow cytometry analysis | 57 |
| 3.1.7 Gene expression by reverse transcription-polymerase chain reaction (RT-PCR) | 58 |
| 3.1.7.1 Total RNA extraction | 58 |
| 3.1.7.2 Primers | 59 |
| 3.1.7.3 Complementary DNA (cDNA synthesis) | 60 |
| 3.1.7.4 Real-time RT-PCR | 60 |
| 3.1.8 Wound healing assay | 61 |
| 3.1.8.1 Induction of diabetic mice | 61 |
| 3.1.8.2 Wound healing model | 62 |
| 3.1.8.3 Wound analysis | 63 |
| 3.1.8.4 Tissue section preparation | 63 |

CONTENTS (Continued)

| | Page |
|---|-------------|
| 3.1.8.5 Hematoxylin and eosin staining | 64 |
| 3.1.8.6 Immunofluorescence | 64 |
| 3.1.9 Statistical analysis | 66 |
| IV RESULTS..... | 68 |
| 4.1 Results..... | 68 |
| 4.1.1 Isolation of CD34 ⁺ cells | 68 |
| 4.1.2 Development of culture medium for CB-CD34 ⁺ cells expansion in serum-free medium | 71 |
| 4.1.3 Determination of phenotype and <i>in vitro</i> hematopoiesis of expanded cells in serum and serum-free cultures | 77 |
| 4.1.4 Comparison of multiple cytokine cocktails for CB-CD34 ⁺ cells expansion in serum-free medium..... | 84 |
| 4.1.5 Determination of phenotype and <i>in vitro</i> hematopoiesis of expanded cells in various cytokine cocktails in serum-free medium | 94 |
| 4.1.6 Pluripotency genes expression in expanded cells | 108 |
| 4.1.7 Wound healing in streptozotocin-induced diabetic mice..... | 112 |
| 4.1.8 Macrophage and capillary contents in treated wounds | 116 |

CONTENTS (Continued)

| | Page |
|--|-------------|
| V DISCUSSION | 128 |
| 5.1 Comparative <i>ex vivo</i> expansion capacity of CB-CD34 ⁺ cells in serum and serum-free medium..... | 128 |
| 5.2 Multiple cocktails comparison for <i>ex vivo</i> expansion of CB-CD34 ⁺ cells in serum-free medium | 133 |
| 5.3 Wound healing in STZ-induced diabetic mice..... | 136 |
| VI CONCLUSION..... | 144 |
| REFERENCES | 145 |
| APPENDICES | 209 |
| APPENDIX A SOLUTION PREPARATION..... | 210 |
| APPENDIX B STATISTICAL DESCRIPTION | 216 |
| CURRICULUM VITAE..... | 217 |

LIST OF TABLES

| Table | Page |
|--|------|
| 4.1 <i>Ex vivo</i> expansion pattern of CD34 ⁺ cells cultured in 2 different cytokine cocktails in cIMDM and KSR medium (n = 3) | 73 |
| 4.2 Total number of colony forming cells derived from day 5 expanded CD34 ⁺ cells obtained from 4F cIMDM, 4FW cIMDM, 4F KSR, and 4FW KSR cultures compared with fresh CD34 ⁺ cells (n = 3) | 80 |
| 4.3 Fold increase in total nucleated cells in all culture conditions in serum-free medium (n = 3) | 87 |
| 4.4 <i>Ex vivo</i> expansion pattern of CD34 ⁺ cells cultured in various cytokine cocktails in serum-free medium (n = 3) | 89 |
| 4.5 Fold increase in total CD34 ⁺ and total CD133 ⁺ cells expansion of cells cultured in various cytokine cocktails in serum-free medium (n = 3) | 93 |
| 4.6 Total number of colony forming cells grown on methylcellulose at day 14 | 99 |

LIST OF FIGURES

| Figure | Page |
|--|------|
| 2.1 Source of blood cells during gestation through after birth | 8 |
| 2.2 Mouse placenta development..... | 12 |
| 2.3 Candidate cellular niches mediated in maintenance and regulation of HSCs in bone marrow; endosteal niche, vascular niche, and reticular niche..... | 18 |
| 2.4 Hierarchy of hematopoiesis | 21 |
| 2.5 Schematic diagram of Wnt/ β -catenin signaling..... | 28 |
| 2.6 Structure and activation of Flt3..... | 35 |
| 2.7 Structure of IL-6 containing the four long helices A, B, C and D..... | 38 |
| 2.8 TPO/c-Mpl signaling pathway | 44 |
| 2.9 A canonical Wnt signaling pathway | 48 |
| 4.1 Assessment of CD34 ⁺ cell fraction in CB-MNCs by flow cytometry | 69 |
| 4.2 Morphology of isolated CB-CD34 ⁺ cells. Scale bar = 5 μ m. | 69 |
| 4.3 Representative of flow cytometry analysis of CD34, CD38 and CD133 expressions in fresh isolated CD34 ⁺ cells (A) and expanded CD34 ⁺ cells (B) cultured in various cytokine cocktails in serum (cIMDM) and serum free medium (KSR) at day 5 and 7 | 70 |
| 4.4 Total CD34 ⁺ CD38 ⁻ cell number in serum and serum-free culture on day 5 and day 7 | 74 |

LIST OF FIGURES (Continued)

| Figure | Page |
|--------|--|
| 4.5 | Total CD34 ⁻ CD38 ⁺ cell number in serum and serum-free culture on day 5 and day 7 75 |
| 4.6 | Total CD133 ⁺ CD38 ⁻ cell number in serum and serum-free culture on day 5 and day 7 76 |
| 4.7 | Immunophenotype of expanded cells. Cell surface markers CD33/CD71 and CD3/CD19 of fresh isolated CD34 ⁺ cells (A) and expanded cells (B) at 5-day and 7-day of each culture condition in serum (cIMDM) and serum- free medium (KSR) 78 |
| 4.8 | Photomicrographs illustrating the colony forming cells; CFU-GEMM (a), CFU-GM (b), and BFU-E (c) on methylcellulose 80 |
| 4.9 | Colony assay (CFU-GEMM, CFU-GM, and BFU-E) of day 5 expanded CD34 ⁺ cells in various culture conditions (CFUs) (n = 3) 81 |
| 4.10 | Differentiation capacities of expanded CB-CD34 ⁺ cells from 4F (A) and 4FW (B) cIMDM <i>in vitro</i> . (a) Undifferentiated day 5 expanded CB-CD34 ⁺ cells, (b) day 7 expanded CD34 ⁺ cells, (c) erythroid lineage differentiation (EPO + SCF, arrow), (d) megakaryocytes differentiation (TPO + SCF), (e) lymphoid lineage differentiation (IL-7 + Flt3-L + SCF + OP9, arrow), (f-g) granulocytes and macrophage lineages differentiation (GM-CSF + IL-3), (h-j) mast cells and granulocyte lineages |

LIST OF FIGURES (Continued)

| Figure | Page |
|--|------|
| differentiation (SCF + IL-3) | 82 |
| 4.11 Differentiation capacities of expanded CB-CD34 ⁺ cells from 4F (A) and 4FW (B) KSR <i>in vitro</i> . (a) Undifferentiated day 5 expanded CB-CD34 ⁺ cells, (b) day 7 expanded CD34 ⁺ cells, (c) erythroid lineage differentiation (EPO + SCF, arrow), (d) megakaryocytes differentiation (TPO + SCF), (e) lymphoid lineage differentiation (IL-7 + Flt3-L + SCF + OP9, arrow), (f-g) granulocytes and macrophage lineages differentiation (GM-CSF + IL-3), (h-j) mast cells and granulocyte lineages differentiation (SCF + IL-3) | 83 |
| 4.12 Fold increase in total nucleated cells in various cytokine cocktails in serum- free culture on day 5 and 7 (n = 3) | 86 |
| 4.13 Representative of flow cytometry analysis of CD34, CD38 and CD133 expressions in expanded CD34 ⁺ cells cultured in P0 (A), P1 (B), P2 (C), P3 (D) and P4 (E) in serum-free medium on day 5 and day 7 (n = 3)..... | 88 |
| 4.14 Total CD34 ⁺ CD38 ⁻ cells in various cytokine cocktail in serum-free culture on day 5 and day 7 (n = 3) | 90 |
| 4.15 Total CD34 ⁻ CD38 ⁺ cells in various cytokine cocktail in serum-free culture on day 5 and day 7 (n = 3) | 91 |

LIST OF FIGURES (Continued)

| Figure | Page |
|---|------|
| 4.16 Total CD133 ⁺ CD38 ⁻ cells in various cytokine cocktail in serum-free culture on day 5 and day 7 (n = 3) | 92 |
| 4.17 Total CD34 ⁺ cells in various cytokine cocktail in serum-free culture on day 5 and day 7 (n = 3)..... | 96 |
| 4.18 Total CD133 ⁺ cells in various cytokine cocktail in serum-free culture on day 5 and day 7 (n = 3)..... | 97 |
| 4.19 Representative of flow cytometry analysis of CD3, CD19, CD33, and CD71 expressions in expanded CD34 ⁺ cells cultured in P0 (A), P1 (B), P2 (C), P3 (D) and P4 (E) in serum-free medium at day 5 and day 7 (n = 3)..... | 98 |
| 4.20 Number of CFU-GEMM on methylcellulose at day 14 (n = 3) | 100 |
| 4.21 Number of CFU-GM on methylcellulose at day 14 (n = 3) | 101 |
| 4.22 Number of BFU-E on methylcellulose at day 14 (n = 3) | 102 |
| 4.23 Differentiation capacities of expanded CB-CD34 ⁺ cells from P0 KSR <i>in vitro</i> . (a) Undifferentiated day 5 expanded CB-CD34 ⁺ cells, (b) day 7 expanded CD34 ⁺ cells, (c) erythroid lineage differentiation (EPO + SCF, arrow), (d) megakaryocytes differentiation (TPO + SCF), (e) lymphoid lineage differentiation (IL-7 + Flt3-L + SCF + OP9, arrow), (f-g) granulocytes and macrophage lineages differentiation (GM-CSF + IL-3), (h-j) | |

LIST OF FIGURES (Continued)

| Figure | Page |
|--|------|
| mast cells and granulocyte lineages differentiation (SCF + IL-3) | 103 |
| 4.24 Differentiation capacities of expanded CB-CD34 ⁺ cells from P1 KSR <i>in vitro</i> . (a) Undifferentiated day 5 expanded CB-CD34 ⁺ cells, (b) day 7 expanded CD34 ⁺ cells, (c) erythroid lineage differentiation (EPO + SCF, arrow), (d) megakaryocytes differentiation (TPO + SCF), (e) lymphoid lineage differentiation (IL-7 + Flt3-L + SCF + OP9, arrow), (f-g) granulocytes and macrophage lineages differentiation (GM-CSF + IL-3), (h-j) mast cells and granulocyte lineages differentiation (SCF + IL-3)..... | 104 |
| 4.25 Differentiation capacities of expanded CB-CD34 ⁺ cells from P2 KSR <i>in vitro</i> . (a) Undifferentiated day 5 expanded CB-CD34 ⁺ cells, (b) day 7 expanded CD34 ⁺ cells, (c) erythroid lineage differentiation (EPO + SCF, arrow), (d) megakaryocytes differentiation (TPO + SCF), (e) lymphoid lineage differentiation (IL-7 + Flt3-L + SCF + OP9, arrow), (f-g) granulocytes and macrophage lineages differentiation (GM-CSF + IL-3), (h-j) mast cells and granulocyte lineages differentiation (SCF + IL-3)..... | 105 |
| 4.26 Differentiation capacities of expanded CB-CD34 ⁺ cells from P3 KSR <i>in vitro</i> . (a) Undifferentiated day 5 expanded CB-CD34 ⁺ cells, (b) day 7 expanded CD34 ⁺ cells, (c) erythroid | |

LIST OF FIGURES (Continued)

| Figure | Page |
|---|------|
| lineage differentiation (EPO + SCF, arrow), (d) megakaryocytes differentiation (TPO + SCF), (e) lymphoid lineage differentiation (IL-7 + Flt3-L + SCF + OP9, arrow), (f-g) granulocytes and macrophage lineages differentiation (GM-CSF + IL-3), (h-j) mast cells and granulocyte lineages differentiation (SCF + IL-3)..... | 106 |
| 4.27 Differentiation capacities of expanded CB-CD34 ⁺ cells from P4 KSR <i>in vitro</i> . (a) Undifferentiated day 5 expanded CB-CD34 ⁺ cells, (b) day 7 expanded CD34 ⁺ cells, (c) erythroid lineage differentiation (EPO + SCF, arrow), (d) megakaryocytes differentiation (TPO + SCF), (e) lymphoid lineage differentiation (IL-7 + Flt3-L + SCF + OP9, arrow), (f-g) granulocytes and macrophage lineages differentiation (GM-CSF + IL-3), (h-j) mast cells and granulocyte lineages differentiation (SCF + IL-3)..... | 107 |
| 4.28 Relative quantitation of <i>Nanog</i> gene expression analyzed by RT real-time PCR of expanded CB-CD34 ⁺ cells cultured in different cytokine cocktails (n = 3)..... | 109 |
| 4.29 Relative quantitation of <i>Oct3/4</i> gene expression analyzed by RT real-time PCR of expanded CB-CD34 ⁺ cells cultured in different cytokine cocktails (n = 3)..... | 110 |
| 4.30 Agarose gel electrophoresis of specific PCR products without | |

LIST OF FIGURES (Continued)

| Figure | Page |
|---|------|
| <p>non-specific amplification of <i>Nanog</i> (A), <i>Oct3/4</i> (B) and <i>GAPDH</i> (C) genes obtained from real-time RT PCR.....</p> | 111 |
| <p>4.31 Percentage of opened wound area as normalized to the day 0. Mice were treated with PBS, fresh isolated CD34⁺ cells, expanded CD34⁺ cells and 4FW cytokine around the full- thickness dermal wound on day 0.....</p> | 113 |
| <p>4.32 Representative photographic pictures of wound healing in mice treated with PBS, fresh isolated CD34⁺ cells, expanded CD34⁺ cells and 4FW cytokine on day 0, day 3, day 5, day 7 and day 9 after wounding. Scale bar = 5 μm.</p> | 114 |
| <p>4.33 Histologic analysis of day 9 wound sections from PBS- (a), fresh isolate CD34⁺ cells- (c), day 5 expanded CD34⁺ cells- (e) and 4FW cytokine- (g) treated wounds. The length of edge measurement of epithelial gap is indicated by arrow. Scale bar = 200 μm. Corresponding higher power magnification (b, d, f, h) represents the right edge of epithelial margin (arrow head) that connected to the original epidermis and superior to the granulation tissue. Scale bar = 100 μm.....</p> | 115 |
| <p>4.34 Epithelial gap of the day 9 wounds treated with PBS, fresh isolated CD34⁺ cells, expanded CD34⁺ cells and 4FW cytokine</p> | 116 |

LIST OF FIGURES (Continued)

| Figure | Page |
|---|------|
| <p>4.35 CD68-positive cells on wounds treated with PBS, fresh isolated CD34⁺ cells, expanded CD34⁺ cells and 4FW cytokine on day 5 and 9 after wounding (n = 6)</p> | 118 |
| <p>4.36 Immunofluorescent staining for macrophage marker CD68 (green) on wound tissue treated with PBS (a), fresh isolated CD34⁺ cells (e), expanded CD34⁺ cells (i) and 4FW cytokine (m) sections at day 5 after wounding (the first column). Counterstaining of nuclei with DAPI (blue) on the same sections are represented on the second column (b, f, j, n). The overlay images of the 2nd and 3rd columns (c, g, k, o) are represented on the third column. Scale bar = 400 μm. High magnification images of CD31-positive cells are represented on the fourth column (d, h, l, p). Scale bar = 80 μm</p> | 119 |
| <p>4.37 Immunofluorescent staining for macrophage marker CD68 (green) on wound tissue treated with PBS (a), fresh isolated CD34⁺ cells (e), expanded CD34⁺ cells (i) and 4FW cytokine (m) sections at day 9 after wounding (the first column). Counterstaining of nuclei with DAPI (blue) on the same sections are represented on the second column (b, f, j, n). The overlay images of the 2nd and 3rd columns (c, g, k, o)</p> | |

LIST OF FIGURES (Continued)

| Figure | Page |
|--|------|
| <p>are represented on the third column. Scale bar = 400 μm.</p> <p>High magnification images of CD31-positive cells are represented on the fourth column (d, h, l, p). Scale bar = 80 μm</p> | 120 |
| <p>4.38 CD31-positive cells on wounds treated with PBS, fresh isolated CD34⁺ cells, expanded CD34⁺ cells and 4FW cytokine on day 5 and 9 after wounding (n = 6)</p> | 121 |
| <p>4.39 Immunofluorescent staining for endothelial marker CD31 (green) on wound tissue treated with PBS (a), fresh isolated CD34⁺ cells (e), expanded CD34⁺ cells (i) and 4FW cytokine (m) sections at day 5 afterwounding (the first column). Counterstaining of nuclei with DAPI (blue) on the same sections are represented on the second column (b, f, j, n). The overlay images of the 2nd and 3rd columns (c, g, k, o) are represented on the third column. Scale bar = 400 μm.</p> <p>High magnification images of CD31-positive cells are represented on the fourth column (d, h, l, p). Scale bar = 80 μm</p> | 122 |
| <p>4.40 Immunofluorescent staining for endothelial marker CD31 (green) on wound tissue treated with PBS (a), fresh isolated CD34⁺ cells (e), expanded CD34⁺ cells (i) and 4FW cytokine (m) sections at day 9 after wounding (the first column).</p> | |

LIST OF FIGURES (Continued)

| Figure | Page |
|---|------|
| <p>Counterstaining of nuclei with DAPI (blue) on the same sections are represented on the second column (b, f, j, n). The overlay images of the 2nd and 3rd columns (c, g, k, o) are represented on the third column. Scale bar = 400 μm. High magnification images of CD31-positive cells are represented on the fourth column (d, h, l, p). Scale bar = 80 μm</p> | 123 |
| <p>4.41 Immunofluorescence analysis of human CD34⁺ cells on wound tissue section treated with fresh isolated CD34⁺ cells at day 5 of wounding (red, a). Counterstaining of nuclei with DAPI (blue) on the same section (b). The overlay images of CD34⁺ cells with nuclei staining (c). Scale bar = 400 μm. High magnification image of human CD34-positive cells (d). Scale bar = 80 μm</p> | 124 |
| <p>4.42 Immunofluorescence analysis of human CD34⁺ cells on wound tissue section treated with expanded CD34⁺ cells at day 5 of wounding (red, a). Counterstaining of nuclei with DAPI (blue) on the same section (b). The overlay images of CD34⁺ cells with nuclei staining (c). Scale bar = 400 μm. High magnification image of human CD34-positive cells (d). Scale bar = 80 μm</p> | 125 |

LIST OF FIGURES (Continued)

| Figure | Page |
|---|-------------|
| 4.43 Immunofluorescence analysis of human CD34 ⁺ cells on wound tissue section treated with fresh isolated CD34 ⁺ cells at day 9 of wounding (red, a). Counterstaining of nuclei with DAPI (blue) on the same section (b). The overlay images of CD34 ⁺ cells with nuclei staining (c). Scale bar = 400 μ m. High magnification image of human CD34-positive cells (d). Scale bar = 80 μ m | 126 |
| 4.44 Immunofluorescence analysis of human CD34 ⁺ cells on wound tissue section treated with expanded CD34 ⁺ cells at day 9 of wounding (red, a). Counterstaining of nuclei with DAPI (blue) on the same section (b). The overlay images of CD34 ⁺ cells with nuclei staining (c). Scale bar = 400 μ m. High magnification image of human CD34-positive cells (d). Scale bar = 80 μ m | 127 |
| B.1 Statistical description of Figure 4.12 | 214 |
| B.2 Statistical description of Figure 4.15 | 215 |

LIST OF ABBREVIATIONS

| | | |
|-----------|---|--|
| Ang-1 | = | angiopoietin-1 |
| AGM | = | aorta-gonad mesonephros |
| BFU-E | = | burst-forming unit-erythroid |
| BM | = | bone marrow |
| BMP-2 | = | bone morphogenic protein 2 |
| BSA | = | bovine serum albumin |
| °C | = | degree celcius |
| CAR cells | = | vascular cell adhesion molecule-1 ⁺ reticular cells |
| CFU | = | colony-forming unit |
| CB | = | cord blood |
| CD | = | cluster of differentiation |
| cDNA | = | complementary deoxyribonucleic acid |
| CFU-G | = | colony-forming unit-granulocyte |
| CFU-GM | = | colony-forming unit-granulocyte and macrophage |
| CFU-M | = | colony-forming unit-macrophage |
| CFU-S | = | colony-forming unit-spleen |
| CKIε | = | casein kinase Iε |
| CLP | = | common lymphoid progenitor |
| CM | = | conditioned medium |
| CMP | = | common myeloid progenitor |

LIST OF ABBREVIATIONS (Continued)

| | | |
|--------|---|---|
| CNC | = | cranial neural crest |
| CRD | = | cysteine rich domain |
| CXCR4 | = | chemokine C-X-C receptor 4 |
| DAPI | = | 4,6-diamidino-2-phenylindole |
| DC | = | dendritic cell |
| DKK1 | = | dickkopf1 |
| dNTP | = | deoxyribonucleic acid |
| DVL | = | Dishevelled |
| EP | = | erythroid progenitor |
| EPO | = | erythropoietin |
| ESC | = | embryonic stem cell |
| FBS | = | fetal bovine serum |
| FITC | = | fluorescein isothiocyanate |
| Flt3L | = | Fms-related tyrosine kinase 3–ligand |
| Fz | = | Frizzled |
| G-CSF | = | granulocyte colony-stimulating factor |
| GEMM | = | granulocyte, erythroid, macrophage, and megakaryocyte |
| GFP | = | green fluorescent protein |
| GM-CSF | = | granulocyte/macrophage colony-stimulating factor |
| GMP | = | granulocyte/macrophage progenitor |
| GP | = | granulocyte progenitor |

LIST OF ABBREVIATIONS (Continued)

| | | |
|--------|---|---|
| GSK | = | glycogen synthase kinase |
| Hh | = | hedgehog |
| HSC | = | hematopoietic stem cell |
| HSPC | = | hematopoietic stem and progenitor cell |
| IGFBP2 | = | insulin-like growth factor-binding protein 2 |
| IL | = | interleukin |
| IMDM | = | Iscove's Modified Dulbecco's Medium |
| iPSC | = | induced pluripotent stem cell |
| JAK-2 | = | Janus kinase 2 |
| KSR | = | knockout serum replacement |
| LEF | = | lymphoid enhancer factor |
| Lin | = | lineage |
| LRP5 | = | LDL-receptor-related proteins 5 |
| LRP6 | = | LDL-receptor-related proteins 6 |
| LSK | = | Lineage ⁻ Sca-1 ⁺ CD117 ⁺ cell |
| LT-HSC | = | long-term repopulating hematopoietic stem cell |
| MacP | = | macrophage progenitor |
| MAPKs | = | mitogen-activated protein kinases |
| M-CSF | = | macrophage colony-stimulating factor |
| MEP | = | megakaryocyte/erythrocyte progenitor |
| mg | = | milligram |
| MGDF | = | megakaryocyte growth and development factor |

LIST OF ABBREVIATIONS (Continued)

| | | |
|----------|---|----------------------------------|
| Mib | = | Mind bomb |
| MkP | = | megakaryocyte progenitor |
| MMP-9 | = | matrix metalloproteinase-9 |
| MNC | = | mononuclear cell |
| MPD | = | myeloproliferative disease |
| MPP | = | multipotent progenitor |
| MSCs | = | mesenchymal stem cells |
| mTOR | = | mammalian target of rapamycin |
| NC | = | neural crest |
| NK | = | natural killer cell |
| NSC | = | neural stem cell |
| NOD mice | = | non-obese diabetic mice |
| PB | = | peripheral blood |
| PBS | = | phosphate buffer saline |
| PE | = | phycoerythrin |
| PI3K | = | phosphatidylinositol 3-kinase |
| Ptc | = | Patched |
| RBC | = | red blood cell |
| RNA | = | ribonucleic acid |
| SCF | = | stem cell factor |
| SCID | = | severe combined immunodeficiency |
| SDF-1 | = | stromal derived factor-1 |

LIST OF ABBREVIATIONS (Continued)

| | | |
|--------------|---|--|
| sIL-6R | = | soluble interleukin-6 receptor |
| SMO | = | Smoothened |
| SNO cell | = | spindle-shaped N-cadherin ⁺ osteoblastic cell |
| SRC | = | SCID-repopulating cell |
| STAT3 | = | signal transducers and activators of transcription |
| STZ | = | streptozotocin |
| TCF | = | T-cell factor |
| TGF- β | = | transforming growth factor- β |
| Th | = | T helper cell |
| TPO | = | thrombopoietin |
| Treg | = | regulatory T cells |
| Tyr | = | tyrosine |
| UBC | = | umbilical cord blood |
| Wnt | = | Wingless |

CHAPTER I

INTRODUCTION

1.1 Introduction

Stem cells are unspecialized cells which contain the self-renewal ability. These cells have the capacity to differentiate into diverse cell types according to their optimal condition. Conversely, progenitor cells lack the self-renewal property but remain the differentiation capacity to differentiate into mature specialized cell types (Alison et al., 2002; Kondo et al., 2003). Two main categories of human stem cells are classified as embryonic stem cells group and somatic stem cell group according to their source and differentiation capacity. First, embryonic stem cells group comprised of embryonic stem cells (ESCs, originated from inner cell mass of blastocyst of embryos) and induced pluripotent stem cells (iPSCs). The iPSCs are embryonic-like stem cells which derived from reprogramming adult cells (Teo and Vallier, 2010). Both ESCs and iPSCs contain differentiation potential into three germ layers; ectoderm, mesoderm, and endoderm. In addition, these stem cells are pluripotent cells and capable of differentiation into all cell types of the body except placenta and umbilical cord. Although, human ESCs and iPSCs are believed to be the ultimate source for stem cell-based therapy studies, however, their safety and ethic in clinical practice remains controversial. There are due to source and immortalized property of the cells that may result in the development of malignant teratocarcinomas. Second,

somatic or adult stem cells are restricted in their differentiation capacity and can be isolated from various tissues such as brain, hematopoietic system, neuron, skin, heart, lung, liver, intestine (Alison et al., 2002), anterior cruciate ligament (Matsumoto et al., 2011), adipose tissue, vascular system (Hung et al., 2011), periodontal ligament, tooth dental pulp (Duailibi et al., 2011; Um et al., 2011), placenta (Sasaki et al., 2010; Tsagias et al., 2011), amniotic fluid (Rosner et al., 2011), and umbilical cord (Sellamuthu et al., 2011; Taghizadeh et al., 2011). Moreover, adult stem cells show a well-defined differentiation to other specialized cell types called 'plasticity'. Hematopoietic stem cells (HSCs), for instance, can differentiate into all blood cell types, endothelial cells (Elkhafif et al., 2011), brain cells (neurons and astrocytes) (Reali et al., 2006), muscles (Jazedje et al., 2009), cardiomyocytes (Pozzobon et al., 2010), liver cells (Khurana and Mukhopadhyay, 2008; Sellamuthu et al., 2011), pancreatic cells (Minamiguchi et al., 2008), fibroblasts/myofibroblasts (Ebihara et al., 2006), adipocytes (Sera et al., 2009), osteochondrocytes (Dominici et al., 2004; Mehrotra et al., 2010), and alveolar epithelial cells (De Paepe et al., 2011), etc. Due to the ease of collection and processing, HSCs have been studied extensively for clinical implications not only hematological disease treatment but also non-hematological diseases such as neurological disorders, cardiovascular, pancreas or liver diseases, and non-healing wounds in regenerative medicine, etc. HSCs can be isolated from several sources including bone marrow and peripheral blood (PB) and umbilical cord blood (CB). Among these three sources, cord blood HSCs (CB-HSCs) are less mature and contain the lowest immunogenicity. The frequency of HSCs is more prominent in CB than bone marrow and peripheral blood as 0.4-4.9% (Pranke et al., 2005), and 0.1-2 % in growth factors stimulation, respectively (Hossle et al., 2002; Krause et al., 1996).

In addition, engraftment ability of CB-HSCs is higher than bone marrow and peripheral blood as determined by engraftment ability of severe combined immunodeficient (SCID)-repopulating cell (SRC) in non-obese diabetic/SCID (NOD/SCID) mice (1 SRC in 9.3×10^5 CB cells compared to 1 SRC in 3.0×10^6 adult BM cells or 1 in 6.0×10^6 mobilized peripheral blood cells) (Wang et al., 1997). Thus, CB-HSCs serve as the great candidate for HSCs studies and in clinical applications. Although, HSCs are rich in CB, the total HSCs obtained from single blood unit remain low which hamper the successive autologous transplantation. Therefore, researchers have been attempting to induce the higher number of HSCs *ex vivo*. Several HSCs cultures have been identified; 1.) co-cultivation with supportive cells simulated the bone marrow niche (Butler et al., 2010; da Silva et al., 2010), 2.) viral-based induction of self-renewal gene expression (Domashenko et al., 2010; Iwama et al., 2004; Miyake et al., 2006), 3.) suppression of the negatively regulator of self-renewal genes (Wang et al., 2008; 2011), and 4.) growth factors and cytokines based medium culture (Bramono et al., 2010; Zhang et al., 2008). The cultivation of HSCs by growth factors and cytokines shows superior advantages than other techniques, which is not related to virus and cell loss by interaction to the supportive cells. In practical, the high yield number of proliferative cells in the culture can differentiate quickly into more mature blood cells and lower the HSCs yield for transplantation. Thus, maintaining their multipotency and stemness capacity during the cultivation is the key role to the way of clinic. Therefore, my dissertation research was focused on the *ex vivo* expansion of cord blood CD34⁺ cells which are the representative of hematopoietic stem and progenitor cells by cytokine-based and medicinal plant extract including studied the role of expanded CD34⁺ cells in wound healing of

streptozotocin-induced diabetic mice. The findings obtained from this work contain the new cytokines cocktails that never studied before and thus will provide as an alternative method to increase the number of available HSCs for successful clinical based HSC transplantation, including apply for regenerative medicine and other hematological research studies.

1.2 Objectives

1.2.1 To determine the efficacy of cytokine cocktails culture between serum and serum-free medium for the *ex vivo* enhancement of human CB-CD34⁺ cells

1.2.2 To determine the efficacy of multi-combination of cytokines and medicinal plant extract for the *ex vivo* enhancement of human CB-CD34⁺ cells and characterization of expanded cells in both cellular and molecular levels

1.2.3 To explore the potential of expanded human CB-CD34⁺ cells in wound healing of streptozotocin-induced diabetic mice

CHAPTER II

LITERATURE REVIEW

2.1 Hematopoietic stem cells origin and development

In the hematopoietic system, the discovery of hematopoietic stem cells (HSCs) has shed the light on stem cell biology studies including linked to other adult stem cells through the basic concepts of differentiation, multipotentiality, and self-renewal. In the early period of those discoveries, lethally irradiated animals were found to be rescued by spleen cells or marrow cells (Jacobson et al., 1951; Lorenz et al., 1951). After mouse bone marrow cells were transplanted into irradiated mice, the clonogenic mixed colony of hematopoietic cells (often composed of granulocyte/megakaryocyte and erythroid precursors) were formed within the spleen, which these colonies were then termed colony-forming unit spleen (CFU-S) (Till and McCulloch, 1961). Some colonies of primary CFU-S could reconstitute hematopoietic system in the secondary irradiated mice after receiving transplantation (Siminovitch et al., 1963). The CFU-S was first proposed that it may be differentiated from HSC, but subsequently CFU-S was demonstrated to be originated from more committed progenitor cells (Schofield, 1978). The discovery by Till and McCulloch embarked on a new journey toward many investigations to clarify HSC biology, functional characterization, purify, cultivation and other stem cells research.

Hematopoiesis and HSC development are the key role in the improvement of efficient HSC expansion. To explore that enigma, embryogenesis study for tracing HSC development in various multiple anatomical sites from different animals such as zebrafish, chicken and mouse including human embryos model have been emerging. The first anatomical site for fetal HSC activity was found in the yolk sac, which generated hematopoietic progenitors that restricted to erythroid and myeloid lineages (Mikkola and Orkin, 2006; Moore and Metcalf, 1970). Moreover, the Runx1 (transcription factor for the onset of definitive hematopoiesis) was first observed to express at embryonic day 7.5 (E7.5) in the yolk sac, the chorionic mesoderm and parts of allantoic mesoderm (Zeigler et al., 2006). However, the yolk sac was found to lack the definitive hematopoietic stem cells which lacking long-term hematopoietic reconstitution in mouse embryo prior to E11.5 (Medvinsky and Dzierzak 1996). On the other hand, long-term repopulating HSCs (LT-HSCs) were demonstrated that HSCs increased largely in the aorta-gonad mesonephros (AGM) region of the mouse embryo including in serially transplantable irradiated mice (Medvinsky and Dzierzak, 1996; Muller et al., 1994). Vitelline and umbilical arteries were also endowed with hematopoietic potential (de Bruijn et al., 2000). The presence of HSC phenotype in the embryo was supported by the evidence that a high number of non-erythroid progenitors with high proliferative potential was observed from which the liver rudiment has been removed (Huyhn et al., 1995). Other evidence to demonstrate the existence of HSC progenitor within the embryonic compartment showed that a dense population of CD34⁺ cells adhering to the ventral side of the aortic endothelium displayed a cell-surface and molecular phenotype of primitive hematopoietic progenitors (CD45⁺, CD34⁺, CD31⁺, CD38⁻, negative for lineage markers, GATA-2⁺,

GATA-3⁺, c-myb⁺, SCL/TAL1⁺, c-kit⁺, flk-1/KDR⁺) (Labastie et al., 1998; Tavian et al., 1996). In addition, the autonomously emergence of myelo-lymphoid lineage from progenitors occurred in splanchnopleural mesoderm and derived aorta within the human embryo proper, while the yolk sac generated restricted progenitors (Tavian et al., 2001). Altogether, AGM region in the embryo is suggested as the source of definitive hematopoiesis as the generation occurs between E10.5 and E12.0 with the enhance activity of HSC after mid-day 11 of gestation (Chen et al., 2009; de Bruijn et al., 2002; Taylor et al., 2010). Even though, the main source of fetal hematopoiesis was considered in AGM including vitelline and umbilical arteries, the question was raised whether the rare population produced in those regions would be enough for the distribution into fetal liver for alternative development of enormous HSCs before the transition of hematopoiesis continues to occur in the fetal thymus and bone marrow in post-natal life. Recently, the placenta, an extra-embryonic organ, has been considered as the other hematopoietic organ for *de novo* hematopoiesis (Barcena et al., 2009; Robin et al., 2009). This may be due to the physiology of the placenta containing highly vascularized blood vessels, and cytokines and growth factors rich environment for proper microenvironment of hematopoiesis and development (Cross, 2005). Additionally, privilege site within the placenta may hide the HSCs from the promoting signal into differentiation stage. Summarization of the source of blood cells during gestation through adult life has been elucidated in Figure 2.1.

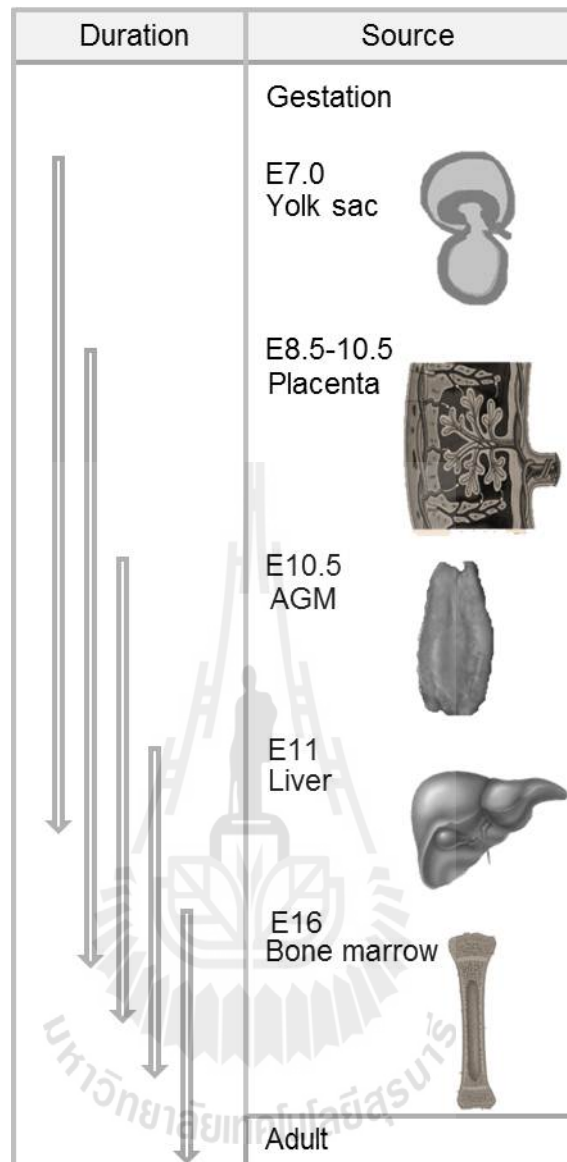


Figure 2.1 Source of blood cells during gestation through after birth (adapted from (Coskun and Hirschi, 2010)). Intraembryonic yolk sac is the first site of blood cells observation at around E7.0-E7.5. The *de novo* hematopoiesis in the placenta and AGM occurs at nearly similar wave of gestation (around E8.5-E10.5) before it circulates into fetal liver where there is the large HSC pool during gestation. At around E16.5, the HSCs migrate and reside within the bone marrow which finally becomes the source of HSC in adult life.

The origin of HSC in the placenta is being question. Understanding how the placenta develops might be useful to define the source and the niches supporting HSC development. Mouse and human placentas are anatomically similar and its genes have analogous identity (Cox et al., 2009; Georgiades et al., 2002). The placenta is formed from trophoblast, mesodermal tissues, chorionic mesoderm and allantois (Figure 2.2) (Rossant and Cross, 2001). At E8.5 of mouse gestation, the allantois develops and fuses with chorionic mesoderm through its distal part generating the chorioallantoic mesenchyme in the chorionic plate and continuing to form the fetal vascular compartment of the placental labyrinth, while the proximal part becomes the umbilical cord (Gekas et al., 2010).

The umbilical cord (a constitution of the fetal arteries and veins and is inserted within chorionic plate of the placenta) is attached to the center of fetal surface for utero-placenta circulation through maternal blood. Maternal blood passes through the placenta from uterine arteries to spiral arteries in the maternal decidua Thereafter, the maternal blood percolates through the villous tree in humans (or the labyrinth in mice) known as chorionic villi which created and lined by fetal trophoblast cells (Georgiades et al., 2002; Rossant and Cross, 2001). The inner core of the chorionic villi consists of allantoic mesenchyme and vasculature which is continuous with that of the umbilical cord. The chorioallantoic vasculature connects the placenta via the dorsal aorta and fetal liver through the umbilical cord vessels. These regions are localized by an equally dense network of fetal capillaries where the fetomaternal exchange occurs (Georgiades et al., 2002).

Because of the mesoderm layer gives rise to all blood cells, the chorionic and allantoic mesoderm are considered as the origin of HSC in the placenta. This can be

explained by the observation that hematopoietic potential emerging from both tissues and has been identified with myeloerythroid potential (Corbel et al., 2007). In addition, hematopoietic cell (CD34⁺CD45⁺) collected from placental villi stroma and highly expression of CD45⁺ cells that appear to be budding from the vasculature have been found from human placenta during midgestation (Robin et al., 2009). Moreover, cells harvested from term human placenta vessels and tissues could generate human hematopoietic repopulation of non-obese diabetic (NOD)-SCID mice, which harbored and/or amplified in vascular labyrinth placenta niche (Robin et al., 2009). These observations imply that the placenta is the HSC source along with umbilical cord blood. At E10.5, first HSC emerge in the dorsal aorta before the onset of heart beat where the circulation has not been formed. One study showed that in the absence of heart beat in *Ncx1* (the sodium and calcium exchange pump1) knockout embryos, the HSC development was verified to initiate in the placental vasculature (Rhodes et al., 2008). Additionally, multilineage hematopoietic potential could obtain from placentas of *Ncx1* knockout embryos. Taken together, these observations support the hypothesis that the placenta is the source of *de novo* hematopoiesis while placenta labyrinth may serve as the niche for the development.

The true origin of HSC in the intraembryonic hematopoiesis remains controversial. One of the main hypotheses is hemangioblasts or hemogenic endothelial while the alternative model is mesodermal precursors. The blood islands originated in the yolk sac are derived from mesodermal cell aggregates, which contain the ability to differentiate into both hematopoietic and endothelial cells. The common precursor by those lineages is suggested to be so called the hemangioblast (Murray, 1932). Hematopoietic phenotype originated from hemogenic endothelium has been

found in avian and mouse during ontogeny (Jaffredo et al., 1998; Nishikawa et al., 1998). Imaging and cell-tracking study explored the hemogenic endothelial cells giving rise to hematopoietic cells (Eilken et al., 2009). Single-cell observation of mouse mesodermal cells by time-lapse imaging showed the generation of endothelial sheet colonies. Some colonies developed the hematopoietic morphology by upregulated the blood-specific proteins CD45, CD41 and CD11b and losing intact morphology. Recently, this evidence has been supported by the emergence of HSCs (Sca^+ , $c-kit^+$, $CD41^+$) directly from ventral aortic endothelial cells using time-lapse confocal imaging from live mouse aorta (Boisset et al., 2010). Moreover, Oberlin and colleagues prove the origin of adult bone marrow HSCs which most of them derived from the vascular endothelial-cadherin ancestor (Oberlin et al., 2010). Taken together, these studies pinpoint the evidence that definitive hematopoietic stem and progenitor cells emerge from an endothelial precursor.

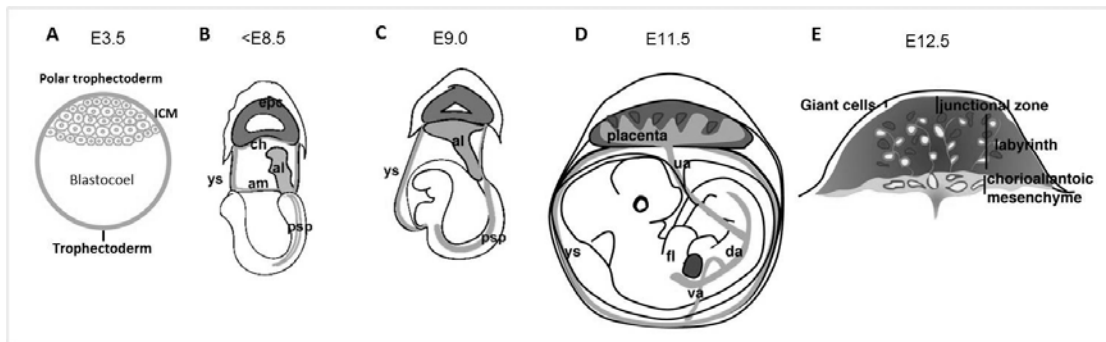


Figure 2.2 Mouse placenta development. A) At E3.5 of early embryogenesis, blastocyst is formed, containing inner cell mass located at one side of the blastocoelic cavity and outer layer (trophoblastic epithelium) which give rise to the placenta. B) Between E7.5-E8.25 mesodermal precursors originating from the primitive streak grow into the allantois (light grey) which then develops toward the ectoplacental cone (dark grey). C) Chorioallantoic fusion between the allantoic and chorionic mesoderm at E8.5. After that, Chorionic villi and vasculature are formed producing and generates extensive villous branching called labyrinth. D) At E11.5, umbilical cord is fully formed to connect the placenta with fetus where feto-maternal bloods circulate. D) Cross-section of the placenta at E12.5 showing the chorioallantoic mesenchyme lies cover the placenta labyrinth with fetal vessels lined by fetal endothelium (dark vessels with lumen) and trophoblast lined by maternal blood spaces (grey vessels surrounded by dark trophoblasts). al, allantois; ch, chorion; am, amnion; epc, ectoplacental cone; ys, yolk sac; psp, para-aortic splanchnopleura; da, dorsal aorta; ua, umbilical artery; va, vitelline artery; fl, fetal liver (modified from (Gekas et al., 2010)).

2.2 HSC niches

Homing of HSC from other definitive hematopoiesis to fetal bone marrow is thought to involve some signaling factors such as stromal derived factor-1 (SDF-1 or CXCL12)/chemokine C-X-C receptor 4 (CXCR4) axis (Ara et al., 2003; Guo et al., 2005). Soluble factors are not only mediated in fetal bone marrow but also in adult bone marrow to maintain HSC in undifferentiated state, and regulate HSC in proliferative and differentiated states within the microenvironments termed 'niche' throughout the life (Nagasawa et al., 2011). Such molecules have been identified to be associated with HSC homing to bone marrow, for example, SDF1- α , β 1-integrins, metalloproteinases (MMP) and serine-threonine protein phosphatase (PP)2A (Basu et al., 2007; Nilsson et al., 2006). By using real-time imaging, it is possible to explore the localization of HSCs with their function (Lo Celso et al., 2009). HSCs lodge in the endosteal surface, osteoblasts and blood vessels, particularly in trabecular regions, in the mouse calvaria. On the contrary, more mature cells reside away from the endosteum. Similarly, a study by developed *ex vivo* real-time imaging in irradiated mice show the homing and lodgment of transplantable HSCs in the endosteal region of the trabecular bone area where they respond to bone marrow damage by rapidly dividing (Xie et al., 2009).

Recently, HSCs niches are suggested to be mediated in three main microenvironments within bone marrow (Figure 2.3). First, osteoblasts derived from mesenchymal precursors are localized in the endosteal regions which are well vascularized. The activation of osteoblastic differentiation is in part mediated by HSC-derived bone morphogenic protein 2 (BMP-2) and BMP-6 (Jung et al., 2008). Osteoblasts are suggested as the niche due to the finding that the number of

osteoblasts is increased from parathyroid hormone activation and results in an increase HSCs number *in vivo* (Calvi et al., 2003). This signal was found to activate through *Jagged1*, a serrate family of Notch ligand, on osteoblasts (Weber et al., 2006). Study by Chitteti and colleagues supports this evidence and shows that enhancing hematopoiesis promoted by osteoblast via Notch signaling not only through *Jagged1* up-regulation, but also *Notch2*, *Jagged2*, *Delta1* and *4*, *Hes1* and *5*, and *Deltex* ligands (Chitteti et al., 2010). Soluble factors produced from osteoblasts function in regulating HSC quiescence, HSC pool and fate such as angiopoietin-1 (Ang-1) (Arai et al., 2004), SDF-1 (CXCL12) (Taichman, 2005), and osteopontin (Stier et al., 2005). Recently, osteoblasts secreted cysteine protease cathepsin X has been found to catalyze the chemokine CXCL-12, a potent chemo-attractive cytokine for HSCs, and ablate the attachment of CD34⁺ cells with the osteoblasts (Staudt et al., 2010). This result suggests the role of osteoblasts in regulate HSCs trafficking in the bone marrow.

A group of de Barros supports this hypothesis by demonstrated that the 3D spheroid of non-induced and one week osteo-induce bone marrow stromal cell (active osteoblasts) form an informative microenvironment that control migration, lodgment, and proliferation of HSCs (de Barros et al., 2010). Bone marrow endosteal cells, particularly, osteoblast-enriched ALCAM⁺Sca-1⁻ cells promote LT-reconstitution activity of HSCs via the up-regulation of genes related in homing and cell adhesion (Nakamura et al., 2010). In addition, HSCs are found to adhere with spindle-shaped N-cadherin⁺ osteoblastic (SNO) cells which are a subpopulation of osteoblasts (Zhang et al., 2003). BMP receptor type IA mutant mice have been showed to increase in the number of SNO cells that correlated to an increase in HSC number (Zhang et al.,

2003). Consistently, green fluorescent protein-positive (GFP⁺) HSCs derived from *Col2.3-GFP*⁺ transgenic mouse are found to attach to SNO cells but not all GFP⁺ HSCs are in contact with SNO cells which show that N-cadherin⁻ component might be the other niche for HSCs (Xie et al., 2009). Cumulatively, osteoblasts and SNO cells are suggested as the niche for hematopoietic stem and progenitor cells where this microenvironment termed “Endosteal niche”.

Nevertheless, some reports suggest that other niches might involve in HSC maintenance inside the bone marrow. There are some observations that osteoblast depletion results in the loss of B lymphopoiesis but not immediately loss of HSC number (Visnjic et al., 2004; Zhu et al., 2007) and few bone marrow HSCs (CD150⁺CD48⁻CD41⁻lineage⁻) localized to the endosteum (Kiel et al., 2007). Mice model defect in osteoblast function confer no changes in LT-reconstitution function of HSCs (Ma et al., 2009). Additionally, loss of N-cadherin does not affect HSC maintenance and hematopoiesis (Kiel et al., 2009). Most HSCs in the bone marrow have been observed to reside in the sinusoid, where fenestrated endothelium persists and allows blood flow for an exchange of blood cells and small molecules. Taken together, the vascular niche is suggested as the other niche for HSC maintenance (Kiel et al., 2007). Bone marrow endothelial cells have been proposed to play a role in HSC controlling within vascular niche. Primary CD31⁺ microvascular endothelial cells can restore hematopoiesis in mice when they receive bone marrow lethal doses of irradiation (Li et al., 2010). Study by a group of Salter shows a consistent observation that endothelial progenitor cells injected in total body irradiated mice can stimulate HSC reconstitution and hematologic recovery (Salter et al., 2009). Furthermore, selective activation of Akt in endothelial cells produces angiocrine factors mediated in

the reconstitution, expansion and maintenance of HSCs (Kobayashi et al., 2010). Nonetheless, constitutive activation of Akt, a binding ligand of phosphoinositide 3 in the phosphoinositide 3-kinase pathway, impairs engraftment ability in mice and preferentially generate leukemia in mice (Kharas et al., 2010). Sinusoidal endothelial cells are essential for engraftment of hematopoietic stem and progenitor cells (HSPCs) and restoration of hematopoiesis after myeloablation (Hooper et al., 2009). Angiocrine factors, such as Notch ligands, released by endothelial cells *in vivo* contribute to the replenishment of the LT-HSC pool and result in reconstitution of hematopoiesis (Butler et al., 2010). Altogether, vascular niche containing endothelial cells is suggested as the major HSC pool and maintenance conferring proliferation and differentiation selection.

The other candidate niche rather than endosteal and vascular microenvironments has been proposed to SDF-1 (CXCL12) producing vascular cell adhesion molecule-1⁺ reticular cells (CAR cells), that line the sinusoid next to the endothelial layer, in which the HSCs are found in contact with (Sugiyama et al., 2006). CAR cells are surrounded by sinusoidal endothelial cells. CXCL12-CXCR4 signaling is essential in maintaining the HSC pool, development of B cells and plasmacytoid dendritic cells (Kohara et al., 2007; Nagasawa, 2006; Nie et al., 2008; Noda et al., 2011). Short-term ablation of CAR cells results in impairment of adipogenic and osteogenic differentiation, thus, CAR cells are suggested as the adipogenic and osteogenic progenitors (Omatsu et al., 2010). HSCs from CAR cell-depleted mice have been shown a reduction in number and cell size, which are more quiescent and an increase in expression of early myeloid selector genes (Omatsu et al., 2010). In addition, CAR cells are suggested to coincide with CD146⁺ stromal progenitors that

express CXCL12 and Ang-1. CD146⁺ cells have been shown to generate osteoblast which form bone and function as skeletal progenitor cells. Thus, those cells provide or generate the hematopoietic microenvironment that link to the hematopoietic regulation in the reticular niche (Sacchetti et al., 2007).

2.3 Hierarchy of human hematopoiesis

Based on the study of molecular marker expression by flow cytometry analysis has led the identification of each blood cell subpopulations in terms of their biology and potential when combine with other functional assays. As a result, schematic demonstration of hematopoietic hierarchy has been proposed (Figure 2.4) (Seita and Weissman 2010). The origin of all blood cell in hematopoietic system is believed to be derived from HSCs that contain self-renewal capacity and give rise to multipotent progenitors (MPPs) which lose self-renewal potential but remain fully differentiate into all multilineages. MPPs further give rise to oligopotent progenitors which are common lymphoid and myeloid progenitors (CLP and CMP, respectively). All these oligopotent progenitors differentiate into their restricted lineage commitment: (1) CMPs advance to megakaryocyte/erythrocyte progenitors (MEPs), granulocyte/macrophage progenitors (GMPs) and dendritic cell (DC) progenitors. (2) CLPs give rise to T cell progenitors, B cell progenitors, NK cell progenitors and DC progenitors. Notably, DC progenitors (CD8 α ⁺ DC, CD8 α ⁻ DC, and plasmacytoid DC) could be derived from both CMPs and CLPs (Manz et al., 2001a; 2001b; Traver et al., 2000).

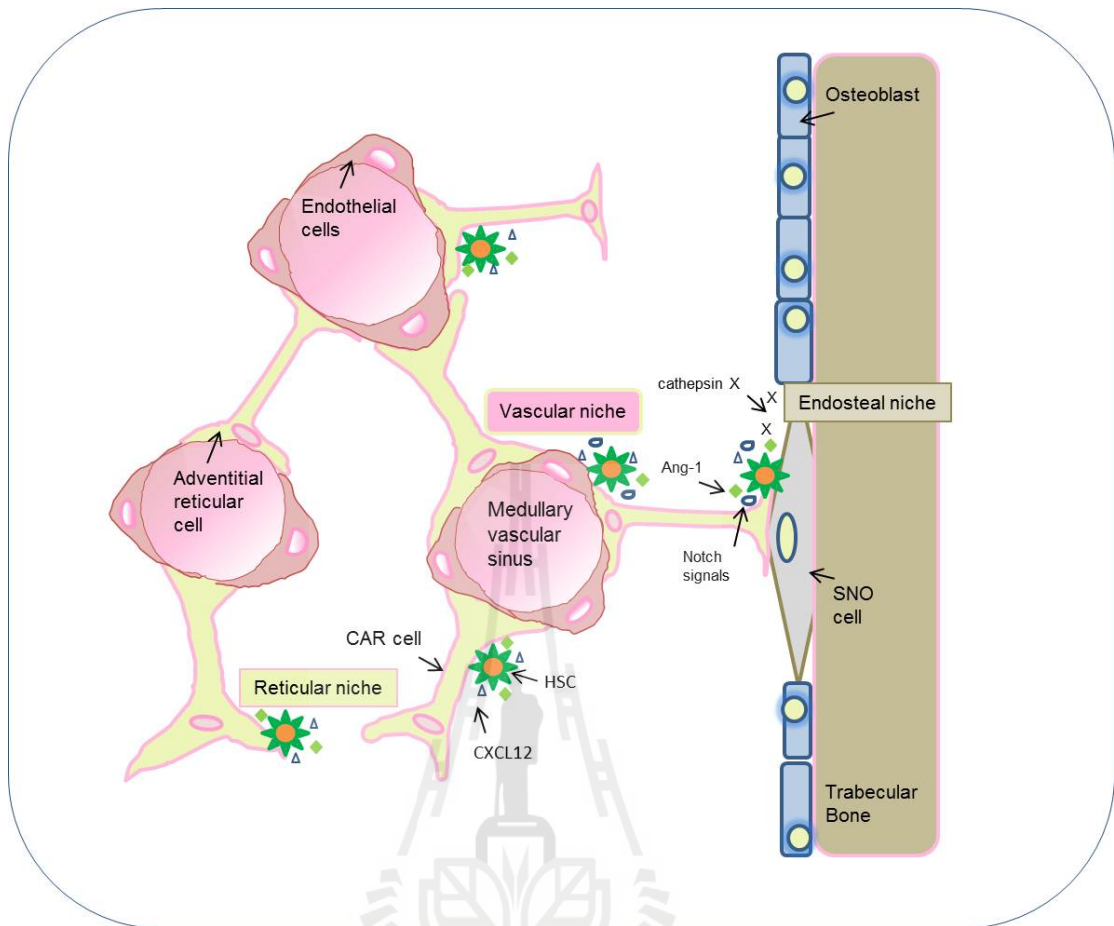


Figure 2.3 Candidate cellular niches mediated in maintenance and regulation of HSCs in bone marrow; endosteal niche, vascular niche, and reticular niche. HSCs are in contact with SNO cells, bone-lining osteoblasts, within endosteal niche. Osteoblasts produce several signal molecules such as Notch ligands, angiopoietin-1 (Ang-1), CXCL12 and cathepsin X mediated in control HSC pool and maintenance. Most HSCs are found in sinusoids, particularly adherence to CAR cells that surround sinusoidal endothelial cells (reticular niche). Similarly, CAR cells produce CXCL12 in association with CXCR4 signaling essentially for HSC maintenance (adapted from Nagasawa et al., 2011).

Among the isolation and characterization of HSCs and progenitors, CD34 molecule is the first widely chosen for the study by several researchers. CD34 is comprised in the CD34 family of cell-surface transmembrane proteins together with podocalyxin and endoglycan (Doyonnas et al., 2001; Sasseti et al., 1998; 2000). CD34 expression on blood cells is about 0.1-4.9% in human cord blood, bone marrow and peripheral blood (Hossle et al., 2002; Krause et al., 1996; Pranke et al., 2005). The first candidate human HSCs was a population of cells expressing CD34⁺CD90⁺(Thy-1)Lin⁻ which could give rise to T and B lymphocytes and myeloerythroid activities in both *in vitro* and *in vivo* human fetal thymus transplanted into SCID mice while some subset of CD34⁻, CD90⁻, Lin⁻ lack of multipotent progenitors (Baum et al., 1992). Further isolation of HSCs are based on the expression of CD38 (Bhatia et al., 1997b; Hao et al., 1995) and CD45RA (Mayani et al., 1993). This can be concluded that Lin⁻CD34⁺CD38⁻CD90⁺CD45RA⁻ population enriches for human HSCs and the candidate human MPP fraction of multipotency with an incomplete self-renewal capacity is enriched in Lin⁻CD34⁺CD38⁻CD90⁻CD45RA⁻ population (Majeti et al., 2007). However, recently observation using HSC xenograft assay in NOD-SCID-IL2Rgc^{-/-} (NSG) mice showed that both Lin⁻CD34⁺CD38⁻CD90⁻CD45RA⁻ and Lin⁻CD34⁺CD38⁻CD90⁺CD45RA⁻ contain LT repopulating activity in secondary recipients with different frequency (Notta et al., 2011). In addition, CD49f (integrin α 6) marker has been shown as a specific HSC marker within Lin⁻CD34⁺CD38⁻CD45RA⁻ population which as single sorted HSC is highly efficient in generating long-term multilineage grafts while the loss of CD49f expression results in the absence of long-term grafts (Notta et al., 2011). Furthermore, Rhodamine-123 marker (efflux of the mitochondrial dye) is added to enrich for HSCs where high Rho

efflux (Rho^{lo})Lin⁻CD34⁺CD38⁻CD90⁺CD45RA⁻ can also repopulate all blood lineages in secondary recipients (Notta et al., 2011). Taken together, these results demonstrate that human HSCs are enriched in the Lin⁻CD34⁺CD38⁻CD90^{+/-}CD45RA⁻Rho^{lo} population of hematopoietic cells (Figure 2.4).

2.4 Molecular niche in self-renewal and maintenance of HSCs

The balance to control between self-renewal and differentiation (or cell fate decision) of HSCs in bone marrow is mediated by several factors. There are a number of animal models promoting the concept that the niches inside bone marrow provide the maintenance and regulation of HSCs by some microenvironmental-dependent signals. Most HSCs are in quiescent state (i.e. in G0/G1 phase of the cell cycle) (Fleming et al., 1993), however, when the hematopoietic cells disturbance occurs, hematopoiesis system will respond by shutting down or turning on the regulators mediated in the regulations. Several pathways have been studied in relation to that circumstance which are; CXCL12/CXCR4 signaling, BMP signaling, Mpl/Thrombopoietin (TPO) signaling, Tie2/Ang-1 signaling, hedgehog and Notch signaling, as well as Wingless (Wnt) signaling.

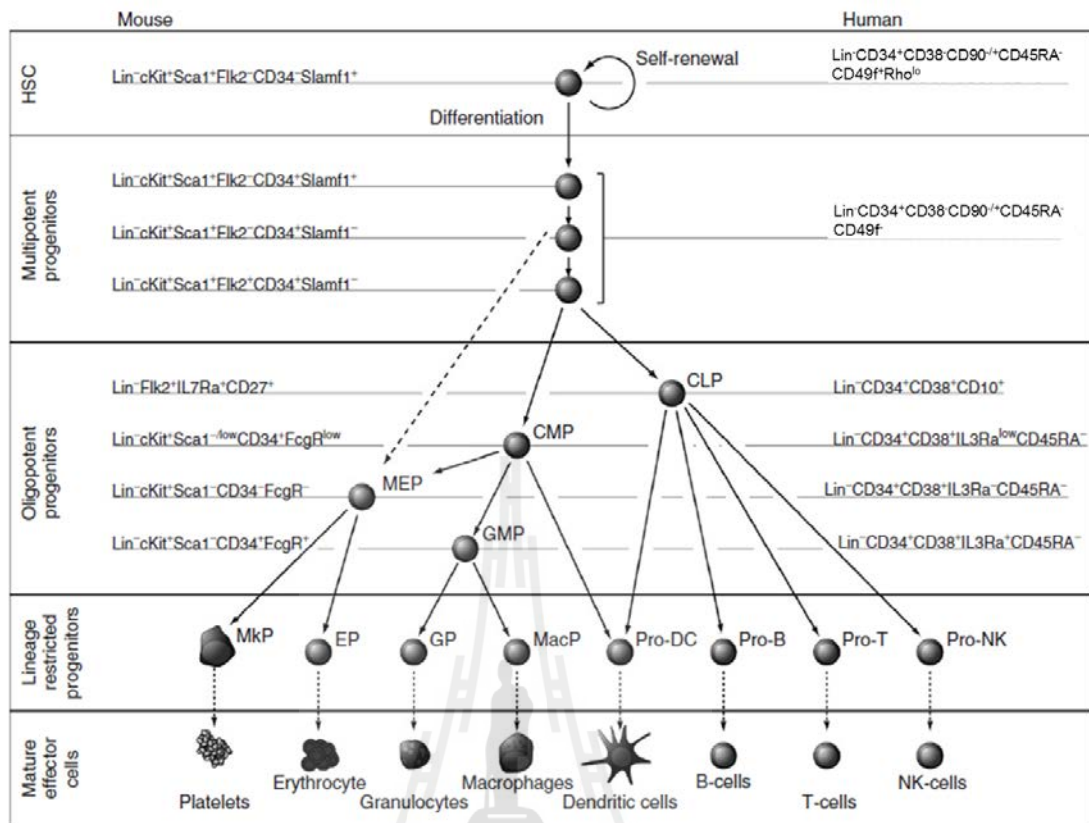


Figure 2.4 Hierarchy of hematopoiesis (modified from Irving Weissman's group (Seita and Weissman, 2010)). The phenotypic cell surface marker of each population of mouse and human blood system is shown. In the mouse hematopoiesis system, MPPs give rise directly to MEPs without passing through CMPs as identified in human system (dash line). CLP, common lymphoid progenitor; CMP, common myeloid progenitor; DC, dendritic cell; EP, erythrocyte progenitor; GMP, granulocyte/ macrophage progenitor; GP, granulocyte progenitor; HSC, hematopoietic stem cell; MacP, macrophage progenitor; MEP, megakaryocyte/erythrocyte progenitor; MkP, megakaryocyte progenitor; NK, natural killer; Lin, lineage markers.

The first pathway is CXCL12 (SDF-1)/CXCR4 signaling as described earlier that its role is essential for HSC maintenance. Specifically, SDF-1 regulated HSC attachment within the niche through matrix metalloproteinase-9 mediated released of soluble Kit-ligand (Heissig et al., 2002). Inactivation or deletion of CXCR4 in mice resulted in HSC pool reduction and hyperproliferation responsive to HSC defects (Nie et al., 2008; Sugiyama et al., 2006). In addition, conditional SDF-1-deficient mice impaired HSC quiescence and endosteal niche localization (Tzeng et al., 2011).

The second pathway is involved in BMP signaling. Besides BMP-4 (a TGF- β family member) regulation during embryogenesis in hematopoietic lineage commitment from mesodermal cell, adult HSC number and function within bone marrow niche is controlled by Bmp-4 (Durand et al., 2007; Goldman et al., 2009). Knowledge of BMP signaling and receptor related adult HSC within bone marrow has been studied in a small number and is elusive. BMP signaling impairment demonstrated an increase in the niche size, leading to the enhancement in the number of HSCs (J. Zhang et al., 2003). Differential response of HSC to soluble BMPs observed by a group of Bhatia showed that higher concentrations of BMP-4 maintained human CB HSCs *in vitro* while at lower concentrations of BMP-4 induced proliferation and differentiation of HSCs (Bhatia et al., 1999). Moreover, BMP-2 and BMP-7 at high concentrations inhibited proliferation which then maintained HSCs (Bhatia et al., 1999).

A third pathway is composed of Mpl and its ligand TPO which is known to regulate megakaryopoiesis (Broudy and Kaushansky, 1995). Mpl/TPO signaling involved in postnatal steady-state HSC maintenance and cell-cycle progression at the endosteal surface (Qian et al., 2007; Yoshihara et al., 2007b). Mpl-expressed LT-

HSCs was found in correlation to cell cycle quiescence and that is closely associated with TPO-producing osteoblastic cells in the bone marrow (Yoshihara et al., 2007b). Additionally, the inhibitory adaptor protein Lnk was demonstrated as a negative regulator of Janus kinase 2 (JAK2) in HSCs following TPO stimulation and that HSC quiescence and self-renewal control was predominantly through Mpl (Bersenev et al., 2008). Therefore, TPO/Mpl/JAK2/Lnk pathway can be concluded as a gatekeeper for HSC quiescence. Recently, TPO knock-in RAG2^{-/-}γc^{-/-} mice has been shown to improve human engraftment in the bone marrow and maintenance of HSPCs pool by serial transplantation (Rongvaux et al., 2011). Taken together, TPO has an important function in maintenance and self-renewal of HSCs.

A fourth pathway includes Tie2/Ang-1 signaling which Ang-1 is the ligand of Tie2 expressed predominantly on osteoblastic cells in endosteum (Arai et al., 2004) and in mesenchymal stem/stromal cells (MSCs) (Sacchetti et al., 2007). Interaction of receptor tyrosine kinase Tie2 expressing HSCs to the bone surface of bone marrow via the interaction of Ang-1, resulted in tightly adhesion of HSCs to the niche and become quiescence (Arai et al., 2004). Moreover, Ang-1 conferred the maintenance of LT-HSCs while Ang-2 did not and antagonized the effects of Ang-1 on gene expression, Akt (also known as protein B) phosphorylation (Gomei et al., 2010).

A fifth pathway, hedgehog (Hh) signaling is proposed as a negative regulator of the HSC quiescence (Trowbridge et al., 2006a). Hh ligand binds to the transmembrane receptor Patched (Ptc) allowing the signaling function of a second transmembrane protein, Smoothed (Smo) essential for the Hh signal to be active. Constitutive activation of the Hh signaling pathway in Ptc heterozygous (Ptc-1^{+/-}) mice resulted in induction of cell cycling and expansion of primitive bone marrow

hematopoietic cells (Trowbridge et al., 2006a). To support this hypothesis, deletion of *Smo* in the in utero of transgenic mice impaired stem cell self-renewal and inhibit the engraftment capacity of HSCs (Zhao et al., 2009). Furthermore, the common downstream positive effector of Hg signaling, *Gli1*, has been shown to play a critical role in normal and stress hematopoiesis (Merchant et al., 2010). However, the discrepancy was shown in studies of Hofmann et al. (2009) and Gao et al. (2009) which suggested that the conditional loss of *Smo* within adult HSCs is dispensable for hematopoiesis. These conflicts might be due to the difference of the mice model and conditional system used to impair Hg signaling.

A sixth pathway is Notch signaling which plays a key role in several fundamental functions including proliferation, differentiation and cell fate decision (Artavanis-Tsakonas et al., 1999; Lin and Hankenson, 2011). Four notch receptors (Notch 1-4) and five ligands (Jagged1-2 and Delta-like 1, 3 and 4) have been identified in mammals (Ranganathan et al., 2011). Cells expressing Notch ligands or engineered immobilized Notch ligands could maintain or enhance HSC self-renewal in culture (Ohishi et al., 2002; Varnum-Finney et al., 2011). Of note, some investigations showed an impair differentiation *in vitro* (Stier et al., 2002; Varnum-Finney et al., 2003) and *in vivo* (Stier et al., 2002; Varnum-Finney et al., 2011) following interaction of Notch receptors and Notch ligands. Transcription factor act upstream of the Notch signaling cascade, *Hes2*, was shown to be essential in HSCs formation in zebrafish embryos when *hes2* expression was knockdown, whereas HSC formation could be rescued by the activation of Notch signal (Rowlinson and Gering, 2010). Increased in *in vitro* maintenance of hematopoietic functions and repopulating potential on osteoblasts and Lineage⁻Sca-1⁺CD117⁺ (LSK) cells co-culture was

mediated with the up-regulation of Notch signal (Notch2, Jagged1 and 2, Delta1 and 4, Hes1 and 5, and Deltex) (Chitteti et al., 2010). Thus, these studies support the role of Notch signaling mediated in HSC hematopoiesis and maintenance. In the contrary, some investigations reported that Notch signaling is not important for HSC self-renewal and maintenance (Maillard et al., 2008; Mancini et al., 2005). Inactivation of Notch1 and Jagged1 in bone marrow progenitors and bone marrow stroma, respectively, did not impair HSC maintenance and reconstitution (Mancini et al., 2005). The inhibition of Notch1-4 signaling via a developed dominant-negative Mastermind-like1 construct was transfected into LSK and demonstrated similar result of LT-reconstitution in bone marrow compared to LSK control, except for T-cells (Maillard et al., 2008). Nevertheless, the study by Kim and colleague explored the important of Notch in normal hematopoiesis (Kim et al., 2008). Mind bomb (Mib)-1, that regulates the endocytosis of Notch ligands and activation, was inactivated in mice leading to myeloproliferative disease (MPD). Surprisingly, when transplanted with wild-type bone marrow cells into the Mib1-null microenvironment resulting in a *de novo* MPD. The MPD progression was suppressed by transplantable Notch activating cells, suggesting that MPD develops from the non-hematopoietic microenvironmental cells with defective Notch signaling. Therefore, Notch signaling is indeed required for normal hematopoiesis. Santaguida and colleague developed *JunB*-deficient mice which resulted in impairment of Notch and transforming growth factor- β (TGF- β) signaling, in part via the transcriptional regulation of Hes1 (Santaguida et al., 2009). This study showed an increase in LT-HSCs proliferation and differentiation without impairing their self-renewal *in vivo*, suggesting that LT-HSC proliferation rate is not

exclusively compelling to self-renewal activity and maintenance of HSC in the BM niches.

Notch signaling is involved in the cross-talk with other pathways particularly Wnt signaling not only in hematopoiesis (Clements et al., 2011) but also in other cellular development (Chalamalasetty et al., 2011; Han et al., 2011; Kim et al., 2011; Lin and Hankenson, 2011; Peter and Davidson, 2011). In addition, Wnt signaling pathway is mediated in the regulation of stem cell fate and maintenance of mouse ESCs and human ESCs in undifferentiated state (Sato et al., 2004; Woll et al., 2008).

A seventh pathway is Wnt signaling. There are at least two independent pathway comprised in Wnt signaling; canonical Wnt and non-canonical Wnt signaling pathways. The canonical Wnt signal interacts with Frizzled (Fz) receptors and single-pass co-receptors LDL-receptor-related proteins 5 and 6 (LRP 5 and 6). The Fz protein contains a conserved motif, a cysteine rich domain (CRD) located on the extracellular domain that binds to multiple Wnts with a high affinity (Wu and Nusse, 2002). The intracellular signaling, then, activates β -catenin stabilization, a multi-functional protein that plays a central role in Wnt signaling pathway to modulate transcription of specific target genes by binding to T-cell factor/lymphoid enhancer binding factor (TCF/LEF) in the nucleus (Figure 2.5) (Miller et al., 1999). In the absence of Wnt, β -catenin is destabilized by phosphorylation of serine-threonine kinase, glycogen synthase kinase 3 β (GSK 3 β) and resulting in a formation of a destruction complex facilitating by Axin, a scaffold protein for the complex (Miller et al., 1999).

In the second pathway, “non-canonical Wnt signal” exerts the independent β -catenin signaling. The Wnt subfamily members, for example, Wnt5a bind to the

Frizzled receptor and stimulate downstream intracellular signaling, resulting in an increase in intracellular Ca^{2+} and then activates protein kinase C and calmodulin-dependent kinase (Miller et al., 1999). The cross-talk between Notch and Wnt signaling pathways was found in the stabilizing β -catenin on bone marrow stroma cells that promoted maintaining and self-renewal of HSCs (Kim et al., 2009). Moreover the induction of Jagged1 and delta-like 1 was observed in Wnt/ β -catenin activated bone marrow stroma or in bone marrow stroma cultured with Wnt3a-conditioned medium (Kim et al., 2009). Mice lacking Wnt3a resulted in prenatal death (Luis et al., 2009). Moreover, Wnt3a deficiency reduced the number of HSCs in fetal liver and impaired the repopulating activity *in vivo* (Luis et al., 2009). However, the exact role of Wnt signaling pathway in regulation of HSCs remains a controversy. Some studies showed that constitutive activation of Wnt/ β -catenin in transgenic mice resulted in the multilineage differentiation block and loss of repopulating stem cell activity due to the induction of quiescent stem cells entering into cell cycle and arresting their differentiation (Kirstetter et al., 2006; Scheller et al., 2006). In contrast to previous works by administration of an inhibitor of GSK-3 β *in vivo* resulted in enhancing the recovery of hematopoietic cells for neutrophil and megakaryocytic lineages as well as primitive LSK cell population together with the up-regulation of *Wnt*, *Notch* and *Hedgehog* genes (Trowbridge et al., 2006b).

In addition, inhibition of Wnt signaling in HSCs by overexpression of the paninhibitor of canonical Wnt signaling, Dickkopf1 (Dkk1), resulted in the induction of cell cycling and reduction in repopulating ability in transplanted induction mice (Fleming et al., 2008). When the inhibitor of GSK-3 β , 6-bromoindirubin 3'-oxime was used to treat CB-CD34⁺ cells, cell cycle progression was delayed including

promoted engraftment of *ex vivo*-expanded HSCs (Ko et al., 2011). Cumulatively, these studies suggest the positive regulatory role of Wnt/ β -catenin signal on the proliferative or repopulating activity of HSCs. 12/15-lipoxygenase-mediated unsaturated fatty acid metabolism has been implicated in canonical Wnt-related signaling in the maintenance of LT-HSC quiescence and number (Kinder et al., 2010). Taken together, the canonical Wnt signal is mediated in the regulation of HSC function by maintaining quiescence and balance in proliferation.

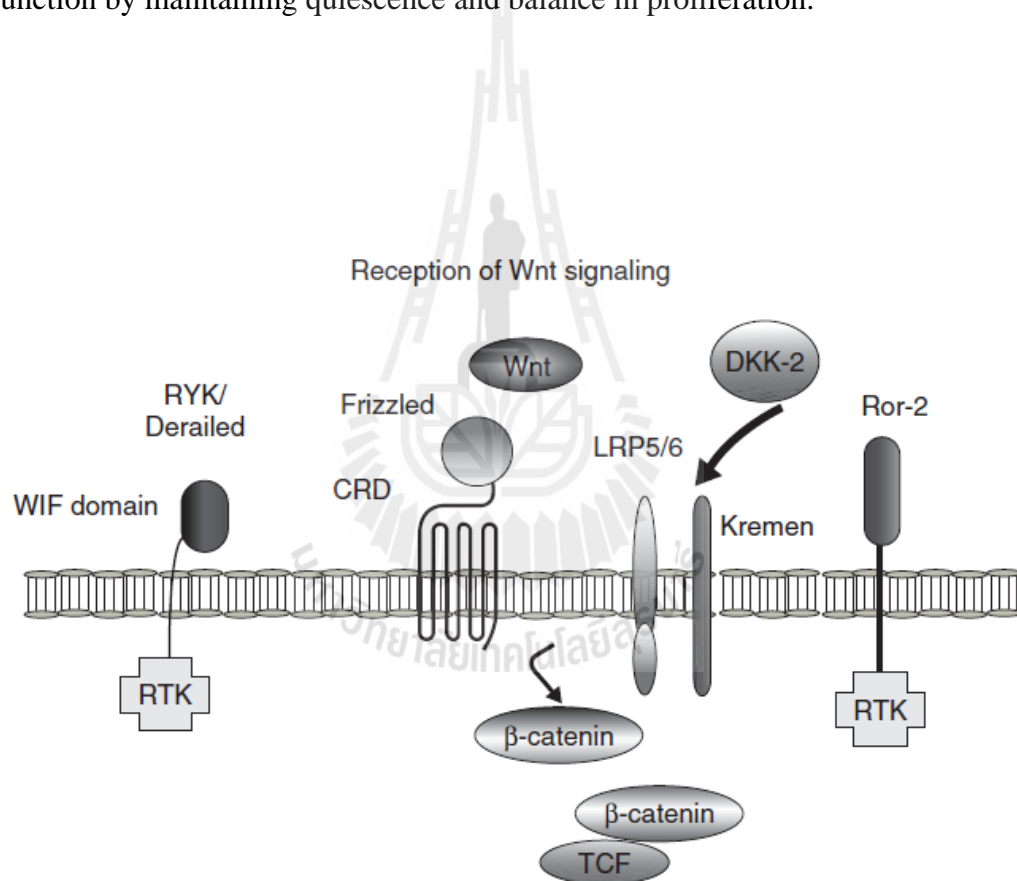


Figure 2.5 Schematic diagram of Wnt/ β -catenin signaling. CRD: cysteine-rich domain, DKK: dickkopf, LRP: LDL-receptor-related proteins, RTK: receptor tyrosine kinase, TCF: T-cell factor, WIF: Wnt inhibitory factor (Oh, 2010).

2.5 *Ex vivo* HSCs expansion

Besides advanced studies in HSC biology, understanding regulatory transcription factors and growth factor mediated in self-renewal and proliferation have led into the development of HSCs culture. Currently, the use of CB as a source for hematopoietic cell transplantation is increasing, primarily due to the ease, availability in collection and wide-applicability for undefined HLA-matched recipients. There are several attempts to expand HSC and MPP (HSPC) numbers *ex vivo* to reach the available dose needed for transplantation, particularly for autologous transplantation to reduce the risk of graft failure. Three main methodologies for *ex vivo* expansion of HSPCs can be classified; cytokine-based culture, viral-based culture and stromal cell support.

2.5.1 Cytokine-based culture

Initial studies in PB-, BM- or CB-CD34⁺ or CD34⁺CD38⁻ cells expansion using Fms-Related Tyrosine Kinase 3-Ligand (Flt3L), stem cell factor (SCF), thrombopoietin (TPO), interleukin-6 (IL-6) and/or granulocyte-colony-stimulating factor (G-CSF) showed significant expansion of hematopoietic cells or moderate increase in CD34⁺CD38⁻ cells with 2- to 6- fold increase in long-term repopulating cells after 4 to 21 days in culture (Bhatia et al., 1997a; Conneally et al., 1997; Gammaitoni et al., 2003; Ueda et al., 2000). In addition, a number of investigators adopted the medium culture usually compose of Flt3L, SCF and TPO for CB-CD34⁺ cells expansion (<14 days) (Lam et al., 2001; Qiu et al., 1999; Yang et al., 2007). Furthermore, some molecules have been found to synergize effect to enhance the proliferation of the CD34⁺ cells, colony-forming cells (CFU) and SRC number such

as angiotensin-(1-7) (Heringer-Walther et al., 2009), angiopoietin-like proteins (Zhang et al., 2006a), serotonin (Yang et al., 2007), insulin-like growth factor-binding protein 2 (IGFBP2) (Zhang et al., 2008) and valproic acid (Seet et al., 2009). Additionally, conditioned medium (CM) containing Wnt proteins (Wnt1 and Wnt3a) were found enhance the proliferative capacity and preserve immature state of CB-CD133⁺ cells, while WNT4-, WNT5a-, and WNT11-CM have been shown to promote non-hematopoietic differentiation (Nikolova et al., 2007).

Preclinical expansion of CB-CD34⁺ cells in the medium supplemented with cytokine cocktail SCF, granulocyte colony-stimulating factor (G-CSF), and megakaryocyte growth and with the development factor (MGDF) could enhance CD34⁺ cells around 100-fold in 10 days of culture and SCID-repopulating cell (SRC) activity was maintained (Ivanovic et al., 2011). Moreover, the addition of IL-3 did not improve the net fold increase significantly. Nevertheless, clinical trial using PB-CD34⁺ expansion in that cocktail containing SCF, G-CSF, and MGDF for 10 days and subjected to autologous transplantation resulted in modest or no effect to abrogate the post-transplantation neutropenia (Boiron et al., 2006; McNiece et al., 2000). Another group by Delaney and colleague point to the role of Notch mediated in *ex vivo* expansion which has been studied in phase I clinical trial (Delaney et al., 2010). Initial analysis showed an extensive expansion of CB-CD34⁺ cells (>100-fold) after 17 days in the culture containing immobilized ligand Delta1 combined with fibronectin fragments and cytokines (SCF, TPO, Flt3L, IL-3, IL-6). Preliminary results of ongoing phase I trial in patients transplanted with non-manipulated CB unit along with manipulated CB unit that have undergone Notch-mediated *ex vivo* expansion resulted in rapid recovery of neutrophil.

2.5.2 Viral-based culture

Intrinsic regulators, directly act on HSCs to regulate cell fate and self-renewal, have been imposed to stimulate HSCs proliferation through viral-mediated expression. HOX transcription factor, particularly HOXB4, overexpressed by retroviral vector demonstrated an extensive *ex vivo* expansion of mouse BM-HSCs without impairing lymphomyeloid repopulating activity in irradiated mice (Antonchuk et al., 2001; 2002). Adapted TAT-HOXB4 fusion protein was introduced to the medium for inducing murine HSCs expansion (Krosl et al., 2003). Moreover, *ex vivo* expansion of HOXB4 overexpression in human CB-CD34⁺ cells was shown to improve proliferation but repopulation activity in NOD/SCID mice was less efficient as compared to murine HSCs (Buske et al., 2002; Schiedlmeier et al., 2003). Similarly, study on nonhuman primate CD34⁺ cells repopulating ability showed a dramatic effect on short-term repopulation ability (less than 7 weeks post-transplant). On the other hand, the repopulating cells were shown to less pronounce in long-term repopulation ability (Zhang et al., 2006b). Combining culture of HOXB4-transduced human CB-CD34⁺ cells with Delta-1 ligand-expressing OP9 cells had better expansion and fully lymphomyeloid repopulating capacity in NOD/SCID mice which cannot be observed with HOXB4 alone (Watts et al., 2010).

Another gene of HOX family, a nucleoporin 98-homeobox A10 fusion gene (NUP98-HOXA10 (NA10)) conferred a remarkable expansion of mouse long-term repopulating cells other than those observed by HOXB4 (Ohta et al., 2007). Of note, the 60 amino acid homeodomain portion in the HOXA10 domain (namely NUP98-HOXA10hd or NA10hd) was found to demonstrate that potent effect on HSC expansion. Furthermore, NA10hd transduced HSCs also maintained lymphomyeloid

repopulating capacity in murine (Ohta et al., 2007). Recently, comparative study on nonhuman primate model has shown that HOXB4 overexpression in monkey CD34⁺ cells contributed more to early hematopoiesis while in those of NA10hd overexpression contributed more to later hematopoiesis (Watts et al., 2011). Based on utilization of retroviral-transduced cells, the clinical setting should be of concern. Recently, new viral system, sendai virus, which shown transient expression of HOXB4 has been introduced for the development of *ex vivo* HSC expression to reduce the risk of leukemogenesis (Abe et al., 2011), however, safety in the clinic remains controversial.

2.5.3 Stromal cell-based culture

HSCs self-renewal is thought to be regulated by their surrounded microenvironment and nonhematopoietic cells that govern molecular signals. As a consequence, those signals may exert in orchestrate in control cell fate decision and proliferation of HSCs during the stress response. Co-cultivation of HSCs with cytokines combined with stromal cells has been an interest in the field of *ex vivo* expansion of HSCs. The most favorable utilization to date is MSCs that mimic the microenvironment in the bone marrow niche. CB-CD34⁺ cells showed a modest expansion in MSC-cocultivation with the improve engraftment in mice model (Jang et al., 2006; Mishima et al., 2010; Xie et al., 2006). Recently, improved co-culture of MSC with multiple cytokines combination (SCF, TPO, fibroblast growth factor-1, IGFBP2, and angiopoietin-like 5 (ANGPTL5)) increased net fold expansions of CB-CD34⁺ cells significantly and enhanced hematopoietic chimerism in a murine transplantation model (Walenda et al., 2011). Nonetheless, MSCs maintenance

requires robust manipulation such as culture medium that requires xeno-free cell culture conditions. MSCs isolation with pooled human platelet lysate instead of FCS is the best selective choice (Horn et al., 2010; Schallmoser et al., 2007); however, the increase risk in bacterial contamination should be of concern. Moreover, long-term culture may affect their stromal function.

2.6 Flt3-Ligand

2.6.1 Structure and expression pattern

Flt3-ligand (Flt3L) is a type I transmembrane protein that exists either in a transmembrane, a membrane-bound or a soluble form which is specific for class III receptor tyrosine kinases; Flt3 (Fms-related tyrosine kinase), also known as FLK-2 (fetal liver kinase 2). Flt3L is encoded by a single locus on chromosome 13 at q12 and contains 24 exons (Abu-Duhier et al., 2001; Agnes et al., 1994). Structurally, Flt3L contains an amino-terminal signaling peptide, four extracellular helical domains, spacer and tether regions, a transmembrane domain and a small cytoplasmic domain. Its structure is similar to M-CSF and SCF receptors c-fms and c-kit, respectively, which also included in the same type 1 transmembrane protein (Lyman and Jacobsen, 1998). Human Flt3L contains at least three isoforms; 1) full-length transmembrane isoform, 2) proteolytic cleavage of the first isoform that lacks the carboxyl end and consists mainly of the extracellular domains of the protein, and 3) an alternatively spliced exon 6 that creates a premature stop codon (Stirewalt and Radich, 2003). Flt3L expression is found in various tissues, including hematopoietic organs (spleen, thymus, peripheral blood and bone marrow) and the prostate, ovary, kidney, lung, colon, small intestine, testis, heart and placenta, with the highest level of expression in

peripheral blood mononuclear cells (Takahashi, 2011). Nonetheless, the Flt3L protein has been found only in stromal fibroblasts presented in the bone marrow microenvironment and T lymphocytes (Antonyamy and Thomson, 2000).

Flt3 expression is found mainly on primitive hematopoietic progenitors in the bone marrow, thymus and lymph nodes, but is also found in the placenta, brain and gonads (Naoe and Kiyoi, 2004). Flt3L can be proteolytically processed and released as a soluble protein, which both membrane-bound and soluble isoforms are biologically active (Lyman, 1995). Flt3L binding to the Flt3 stimulates the dimerization of the receptors, phosphorylation of the tyrosine-kinase domains and activating the receptor and downstream effectors that regulate the proliferation and differentiation of immature hematopoietic cells (Hannum et al., 1994; Stirewalt and Radich, 2003). The representative model of Flt3 binding to Flt3L and its activation is shown in Figure 2.6.

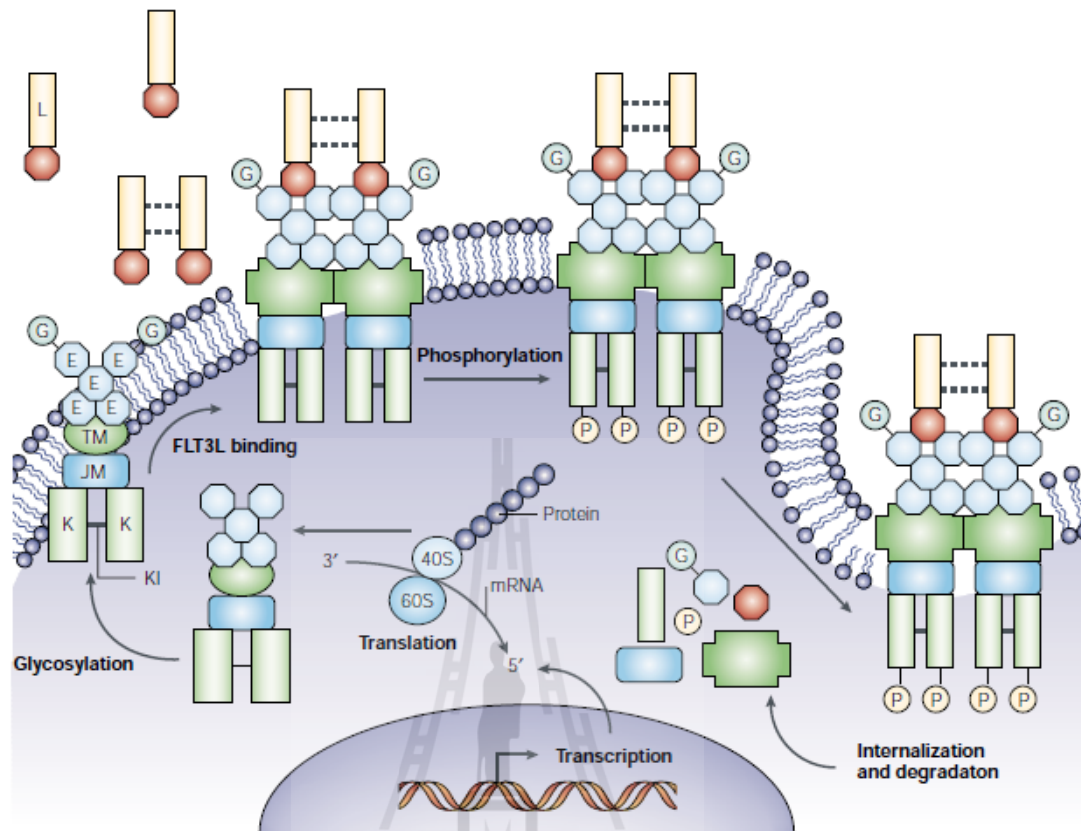


Figure 2.6 Structure and activation of Flt3. Transcription of the FMS-like tyrosine kinase 3 (Flt3) gene produces Flt3 mRNA, which is translated to Flt3 protein. Flt3 contains five extracellular immunoglobulin-like domains (E), a transmembrane domain (TM), a juxtamembrane domain (JM) and two tyrosine-kinase domains (K) that are linked through the tyrosine-kinase insert (KI). Cytoplasmic Flt3 undergoes glycosylation (G), which promotes localization of the receptor to the membrane. Wild-type Flt3 remains as a monomeric, inactivated protein on the cell surface until Flt3L (L), probably in a dimeric form, binds the receptor and induces receptor dimerization. Flt3 dimerization promotes phosphorylation (P) of the tyrosine-kinase domains, thereby activating the receptor and downstream effectors. The dimerized receptors are quickly internalized and degraded (Stirewalt and Radich, 2003).

2.6.2 Biological function

Flt3L alone does not effective enough for hematopoietic cells growth and functions. Despite using Flt3L only, combination of other cytokines and growth factors are used for pleiotropic effects on HSCs (as previously described) and precursors of myeloid and lymphoid lineages. For instance, Flt3L in combination with growth factors such as IL-3, G-CSF, M-SCF (CSF1), GM-CSF, EPO and KIT ligand produce synergistic effect for proliferative response (Rusten et al., 1996; Shah et al., 1996). Administration of Flt3L and G-SCF enhance the mobilization of bone marrow cells which improved the functional outcome after spinal cord injury in the rat (Urdzikova et al., 2011). Flt3L displays a role in lymphoid development where progenitor lymphocytes depend on Flt3 signaling. Besides the effect of Flt3L on the mobilization of HSCs and progenitor cells, Flt3L increases the number of dendritic cells in the circulatory system (Antonysamy and Thomson, 2000; Bertrand et al., 2000; McKenna et al., 2000). A combination of Flt3L and IL-7 promotes stromal-cell-independent growth of pro-B cells and the differentiation of pro-B cells to pre-B cells (Namikawa et al., 1996). Recently, *in vivo* study has been shown that haploinsufficiency of FL (FL(+/-)) reduces the numbers of lymphohematopoietic progenitors, common lymphoid progenitors, and pro-B cells in bone marrow suggesting that Flt3L level regulates the generation and survival of lymphoid progenitors and B-cell precursors (Dolence et al., 2011). *Ex vivo* expansion of plasmacytoid DCs and DCs from murine bone marrow or spleen could be performed by culture with recombinant Flt3L (Brawand et al., 2002; Gilliet et al., 2002; Naik et al., 2005). Moreover, recent observation has shown the mechanism of Flt3 signaling in regulation of DC. The results show that DC progenitor survival and DC

development requires prostaglandin E(2) signaling through EP1/EP3 receptors that regulate Flt3 expression, downstream signal transducers and activators of transcription 3 (STAT3) activation and Survivin expression (Singh et al., 2012).

2.7 Interleukin-6

2.7.1 Structure and expression pattern

IL-6 belongs to the family of IL-6 cytokines which also includes IL-11, leukemia inhibitory factor, oncostatin M, ciliary inhibitory factor, cardiotropin-1, cardiotrophin-like related cytokine and stimulating neurotrophin-1/B-cell stimulating factor 3, neuropoietin, IL-27, and IL-31 (Scheller et al., 2011). IL-6 is a glycosylated protein of 21–28 kDa and comprises the helix bundle structure characteristic for all IL-6-type cytokines (Heinrich et al., 2003). Typically, the four long α -helices (A, B, C, D) arrange in an up-up-down-down topology. Three distinct receptor-binding sites of IL-6 have been identified. Site 1 is structurally mediated by the formation of the C-terminal residues of helix D and the C-terminal part of the AB-loop that determines the specificity of IL-6R binding. Site 2 has gp130 residue contact located in between helices A and C. Site 3 comprises of two residues; one located at N-terminal part of the AB-loop and another located at the C-terminal residues of the D-helix (Ig-like domain of gp130). The representative picture of IL-6 structure is shown in Figure 2.7. All except IL-31 contain the common membrane glycoprotein gp130 as a receptor and signal transducer subunit (Heinrich et al., 2003). Signal transduction initially starts from the binding of IL-6 to the membrane bound α receptors IL-6 receptor (IL-6R; type I transmembrane glycoprotein). Subsequently, IL-6/IL-6R complex binds to two molecules of gp130, leading to gp130-homodimer formation and signal initiation via

JAK/STAT, ERK, and phosphatidylinositol 3-kinase (PI3K) signal transduction pathways (Scheller et al., 2011). The resulting signals not only effect proliferation of HSCs but also control immune system and communications among cells including epithelial cells, neutrophils, macrophages and T cells (Fielding et al., 2008; Hou et al., 2008; Hurst et al., 2001; Jones et al., 2005). IL-6 is produced by T cells, B cells, monocytes, fibroblasts, keratinocytes, endothelial cells, and mesengial cells (Ghazizadeh, 2007). Typically, large amount of IL-6 is produced by adipose tissue *in vivo* and may be mediate in fat metabolism (Mohamed-Ali et al., 1997). Besides the adipocytes that secretes IL-6 (Fried et al., 1998), other cells such as primarily nonfat cells in the adipose tissue are capable of IL-6 production (Fain, 2010; Fain et al., 2004; Weisberg et al., 2003).

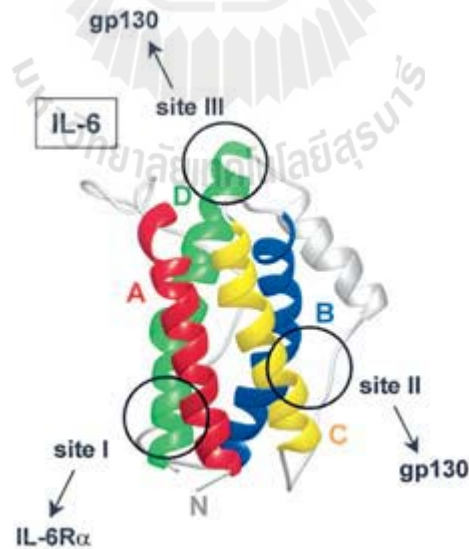


Figure 2.7 Structure of IL-6 containing the four long helices A, B, C and D. Receptor-binding sites I, II and III of IL-6 are indicated by circles (Heinrich et al., 2003).

2.7.2 Biological function

IL-6 is pleiotropic cytokines that function in inflammation, hematopoiesis, immune responses, cardiovascular action, and neuronal survival (Heinrich et al., 2003). The major role of IL-6 in the inflammation is the synthesis of acute phase proteins such as C-reactive protein. Another role is the regulation of T cell differentiation and activation (Weinhold et al., 1997; Weinhold and Ruther, 1997). T helper 2 (Th2) cell cytokine production in CD4⁺ T lymphocytes is activated by IL-6 through the transcription factor C/EBP (Rincon et al., 1997). The balance between IL-17-producing Th17 cells and regulatory T cells (Treg) is also regulated by IL-6 (Kimura and Kishimoto, 2010). Specifically, IL-6 and TGF- β induce the development of Th17 cells from naive T cells. On the other hand, IL-6 inhibits differentiation of TGF- β -induced Treg. Some evidences also suggested the correlation of IL-6 inflammatory response in obese humans by showed that human adipose tissue in obesity contains the elevation of IL-6 in circulation (Fain, 2010; Khaodhiar et al., 2004; Madani et al., 2009). In addition, IL-6 is mediated in wound healing. Proinflammatory cytokines (IL-6, IL-1 α , IL-1 β and TNF- α) response in the wound repair were found to strongly up-regulated during the inflammatory phase (Grellner 2002; Grellner et al., 2000; Hubner et al., 1996). The major targets of these cytokines were macrophages, fibroblasts and lymphocytes. Moreover, during the proliferative phase, fibroblasts produced keratinocyte growth factor (KGF)-1, KGF-2, and IL-6, which simulated keratinocytes nearby migrated into the wound site, proliferated, and differentiated in the epidermis (Smola et al., 1993; Xia et al., 1999). Gallucci and colleague showed that IL-6-deficient transgenic mice displayed prolong wound healing compared to wild-type control (Gallucci et al., 2000). More multiple effects

were observed which were delayed re-epithelialization, greatly decreased granulation tissue, inhibited neovascularization and delayed wound closure (Gallucci et al., 2001; Lin et al., 2003).

Additionally, IL-6 has been implicated its role in bone metabolism and aging (Hashizume et al., 2008; Maggio et al., 2006). Epidemiology studies have been shown to clarify the relationship among risk factors for elevated markers of inflammation in older adults. The data has demonstrated that IL-6 is the robustly predicted disease, disability and mortality in old age (Singh and Newman, 2011; S. Zhu et al., 2009). This data also suggests that IL-6 may be a common cause of multiple age-related diseases or a final common pathway, thereby resulting in the reducing disability in older adults. RANK ligand (RANKL) is an essential factor for osteoclastogenesis. RANKL binding to its signaling receptor (RANK) stimulates differentiation of myeloid precursor cells into osteoclasts. In particular, IL-6 and sIL-6R complex induces RANKL expression via the JAK/STAT signaling pathway (Hashizume et al., 2008). Thus, IL-6 functions in trans-signaling to regulate the bone homeostasis.

2.8 Stem cell factor

2.8.1 Structure and expression pattern

Stem Cell Factor (SCF; also known as Kit ligand, mast cell growth factor, or steel factor) is the ligand of c-kit which is encoded by the *Steel (Sl)* locus on chromosome 12 in humans and chromosome 10 in mice (Besmer, 1991; Geissler et al., 1991). Alternative splicing of exon 6 of the mRNA results in two isoforms. The first isoform contains 248 amino acids translation product containing proteolytic cleavage site and post-translational processing at this site results in the soluble form

of SCF comprising 165 amino acid residues. While, the second form comprises of 220 amino acid that lacks the proteolytic cleavage site, thereby remaining in the membrane-bound form (Ray et al., 2008). SCF binds to c-kit that is a type III tyrosine kinase receptor. Subsequently, two c-kit receptors homodimerize and are phosphorylated by selective tyrosine residues 719 of c-kit by p85 regulatory subunit of PI3K. The resulting effect is the unmasked docking sites for the Src-homology2 (SH2)-containing signal transducers (Blume-Jensen et al., 1998).

SCF is expressed during the development of embryo and primordial germ cells (De Felici and Pesce, 1994), in the sources where hematopoietic system is developed including the yolk sac, fetal liver, bone marrow (Kallianpur et al., 1994), melanocytes (Wehrle-Haller, 2003; Wehrle-Haller and Weston, 1995), oocytes (Manova et al., 1993), testis (Ballow et al., 2006), retina (Blackshaw et al., 2004), stromal cells, thymic stroma, fibroblasts and endothelial cells (Heinrich et al., 1993). Moreover, the c-kit is expressed by approximately 70% of CD34⁺ cells in bone marrow including more committed progenitor cells (Papayannopoulou et al., 1991), in neurons and neural stem cells/neural progenitor cells of adult brain (Zhao et al., 2007).

2.8.2 Biological function

The SCF/c-kit signaling has been reported as an important survival factor for many progenitor cell types including primordial germ cells (Guerif et al., 2002; Yan et al., 2000), HSCs (Engstrom et al., 2003), NSCs (Erlandsson et al., 2004), melanocyte precursors (Ito et al., 1999), and ESCs (Bashamboo et al., 2006). The main mechanism that promotes survival of these cell types is the suppression of apoptosis. Neuronal lineage commitment from NSCs has been shown by the use of

combination of SCF and G-CSF, suggesting the role of SCF in neurogenesis (Piao et al., 2012). In the normal stage, the brain produces high amount of SCF (Huang et al., 1992). However, when the injury occurs, the membrane-bound SCF is enhanced. The latter form of ligand recruits NSCs to the injury site and stimulates c-kit expression on stem cells for further healing process (Sun et al., 2004). Besides the proliferation effect on HSCs, SCF has been shown to control the regulatory effect of TGF- β , thereby promoting proliferation of prostate cells from the proximal and distal regions of prostatic ducts where stem cell niche exists (Salm et al., 2011). As mentioned earlier that Flt3L and IL-7 mediate in the T cell development, another possible thymopoietic agent is SCF. Specifically, SCF/c-kit signaling is essential in early T cell differentiation into the T cell lineage and thymic niche availability (Fewkes et al., 2010; Massa et al., 2006; Rodewald et al., 1995).

2.9 Thrombopoietin

2.9.1 Structure and expression pattern

Thrombopoietin (TPO) is also known as megapoietin, MGDF, and c-mpl ligand. Human TPO gene is located on chromosome 3q26.33-q27 (Foster et al., 1994; Sohma et al., 1994) and is approximately 8 kb long containing 7 exons (Chang et al., 1995). TPO is originally translated from TPO gene into 353 amino acids precursor (35 kDa). Processing by cleavage of the 21 amino acid signal peptide and glycosylation results in 332 amino acids with 60-70 kDa glycoprotein that contains an amino-terminal receptor-binding domain (residues 1-153) and a carboxyl-terminal carbohydrate-rich domain (residues 154-332). Both domains are separated by the arginine residues in positions 153 and 154 (Bartley et al., 1994; de Sauvage et al.,

1994). TPO is a member of the four-helix bundle family of cytokines, which also contains erythropoietin, G-CSF, growth hormone and leukemia inhibitory factor among others. TPO mRNA is expressed widely in several tissues including liver, kidney, brain, skeletal muscle and intestine. The main site for TPO synthesis is found in the liver, particularly hepatocytes (Ogami, 1996; Sungaran et al., 1997).

TPO receptor is a member of the class I hematopoietic growth factor receptor superfamily, a group of integral membrane proteins. By cDNA sequencing, the TPO receptor can be differentiated into three forms which are c-Mpl-P, c-Mpl-K and c-Mpl-S (Kiladjian et al., 1997; Vigon et al., 1992). Of note, c-Mpl-P is the only demonstrating functional receptor. The alternative splicing confers the difference in intracellular domains of those isoforms. TPO mRNA is expressed mainly on HSCs, with a lesser extent on megakaryocytic progenitors, megakaryocytes and platelets (Debili et al., 1995). Various tissues that express c-Mpl are mediated in hematopoiesis, including bone marrow, spleen, and fetal liver (Chou and Mulloy, 2011). By crystallographic EPO receptor study and based on the its analogy to the TPO receptor have led to postulation that TPO initiates the signal transduction by binding to the c-Mpl at the distal part, which in turn a homodimer of c-Mpl becomes active (Livnah et al., 1999). Consequently, JAK2 can phosphorylate tyrosine residues within the receptor itself and phosphorylate c-Mpl on at least Tyr625 and Tyr630 (Drachman and Kaushansky, 1997; Figure 2.8), thereby stimulating the down-stream cascade STATs, PI3K, the mitogen-activated protein kinases (MAPKs), and extracellular signal regulated kinases-1 and -2 (Tortolani et al., 1995; Witthuhn et al., 1993).

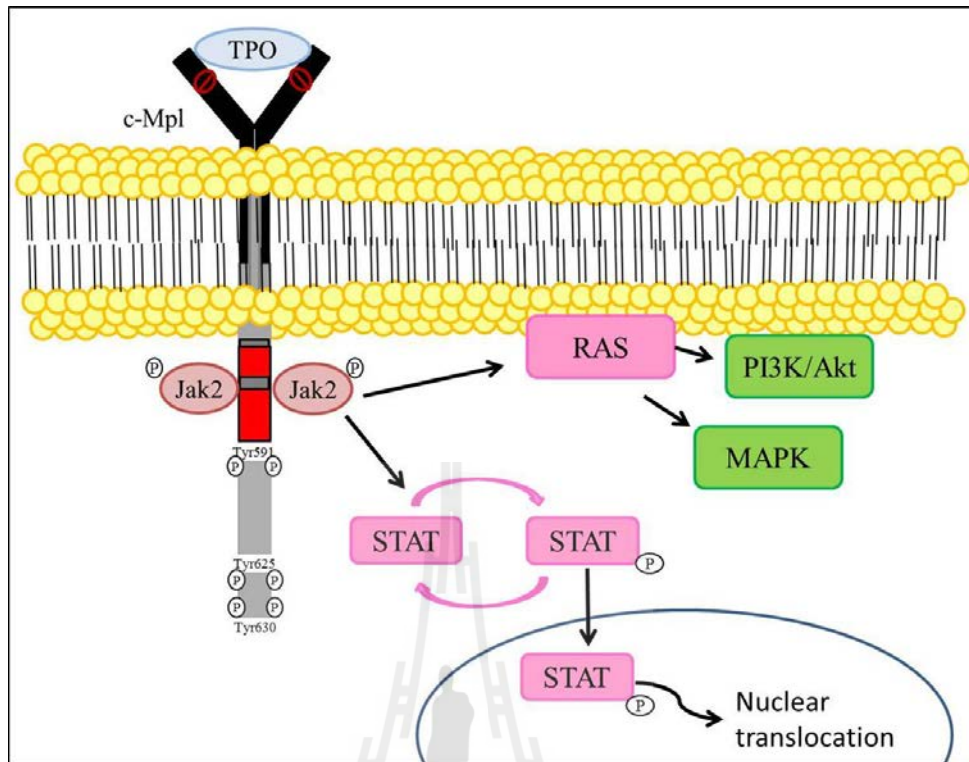


Figure 2.8 TPO/c-Mpl signaling pathway (modified from Chou and Mulloy, and Geddis (Chou and Mulloy, 2011; Geddis, 2010)).

2.9.2 Biological function

TPO plays a role in megakaryopoiesis. Typically, mice genetically modified lacking of TPO conferred an approximately 85% reduction in circulating platelets and markedly decreased the number of bone marrow megakaryocyte (Carver-Moore et al., 1996; Gurney et al., 1994). TPO stimulates the megakaryocytic colony-forming units (CFU-Meg) and more mature megakaryocytes development such as the number size and ploidy of megakaryocytes (Broudy et al., 1995; Wendling et al., 1994). TPO induces PI3K phosphorylates and activates the serine/threonine kinase Akt (Geddis et al., 2001). TPO-induced cell cycle progression of primary megakaryocyte progenitors is mediated by PI3K/Akt pathway (Chanprasert et al., 2006). Moreover, p27^{Kip1}

expression is shown to be regulated by PI3K/Akt/FOXO3a pathway, suggesting that PI3K/Akt/FOXO3a/p27^{Kip1} pathway contributes to normal TPO-induced megakaryocyte proliferation (Nakao et al., 2008). One downstream target of PI3K/Akt, mammalian target of rapamycin (mTOR) controls proliferation and maturation of megakaryocytic progenitors via 2 effector proteins, p70S6K1 and 4E-BP1 (Guerriero et al., 2006; Raslova et al., 2006). Recent data has shown that neonatal megakaryocyte progenitors, which are hyperproliferative, contain up-regulation of TPO signaling through mTOR during the development to mature megakaryocytes (Liu et al., 2011). This study suggests that TPO signaling has the role in rapidly repopulate of megakaryocyte progenitors from bone marrow in neonatal. Furthermore, HSC maintenance mediating TPO/c-Mpl signaling was demonstrated by overexpression of Bcl2 (anti-apoptotic molecule) in $MPL^{-/-}$ mice which resulted in a failure to rescue $Lin^{-}Sca^{+}Kit^{+}CD34^{-}Flt3^{-}$ cells (Qian et al., 2007). Several investigators has also been studies the regulation, expansion and maintenance of quiescent HSC by TPO (Bryder and Jacobsen, 2000; Buza-Vidas et al., 2006; Ema et al., 2000; Fox et al., 2002; Hiroki Yoshihara et al., 2007a).

2.10 Wnt1

2.10.1 Structure and expression pattern

The human Wnt gene family comprises of 19 members that encode cysteine-rich glycoproteins of 45 kDa and express distinctively in mammal during embryogenesis and adulthood. After glycosylation, they are transported to the cell membrane and bind to the cell surface or the extracellular matrix through heparin-like binding sites (Katoh, 2002; Lo Muzio, 2001). Wnt1 is encoded by human

chromosome 12q13 as well as Wnt10B (Katoh, 2002). Wnt1 signal is transduced to the canonical pathway via the Frizzled (FZD) family receptors and LRP5/LRP6 co-receptor as shown in Figure 2.9 (Bhanot et al., 1996; Katoh, 2007; Pinson et al., 2000). Specifically, Dishevelled (DVL) is phosphorylated by casein kinase I ϵ (CKI ϵ), which then binds typically to FRAT and confers the assembly between FZD to DVL (FZD-DVL complex) and LRP5/6 to AXIN and FRAT (LRP5/6-AXIN-FRAT complex) (Tolwinski et al., 2003; Wong et al., 2003). After that, β -catenin is protected and released from phosphorylation by CKI α and GSK3 β . Then, β -catenin forms the complex with TCF/LEF family transcription factors and also with Legless family docking proteins (BCL9 and BCL9L) associated with PYGO family co-activators for stabilization and nuclear accumulation (Katoh, 2003; Kramps et al., 2002). Typically, the down-stream effectors for transcriptional activation target genes are *FGF20*, *DKK1*, *WISP1*, *MYC* and *CCND1* (Chamorro et al., 2005; He et al., 1998; Pennica et al., 1998; Tetsu and McCormick, 1999). On the other hand, if the canonical Wnt signaling is absent, phosphorylation to β -catenin by CKI α and GSK3 β in the NH₂-terminal degradation box occurs and results in forming of the β -catenin-APC-AXIN complex that is polyubiquitinated by β TRCP1 or β TRCP2 complex for the degradation by proteasome (Price, 2006).

2.10.2 Biological function

Wnt1 plays a role in regulation of cell fate and patterning during embryogenesis. Wnt1 is expressed in the dorsolateral region of the neural tube that gives rise to cranial neural crest (CNC). The expression of Wnt1 is restricted to the midbrain which is essential for the midbrain patterning during the development of

embryo (McMahon et al., 1992). Mice lacking Wnt1 and Wnt3a genes conferred a marked deficiency in CNC derivatives that originated from the dorsal neural tube (Ikeya et al., 1997). Besides the functional role in stimulating proliferation of embryonic neural crest (NC) progenitors by Wnt1, it has been shown that BMP2 and Wnt1 enrich the NC progenitors from adult bone marrow cells that normally NC progenitors persist in a few number during adulthood (Glejzer et al., 2011). Additional data also showed that satellite cells which are mediated in muscle regeneration could be induced to proliferate by overexpressed Wnt1, Wnt3a or Wnt5a protein (Otto et al., 2008). Furthermore, the marked increase in mouse ESCs proliferation by BMP-4 was found to be mediated by Wnt1/ β -catenin, Smad and PI3K/Akt signaling (Lee et al., 2009). Another role of Wnt1 as a proangiogenic molecule has been shown by injection of human endothelial progenitor cells expressing Wnt1 in murine ischemic hindlimbs can enhance blood flow and capillary density to the ischemic tissues (Gherghe et al., 2011). Moreover, the expression of Wnt1 has been implicated in pathogenesis of different tumors. Overexpression of Wnt1 is associated with pathogenesis and progression in non-small cell lung cancer and mammary phyllodes tumors (Huang et al., 2008; Karim et al., 2009). When using anti-Wnt1 siRNA transduced into tumor cell lines from sarcomas, colon cancer, and breast cancers that expressed Wnt1 could induce tumor cell apoptosis effectively (He et al., 2004; 2005; Mikami et al., 2005).

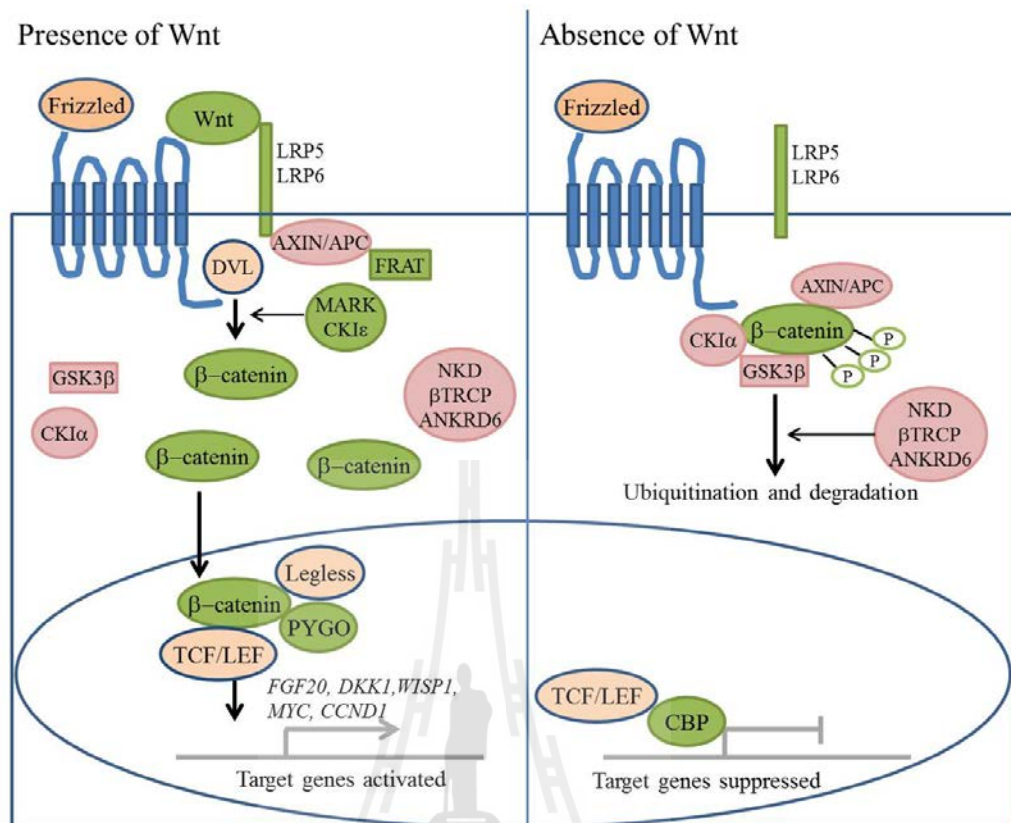


Figure 2.9 A canonical Wnt signaling pathway. In the presence of Wnt, the signals are transduced through Frizzled family receptors and LRP5/LRP6 coreceptor to the β -catenin signaling cascade which then stabilize hypophosphorylated β -catenin and interact with TCF/LEF, Legless and PYGO for target gene activations. MARK and CK1 ϵ are the positive regulators of canonical Wnt pathway, while APC, AXIN1, AXIN2, CK1 α , NKD1, NKD2, β TRCP1, β TRCP2 and ANKRD6 are negative regulators. In the absence of Wnt, β -catenin forming complex with AXIN and APC is phosphorylates, leading to be a target for ubiquitination and degradation by proteasome (adapted from Katoh (Katoh, 2007)).

2.11 Wound healing in diabetes mellitus by stem cells

Diabetes, a chronic and progressive disease, has increasingly affected people worldwide during the last three decades (Danaei et al., 2011). The prevalence of diabetes in Thai adults (≥ 20 years) was 7.5% as reported by the multistage cross-sectional National Health Examination Survey (NHES) IV in 2009 (Aekplakorn et al., 2011). Nonhealing foot ulceration is affecting diabetes patients which lead to high mortality rate (Boyko et al., 1996; Iversen et al., 2009; Junrungsee et al., 2011). More specifically, Sriwijitkamol and coworkers showed that the diabetic foot occurred 40% in Thai patients with type 2 diabetes. (Sriwijitkamol et al., 2011). Normal wound healing is a dynamic process mediated by three phases; inflammation, tissue formation (epithelialization), and tissue remodeling (granulation tissue formation) that overlap in time (Singer and Clark, 1999). Directly after wounding, the coagulation process is activated and forming a fibrin clot that prevent the blood loss from the wound. Subsequently, the inflammatory phase performing by recruitment of neutrophils and macrophages to the site of injury (Broughton et al., 2006). As a circumstance, these cells release several mediators and cytokines to promote epithelial cells and fibroblasts migration from the surrounding tissue and proliferation within the wound area which in turn produce extracellular matrix components (Ehrlich and Krummel, 1996; Smola et al., 1993; Xia et al., 1999). Finally, the maturation and remodeling are mainly compose of keratinocytes migration over the matrix to close the wound with collagen synthesis and deposition, and fibroblasts differentiation into myofibroblasts to increase the contractility (Broughton et al., 2006).

Wound healing in diabetes is thought to be impaired by several factors; deregulatory in pro-inflammatory cytokine interaction and production by immune and

non-immune cells, dysfunction of leukocytes, impaired neovascularization, neuropathy and peripheral vascular disease (Pradhan et al., 2009). In particular, abnormality in cytokine production and recruitment by local inflammatory cells including reduced angiogenesis are believed to be crucial in impaired wound healing. Thus, advance methodologies are required for the treatment or accelerate wound repair in diabetic patients.

Peripheral blood-CD34⁺ cells were shown to accelerate neovascularization and healing in diabetic wounds (Sivan-Loukianova et al., 2003). However, it has been shown that circulating CD34⁺ cell from diabetic patients had impaired vasculature potential (Caballero et al., 2007). Murine bone marrow stem cell population, Sca-1⁺c-kit⁺Lin^{neg/low}CD34⁻ and purified based on its ability to efflux Hoechst dye (side population), was found to improve wound healing in diabetic mice (Chan et al., 2007). In addition, human fetal aorta-derived CD133⁺ was found to promote diabetic ischemic ulcers, which suggested the potential use of fetus-derived cells, however, the future therapy in clinics may be difficult to obtain (Barcelos et al., 2009). Furthermore, improvement in wound healing has been developed by the combined use of CB-CD34⁺ cells and CD34⁺-derived endothelial cells encapsulated in a fibrin gel (Pedroso et al., 2011). Recent studies have shown that human CB- and rat adipose-tissue-derived MSCs were also shown to promote wound healing in diabetic mice and rat, respectively. (Maharlooei et al., 2011; Tark et al., 2010). CB-derived cells seem to be more useful than adipose tissue due to the aging and disease related isolation. Other evidence showed that mouse ESCs was also found to enhance wound healing in diabetic rates (K.B. Lee et al., 2011a), yet, ethical concern remains.

CHAPTER III

MATERIALS AND METHODS

3.1 Materials and Methods

3.1.1 Human cord blood collection and separation

Umbilical cord blood (UCB) samples were collected from normal full term cesarean section in the Department of Obstetrics and Gynecology at Por-Pat hospital, St. Mary Hospital, and Fort Suranari Hospital, Nakhon Ratchasima, Thailand (n = 45). Written inform of consent was obtained from the mother according to the approval of Institute of Research and Development of Suranaree University of Technology, Suranaree University of Technology, Nakhon Ratchasima, Thailand.

After removal of the newborn from the operative field, the free end of the cord was clamped and cord blood was collected. The UCB units were stored at room temperature until delivered to the laboratory and processing.

3.1.2 CD34⁺ cell purification

Total cord blood was centrifuged at 2,003 x g for 10 minutes at 25°C to separate plasma from whole blood. Mononuclear cells (MNCs) were isolated by density gradient centrifugation using Ficoll-Paque PREMIUM (1.077 g/ml; GE Healthcare, Sweden). Diluted packed RBCs were over layered on the Ficoll-Paque (dilution 1:1) and centrifuged at 400 x g for 30 minutes at 25°C. MNCs layer was collected and

washed twice with washing buffer (PBS pH 7.4, 0.1% BSA, 2 mM EDTA) by centrifugation at 235 x g for 5 minutes each at 25°C. Total number of MNCs was stained with trypan blue and counted by hemacytometer. Before performing CD34 positive cell selection, MNCs (1.5×10^5 cells) were subjected for CD34⁺ cells determination by flow cytometry analysis as describe below. After that, CD34⁺ cells were purified with Dynal CD34 Progenitor Cell Selection System (Invitrogen Dynal AS, Norway) from MNCs. Dynabeads CD34 (4×10^7 in 100 μ l/1 ml MNCs) were used for the CD34⁺ cells separation by incubation with MNCs for 30 minutes at 4°C. Rosetted cells were separated from other MNCs by placing the tube into a magnet for 2 minutes and discarded the supernatant. The rosette cells were washed four times with washing buffer (8 ml) by placing the tube into a magnet for 2 minutes each. After that, the beads were detached from the CD34⁺ cells with DETACHaBEAD CD34 (100 μ l/1 ml total volume of MNCs starter). The mixture was incubated for 45 minutes at room temperature. Enhancement the detached beads from the cells by adding 2 ml washing buffer. Isolated CD34⁺ cells were collected after placing the tube into the magnet for 2 minutes. After that, the residual cells were obtained by washing four times with washing buffer (2 ml) and placed the tube into the magnet for 2 minutes each. Isolated cells were then pooled together. All collected cells were washed thoroughly twice in 10 ml washing buffer and centrifuged at 400 x g for 5 minutes each. Finally, the isolated cells were suspended in 100 μ l washing buffer and subjected to cell count by trypan blue dye exclusion. To identify the purity and percentage of CD34⁺ cells recovery, isolated CD34⁺ cells were subjected for flow cytometry analysis. The percentage recovery of selected CD34⁺ cells was calculated as the following equation as previously described (Imai et al., 2005).

$$\text{Recovery (\%)} = \frac{\text{total number of CD34}^+ \text{ cells after selection}}{\text{total number of CD34}^+ \text{ cells before selection}} \times 100$$

3.1.3 Expansion of enriched CD34⁺ cells *in vitro*

3.1.3.1 Cytokines

Cytokines used in the *ex vivo* expansion were Flt3-Ligand (Flt3L), interleukin-6 (IL-6), thrombopoietin (TPO), and Wnt1 (PeproTech, Rocky Hill, NJ, USA).

3.1.3.2 *Ex vivo* expansion

On day 0, enriched CD34⁺ cells from cord blood were seeded at a concentration of 1×10^5 cells/ml in a flat-bottomed 24-well plate in Iscove's Modified Dulbecco's Medium (IMDM; Invitrogen, USA) supplemented with 10% fetal bovine serum (FBS; Hyclone, USA) or 10% knockout serum replacement (KSR; Invitrogen, USA), 4 µg/ml amphotericin B, 200 U/mL penicillin and 200 µg/ml streptomycin (Sigma, USA). The cultures will be incubated at 37°C in a humidified atmosphere of 5% O₂, 5% CO₂ for 7 days. At initiation and every 48 h thereafter, cultures were supplemented with different combinations of recombinant human cytokines and growth factors as follow:

a. Flt3-L (100 ng/ml), IL-6 (100 ng/ml), SCF (100 ng/ml), and TPO (10 ng/ml) in 10% FBS (designated as 4F cIMDM)

b. Flt3-L (100 ng/ml), IL-6 (100 ng/ml), SCF (100 ng/ml), TPO (10 ng/ml), and Wnt1 (20 ng/ml) in 10% FBS (designated as 4FW cIMDM)

c. Flt3-L (100 ng/ml), IL-6 (100 ng/ml), SCF (100 ng/ml), and TPO (10 ng/ml) in 10% KSR (designated as 4F KSR)

d. Flt3-L (100 ng/ml), IL-6 (100 ng/ml), SCF (100 ng/ml), TPO (10 ng/ml), and Wnt1 (20 ng/ml) in 10% KSR (designated as 4FW KSR)

e. Cocktail P0 (confidential) designated as P0

f. Cocktail P1 (confidential) designated as P1

g. Cocktail P2 (confidential) designated as P2

h. Cocktail P3 (confidential) designated as P3

i. Cocktail P4 (confidential) designated as P4

By the third and fifth day, all cultures were demipopulated by removal of one half the culture volumes, which were replaced by fresh medium and growth factors. The total number of amplified cells and viable cell staining with trypan blue were determined every two days by counting in triplicate with in the single expansion assay. On day 5 and day 7, some cells were harvested to determine flow cytometry analysis. On day 7, cells were subjected for colony forming cell assay, liquid differentiation, and pluripotency genes expression. Each culture was performed in three independent CB samples. Fold increase in expansion of total amplified cells was calculated by dividing total number of viable cells at indicated time point by number of isolated CD34⁺ cells in starting culture.

3.1.4 Liquid differentiation assay

3.1.4.1 Feeder cell preparation for lymphoid differentiation

Mouse stromal (OP9) cell line was cultured in α -MEM (Invitrogen, USA) supplemented with 10% FBS, 2 μ g/ml amphotericin B, 100 U/ml penicillin and

100 µg/ml streptomycin. The OP9 cells were plated to subject 90% confluent by growing at 37°C in a humidified atmosphere of 5% O₂ and 5% CO₂ overnight.

3.1.4.2 *In vitro* liquid differentiation

Five-days expanded cells (1.5×10^5 cells/well) were determined the capability of primitive HSPCs to differentiate into each cell lineages. Five different groups containing different human recombinant cytokine factors (PeproTech, USA) were performed to study the differentiation and proliferation of cells as follow:

- a. Erythrocytes; EPO (20 ng/ml) + SCF (100 ng/ml)
- b. Megakaryocytes; TPO (100 ng/ml) + SCF (100 ng/ml)
- c. Mast cells + granulocytes; IL-3 (30 ng/ml) + SCF (100 ng/ml)
- d. Granulocytes + macrophages; GM-CSF (20 ng/ml) + SCF (100 ng/ml)
- e. Lymphocytes; Flt3-L (100 ng/ml) + SCF (100 ng/ml) + IL-7 (50 ng/ml)

Additionally, the culture of lymphocytes was co-cultured with confluent OP9 cells. All cultures were cultured in IMDM, 10% FBS, 4 µg/ml amphotericin B, 200 U/mL penicillin and 200 µg/ml streptomycin incubated at 37°C in a humidified, 5% O₂ and 5% CO₂ for 14-28 days. Differentiated cells were then subjected for cytopspin (1.5×10^5 cells/well; Centurion Scientific, UK) onto slides at 800 rpm for 5 minutes and stained with Wright-Giemsa staining. Slides were mounted with aqueous mounting solution (Merck, Germany). Image analysis was visualized by microscope (Olympus BX51; Olympus Corporation, Japan) and captured by a digital CCD camera (Olympus DP72, Olympus Corporation, Japan).

3.1.5 Colony forming cell assay

For colony forming cell assay, 2×10^3 expanded cells were collected from day 5-expanded CD34⁺ cells and washed with PBS by centrifugation at $235 \times g$ for 5 minutes at 4°C. Cells were resuspended with 100 µl of IMDM with 2% FBS and grown in 1 ml of methylcellulose H4434 (Stem Cell Technologies, Canada) which contained rhSCF, rhGM-CSF, rhIL-3, and rhEPO. The mixtures were plated onto 35 mm suspension culture dish (Corning, USA). There were duplicated plates from each sample. Then, the plates were incubated at 37°C in a humidified containing 5% O₂ and 5% CO₂. The resulting Colony-Forming Unit-Granulocyte, Erythroid, Macrophage, and Megakaryocyte (CFU-GEMM), CFU-Granulocyte and Macrophage (CFU-GM) and Burst-Forming Unit-Erythroid (BFU-E) colonies were scored on day 14 according to their morphologies (Pereira et al., 2007) under inverted microscope (CKX41, Olympus, Japan). CFU-GEMM comprises a multi-potential progenitor that produces a colony containing a highly a large dense with an indistinct border between the core and the peripheral cells. Erythroblast clusters can be visible along the periphery of the CFU-GEMM colony. Monocytic and granulocytic cells are easily identifiable and clusters of large megakaryocytic cells are usually seen. BFU-E colonies were identified as a colony containing erythroid clusters and a minimum of 30 cells (red). Each individual cluster contains a group of cells that are tiny, irregular in shape, and difficult to distinguish. CFU-GM produces a colony containing at least 30 granulocyte cells (CFU-G), macrophages (CFU-M), or cells of both lineages (CFU-GM). The monocytic lineage cells are large cells with an oval to round shape and appear to have a grainy or grey center. The granulocytic lineage cells are round, bright and are much smaller and more uniform in size than macrophage cells (Pereira

et al., 2007). The experiments were performed from three different cord blood samples for each cytokine cocktail.

3.1.6 Flow cytometry analysis

Day 5 and day 7 expanded cells were obtained from each culture to characterize the stemness and differentiation state of expanded cells. The cells were collected and washed with PBS two times at 235 x g for 5 minutes each before subjected to immunofluorescent staining. There were three reaction tubes per each sample (1.5×10^5 cells/tube) as follow:

a. mouse anti-human CD34-PE (5 μ l; BD biosciences, USA), CD133-APC (5 μ l; MACS, Miltenyi Biotec GmbH, Germany) and CD38-FITC monoclonal antibodies (3 μ l; BD biosciences, USA) were used to identify hematopoietic stem and progenitor cells.

b. mouse anti-human CD33-PE (5 μ l; BD biosciences, USA) and CD71-FITC monoclonal antibodies (5 μ l; BD biosciences, USA) were used to identify myeloid and erythroid lineages.

c. mouse anti-human CD3-FITC (5 μ l; BD biosciences, USA) and CD19-PE monoclonal antibodies (5 μ l; BD biosciences, USA) monoclonal antibodies (mAbs) were performed to identify lymphoid lineages.

The reactions were incubated at 4°C for 30 minutes in the dark. Then, the cells were washed with PBS twice by centrifugation at 235 x g for 5 minutes each at 4°C and fixed with 300 μ l of 4% paraformaldehyde. Next, the cells were analyzed by flow cytometer (FACSCalibur, Becton Dickinson, USA) using CellQuest Pro Software

version 5.2.1. As a control, fresh isolated CD34⁺ cells were stained at identical cell concentrations. As a negative cell control, the experiment was done in parallel without the addition of antibody. The experiments were performed on three different cord blood samples for each cytokine cocktail. The analysis of proportion of CD34⁺ cells in MNCs was prepared, stained with mouse anti-human CD34-PE (5 µl) and performed similarly to the method as described above.

Total number of each subpopulation at indicated time point was calculated as the following equation.

$$\text{Total number of subpopulation} = A \times B \times C$$

A: Total cell at the starting culture

B: The percentage of positive cells in each subpopulation

C: The fold expansion of amplified cells

Fold expansion of each subpopulation was calculated as the equation below.

$$\text{Fold expansion} = \frac{\text{total cell number in each population}}{\text{the number of subpopulation at starting culture}}$$

3.1.7 Gene expression by reverse transcription-polymerase chain reaction (RT-PCR)

3.1.7.1 Total RNA extraction

Total RNA from each sample was extracted by Total RNA Purification Mini Kit (Geneaid, Taiwan). Cells were collected on day 5 of the culture. Cell pellets were collected by centrifugation at 6,000 x g for 20 seconds. Then, cells were resuspended in 100 µl of PBS. RB buffer (400 µL) and β-mercaptoethanol (4 µL)

were added to the suspension and incubated for 5 minutes at room temperature. The sample lysate was added with 500 μ L of 70% ethanol and transferred into RB column. The residual was removed by centrifugation at 14,000 x g for 1 minute. W1 Buffer (500 μ L) was added into the RB column and washed by centrifugation at 14,000 x g for 30 seconds. Wash Buffer (600 μ L) was added into the RB column twice at 14,000 x g for 30 seconds, followed by centrifugation at 14,000 x g for 3 minutes to dry the column. The dried column was applied to the 1.5 ml microcentrifuge tube and RNase-free water (30 μ L) was added into the column matrix. The column was incubated for 5 minutes at room temperature and then centrifuged at 14,000 x g for 1 minute to elute the purified RNA. Total RNA was finally measured the concentration by Nanodrop ND-1000 spectrophotometer (Thermo Fisher Scientific Inc., USA).

3.1.7.2 Primers

Two set of primers (human Oct3/4 and Nanog) were used to identify pluripotency gene expression. A house keeping gene; GAPDH was used as a control. Sequence of primers are as follows; human Oct3/4 (230 bp), forward: 5'-CTCACCTGGGGGTTCTATT-3', reverse: 5'-CTCCAGGTTGCCTCTCACTC-3' (Pessina et al., 2010) and human Nanog (255 bp), forward: 5'-GCTTGCCTTGCTTTGAAGCA-3' and reverse: 5'-TTCTTGACTGGGACCTTGTC-3'. As a housekeeping gene; GAPDH (302 bp), forward: 5'-AGCCACATCGCTCAGACACC-3', reverse: 5'-GTACTCAGCGGCCAGCATCG-3' (Yao et al., 2006). The annealing temperatures were 60°C for all genes.

3.1.7.3 Complementary DNA (cDNA synthesis) RT-PCR

Total RNA of each cell samples were reverse transcribed into cDNA using Superscript First-Strand Synthesis System (Invitrogen, USA). The mixture in the first reverse transcription step comprised of 700 ng total RNA, 1 mM deoxynucleotide triphosphate solution (dNTP mix), and 5 μ M oligo(dT) primer. The denaturation was performed at 65°C for 5 minutes and chilled at 4°C for 1 minute. The cDNA was synthesized from the supplement mixture of 1x RT buffer, 5 mM MgCl₂, 0.02 M DTT, 2 Unit RnaseOUT, and 10 Unit Superscript III RT by amplify in a Px2 Thermal Cyclers (Thermo Electron, UK) at 50°C for 50 minutes followed by termination reaction at 85°C for 5 minutes. The reaction mixture was then chilled at 4°C for 5 minutes. cDNA mixture was added with 0.1 Unit RNase H to remove residual RNA template and incubated at 37°C for 5 minutes.

3.1.7.4 Real-time PCR

The level of mRNA expression of Nanog and Oct3/4 was quantified by real-time quantitative PCR. Amplification of PCR products from cDNA of each cells was quantified using Power SYBR green PCR master mix (Applied Biosystems, USA) according to the manufacturer's instructions and fluorescence monitored on a ABI 7900HT Fast Real-Time PCR System (Applied Biosystems, USA) in a 25 μ l final reaction volume containing 1.5 μ l cDNA, 1x SYBR green PCR master mix, 0.2 μ M forward primer, and 0.2 μ M reverse primer. Melting curve analysis was also performed. The following cycling conditions were used: initial denaturation at 95°C for 10 min, followed by 40 cycles of 95°C for 15 s, 60°C for 15 s, and 60°C for 60 s. Measurement of fluorescence of each sample in every cycle at the end of the

extension was performed. The comparative threshold cycle method was used to enable quantification of the mRNA of these genes by normalized to an endogenous control and relative to a calibrator using the equation:

$$\text{Relative quantification} = 2^{-\Delta\Delta C_T}$$

$$\text{Where } \Delta\Delta C_T = \Delta C_{T(\text{target})} - \Delta C_{T(\text{calibrator})}$$

$$\Delta C_{T(\text{target})} = C_{T(\text{Nonog or Oct3/4})} - C_{T(\text{GAPDH})} \text{ of expanded cells obtained from each cocktail.}$$

$$\Delta C_{T(\text{calibrator})} = C_{T(\text{Nonog or Oct3/4})} - C_{T(\text{GAPDH})} \text{ of fresh CD34}^+ \text{ cells.}$$

Graphs represent the combined results for three independent replicates. After PCR operation, a melting curve was obtained and analyzed to verify the single band PCR product. PCR products were analyzed by 1% agarose gel (Invitrogen, USA) electrophoresis in 1x TBE buffer (Sambrook, 2001). The DNA sample was prepared by mixing eight parts of the sample with two parts of 6x DNA loading buffer and applied into the gel wells. Electrophoresis was performed on the electrophoresis unit (Cosmo Bio, Japan) at a constant voltage of 100 V for 120 minutes. The gel was then stained with 0.5 $\mu\text{g/ml}$ ethidium bromide for 10 minutes and destained with distilled water for 20 minutes. Gel image was visualized under UV light and captured by Gel Documentation System (MiniBIS, DNR Bio Imaging Systems Ltd., Israel).

3.1.8 Wound healing assay

3.1.8.1 Induction of diabetic mice

All procedures were performed in accordance with the Guidelines for the Care and Use of the Animal Care Unit of the Center for Scientific and Technological Equipment. Male ICR mice (approximate eight weeks, body weight 30-40 mg) were

intraperitoneal injected by multi-low dose of streptozotocin (STZ, 40 mg/kg; Sigma, USA) in 0.1 M citrate buffer pH 4.5 for 5 days (Motyl and McCabe, 2009; Tesch and Allen, 2007). After 7 days of injection, the blood samples were obtained from the tail vein of non-fasting mice and the glucose level was measured using Accu-Check Performa glucometer (Roche, USA). Mice were considered diabetes when non-fasting blood glucose level higher than 300 mg/dl for two consecutive days (Motyl and McCabe, 2009). Twenty-four hours before start the wound, mice were immunosuppressed by injection subcutaneously with cyclosporine A (10 mg/kg). One day after the wound and every two days after that, mice were also injected with cyclosporine A (20 mg/kg) for the entire experiment period (Nishio et al., 2006).

3.1.8.2 Wound healing model

STZ-induced diabetic mice were anesthetized by Zoletil (80 mg/kg; Virbac Laboratories, Carros, France). Hair on dorsal area was shaved and sterile with 70% alcohol. Two full-thickness excisional wounds were generated on dorso-lateral area using a standard skin biopsy punch (0.5 cm in diameter; Keyes, Germany). After the creation of wound, mice were injected subcutaneous with fresh isolated CD34⁺ cells or 5 day-expanded CD34⁺ cells in 4FW KSR (1 x 10⁵ cells in 100 µl PBS per wound) or 4FW cytokine (100 ng of each SCF, Flt3-L, IL-6 and 10 ng TPO in 100 µl PBS per wound) on four different sites surrounding the wound area. As a control, STZ-induced diabetic mice were injected with PBS alone. The wounds were dressed with an occlusive polyurethane film (Tegaderm, 3M Health Care, USA).

3.1.8.3 Wound analysis

The open wound areas on the left and right side of each mouse were documented using a digital camera (Canon S90, Japan) on days 0, 3, 5, 7 and 9 after wounding. The wound areas were then analyzed by Adobe Photoshop CS5 Extended software (version 12.0, Adobe Systems Incorporated) by calculating the pixel area from the tracing wound margin. After that, wound areas were normalized to the pixel count of the metric ruler scale that was photographed with each wound. Thereafter, the open wound area was calculated as follow (Templin et al., 2009):

$$\% \text{ wound area} = \frac{\text{wound area at each indicated time point}}{\text{wound area (day 0)}} \times 100$$

Wound area of each mouse was calculated from duplicated wound areas on both sides of the mouse.

3.1.8.4 Tissue section preparation

On day 5 and day 9 of the wound, mice were sacrificed by cervical dislocation. Wounds with 0.3 cm margin of normal skin surrounding them were excised by skin biopsy punch from both sides of dorso-lateral area. A half piece of each wound was excised and embedded with tissue freezing medium (Richard-Allan Scientific, USA). Ten micron thick tissue sections from the 25th section were cut perpendicular to the wound surface by microtome cryostat (HM 525, MICROM International GmbH, Germany) and placed on slide. The sections were kept at -80°C until further processed for hematoxylin and eosin staining and immunohistochemistry analysis.

3.1.8.5 Hematoxylin and eosin staining

In order to determine the histopathology of the wound and epithelial gap analysis, hematoxylin and eosin staining was performed according to the manufacturer's instruction. Fresh frozen sections were fixed in 10% neutral buffered formalin for 10 minutes and washed with PBS. Then, the slides were rinsed in distilled water and stained with Harris hematoxylin (Bio Optica, Italy) for 5 minutes. After that the slides were washed in the tap water for 5 minutes and dehydrated with 95% ethanol for 5 minutes. The sections were counterstained with Eosin (1% aqueous solution Eosin Y, Bio Optica, Italy) for 1 minute, followed by dehydration with 95% ethanol for 2 minutes each (twice), 100% ethanol for 2 minutes each (twice) and xylene for 2 minutes each (twice). Finally, slides were mounted with mounting medium (Merck, Germany). Microscopic images of wound tissue sections were visualized by a light microscope (Olympus BX51, Olympus Corporation, Japan). Digital images were captured with a digital camera CCD camera (Olympus DP72, Olympus Corporation, Japan). The epithelial gaps were determined by measuring the distance between encroaching epidermal elements (at least three cell layers thick) near the normal epidermis on both sides (Badillo et al., 2007) as performed by DP2-BSW program (version 2.2, Olympus Corporation, Japan; n = 6 per group).

3.1.8.6 Immunofluorescence

To analyze capillary density and macrophage content, wound sections were processed for immunofluorescent staining adapted from previously described (Templin et al., 2009). Briefly, tissue sections were fixed in cold acetone for 10 minutes at -20°C and let in the air for 20 minutes. The sections were blocked for non-specific

protein binding with 5% bovine serum albumin (BSA, Sigma, USA) in PBS for 10 minutes. Then, the sections were incubated with 50 μ l primary rat anti-mouse CD31 or CD68 monoclonal antibodies (diluted 1:100 with 1% BSA in PBS, AbD Serotec, UK) at 4°C in a moist chamber for 16 hours. After removal of excess antibody, the sections were washed with 0.1% Tween (Sigma, USA) in PBS three times for 5 minutes each. After that, the slides were incubated with secondary antibody Dylight-488 conjugated goat anti-rat IgG (dilution 1:300 in PBS with 1% BSA; AbD Serotec, UK) in a moist dark chamber at room temperature for 1 hour. The slides were then washed with 0.1% Tween in PBS three times for 5 minutes each and for nuclei staining with 4',6-diamidino-2-phenylindole (DAPI, diluted 1:100 with PBS) in a moist dark chamber at room temperature for 5 minutes. The slides were again washed with 0.1% Tween in PBS three times for 3 minutes each. Negative slides were stained in parallel with primary rat IgG2a isotype control (dilution 1:300 in PBS with 1% BSA; AbD Serotec, UK) or without using primary antibody to verify non-specific binding of secondary antibody. Finally, the slides were mounted in Fluorescence mounting medium (Vectashield, Vector Laboratories Inc., USA) and the edges were sealed with nail polish. Microscopic images of wound tissue sections were visualized by a fluorescence microscope (Olympus BX51, Olympus Corporation, Japan). Digital images were captured with a digital camera CCD camera (Olympus DP72, Olympus Corporation, Japan). CD31- or CD68-positive area was counted in the area where contain the most cells found in relative to five high power field (x400) on each slide (n = 6 per group).

Analysis of fresh human isolate CD34⁺ cells and expanded-CD34⁺ cells within the wound tissues were performed using mouse anti-human CD34-PE monoclonal antibody. Fixed tissue sections were blocked with 10% normal mouse serum for 10 minutes. Then, the sections were incubated with 50 μ l mouse anti-human CD34-PE monoclonal antibody (dilution 1:15 with 1% BSA in PBS) at 4°C in a moist chamber for 16 hours. Next, after removal of excess antibody, the sections were washed with 0.1% Tween in PBS 3 times for 5 minutes each. The slides were then stained with DAPI (diluted 1:100 with PBS) in a moist dark chamber at room temperature for 5 minutes and washed with 0.1% Tween in PBS 3 times for 3 minutes each. Negative slides were stained in parallel with mouse IgG1-PE (BD biosciences, USA) as an isotype control. Finally, the slides were mounted in Fluorescence mounting medium and sealed the edges with nail polish. Microscopic images of wound tissue sections were visualized by with a fluorescence microscope (Olympus BX51, Olympus Corporation, Japan). Digital images were captured with a digital camera CCD camera (Olympus DP72, Olympus Corporation, Japan).

3.1.9 Statistical analysis

Data were presented as the mean values \pm the standard deviation (SD). Significant differences of total cells and fold increase in each subpopulation, colony forming cells, and relative quantification of genes expression between different cytokine cocktails were analyzed with one way analysis of variance (ANOVA) followed by Tukey's HSD test for multiple comparisons. Comparison of total cells and fold increase in subpopulation between day 5 and day 7 of culture, and values between two groups of control and test medium or between two different experiment groups in wound

healing assay were analyzed with unpaired Student's *t* test. P value (P) < 0.05 was considered statistically significant. All statistic tests were calculated with SPSS software (version 17.0, SPSS Inc, USA).



CHAPTER IV

RESULTS

4.1 Results

4.1.1 Isolation of CD34⁺ cells

The mean mononuclear cell (MNC) concentration in fresh cord blood (CB) was $2.1 \pm 2.7 \times 10^9/l$ (range $0.1 - 18.5 \times 10^9$) and the mean MNCs per product was $9.9 \pm 8.5 \times 10^7$ cells (range $1.1 - 47.5 \times 10^7$; $n = 45$). The mean proportion of CD34⁺ cells in MNCs were $6.9 \pm 2.3\%$ (range $3.5 - 10.6$, $n = 6$) as analyzed by flow cytometry analysis before subjected for CD34 positive selection (Figure 4.1).

After using the Dynal CD34 Progenitor Cell Selection System, the mean number of isolated CB-CD34⁺ cells in each product was $6.9 \pm 10.1 \times 10^5$ cells (range $0.3 - 55.5 \times 10^5$, $n = 45$). The purity of CD34⁺ cells in each product was $>93\%$ (Figure 4.3) with a mean recovery of $10.7 \pm 9.0\%$ (range $4.1 - 28.0$, $n = 6$). CB-CD34⁺ cells morphology was homogeneous and contained the diameter approximately $9.7 \mu\text{m}$ (range $5.3 - 13.9 \mu\text{m}$; Figure 4.2). The evaluation of cell surface expression molecules (CD34, CD38 and CD133) on freshly isolated CD34⁺ cells showed that the majority of isolated cells co-expressed with CD133 ($74.3 \pm 6.2\%$) and CD38 ($86.2 \pm 1.3\%$, $n = 3$) which corresponded to previous reports (Mayani and Lansdorp, 1998; Scheinecker et al., 1995) as shown in Figure 4.3A.

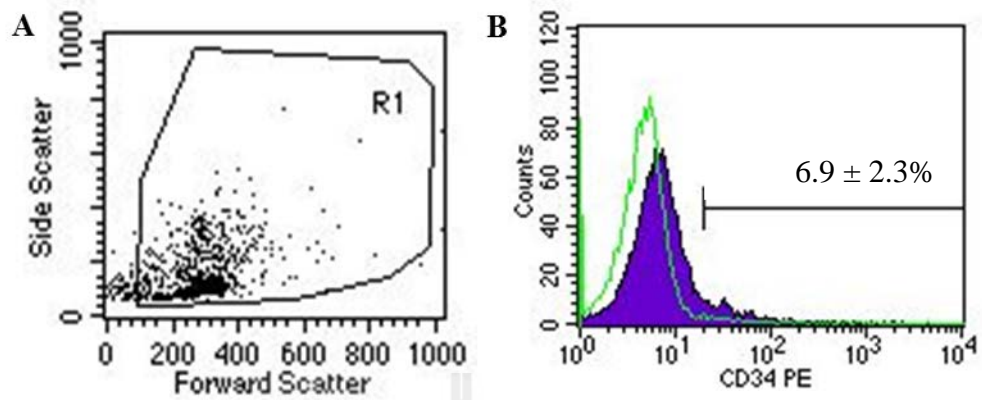


Figure 4.1 Assessment of CD34⁺ cell fraction in CB-MNCs by flow cytometry. (A) Forward scatter and side scatter of MNCs. (B) Percentage of CD34⁺ cells in MNCs fraction (violet) compared to negative control (green line). Data represent as mean \pm SD (n = 6).

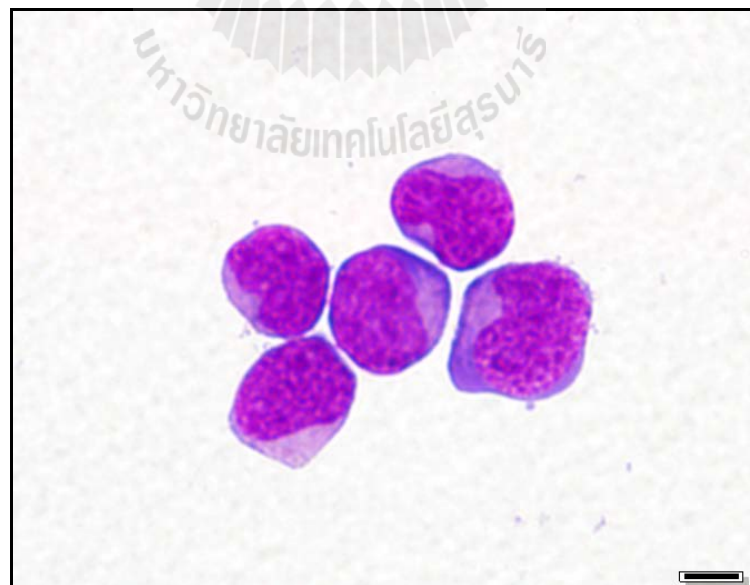


Figure 4.2 Morphology of isolated CB-CD34⁺ cells. Bar = 5 μ m.

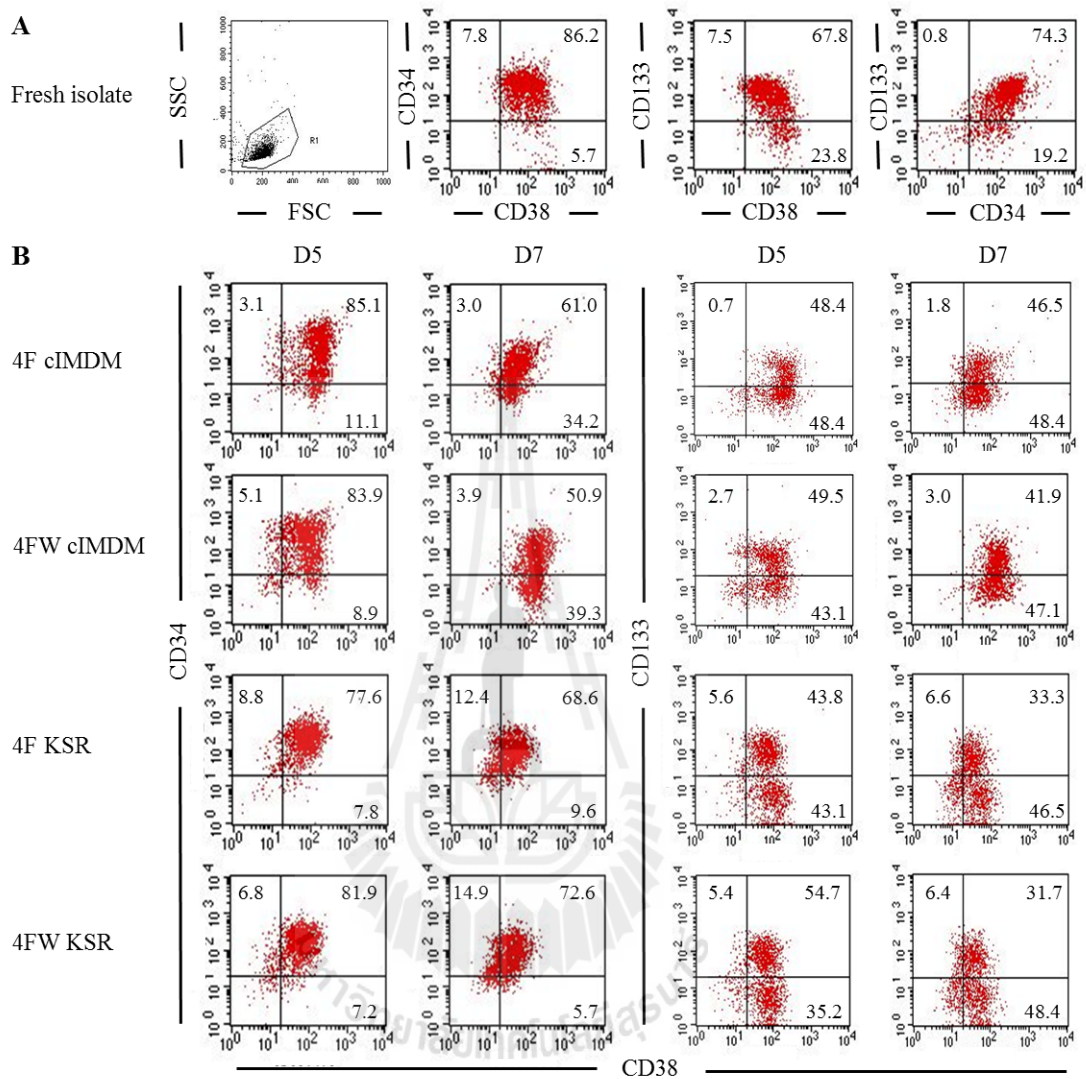


Figure 4.3 Representative of flow cytometry analysis of CD34, CD38 and CD133 expressions in freshly isolated CD34⁺ cells (A) and expanded CD34⁺ cells (B) cultured in various cytokine cocktails in serum (cIMDM) and serum-free medium (KSR) at day 5 and 7. Values are expressed as the mean (n = 3).

4.1.2 Development of culture medium for CB-CD34⁺ cells expansion in serum-free medium

Due to the limit number of CD34⁺ cells in a single unit, the expansion of the cells is required. Cultivation of CD34⁺ cells in a medium containing the growth factors and fetal serum resulted in the contamination of animal residual. Thus, to increase the efficiency of the culture method for clinical purpose, 2 different culture medium, with and without fetal serum (cIMDM and KSR, respectively), that could accelerate cells proliferation and preserve hematopoietic stem cells phenotype throughout the culture period were assessed.

There were 4 groups of CB-CD34⁺ cells culture: 4F cIMDM, 4FW cIMDM, 4F KSR and 4FW KSR. The fold increase of the cells after expansion was investigated by stained the cells with CD34, CD38 and CD133 monoclonal antibodies. The representative characteristic patterns of expanded cells derived on day 5 and 7 of each culture condition when analyzed by flow cytometry analysis were shown in Figure 4.3B. The CD34⁺CD38⁻ cells represent primitive HSC population which is very crucial for therapeutic purpose. When normalize the number of data value with the input cell culture, the results showed that there were a slightly increase in fold expansion of CD34⁺CD38⁻ population in the expanded cells cultured in 4F cIMDM (2.6 ± 1.1 fold) and 4FW cIMDM (3.9 ± 1.0 fold) at day 5 as compared with day 0 of the control cells (Table 4.1, n = 3). These cells continuously expanded more over time as 4.2 ± 1.3 and 6.6 ± 1.4 folds at day 7 of expansion process, respectively (Table 4.1).

Interestingly, cells that maintained in 4F KSR and 4FW KSR for 7 days revealed a significant multiplication of CD34⁺CD38⁻ population as 18.5 ± 0.4 and

24.3 ± 2.1 folds, respectively (Table 4.1). Total CD34⁺CD38⁻ cells in 4F KSR (4.8 ± 1.1 × 10⁴ cells) and 4FW KSR (4.5 ± 0.8 × 10⁴ cells) were higher than those of 4F cIMDM (1.9 ± 0.5 × 10⁴ cells) and 4FW cIMDM (3.0 ± 0.3 × 10⁴ cells), respectively, on day 5 of the culture (Figure 4.4). In addition, total CD34⁺CD38⁻ number slightly increased in serum containing medium and gradually increased in serum-free medium as observed on day 7. The highest CD34⁺CD38⁻ number was observed in 4FW KSR (1.9 ± 0.3 × 10⁵ cells) which enhanced significantly than other culture conditions (4F cIMDM: 3.1 ± 0.3 × 10⁴, 4FW cIMDM: 5.0 ± 0.3 × 10⁴, and 4F KSR: 1.4 ± 0.3 × 10⁵ cells) as shown in Figure 4.4. Moreover, cells cultured in 4F KSR and 4FW KSR conditions contained significantly fewer number of CD34⁻CD38⁺ cells (differentiated cells; 1.1 ± 0.2 × 10⁵ and 7.2 ± 1.2 × 10⁴ cells with 20.1 ± 6.8 and 13.0 ± 3.7 folds, respectively) than those of 4F cIMDM and 4FW cIMDM (3.6 ± 0.5 × 10⁵ and 5.0 ± 0.3 × 10⁵ cells with 62.8 ± 5.0 and 89.7 ± 12.2 folds, respectively) on day 7 of cultures (Figure 4.5 and Table 4.1). These data indicate that 4F KSR and 4FW KSR conditions could preserve HSCs phenotype of the cells better than serum containing medium.

Surprisingly, culture condition of 4F KSR and 4FW KSR also revealed the enhancement of CD133⁺CD38⁻ subpopulation proliferation statistical significance as 11.5 ± 3.4 and 12.3 ± 4.0 folds, respectively, on day 7 of cultures when compared to that of 4F cIMDM (0.7 ± 0.4 fold, Table 4.1). In addition, total CD133⁺CD38⁻ number observed in 4F KSR and 4FW KSR (at day 5: 3.0 ± 0.7 × 10⁴ and 3.5 ± 0.7 × 10⁴, day 7: 7.7 ± 1.6 × 10⁴ and 8.0 ± 1.3 × 10⁴ cells, respectively) were significantly higher than those of 4F cIMDM and 4FW cIMDM (at day 5: 0.4 ± 0.1 × 10⁴ and 1.6 ± 0.2 × 10⁴, day 7: 1.9 ± 0.3 × 10⁴ and 3.8 ± 0.2 × 10⁴ cells, respectively) throughout the study

period (Figure 4.6). These cells also contain blood cells repopulating capacity *in vivo* (Boxall et al., 2009; Koutna et al., 2011). Altogether, these findings suggest that 4F KSR and 4FW KSR can augment CD133⁺CD38⁻ subpopulation proliferation along with CD34⁺CD38⁻ cells expansion. Moreover, these data demonstrate that Wnt1 is a potent stimulator of CD34⁺CD38⁻ and CD133⁺CD38⁻ cells proliferations.

Table 4.1 *Ex vivo* expansion pattern of CD34⁺ cells cultured in 2 different cytokine cocktails in cIMDM and KSR medium. Values are expressed as the mean \pm SD (n = 3).

| Culture conditions | | Day | Fold expansion | | |
|--------------------|------------------------------|-----|-------------------------------------|--------------------------------------|-------------------------------------|
| Name | Cytokines | | CD34 ⁺ CD38 ⁻ | CD133 ⁺ CD38 ⁻ | CD34 ⁺ CD38 ⁺ |
| 4F cIMDM | Flt3-L, SCF, TPO, IL-6 | 5 | 2.6 \pm 1.1 | 0.7 \pm 0.4 | 12.0 \pm 1.4 |
| | | 7 | 4.2 \pm 1.3 | 3.1 \pm 1.6 | 62.8 \pm 5.0 [†] |
| 4FW cIMDM | Flt3-L, SCF, TPO, IL-6, Wnt1 | 5 | 3.9 \pm 1.0 | 2.5 \pm 1.2 | 9.3 \pm 1.3 |
| | | 7 | 6.6 \pm 1.4 | 6.0 \pm 2.6 | 89.7 \pm 12.2 [†] |
| 4F KSR | Flt3-L, SCF, TPO, IL-6 | 5 | 6.3 \pm 1.6* | 4.7 \pm 2.0 | 7.6 \pm 2.2 |
| | | 7 | 18.5 \pm 0.4 ^{**†} | 11.5 \pm 3.4 ^{***†} | 20.1 \pm 6.8 ^{**†} |
| 4FW KSR | Flt3-L, SCF, TPO, IL-6, Wnt1 | 5 | 5.9 \pm 1.2 | 5.4 \pm 2.2* | 8.4 \pm 2.2 |
| | | 7 | 24.3 \pm 2.1 ^{**†} | 12.3 \pm 4.0 ^{***} | 13.0 \pm 3.7 ^{**} |

Note: *P<0.05 when comparing with 4F cIMDM on day 5 (on the same column), **P<0.05 when comparing with 4F and 4FW cIMDM on day 7 (on the same column), ***P<0.01 when comparing with 4F cIMDM on day 7 (on the same column), [†]P<0.05 when comparing between day 5 and day 7 of each culture condition.

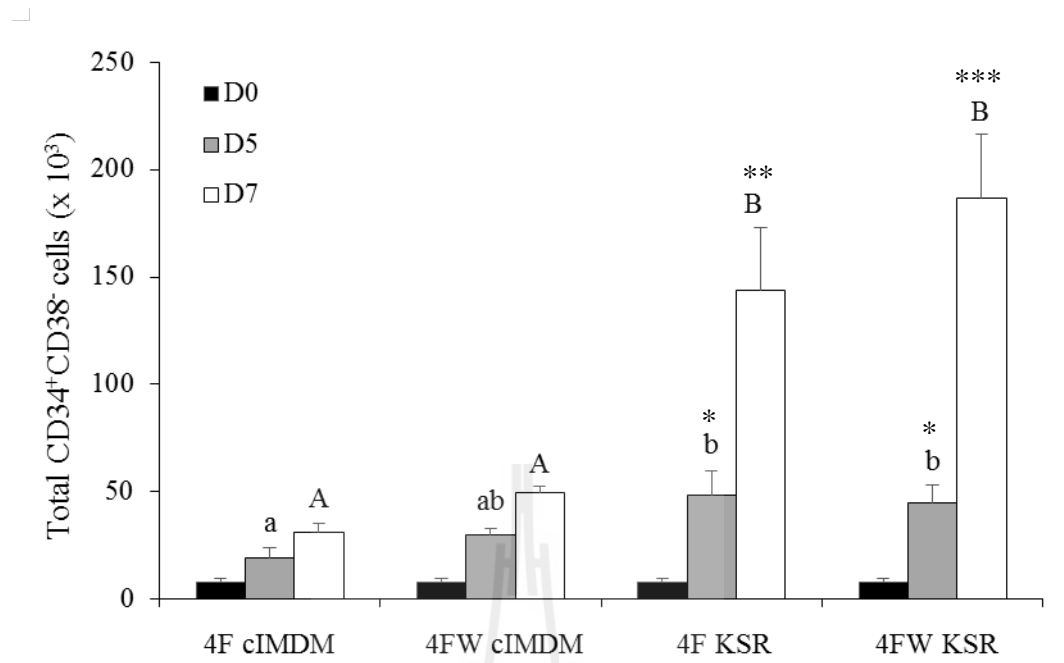


Figure 4.4 Total CD34⁺CD38⁻ cell number in serum and serum-free culture on day 5 and day 7. Values are expressed as the mean \pm SD (n = 3). Values with different letters on the same day of culture are significantly different. *P<0.02 when comparing cultures of KSR with 4F cIMDM on day 5. **P<0.004 when comparing 4F KSR with cultures of cIMDM on day 7. ***P<0.001 when comparing 4FW KSR with cultures of cIMDM on day 7.

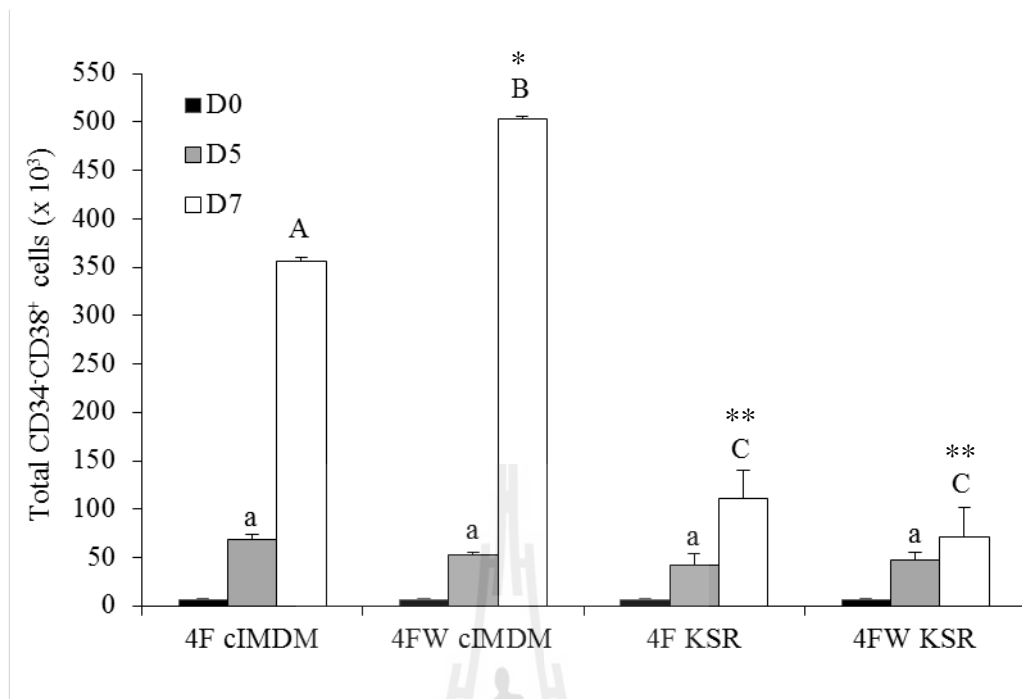


Figure 4.5 Total CD34⁻CD38⁺ cell number in serum and serum-free culture on day 5 and day 7. Values are expressed as the mean \pm SD (n = 3). Values with different letters on the same day of culture are significantly different. *P<0.003 when comparing 4FW cIMDM with 4F cIMDM on day 7. **P<0.001 when comparing cultures of KSR with 4F cIMDM on day 7.

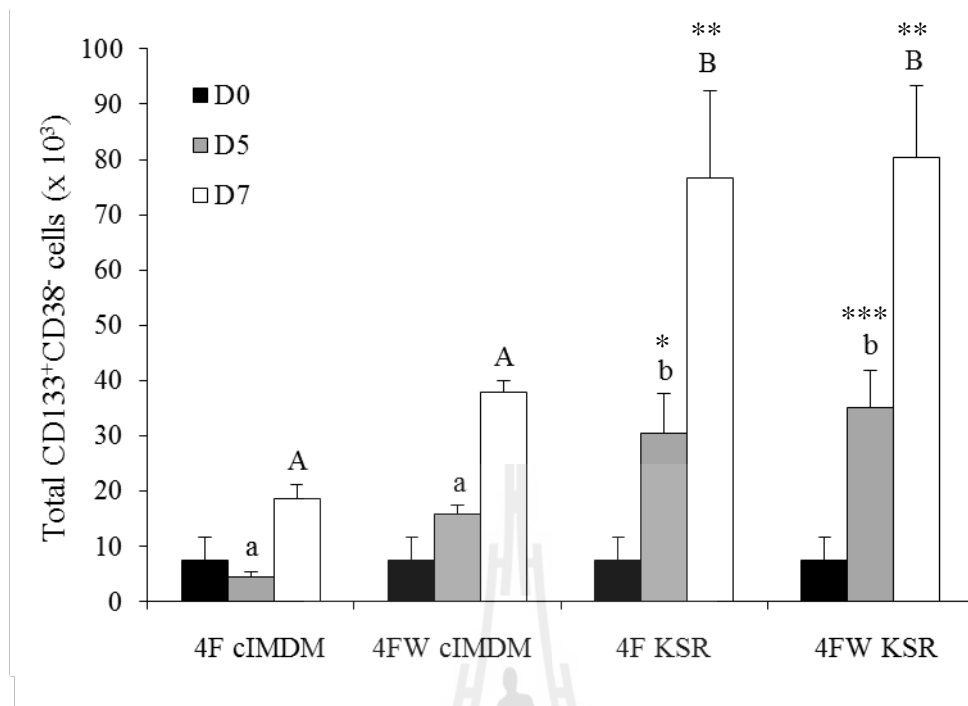


Figure 4.6 Total CD133⁺CD38⁻ cell number in serum and serum-free culture on day 5 and day 7. Values are expressed as the mean \pm SD (n = 3). Values with different letters on the same day of culture are significantly different. *P<0.03 when comparing 4F KSR with cultures of cIMDM on day 5. **P<0.01 when comparing cultures of KSR with cultures of cIMDM on day 7. ***P<0.005 when comparing 4FW KSR with cultures of cIMDM on day 5.

4.1.3 Determination of phenotype and *in vitro* hematopoiesis of expanded cells in serum and serum-free cultures

To further investigate more phenotypes of progenitor cells in these expanded cells, cells from four conditions were separately harvested and subjected for myeloid, lymphoid and erythroid lineages analysis using CD33 (myeloid), CD71 (erythroid), CD3 and CD19 (lymphoid) markers. The results demonstrated the significant presence of early markers of myeloid/erythroid progenitors (CD33⁺CD71⁺ cells, 4F cIMDM: 86.7 ± 3.7%, 4FW cIMDM: 85.5 ± 7.7%, 4F KSR: 72.2 ± 15.6%, 4FW KSR 71.3 ± 14.2%) but not lymphoid progenitors in all culture conditions at day 7 (Figure 4.7). However, cells cultured in 4F cIMDM and 4FW cIMDM contained more myeloid/erythroid progenitors than cells cultured in both 4F KSR and 4FW KSR. In addition, the results showed that medium containing serum induced alteration of cell phenotypes by the loss of CD34⁺ cells and obtained more CD34⁻CD38⁺ population than those observed in serum-free medium. This data suggests the effect of serum in enhancement of spontaneous differentiation.

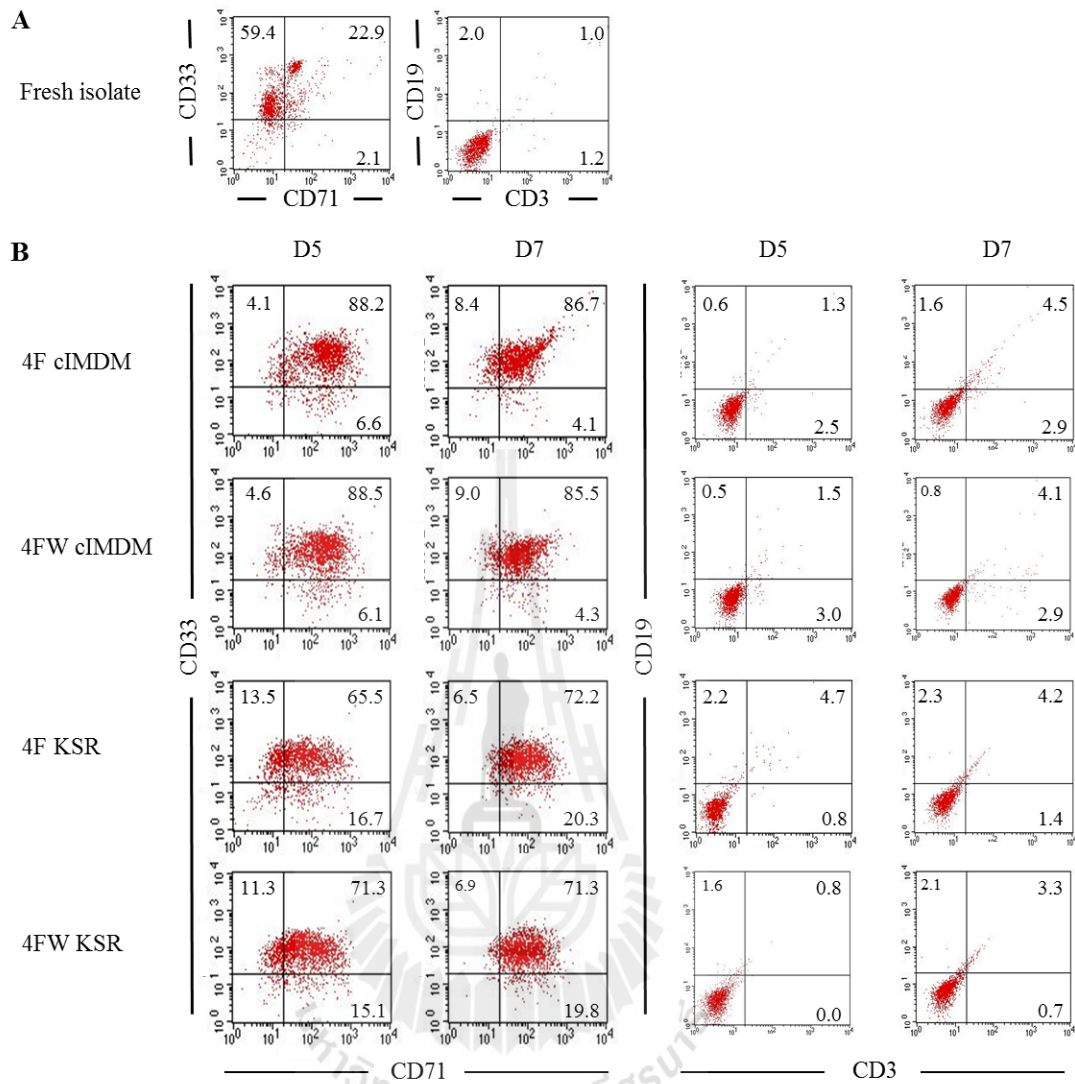


Figure 4.7 Immunophenotype of expanded cells. Cell surface markers CD33/CD71 and CD3/CD19 of freshly isolated CD34⁺ cells (A) and expanded cells (B) at 5-day and 7-day of each culture condition in serum (cIMDM) and serum-free medium (KSR). Values are expressed as the mean (n = 3).

In addition, to support the evidence that expanded CD34⁺ cells in the serum-free medium culture could differentiate into all 3 hematopoietic lineages; myeloid, lymphoid and erythroid lineages, clonogenic assay and liquid differentiation were performed. The results demonstrated that expanded cells in all 4 various culture conditions contained the ability to produce clonogenic progenitor cells (CFUs); CFU-GEMM (4F cIMDM: 5 ± 3 , 4FW cIMDM: 4 ± 2 , 4F KSR: 3 ± 1 , and 4FW KSR: 3 ± 1 colonies), CFU-GM (4F cIMDM: 15 ± 3 , 4FW cIMDM: 15 ± 4 , 4F KSR: 9 ± 4 , and 4FW KSR: 13 ± 8 colonies), and BFU-E (4F cIMDM: 77 ± 7 , 4FW cIMDM: 78 ± 3 , 4F KSR: 70 ± 14 , and 4FW KSR: 75 ± 10 colonies) similar to the freshly isolated CD34⁺ cells (CFU-GEMM: 6 ± 4 , CFU-GM: 16 ± 6 , and BFU-E: 80 ± 4 colonies) as shown in Figures 4.8-4.9 and Table 4.2. Additionally, expanded HSPCs in 4F KSR and 4FW KSR could generate more mature blood cells; megakaryocytes, erythroid cells, lymphocytes, macrophages, granulocytes, and mast cells in liquid culture differentiation (Figure 4.10) as well as those cultured in cIMDM conditions (Figure 4.11). These findings indicated the achievement of repopulating capacity of expanded HSPCs population *in vitro*.

Table 4.2 Total number of colony forming cells derived from day 5 expanded CD34⁺ cells obtained from 4F cIMDM, 4FW cIMDM, 4F KSR, and 4FW KSR cultures compared with fresh CD34⁺ cells. Values are expressed as the mean \pm SD (n = 3).

| Media | CFU-GEMM | CFU-GM | BFU-E |
|---------------|-----------|------------|-------------|
| Fresh isolate | 6 \pm 4 | 16 \pm 6 | 80 \pm 4 |
| 4F cIMDM | 5 \pm 3 | 15 \pm 3 | 77 \pm 7 |
| 4FW cIMDM | 4 \pm 2 | 15 \pm 4 | 78 \pm 3 |
| 4F KSR | 3 \pm 1 | 9 \pm 4 | 70 \pm 14 |
| 4FW KSR | 3 \pm 1 | 13 \pm 8 | 75 \pm 10 |

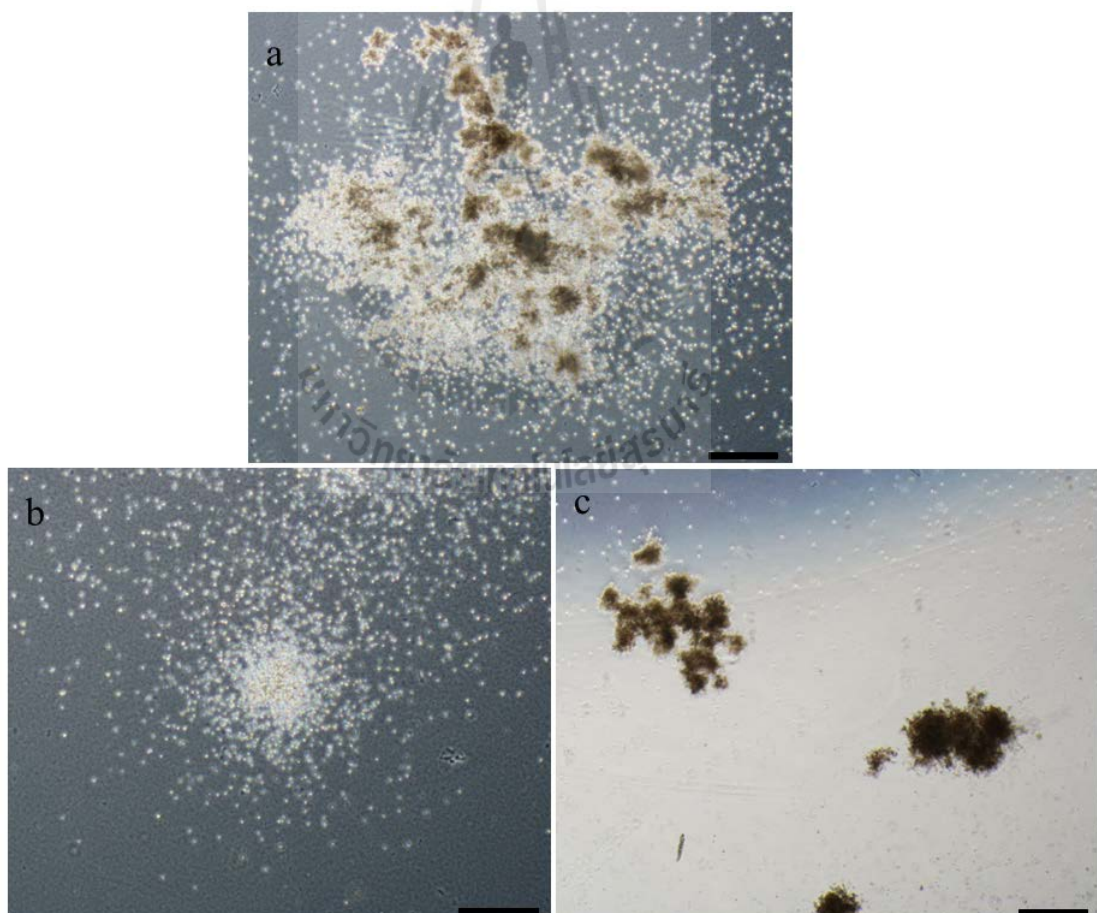


Figure 4.8 Photomicrographs illustrating the colony forming cells; CFU-GEMM (a), CFU-GM (b), and BFU-E (c) on methylcellulose. Scale bar = 400 μ m.

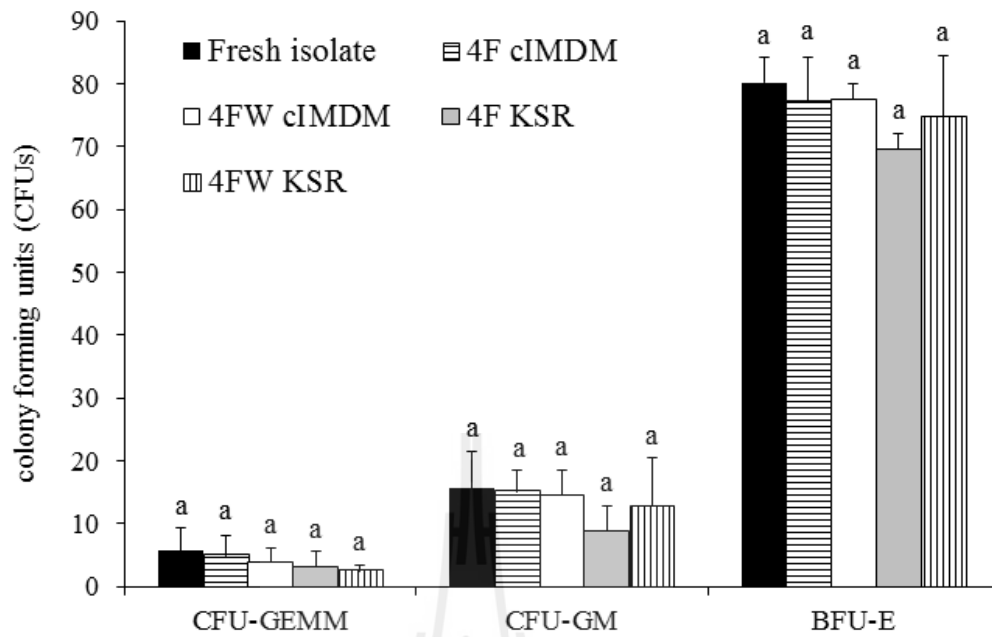


Figure 4.9 Colony forming cell assay (CFU-GEMM, CFU-GM, and BFU-E) of day 5 expanded CD34⁺ cells in various culture conditions. Values are expressed as the mean \pm SD (n = 3).

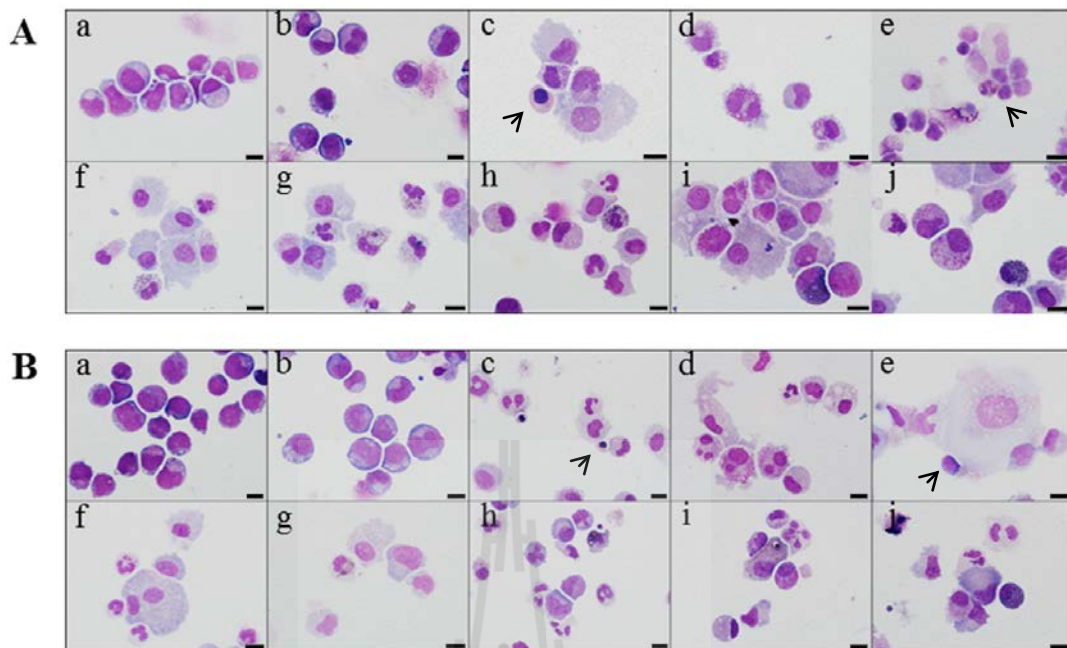


Figure 4.10 Differentiation capacities of expanded CB-CD34⁺ cells from 4F (A) and 4FW (B) cIMDM *in vitro*. (a) Undifferentiated day 5 expanded CB-CD34⁺ cells, (b) day 7 expanded CD34⁺ cells, (c) erythroid lineage differentiation (EPO + SCF, arrow), (d) megakaryocytes differentiation (TPO + SCF), (e) lymphoid lineage differentiation (IL-7 + Flt3-L + SCF + OP9, arrow), (f-g) granulocytes and macrophage lineages differentiation (GM-CSF + IL-3), (h-j) mast cells and granulocyte lineages differentiation (SCF + IL-3). Scale bar = 10 μ m.

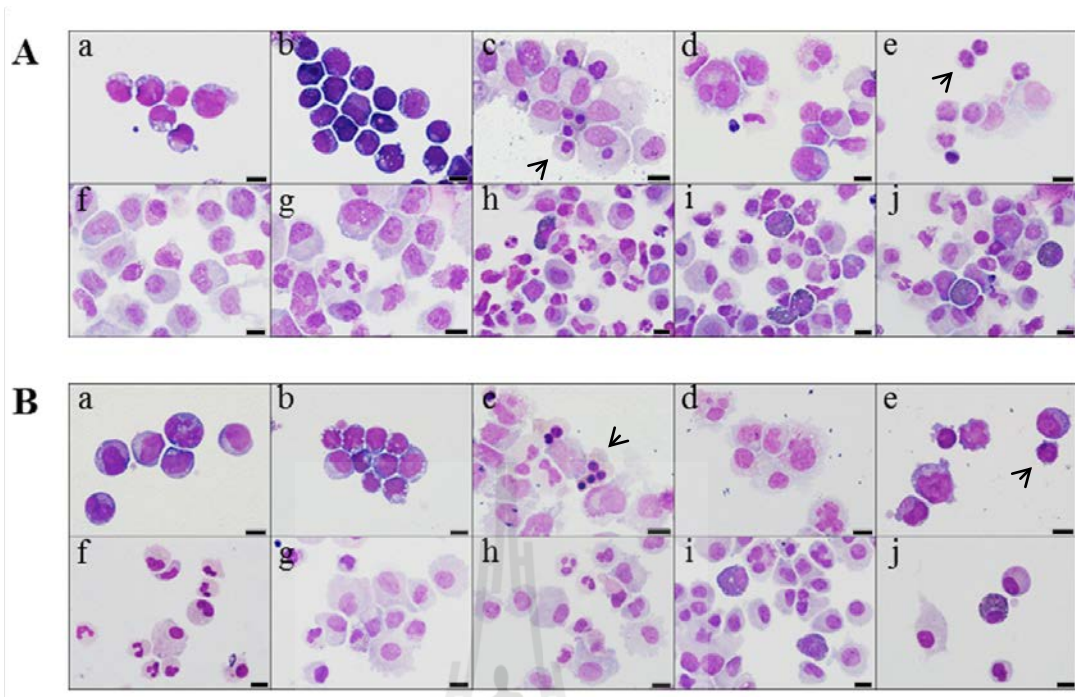


Figure 4.11 Differentiation capacities of expanded CB-CD34⁺ cells from 4F (A) and 4FW (B) KSR *in vitro*. (a) Undifferentiated day 5 expanded CB-CD34⁺ cells, (b) day 7 expanded CD34⁺ cells, (c) erythroid lineage differentiation (EPO + SCF, arrow), (d) megakaryocytes differentiation (TPO + SCF), (e) lymphoid lineage differentiation (IL-7 + Flt3-L + SCF + OP9, arrow), (f-g) granulocytes and macrophage lineages differentiation (GM-CSF + IL-3), (h-j) mast cells and granulocyte lineages differentiation (SCF + IL-3). Scale bar = 10 μ m.

4.1.4 Comparison of multiple cytokine cocktails for CB-CD34⁺ cells expansion in serum-free medium

Additional cytokine cocktails were performed and compared with 4F and 4FW cocktails to determine the efficiency of *ex vivo* expansion of HSCs in serum-free medium, which were P0, P1, P2, P3 and P4 (the composition of each cocktail were described in the materials and methods, n = 3).

Culture of CD34⁺ cells in all culture condition showed slightly increased in expansion of nucleated cells during a few days of culture (Figure 4.12). The number of nucleated cells continually enhanced and demonstrated the highest fold expansion in P4 culture (15.4 ± 2.5 fold) compared to other culture conditions (4F: 11.5 ± 2.4 , 4FW: 12.5 ± 2.0 , P0: 13.9 ± 0.8 , P1: 12.3 ± 0.8 , P2: 9.6 ± 1.4 and P3: 10.6 ± 0.4 folds) on day 7 (Figure 4.12 and Table 4.3).

On 5 and 7 days of the cultures, cells were subjected for CD34, CD38 and CD133 molecules expression which analyzed by flow cytometry analysis (Figure 4.13). When normalized the number to the input cell number at day 0, the results showed that the highest CD34⁺CD38⁻ cells were found in P0 culture ($7.5 \pm 0.3 \times 10^4$ cells) compared to other cocktails significantly (4F: $4.8 \pm 1.1 \times 10^4$, 4FW: $4.5 \pm 0.8 \times 10^4$, P1: $4.9 \pm 0.1 \times 10^4$, P3: $4.6 \pm 0.4 \times 10^4$ and P4: $4.1 \pm 0.9 \times 10^4$ cells) at day 5, except, in P2 culture that did not show statistical significance ($5.7 \pm 0.7 \times 10^4$ cells; Figure 4.14). Similarly, the highest fold increase in CD34⁺CD38⁻ cells at day 5 was found in P0 culture (10.0 ± 2.2 fold) compared to other cocktails (4F: 6.3 ± 1.6 , 4FW: 5.9 ± 1.2 , P1: 6.6 ± 1.3 , P2: 7.4 ± 1.1 , P3: 6.1 ± 1.4 and P4: 5.6 ± 2.1 folds) as shown in Table 4.4. On day 7, the number of CD34⁺CD38⁻ cells was gradually increased significantly in all culture conditions and the culture in 4FW cocktail demonstrated

the highest expansion at $1.9 \pm 0.3 \times 10^5$ cells with 24.3 ± 2.1 fold compare to other cultures (4F: $1.4 \pm 0.3 \times 10^5$ cells and 18.5 ± 0.4 fold, P0: $1.5 \pm 0.1 \times 10^5$ cells and 19.4 ± 2.9 fold, P1: $1.5 \pm 0.1 \times 10^5$ cells and 19.9 ± 4.9 fold, P2: $1.3 \pm 0.2 \times 10^5$ cells and 16.9 ± 2.2 fold, P3: $1.4 \pm 0.1 \times 10^5$ cells and 18.6 ± 3.3 fold, and P4: $1.6 \pm 0.3 \times 10^5$ cells and 20.7 ± 3.5 fold) as can be seen in Figure 4.14 and Table 4.4. In addition, total CD34⁻CD38⁺ cells were observed to be highest in P2 culture ($12.1 \pm 1.4 \times 10^4$ cells and 21.6 ± 3.0 fold) compared to other culture conditions (4F: $4.3 \pm 1.1 \times 10^4$ cells and 7.6 ± 2.2 fold, 4FW: $4.7 \pm 0.9 \times 10^4$ cells and 8.4 ± 2.2 fold, P0: $4.4 \pm 0.1 \times 10^4$ cells and 7.8 ± 1.0 fold, P1: $7.3 \pm 0.1 \times 10^4$ cells and 13.1 ± 1.9 fold, P3: $5.5 \pm 0.5 \times 10^4$ cells and 9.9 ± 1.7 fold, and P4: $7.2 \pm 1.5 \times 10^4$ cells and 12.6 ± 2.2 fold) at day 5 (Figure 4.15 and Table 4.4). On the other hand, the number of total CD34⁻CD38⁺ cells at day 7 was highest in P0 culture ($3.3 \pm 0.2 \times 10^5$ cells and 58.6 ± 6.9 fold) compared to other cocktails (4F: $1.1 \pm 0.1 \times 10^5$ cells and 20.1 ± 6.8 fold, 4FW: $0.7 \pm 0.1 \times 10^5$ cells and 13.0 ± 3.7 fold, P1: $2.5 \pm 0.2 \times 10^5$ cells and 44.2 ± 5.6 fold, P2: $2.4 \pm 0.3 \times 10^5$ cells and 42.0 ± 5.4 fold, P3: $1.8 \pm 0.1 \times 10^5$ cells and 33.0 ± 5.8 fold, and P4: $3.3 \pm 0.5 \times 10^5$ cells and 58.3 ± 10.0 fold) as shown in Figure 4.15.

Moreover, total CD133⁺CD38⁻ cells expanded in the P0 culture ($5.7 \pm 0.2 \times 10^4$ cells and 9.2 ± 4.1 fold) were found higher than those of other culture conditions (4F: $3.0 \pm 0.7 \times 10^4$ cells and 4.7 ± 0.2 fold, 4FW: $3.5 \pm 0.7 \times 10^4$ cells and 5.4 ± 2.2 fold, P1: $1.3 \pm 0.01 \times 10^4$ cells and 2.0 ± 0.8 fold, P2: $3.7 \pm 0.5 \times 10^4$ cells and 5.9 ± 2.4 fold, P3: $2.5 \pm 0.2 \times 10^4$ cells and 4.1 ± 1.9 fold, and P4: $3.4 \pm 0.7 \times 10^4$ cells and 5.7 ± 3.2 fold) significantly on day 5 (Figure 4.16 and Table 4.4). As a consequence, total CD34⁺CD38⁻ cells continued to increase and remained highest in P0 culture ($11.2 \pm 0.7 \times 10^4$ cells and 18.2 ± 7.3 fold) compared to those of other cultures (4F: 7.7 ± 1.6

$\times 10^4$ cells and 11.5 ± 3.4 fold, 4FW: $8.0 \pm 1.3 \times 10^4$ cells and 12.3 ± 4.0 fold, P1: $10.3 \pm 0.7 \times 10^4$ cells and 16.2 ± 6.5 fold, P2: $9.2 \pm 1.3 \times 10^4$ cells and 14.2 ± 5.5 fold, P3: $6.0 \pm 0.2 \times 10^4$ cells and 9.6 ± 4.1 fold, and P4: $8.3 \pm 1.3 \times 10^4$ cells and 13.0 ± 5.4 fold) on day 7 (Figure 4.16 and Table 4.4).

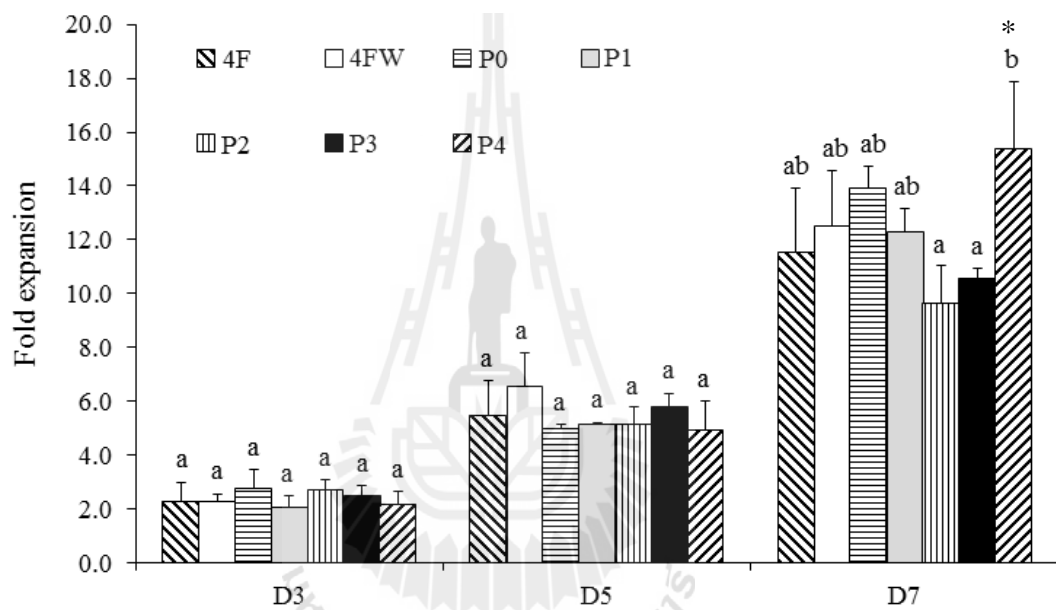
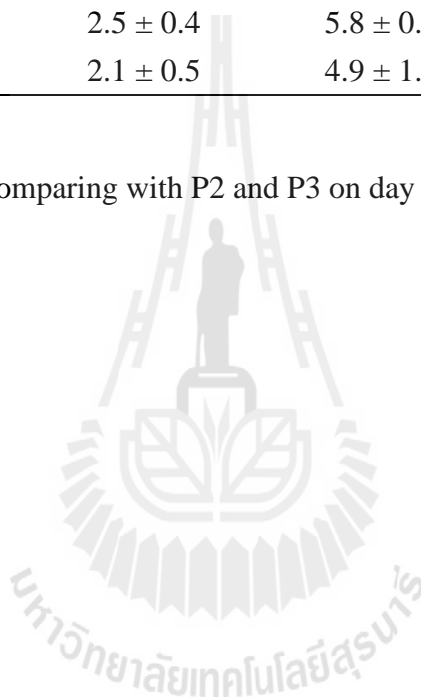


Figure 4.12 Fold increase in total nucleated cells in various cytokine cocktails in serum-free culture on day 5 and day 7. Values are expressed as the mean \pm SD (n = 3). Values with different letters are significantly different on the same day of culture (see appendix B for statistical description). *P<0.05 when comparing P4 with P2 and P3 on day 7.

Table 4.3 Fold increase in total nucleated cells in all culture conditions in serum-free medium. Values are expressed as the mean \pm SD (n = 3).

| Cocktail | D3 | D5 | D7 |
|----------|---------------|---------------|-----------------|
| 4F | 2.3 \pm 0.7 | 5.5 \pm 1.3 | 11.5 \pm 2.4 |
| 4FW | 2.3 \pm 0.3 | 6.5 \pm 1.2 | 12.5 \pm 2.0 |
| P0 | 2.8 \pm 0.7 | 5.0 \pm 0.2 | 13.9 \pm 0.8 |
| P1 | 2.1 \pm 0.4 | 5.2 \pm 0.1 | 12.3 \pm 0.8 |
| P2 | 2.7 \pm 0.4 | 5.2 \pm 0.6 | 9.6 \pm 1.4 |
| P3 | 2.5 \pm 0.4 | 5.8 \pm 0.5 | 10.6 \pm 0.4 |
| P4 | 2.1 \pm 0.5 | 4.9 \pm 1.1 | 15.4 \pm 2.5* |

Note: *P<0.05 when comparing with P2 and P3 on day 7.



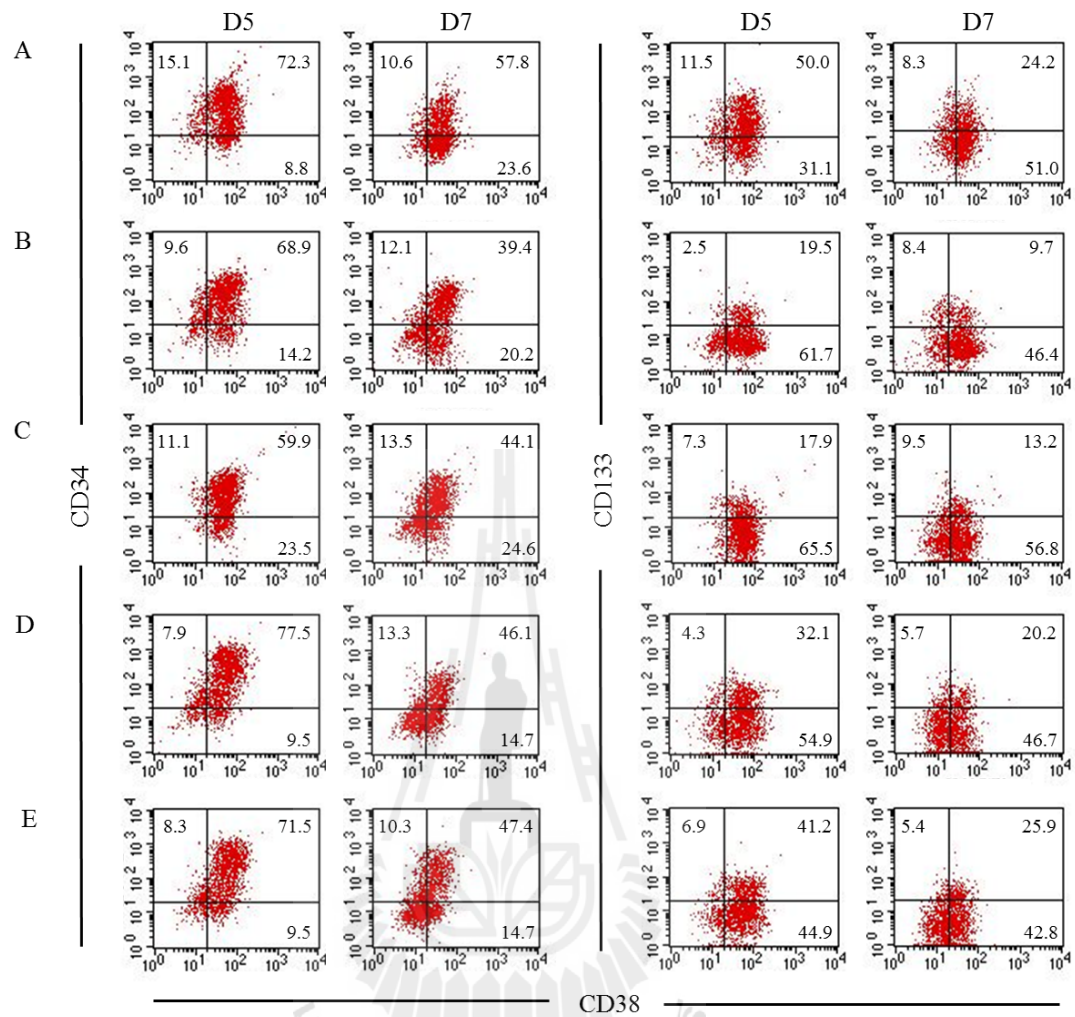


Figure 4.13 Representative of flow cytometry analysis of CD34, CD38 and CD133 expressions in expanded CD34⁺ cells cultured in P0 (A), P1 (B), P2 (C), P3 (D) and P4 (E) in serum-free medium on day 5 and day 7. Values are expressed as the mean (n = 3).

Table 4.4 *Ex vivo* expansion pattern of CD34⁺ cells cultured in various cytokine cocktails in serum-free medium. Values are expressed as the mean \pm SD (n = 3).

| Cytokine cocktail | CD34 ⁺ CD38 ⁻ | | CD133 ⁺ CD38 ⁻ | | CD34 ⁻ CD38 ⁺ | |
|-------------------|-------------------------------------|-----------------------------|--------------------------------------|-----------------------------|-------------------------------------|---------------------------------|
| | D5 | D7 | D5 | D7 | D5 | D7 |
| 4F | 6.3 \pm 1.6 | 18.5 \pm 0.4 [†] | 4.7 \pm 2.0 | 11.5 \pm 3.4 [†] | 7.6 \pm 2.2 | 20.1 \pm 6.8 [†] |
| 4FW | 5.9 \pm 1.2 | 24.3 \pm 2.1 [†] | 5.4 \pm 2.2 | 12.3 \pm 4.0 | 8.4 \pm 2.2 | 13.0 \pm 3.7 |
| P0 | 10.0 \pm 2.2 | 19.4 \pm 2.9 [†] | 9.2 \pm 4.1* | 18.2 \pm 7.3 | 7.8 \pm 1.0 | 58.6 \pm 6.9 ^{***†} |
| P1 | 6.6 \pm 1.3 | 19.9 \pm 4.9 [†] | 2.0 \pm 0.8 | 16.2 \pm 6.5 | 13.1 \pm 1.9 | 44.2 \pm 5.6 [†] |
| P2 | 7.4 \pm 1.1 | 16.9 \pm 2.2 [†] | 5.9 \pm 2.4 | 14.2 \pm 5.5 | 21.6 \pm 3.0 ^{**} | 42.0 \pm 5.4 [†] |
| P3 | 6.1 \pm 1.4 | 18.6 \pm 3.3 [†] | 4.1 \pm 1.9 | 9.6 \pm 4.1 | 9.9 \pm 1.7 | 33.0 \pm 5.8 [†] |
| P4 | 5.6 \pm 2.1 | 20.7 \pm 3.5 [†] | 5.7 \pm 3.2 | 13.0 \pm 5.4 | 12.6 \pm 2.2 | 58.3 \pm 10.0 ^{***†} |

Note: *P<0.05 when comparing with P1 on day 5 (on the same column), **P<0.005 when comparing with other culture conditions on day 5 (on the same column), ***P<0.01 when comparing with 4F, 4FW and P3 on day 7 (on the same column), [†]P<0.05 when comparing between day 5 and day 7 of each population on the same culture condition.

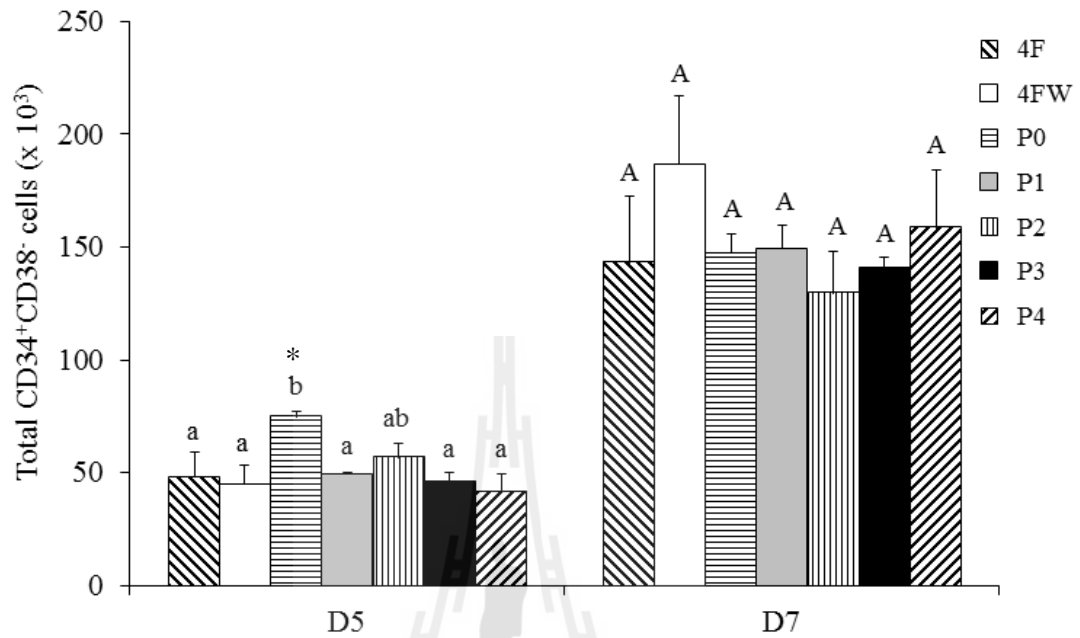


Figure 4.14 Total CD34⁺CD38⁻ cells in various cytokine cocktail in serum-free culture on day 5 and day 7. Values are expressed as the mean \pm SD (n = 3). Values with different letters are significantly different. *P<0.01 when comparing P0 with other cultures except P2 on day 5.

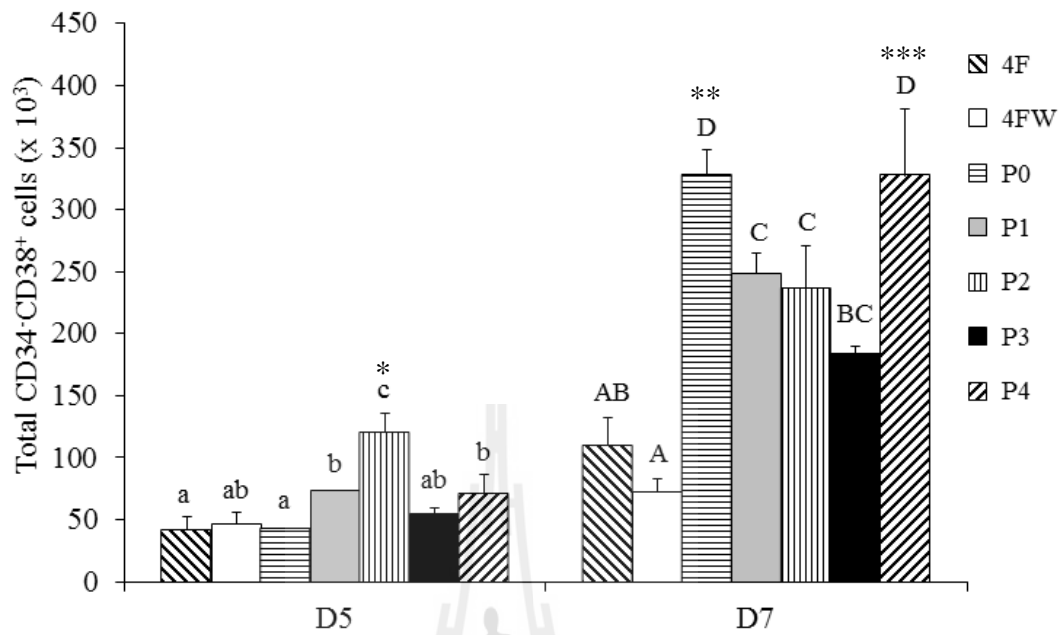


Figure 4.15 Total CD34⁺CD38⁺ cells in various cytokine cocktail in serum-free culture on day 5 and day 7. Values are expressed as the mean \pm SD (n = 3). Values with different letters are significantly different (P < 0.05, see appendix B for statistical description). *P < 0.01 when comparing P2 with other cultures on day 5. **P < 0.04 when comparing P0 with other cultures on day 7. ***P < 0.05 when comparing P4 with other cultures on day 7.

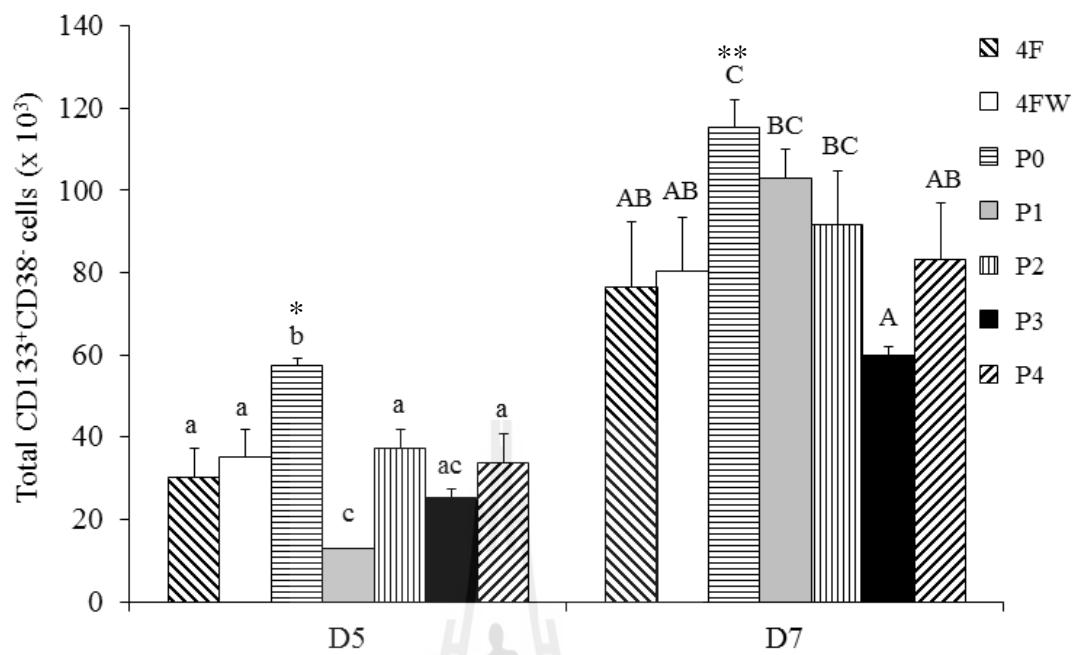


Figure 4.16 Total CD133⁺CD38⁻ cells in various cytokine cocktail in serum-free culture on day 5 and day 7. Values are expressed as the mean \pm SD (n = 3). Values with different letters are significantly different (P<0.05). *P<0.005 when comparing P0 with other cultures on day 5. **P<0.05 when comparing P0 with other cultures except P1 and P2 on day 7.

Table 4.5 Fold increase in total CD34⁺ and total CD133⁺ cells expansion of cells cultured in various cytokine cocktails in serum-free medium. Values are expressed as the mean \pm SD (n = 3).

| Cytokine cocktail | Total CD34 ⁺ cells | | Total CD133 ⁺ | |
|-------------------|-------------------------------|------------------------------|-----------------------------|-------------------------------|
| | D5 | D7 | D5 | D7 |
| 4F | 5.0 \pm 1.2 | 9.9 \pm 2.0 ^{*†} | 3.5 \pm 0.7 | 6.0 \pm 0.7 ^{***†} |
| 4FW | 6.2 \pm 1.2 [*] | 11.7 \pm 1.9 ^{*†} | 5.2 \pm 0.7 ^{**} | 6.3 \pm 0.4 ^{***} |
| P0 | 4.6 \pm 0.2 | 10.1 \pm 0.5 ^{*†} | 4.1 \pm 0.4 | 5.8 \pm 0.4 ^{***†} |
| P1 | 4.3 \pm 0.1 | 6.8 \pm 0.5 [†] | 1.4 \pm 0.1 | 2.9 \pm 0.4 [†] |
| P2 | 3.9 \pm 0.4 | 5.9 \pm 0.8 [†] | 1.7 \pm 0.2 | 3.0 \pm 0.4 [†] |
| P3 | 5.3 \pm 0.4 | 6.7 \pm 0.2 [†] | 2.8 \pm 0.4 | 3.5 \pm 0.3 |
| P4 | 4.2 \pm 0.9 | 9.4 \pm 1.5 ^{*†} | 3.2 \pm 0.9 | 5.9 \pm 1.0 ^{***†} |

Note: *P<0.05 when comparing with P2 on the same day of culture (on the same column), **P<0.05 when comparing with other culture conditions except P0 on day 5 (on the same column), ***P<0.01 when comparing with P1, P2 and P3 on day 7 (on the same column), [†]P<0.01 when comparing between day 5 and day 7 of each population on the same culture condition.

Overall, total CD34⁺ cells were found in the highest amount in 4FW culture throughout the culture period (D5: $5.8 \pm 1.1 \times 10^5$ and D7: $11.0 \pm 1.8 \times 10^5$ cells) compared to other culture (4F: $4.7 \pm 1.1 \times 10^5$ and $9.3 \pm 1.9 \times 10^5$, P0: $4.4 \pm 0.1 \times 10^5$ and $9.5 \pm 0.6 \times 10^5$, P1: $4.0 \pm 0.04 \times 10^5$ and $6.3 \pm 0.4 \times 10^5$, P2: $3.7 \pm 0.4 \times 10^5$ and $5.5 \pm 0.8 \times 10^5$, P3: $4.9 \pm 0.4 \times 10^5$ and $6.3 \pm 0.2 \times 10^5$, P4: $3.9 \pm 0.8 \times 10^5$ and $8.9 \pm 1.4 \times 10^5$ cells, respectively) as can be seen in Figure 4.17. Similarly, total CD133⁺ cells were found to be highest in 4FW culture (D5: $3.9 \pm 0.7 \times 10^5$ and D7: $4.7 \pm 0.8 \times 10^5$ cells) throughout 7 days of culture compared to other cocktails (4F: $2.7 \pm 0.6 \times 10^5$ and $4.5 \pm 0.9 \times 10^5$, P0: $3.1 \pm 0.1 \times 10^5$ and $4.3 \pm 0.3 \times 10^5$, P1: $1.1 \pm 0.01 \times 10^5$ and $2.1 \pm 0.1 \times 10^5$, P2: $1.3 \pm 0.1 \times 10^5$ and $2.2 \pm 0.3 \times 10^5$, P3: $2.1 \pm 0.2 \times 10^5$ and $2.6 \pm 0.1 \times 10^5$, P4: $2.4 \pm 0.5 \times 10^5$ and $4.4 \pm 0.7 \times 10^5$ cells, respectively; Figure 4.18). The summary of fold increase in expansion of total CD34⁺ cells and CD133⁺ cells were demonstrated in Table 4.5.

4.1.5 Determination of phenotype and *in vitro* hematopoiesis of expanded cells in various cytokine cocktails in serum-free medium

Phenotypic characteristics of progenitor cells in all cultures were further investigated for myeloid, lymphoid and erythroid lineages analysis as previously described. The data showed the significant presence of early markers of myeloid/erythroid progenitors (CD33⁺CD71⁺ cells, P0: $72.1 \pm 12.3\%$, P1: $65.9 \pm 0.9\%$, P2: $61.2 \pm 5.7\%$, P3: $65.4 \pm 14.9\%$, and P4: $63.7 \pm 8.9\%$, n = 3) whereas lymphoid progenitors were found in a few number (CD3⁺CD19⁺, P0: $3.5 \pm 2.6\%$, P1: $2.7 \pm 0.9\%$, P2: $1.9 \pm 0.8\%$, P3: $4.5 \pm 2.9\%$, and P4: $3.8 \pm 2.1\%$) as shown in Figure

4.19. These data suggest the differentiation toward myeloid/erythroid lineage rather than lymphoid lineage in all cultures.

Next, hematopoiesis of expanded CD34⁺ cells in all cytokine cocktails were verified by clonogenic assay and liquid differentiation. The number of colony forming cells; CFU-GEMM, CFU-GM, and BFU-E obtained from each cytokine cocktail culture were summarized in Table 4.6 (n = 3 per group). The number of CFU-GEMM, CFU-GM, and BFU-E grown in methylcellulose that obtained from cells expanded in all cultures did not show difference than those of fresh CD34⁺ cells control (Figures 4.20-4.22). The number of CFU-GEMM was highest in the group P2 culture (9 ± 1 colonies) compared to other culture medium (4F: 3 ± 1, 4FW: 3 ± 1, P0: 7 ± 2, P1: 5 ± 3, P3: 7 ± 1, P4: 5 ± 1 colonies) as shown in Figure 4.20. On the contrary, the highest numbers of CFU-GM and BFU-E were found in the group of P0 culture (18 ± 1 and 90 ± 3 colonies, respectively) compared to other culture medium (4F: 9 ± 2 and 70 ± 8, 4FW: 13 ± 8 and 75 ± 6, P1: 9 ± 1 and 77 ± 4, P2: 11 ± 3 and 60 ± 3, P3: 15 ± 2 and 69 ± 3, and P4: 13 ± 3 and 69 ± 4 colonies, respectively) as shown in Figures 4.21 and 4.22, respectively. Furthermore, expanded cells in P0, P1, P2, P3 and P4 cocktails could differentiate into more mature blood cells; megakaryocytes, erythroid cells, lymphocytes, macrophages, granulocytes, and mast cells in liquid culture differentiation assay (Figures 4.23-4.27). These data suggest the potency of expanded cells in *in vitro* hematopoiesis.

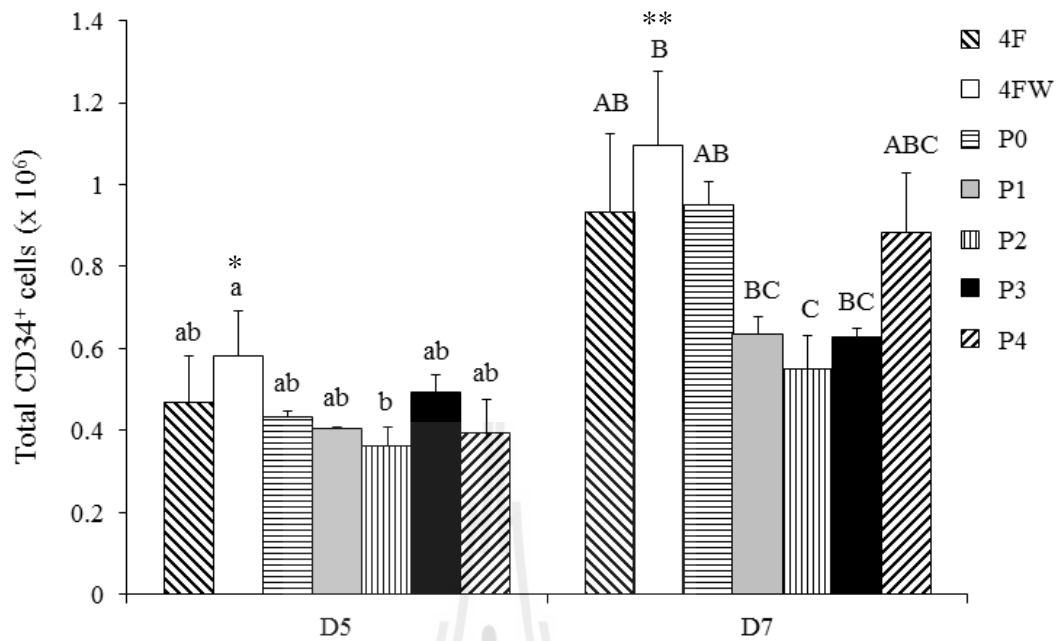


Figure 4.17 Total CD34⁺ cells in various cytokine cocktail in serum-free culture on day 5 and day 7. Values are expressed as the mean \pm SD (n = 3). Values with different letters are significantly different (P<0.05). *P<0.04 when comparing 4FW with P2 on day 5. **P<0.01 when comparing 4FW with P2 on day 7.

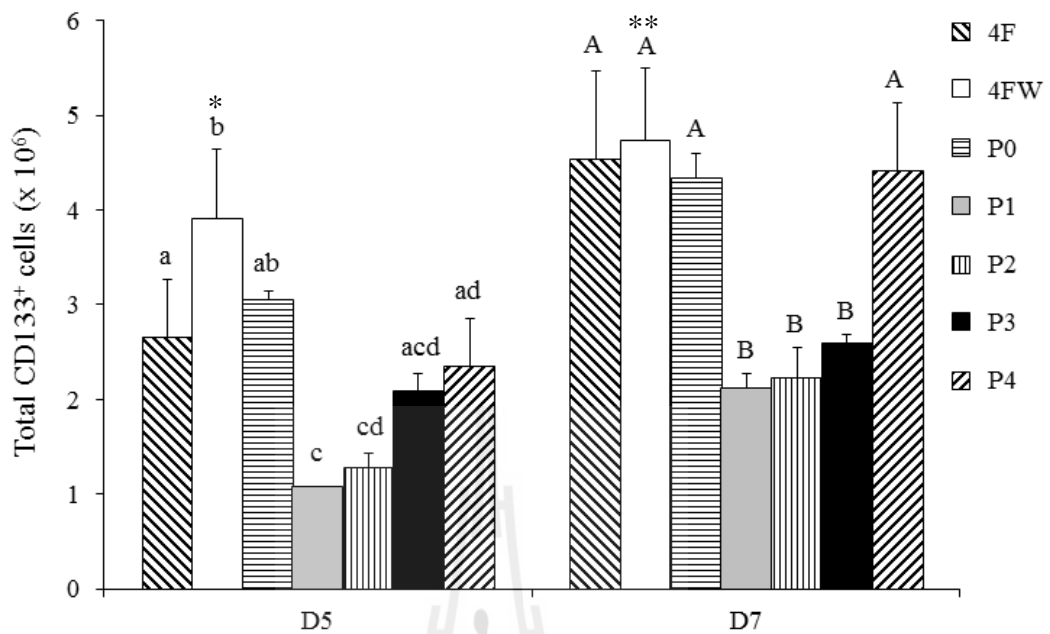


Figure 4.18 Total CD133⁺ cells in various cytokine cocktail in serum-free culture on day 5 and day 7. Values are expressed as the mean \pm SD (n = 3). Values with different letters are significantly different (P<0.05). *P<0.01 when comparing 4FW with other cultures except P0 on day 5. **P<0.006 when comparing 4FW with P1, P2, and P3 on day 7.

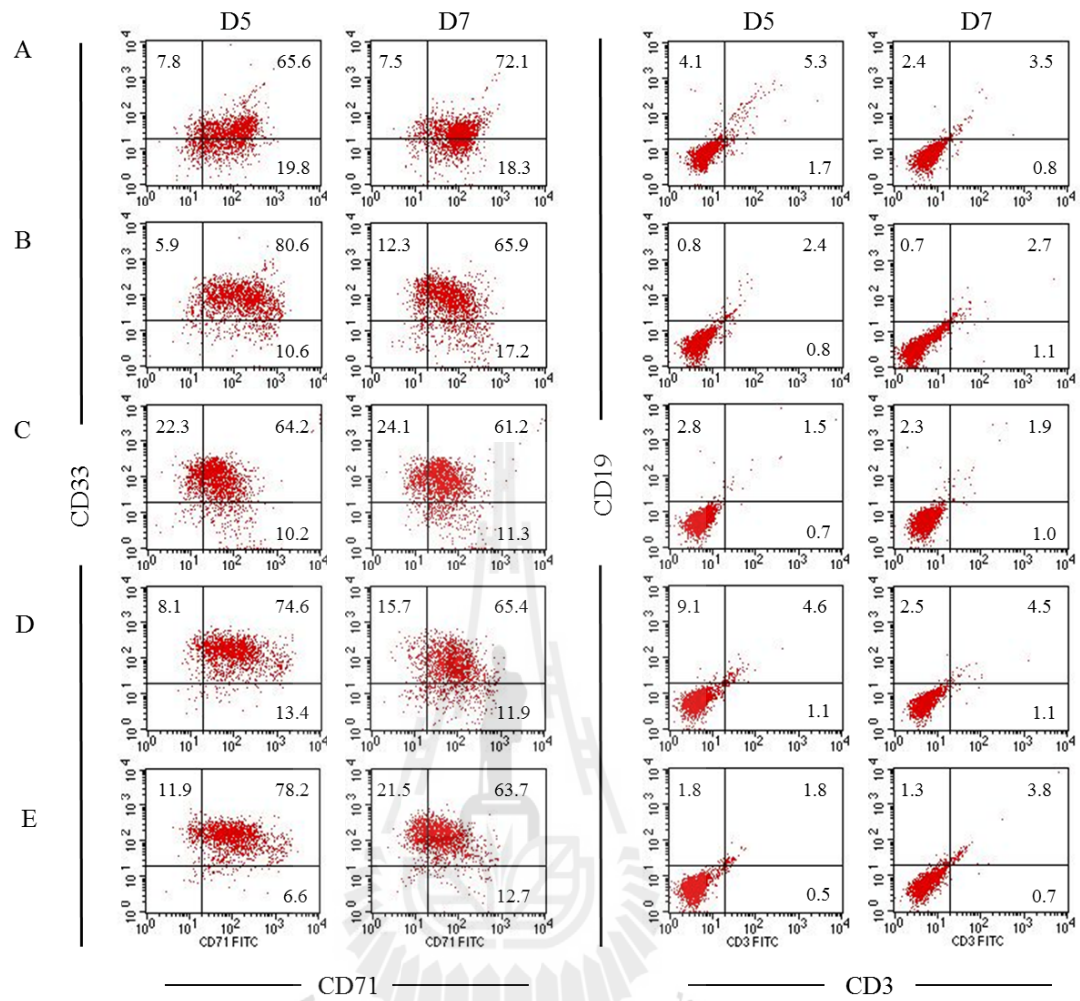


Figure 4.19 Representative of flow cytometry analysis of CD3, CD19, CD33 and CD71 expressions in expanded CD34⁺ cells cultured in P0 (A), P1 (B), P2 (C), P3 (D) and P4 (E) in serum-free medium at day 5 and day 7. Values are expressed as the mean (n = 3).

Table 4.6 Total number of colony forming cells grown on methylcellulose at day 14. Cells cultured on methylcellulose obtained from day 5 expanded CD34⁺ cells obtained various cocktails in serum-free medium compared to fresh CD34⁺ cells. Values are expressed as the mean \pm SD (n = 3).

| Medium | CFU-GEMM | CFU-GM | BFU-E |
|---------------|-----------|------------|-------------|
| Fresh isolate | 6 \pm 4 | 16 \pm 4 | 80 \pm 4 |
| 4F | 3 \pm 1 | 9 \pm 6 | 70 \pm 14 |
| 4FW | 3 \pm 1 | 13 \pm 8 | 75 \pm 10 |
| P0 | 7 \pm 3 | 18 \pm 2 | 90 \pm 6 |
| P1 | 5 \pm 3 | 9 \pm 2 | 77 \pm 6 |
| P2 | 9 \pm 2 | 11 \pm 5 | 60 \pm 6 |
| P3 | 7 \pm 1 | 15 \pm 3 | 69 \pm 5 |
| P4 | 5 \pm 3 | 13 \pm 5 | 69 \pm 7 |

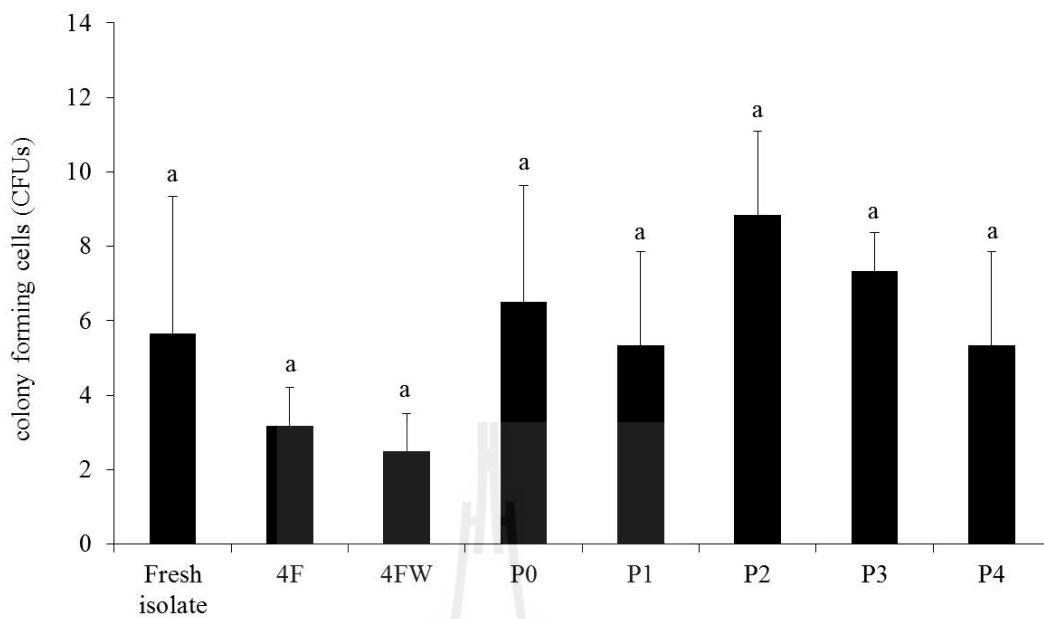
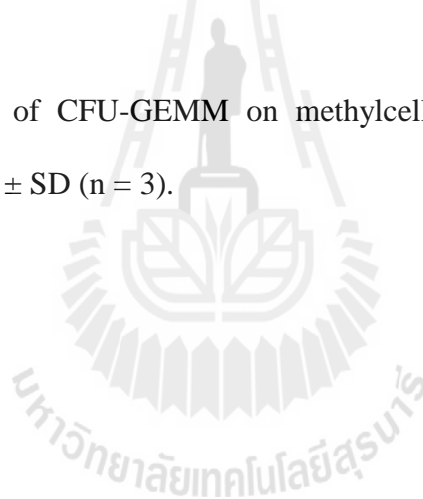


Figure 4.20 Number of CFU-GEMM on methylcellulose at day 14. Values are expressed as the mean \pm SD (n = 3).



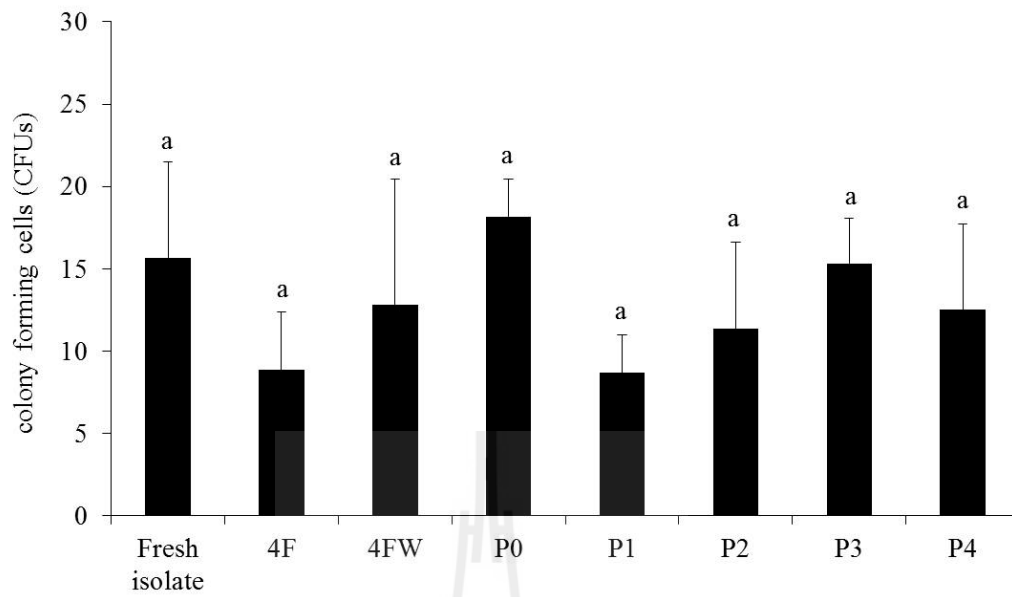


Figure 4.21 Number of CFU-GM on methylcellulose at day 14. Values are expressed as the mean \pm SD (n = 3).

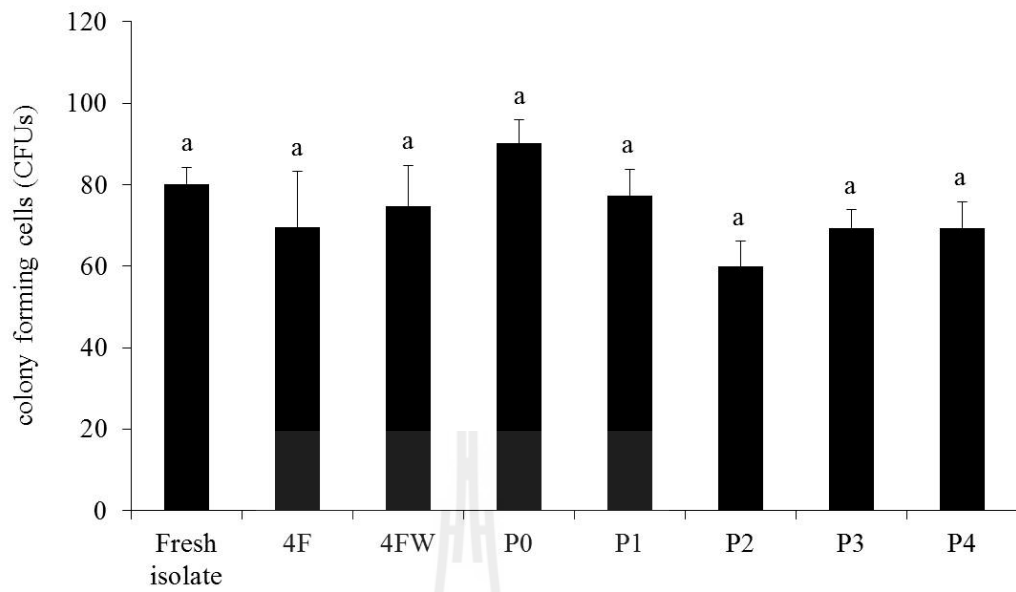
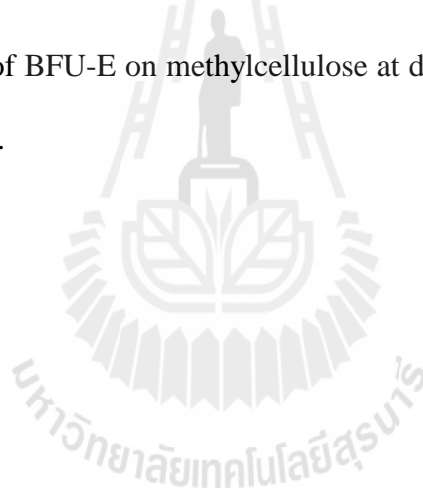


Figure 4.22 Number of BFU-E on methylcellulose at day 14. Values are expressed as the mean \pm SD (n = 3).



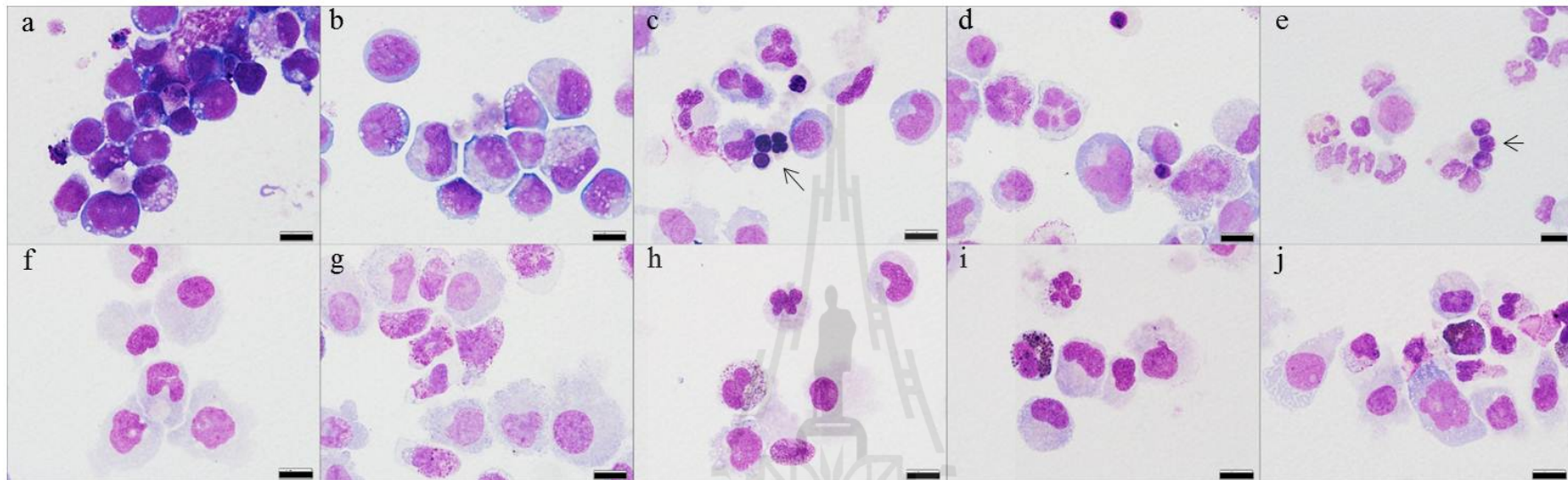


Figure 4.23 Differentiation capacities of expanded CB-CD34⁺ cells from P0 KSR *in vitro*. (a) Undifferentiated day 5 expanded CB-CD34⁺ cells, (b) day 7 expanded CD34⁺ cells, (c) erythroid lineage differentiation (EPO + SCF, arrow), (d) megakaryocytes differentiation (TPO + SCF), (e) lymphoid lineage differentiation (IL-7 + Flt3-L + SCF + OP9, arrow), (f-g) granulocytes and macrophage lineages differentiation (GM-CSF + IL-3), (h-j) mast cells and granulocyte lineages differentiation (SCF + IL-3). Scale bar = 10 μ m.

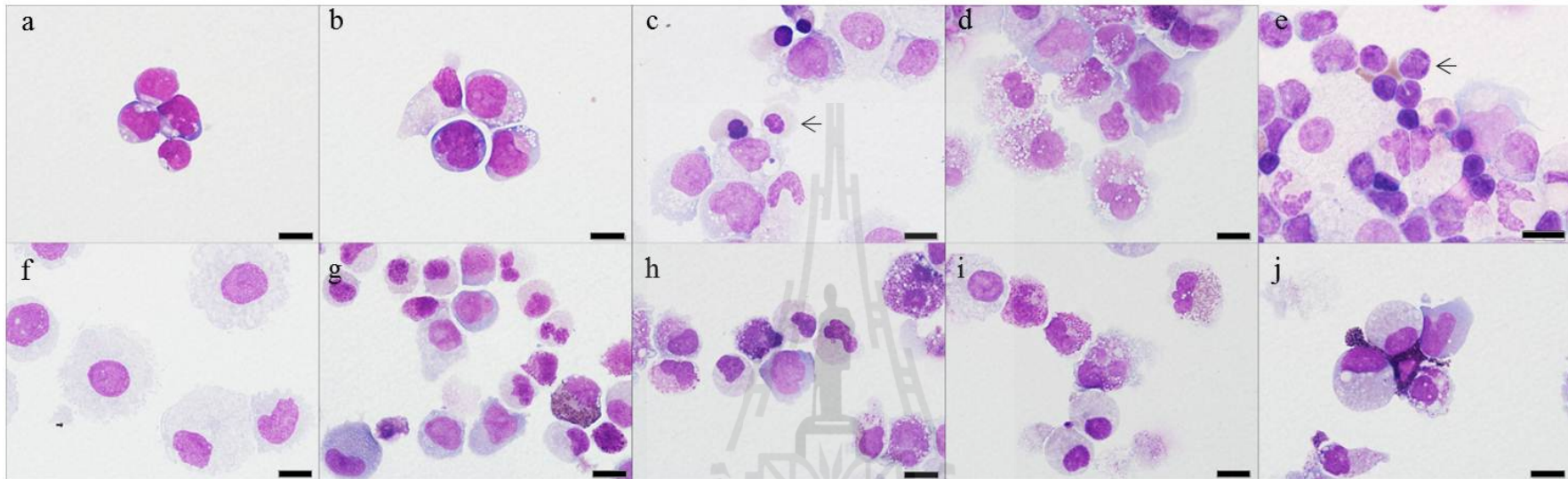


Figure 4.24 Differentiation capacities of expanded CB-CD34⁺ cells from P1 KSR *in vitro*. (a) Undifferentiated day 5 expanded CB-CD34⁺ cells, (b) day 7 expanded CD34⁺ cells, (c) erythroid lineage differentiation (EPO + SCF, arrow), (d) megakaryocytes differentiation (TPO + SCF), (e) lymphoid lineage differentiation (IL-7 + Flt3-L + SCF + OP9, arrow), (f-g) granulocytes and macrophage lineages differentiation (GM-CSF + IL-3), (h-j) mast cells and granulocyte lineages differentiation (SCF + IL-3). Scale bar = 10 μ m.

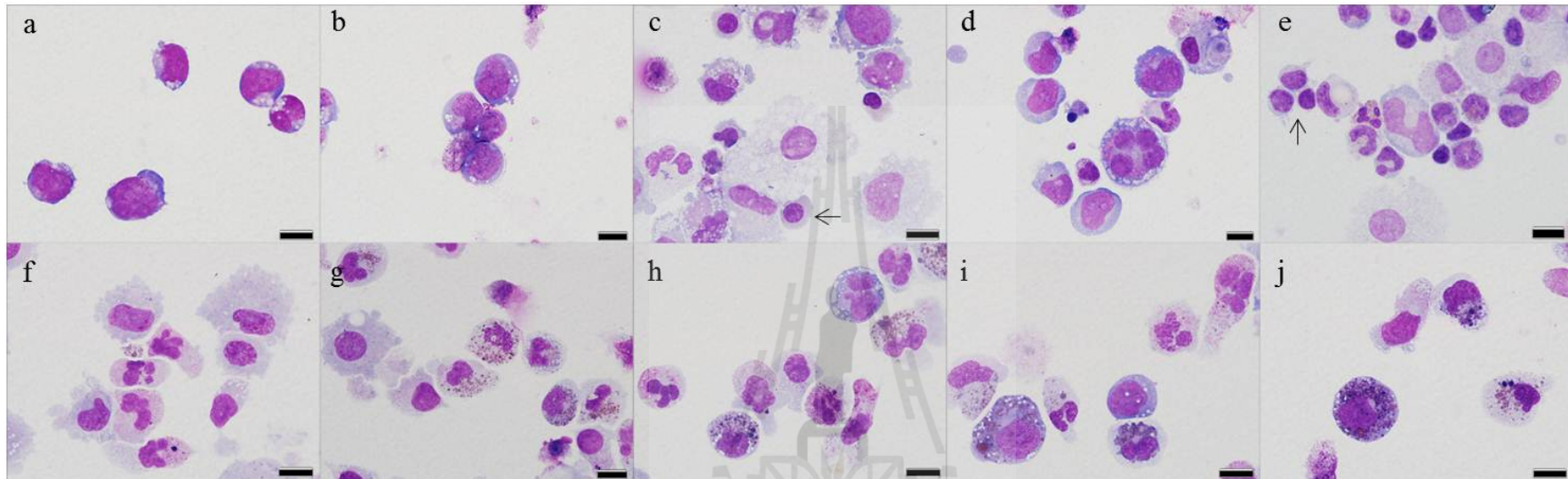


Figure 4.25 Differentiation capacities of expanded CB-CD34⁺ cells from P2 KSR *in vitro*. (a) Undifferentiated day 5 expanded CB-CD34⁺ cells, (b) day 7 expanded CD34⁺ cells, (c) erythroid lineage differentiation (EPO + SCF, arrow), (d) megakaryocytes differentiation (TPO + SCF), (e) lymphoid lineage differentiation (IL-7 + Flt3-L + SCF + OP9, arrow), (f-g) granulocytes and macrophage lineages differentiation (GM-CSF + IL-3), (h-j) mast cells and granulocyte lineages differentiation (SCF + IL-3). Scale bar = 10 μ m.

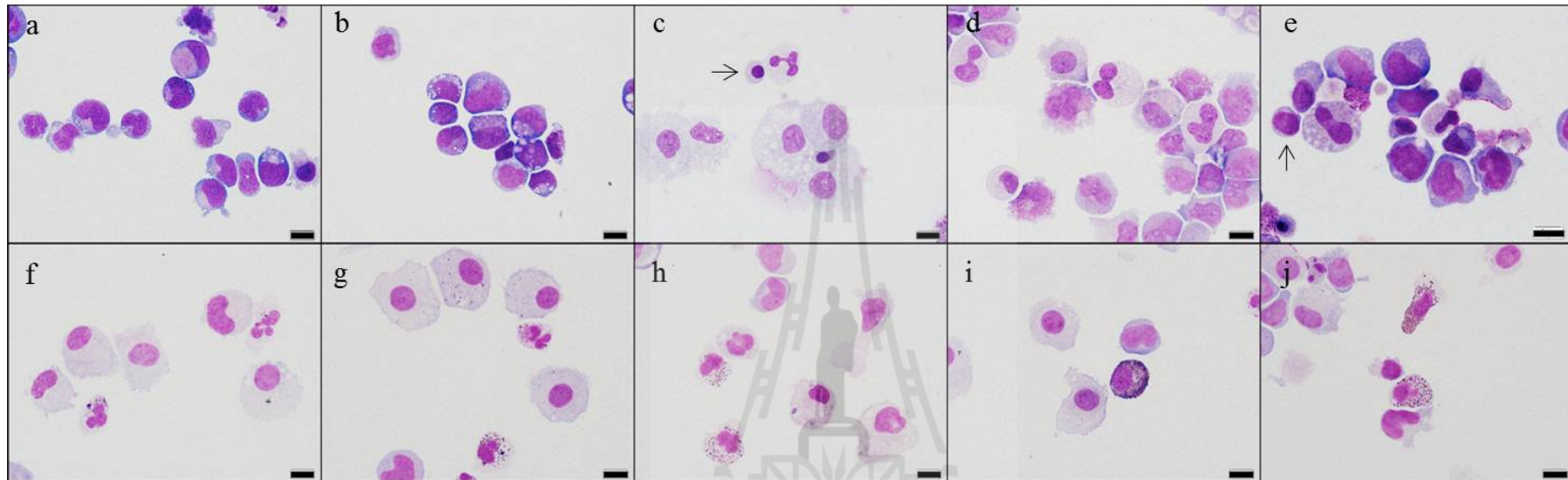


Figure 4.26 Differentiation capacities of expanded CB-CD34⁺ cells from P3 KSR *in vitro*. (a) Undifferentiated day 5 expanded CB-CD34⁺ cells, (b) day 7 expanded CD34⁺ cells, (c) erythroid lineage differentiation (EPO + SCF, arrow), (d) megakaryocytes differentiation (TPO + SCF), (e) lymphoid lineage differentiation (IL-7 + Flt3-L + SCF + OP9, arrow), (f-g) granulocytes and macrophage lineages differentiation (GM-CSF + IL-3), (h-j) mast cells and granulocyte lineages differentiation (SCF + IL-3). Scale bar = 10 µm.

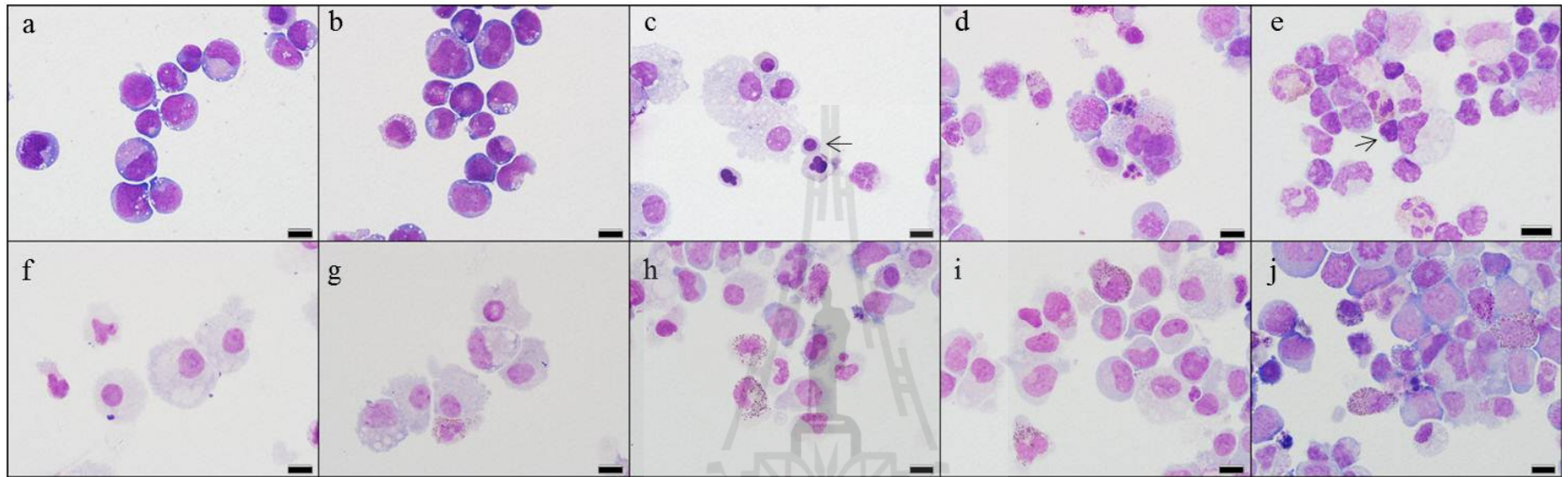


Figure 4.27 Differentiation capacities of expanded CB-CD34⁺ cells from P4 KSR *in vitro*. (a) Undifferentiated day 5 expanded CB-CD34⁺ cells, (b) day 7 expanded CD34⁺ cells, (c) erythroid lineage differentiation (EPO + SCF, arrow), (d) megakaryocytes differentiation (TPO + SCF), (e) lymphoid lineage differentiation (IL-7 + Flt3-L + SCF + OP9, arrow), (f-g) granulocytes and macrophage lineages differentiation (GM-CSF + IL-3), (h-j) mast cells and granulocyte lineages differentiation (SCF + IL-3). Scale bar = 10 µm.

4.1.6 Pluripotency genes expression in expanded cells

Real-time RT PCR was performed to determine the relative expression of pluripotency genes; *Nanog* and *Oct3/4* in expanded CD34⁺ cells that culture in all cocktails in serum-free medium. The results demonstrated that cells expanded in 4F, 4FW, P0, and P3 did not revealed significantly change in relative expression of *Nanog* compared to that of freshly isolated CD34⁺ cells (4F: 0.4 ± 0.1 , 4FW: 58.5 ± 27.5 , P0: 67.2 ± 25.6 and P3: 34.1 ± 20.1 ; Figure 4.28). Interestingly, the expression of *Nanog* increased significantly in the culture of P1 (98.5 ± 38.7), P2 (114.62 ± 35.5) and P4 (74.4 ± 3.3). On the contrary, expanded cells cultured in all cytokine cocktails conferred the significantly increase in relative expression of *Oct3/4* except in those of 4F cocktail (4F: 0.5 ± 0.1 , 4FW: 45.4 ± 16.0 , P0: 49.4 ± 4.5 , P1: 106.1 ± 25.8 , P2: 102.6 ± 24.6 , P3: 63.6 ± 23.0 and P4: 42.7 ± 17.7 ; Figure 4.29). Of note, P2 and P1 displayed the highest *Nanog* and *Oct3/4* gene expressions, respectively. The cDNA PCR products of *Nanog* (255 bp), *Oct3/4* (230 bp) and GAPDH (302 bp) are shown in Figure 4.30. These data indicate that expanded cells could be preserved in stemness like state in the new cytokine cocktails.

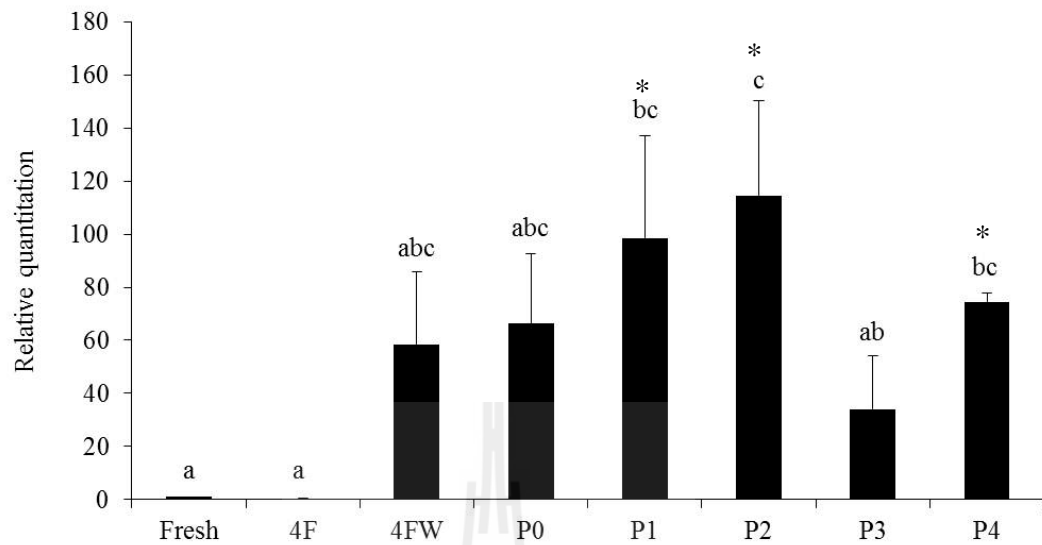


Figure 4.28 Relative quantitation of *Nanog* gene expression analyzed by RT real-time PCR of expanded CB-CD34⁺ cells cultured in different cytokine cocktails. Values are expressed as the mean \pm SD (n = 3). Values with different letters are significantly different (P<0.05). *P<0.03 when comparing P1, P2 and P4 with fresh isolate.

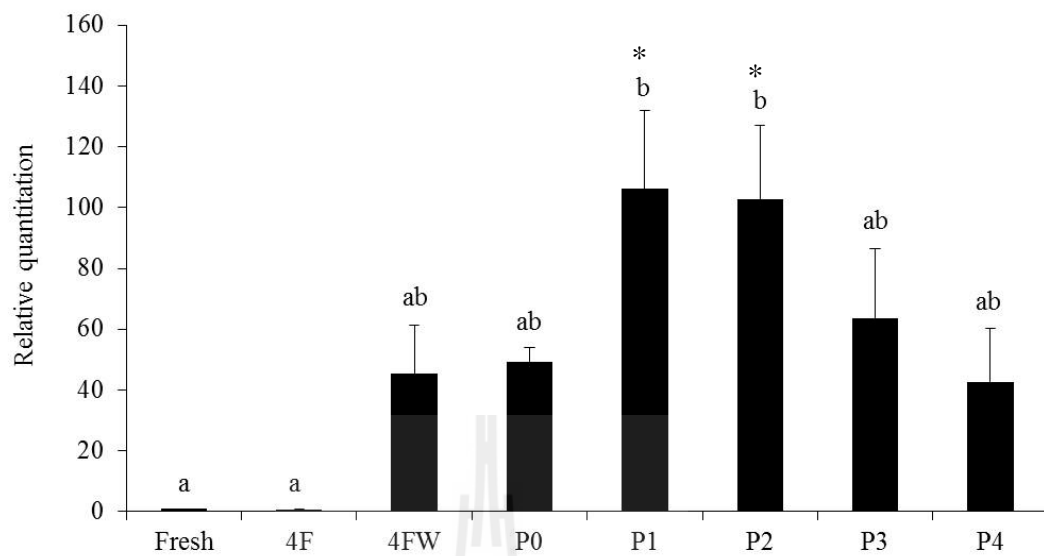


Figure 4.29 Relative quantitation of *Oct3/4* gene expression analyzed by RT real-time PCR of expanded CB-CD34⁺ cells cultured in different cytokine cocktails. Values are expressed as the mean \pm SD (n = 3). Values with different letters are significantly different (P<0.05). *P<0.003 when comparing P1 and P2 with fresh isolate.

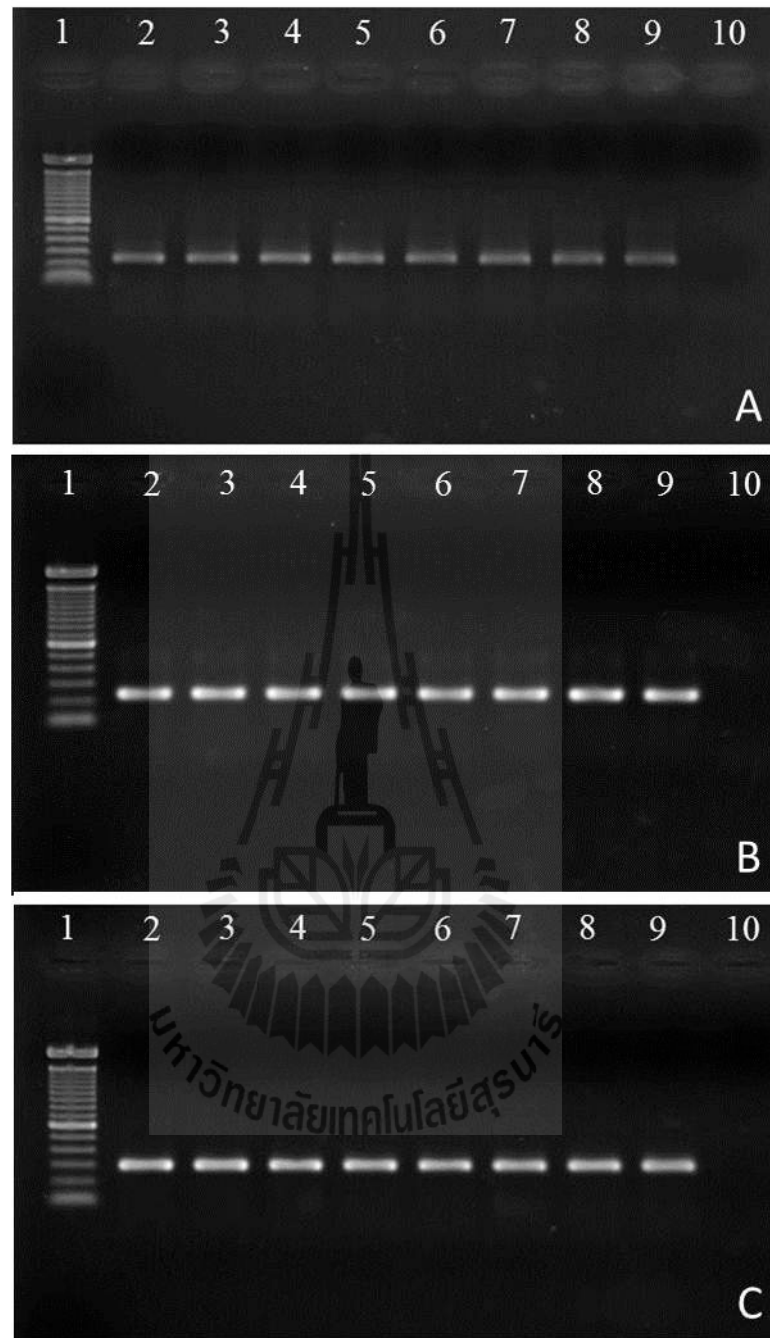


Figure 4.30 Agarose gel electrophoresis of specific PCR products without non-specific amplification of *Nanog* (A), *Oct3/4* (B) and *GAPDH* (C) genes obtained from real-time RT PCR. The bands were 100 bp marker (1), cDNA products obtained from fresh CD34⁺ cells (2), and expanded cells cultured in 4F (3), 4FW (4), P0 (5), P1 (6), P2 (7), P3 (8), P4 (9) and negative control (10).

4.1.7 Wound healing in streptozotocin-induced diabetic mice

In order to identify the use of expanded cells obtained from the new cytokine cocktail for translation medicine, wound assay in diabetic mice was performed. ICR mice injected with multi-low dose injection of STZ could induce diabetic in all mice with blood glucose level of 368 ± 50 mg/dl (normal blood glucose; 144 ± 50 mg/dl, $n = 24$) before start the wound assay. STZ-induced diabetic mice achieved the 50% wound closure by day 7 after wounding (Figure 4.31). When freshly isolated $CD34^+$ cells were injected around full-thickness dermal wounds created on the diabetic mice, wound closure achieved the 50% as early as day 3. Moreover, fresh $CD34^+$ cells significantly accelerated the wound closure at day 5 after injury compared to PBS-treated wounds (fresh isolate: $38.3 \pm 9.1\%$, PBS: $67.2 \pm 13.6\%$, $n = 3$; Figures 4.31-4.32). This significant reduction was also observed on the day 9 of the wounding (fresh isolate: $16.4 \pm 3.3\%$, PBS: $26.8 \pm 5.3\%$). Expanded $CD34^+$ cells injection could achieve 50% wound closure on day 5 of wounding ($41.3 \pm 10.3\%$) and accelerate wound closure as compared to PBS-treated wounds but not statistical significance (Figures 4.31 and 4.32). However, the significant reduction of wound closure was found on day 9 after wound ($14.9 \pm 3.6\%$) compared to PBS-treated wounds. On the other hand, cytokine-injected wounds did not improve wound closure when compared to PBS-treated wounds throughout the study period. All mice after day 9 of wounding remained diabetic with blood glucose level higher than 600 mg/dl for three mice and the remaining were 551.4 ± 53.0 mg/dl.

Histologic analysis of wound sections confirmed the acceleration of wound healing in fresh $CD34^+$ cells- or expanded $CD34^+$ cells-treated diabetic wounds. The results showed the advanced re-epithelialization over the wound bed area and a more

arrangement of collagen than those observed in PBS-treated group (Figure 4.33). In addition, fresh CD34⁺ cells- (1.2 ± 0.4 mm) and expanded CD34⁺ cells-treated (1.3 ± 0.3 mm) wounds showed a significant reduction in epithelial gap range than that of PBS-treated wound (2.0 ± 0.5 mm), whereas, the epithelial gap of 4FW cytokine-treated wound (1.8 ± 0.5 mm) was not different (Figure 4.34; n= 6).

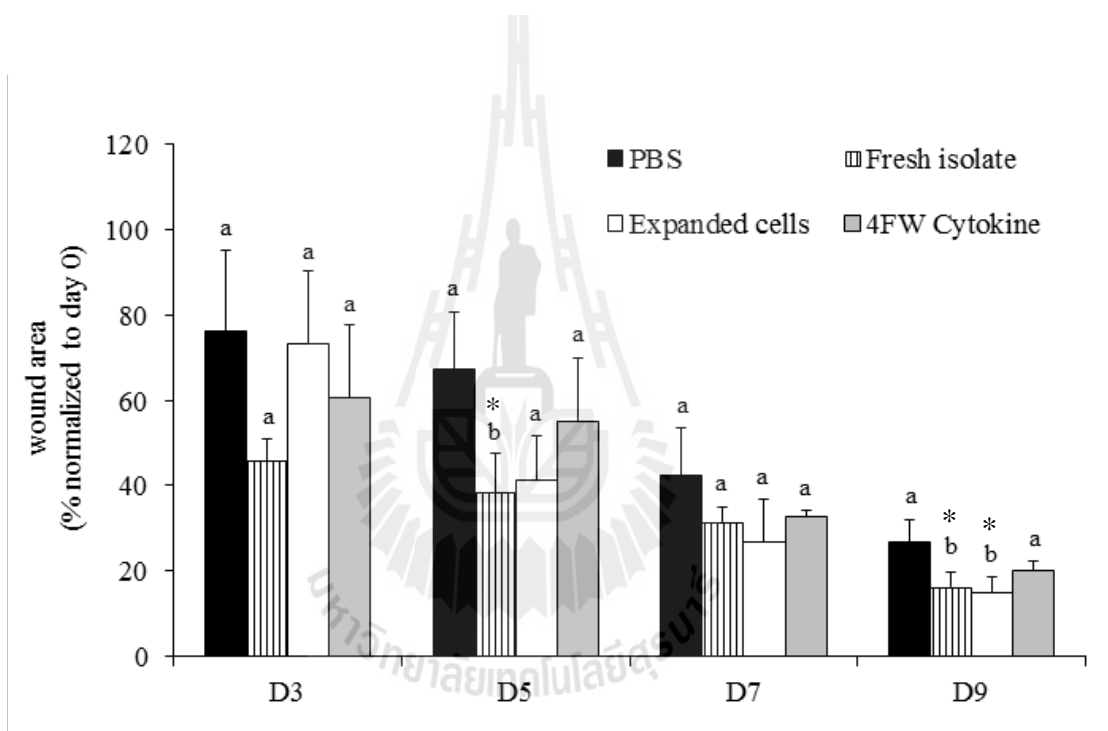


Figure 4.31 Percentage of opened wound area as normalized to the day 0. Mice were treated with PBS, freshly isolated CD34⁺ cells, expanded CD34⁺ cells and 4FW cytokine around the full-thickness dermal wound on day 0 (n = 6). Values are expressed as the mean \pm SD. Values with different letters on the same day of wounding are significantly different. *P<0.05 when comparing with PBS control on the same day of observation.

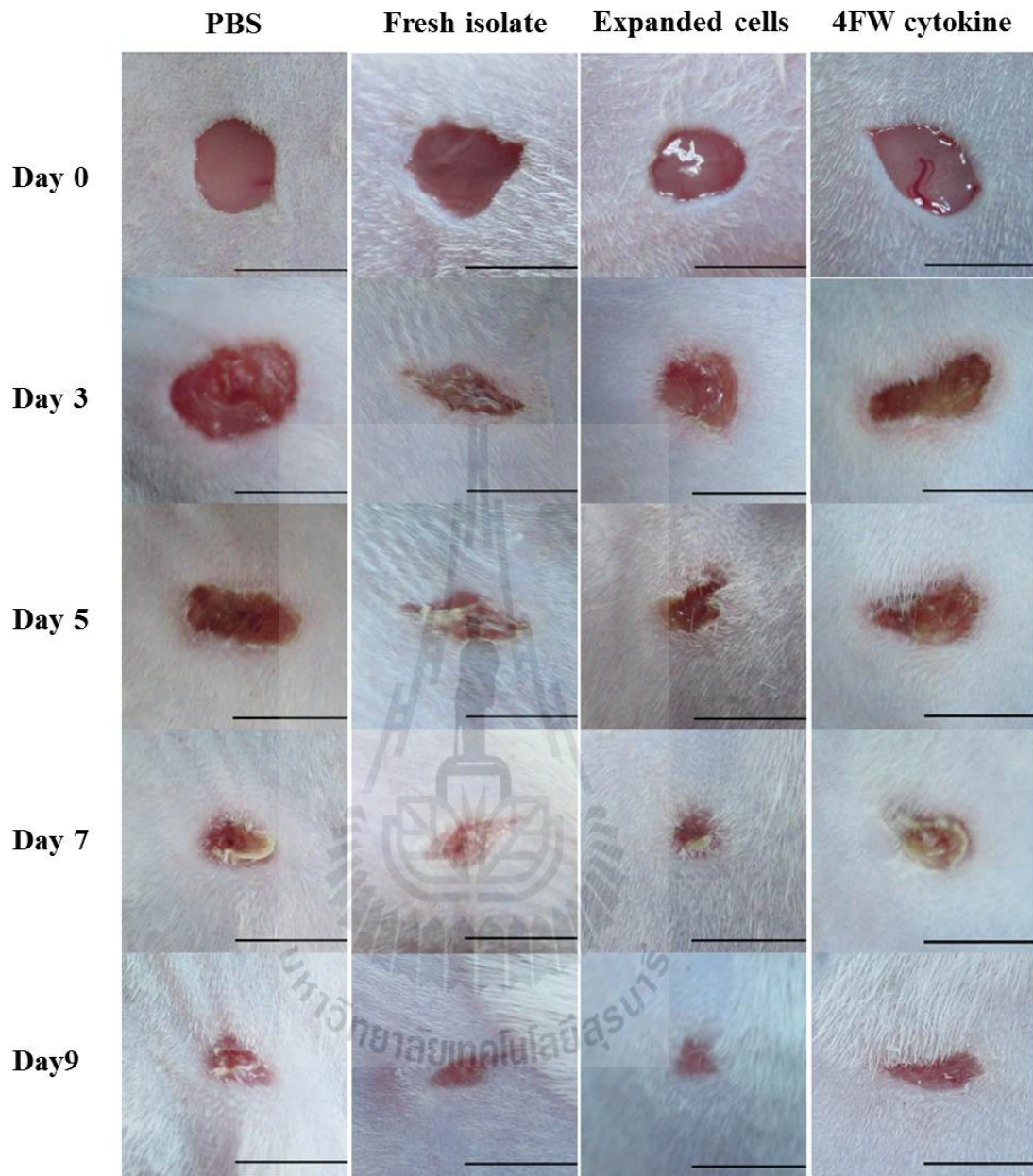


Figure 4.32 Representative photographic pictures of wound healing in mice treated with PBS, freshly isolated CD34⁺ cells, expanded CD34⁺ cells and 4FW cytokine on day 0, day 3, day 5 and day 9 after wounding. Scale bar = 5 μ m.

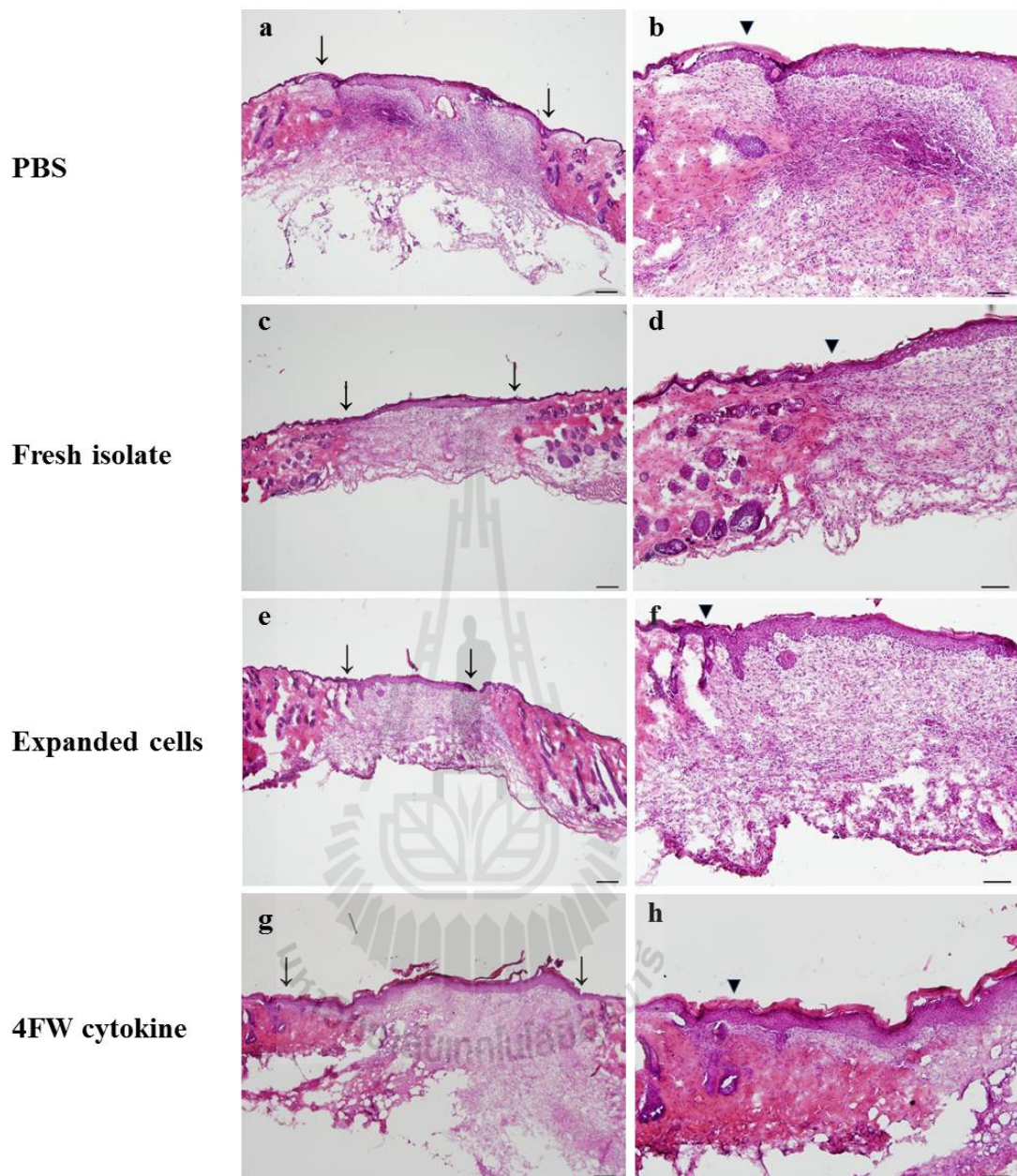


Figure 4.33 Histologic analysis of day 9 wound sections from PBS- (a), freshly isolated $CD34^+$ cells- (c), day 5 expanded $CD34^+$ cells- (e) and 4FW cytokine- (g) treated wounds. The length of edge measurement of epithelial gap is indicated by arrow. Scale bar = 200 μm . Corresponding higher power magnification (b, d, f, h) represents the right edge of epithelial margin (arrow head) that connected to the original epidermis and superior to the granulation tissue. Scale bar = 100 μm .

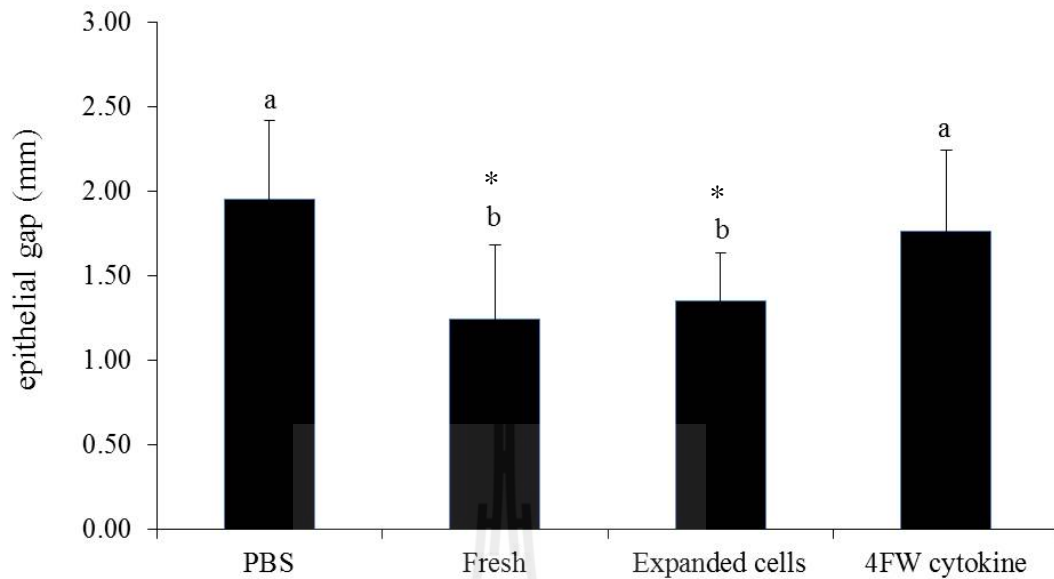


Figure 4.34 Epithelial gap of the day 9 wounds treated with PBS, freshly isolated CD34⁺ cells, expanded CD34⁺ cells and 4FW cytokine. Values are expressed as the mean \pm SD (n = 6). Values with different letters are significantly different when compared to the PBS control. *P<0.03 when comparing with PBS control.

4.1.8 Macrophage and capillary contents in treated wounds

Immunofluorescent staining of tissue section for CD68-positive macrophages revealed the significant increase number in wound treated with freshly isolated CD34⁺ cells (93 ± 8 cells/HPF), expanded CD34⁺ cells (104 ± 20 cells/HPF), and 4FW cytokine (96 ± 11 cells/HPF) compared to PBS-treated wound tissue (81 ± 10 cells/HPF) at day 5 after dermal excision as shown in Figure 4.35. The representative images are shown in Figure 4.36. On the other hand, the number of macrophage contents on freshly isolated CD34⁺ cells- (61 ± 11 cells/HPF), expanded CD34⁺ cells- (65 ± 9 cells/HPF) and 4FW cytokine- (48 ± 12 cells/HPF) treated wound decreased

significantly at day 9 of wounding when compared to the PBS control (92 ± 12 cells/HPF) as shown in Figure 4.35. The representative images are shown in Figure 4.37.

Similarly, endothelial cell-specific staining for CD31 showed a significant increase in capillary content on wound treated with freshly isolated CD34⁺ cells (37 ± 4 cells/HPF), expanded CD34⁺ cells (41 ± 8 cells/HPF), and 4FW cytokine (27 ± 2 cells/HPF) compared to PBS-treated wound tissue (14 ± 3 cells/HPF) at day 5 after dermal excision (Figures 4.38-4.39). Of note, the endothelial cells were generated at the lateral transitional zone of the normal epidermis at day 5 of the wound treated with PBS, while the other experimental groups contained the more advanced filtration of endothelial cells inside the wound tissue area and formed microvessels (Figure 4.39). At day 9, the number of CD31-positive cells in freshly isolated CD34⁺ cells (41 ± 5 cells/HPF), expanded CD34⁺ cells (44 ± 8 cells/HPF), and 4FW cytokine (37 ± 5 cells/HPF) remained higher than those observed in PBS-treated wound (27 ± 4 cells/HPF). Moreover, all experimental groups showed a gradually increase in CD31-positive cells than those of day 5 after dermal excisional (Figures 4.38-4.40).

Additionally, the human CD34⁺ cells were observed within the wound area and normal epidermis nearby in the small quantity of wound tissue treated with freshly isolated CD34⁺ cells and expanded CD34⁺ cells at day 5 and day 9 after wounding (Figures 4.41-4.44). Thus, these data suggest the role of fresh CD34⁺ cells and expanded CD34⁺ cells obtained from 4FW culture in the acceleration of wound healing in diabetic mice.

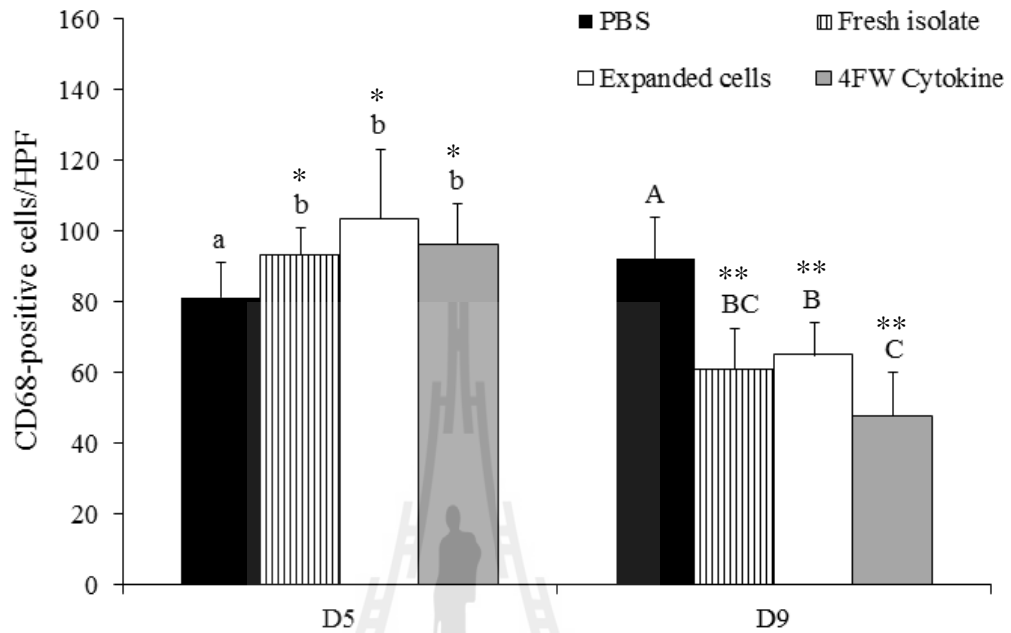


Figure 4.35 CD68-positive cells on wounds treated with PBS, freshly isolated CD34⁺ cells, expanded CD34⁺ cells and 4FW cytokine on day 5 and 9 after wounding. Values are expressed as the mean \pm SD (n = 6). Values with different letters are significantly different when compared to the PBS control (P<0.05). *P<0.05 when comparing with PBS control. **P<0.002 when comparing with PBS control.

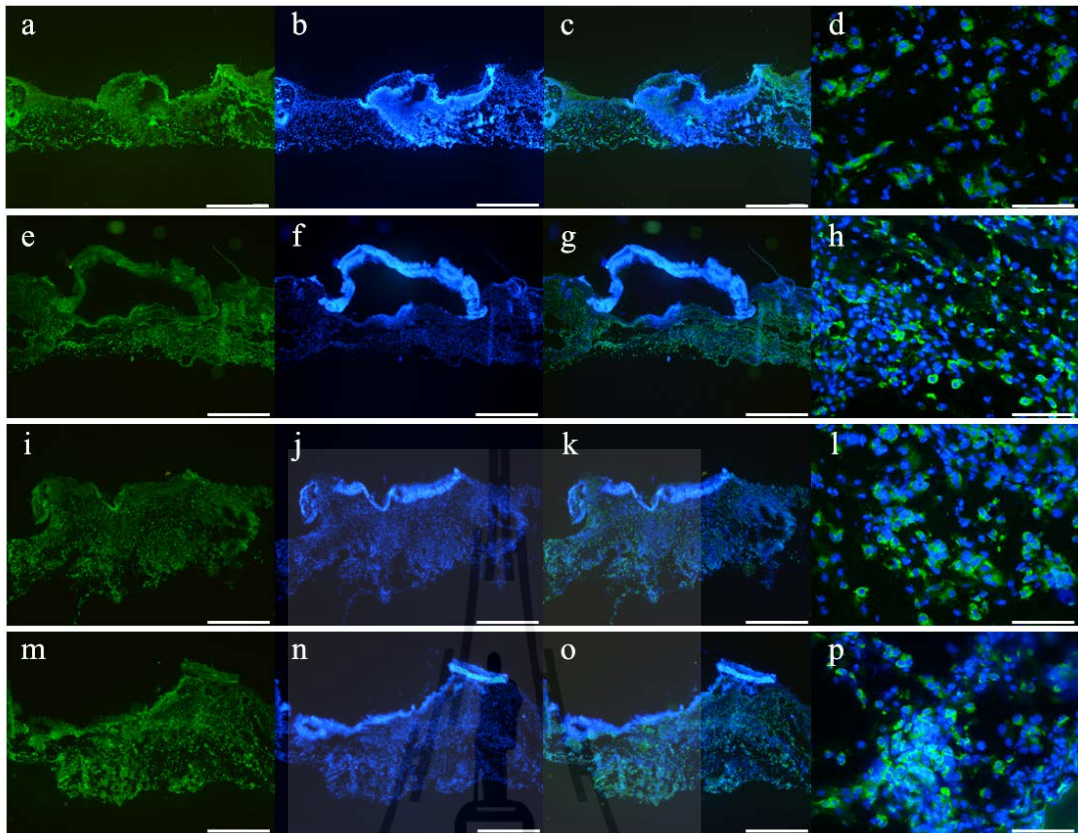


Figure 4.36 Immunofluorescent staining for macrophage marker CD68 (green) on wound tissue treated with PBS (a), freshly isolated CD34⁺ cells (e), expanded CD34⁺ cells (i) and 4FW cytokine (m) sections at day 5 after wounding (the first column). Counterstaining of nuclei with DAPI (blue) on the same sections are represented on the second column (b, f, j, n). The overlay images of the 2nd and 3rd columns (c, g, k, o) are represented on the third column. Scale bar = 400 μm . High magnification images of CD31-positive cells are represented on the fourth column (d, h, l, p). Scale bar = 80 μm .

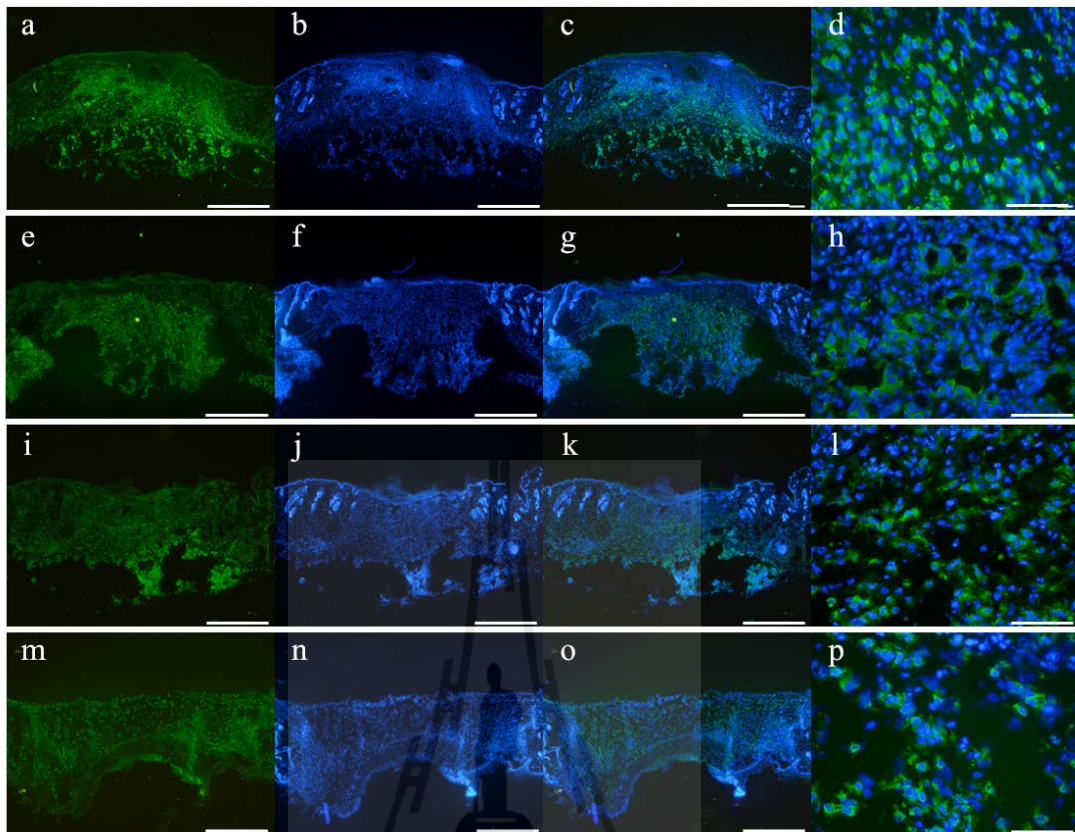


Figure 4.37 Immunofluorescent staining for macrophage marker CD68 (green) on wound tissue treated with PBS (a), freshly isolated CD34⁺ cells (e), expanded CD34⁺ cells (i) and 4FW cytokine (m) sections at day 9 after wounding (the first column). Counterstaining of nuclei with DAPI (blue) on the same sections are represented on the second column (b, f, j, n). The overlay images of the 2nd and 3rd columns (c, g, k, o) are represented on the third column. Scale bar = 400 μm . High magnification images of CD31-positive cells are represented on the fourth column (d, h, l, p). Scale bar = 80 μm .

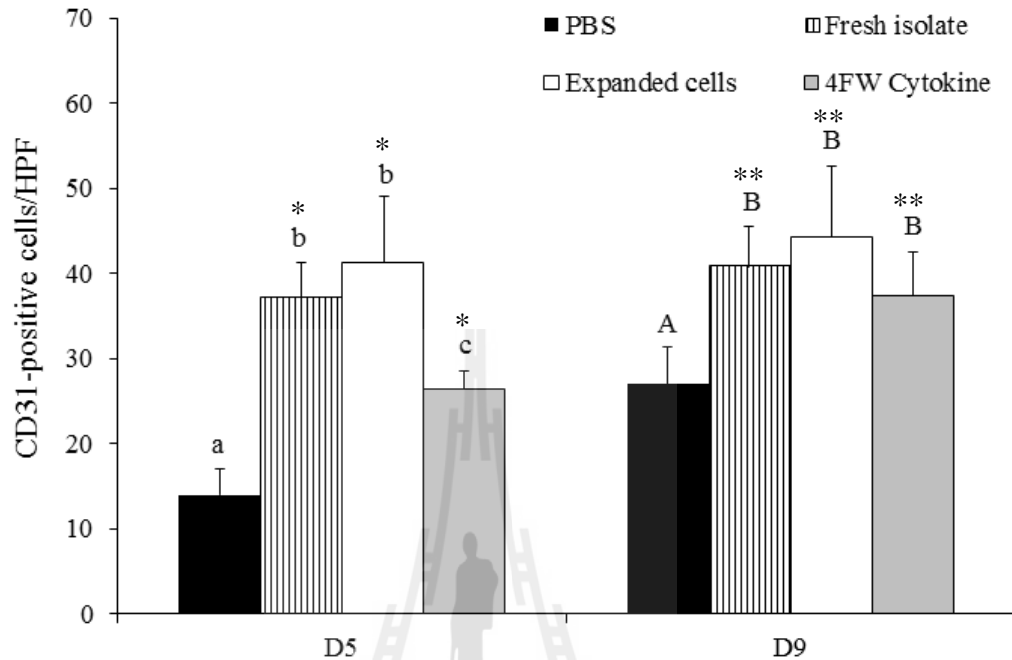


Figure 4.38 CD31-positive cells on wounds treated with PBS, freshly isolated CD34⁺ cells, expanded CD34⁺ cells and 4FW cytokine on day 5 and 9 after wounding. Values are expressed as the mean \pm SD (n = 6). Values with different letters are significantly different when compared to the PBS control (P<0.05). *P<0.001 when comparing with PBS control. **P<0.005 when comparing with PBS control.

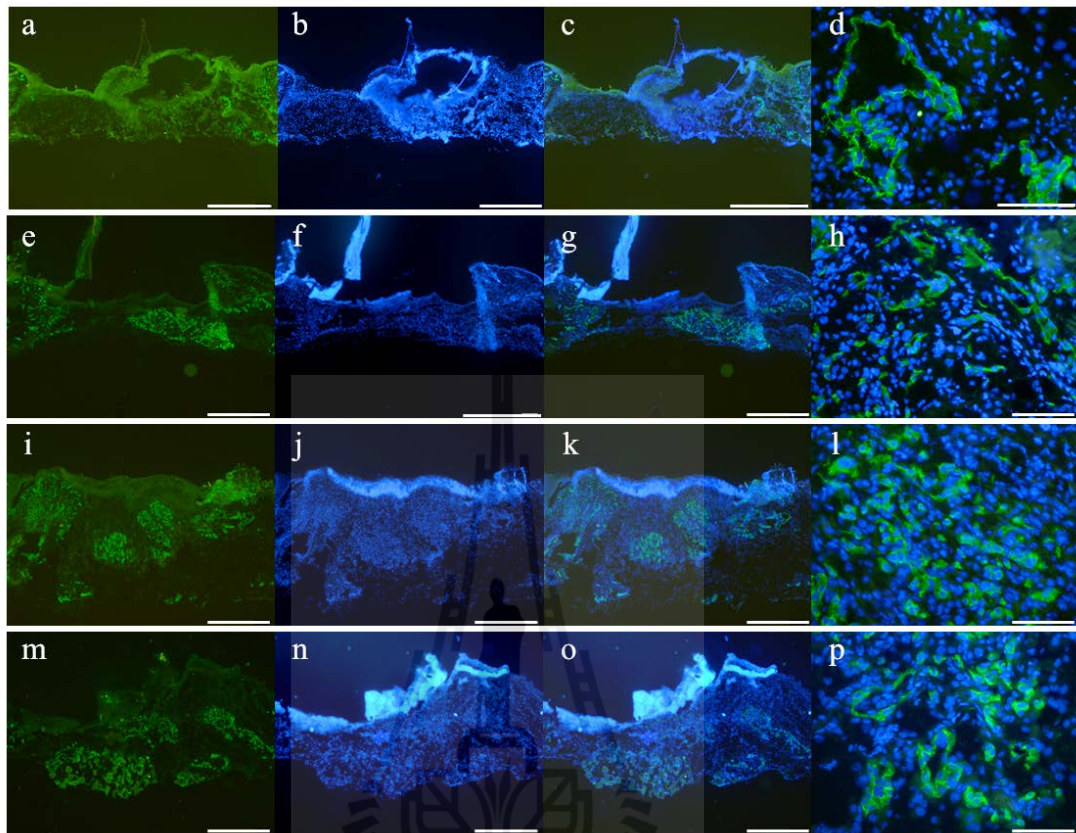


Figure 4.39 Immunofluorescent staining for endothelial marker CD31 (green) on wound tissue treated with PBS (a), freshly isolated CD34⁺ cells (e), expanded CD34⁺ cells (i) and 4FW cytokine (m) sections at day 5 after wounding (the first column). Counterstaining of nuclei with DAPI (blue) on the same sections are represented on the second column (b, f, j, n). The overlay images of the 2nd and 3rd columns (c, g, k, o) are represented on the third column. Scale bar = 400 μm . High magnification images of CD31-positive cells are represented on the fourth column (d, h, l, p). Scale bar = 80 μm .

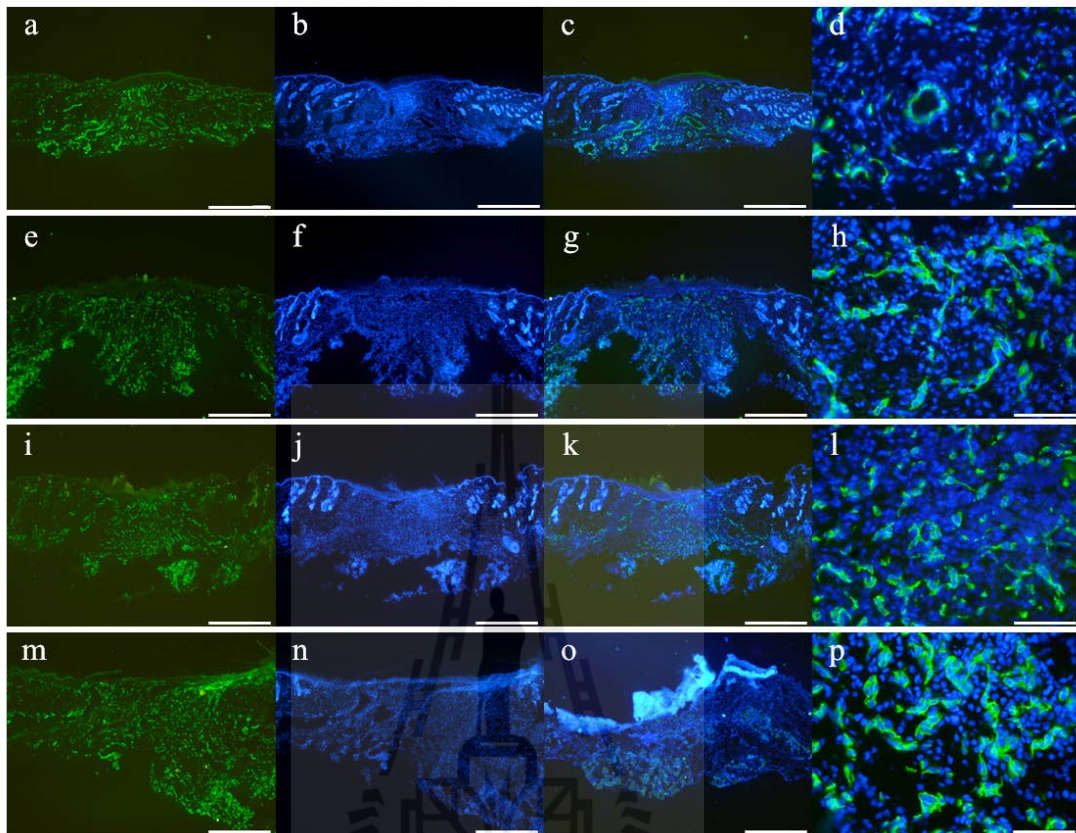


Figure 4.40 Immunofluorescent staining for endothelial marker CD31 (green) on wound tissue treated with PBS (a), freshly isolated CD34⁺ cells (e), expanded CD34⁺ cells (i) and 4FW cytokine (m) sections at day 9 after wounding (the first column). Counterstaining of nuclei with DAPI (blue) on the same sections are represented on the second column (b, f, j, n). The overlay images of the 2nd and 3rd columns (c, g, k, o) are represented on the third column. Scale bar = 400 μm . High magnification images of CD31-positive cells are represented on the fourth column (d, h, l, p). Scale bar = 80 μm .

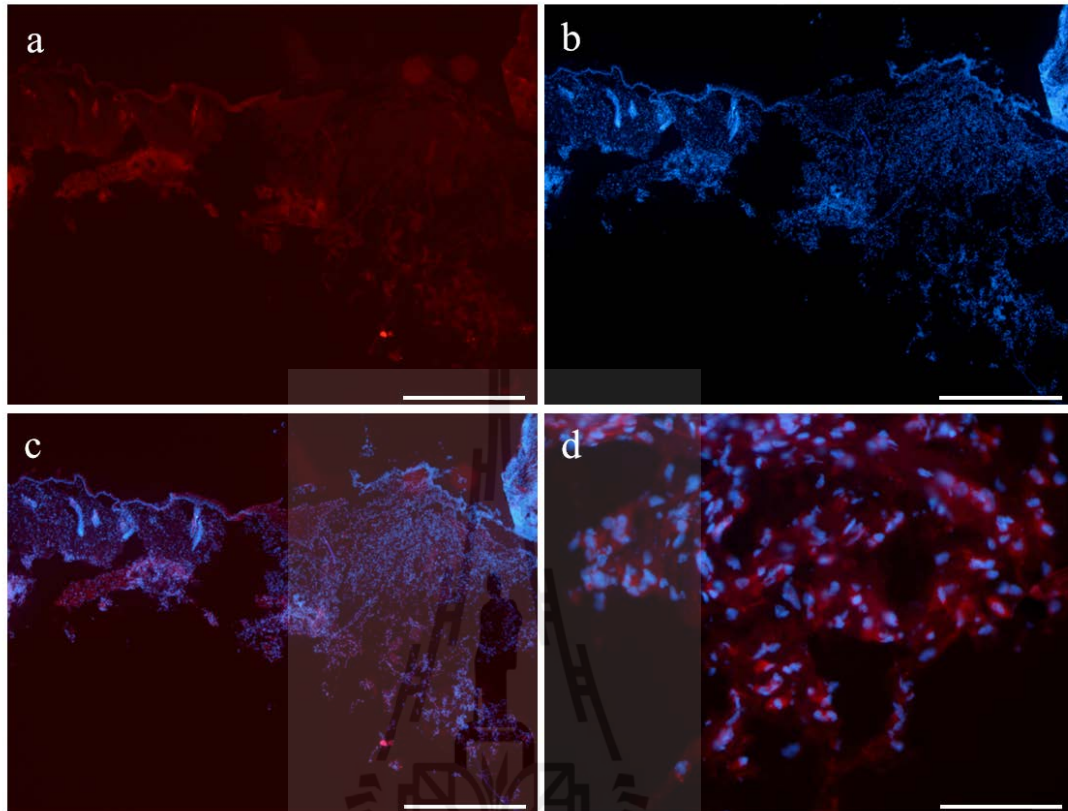


Figure 4.41 Immunofluorescence analysis of human CD34⁺ cells on wound tissue section treated with freshly isolated CD34⁺ cells at day 5 of wounding (red, a). Counterstaining of nuclei with DAPI (blue) on the same section (b). The overlay images of CD34⁺ cells with nuclei staining (c). Scale bar = 400 μm . High magnification image of human CD34-positive cells (d). Scale bar = 80 μm .

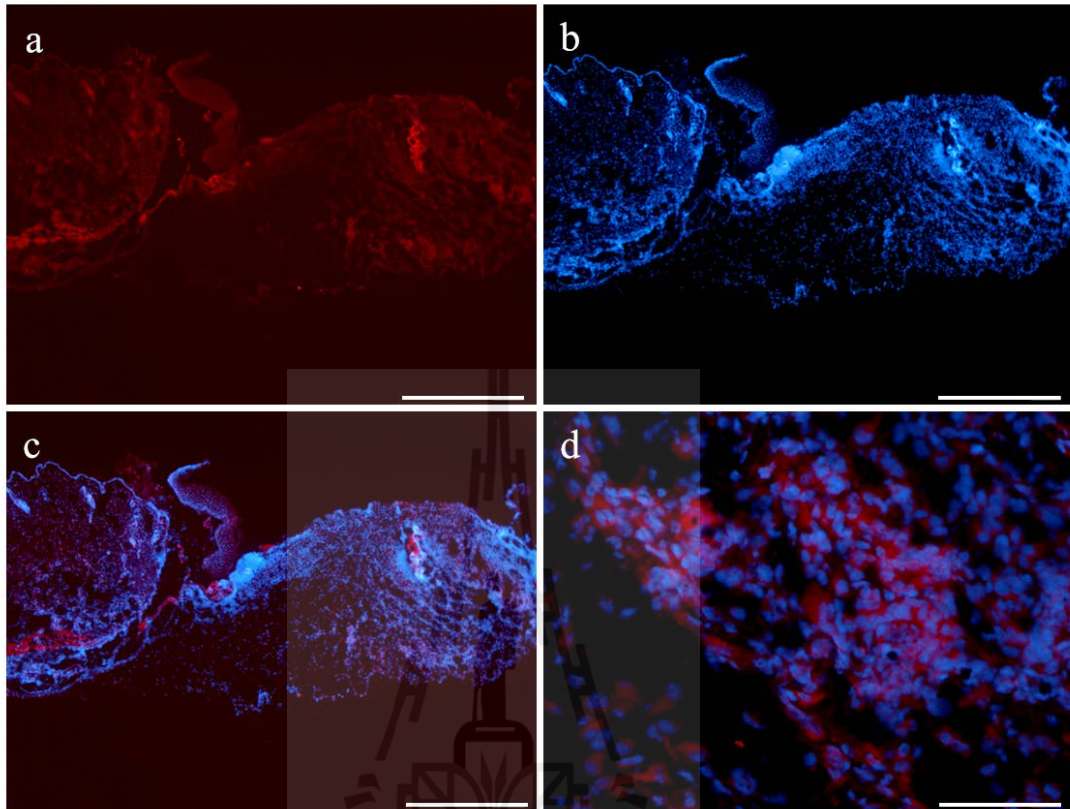


Figure 4.42 Immunofluorescence analysis of human CD34⁺ cells on wound tissue section treated with expanded CD34⁺ cells at day 5 of wounding (red, a). Counterstaining of nuclei with DAPI (blue) on the same section (b). The overlay images of CD34⁺ cells with nuclei staining (c). Scale bar = 400 μm . High magnification image of human CD34-positive cells (d). Scale bar = 80 μm .

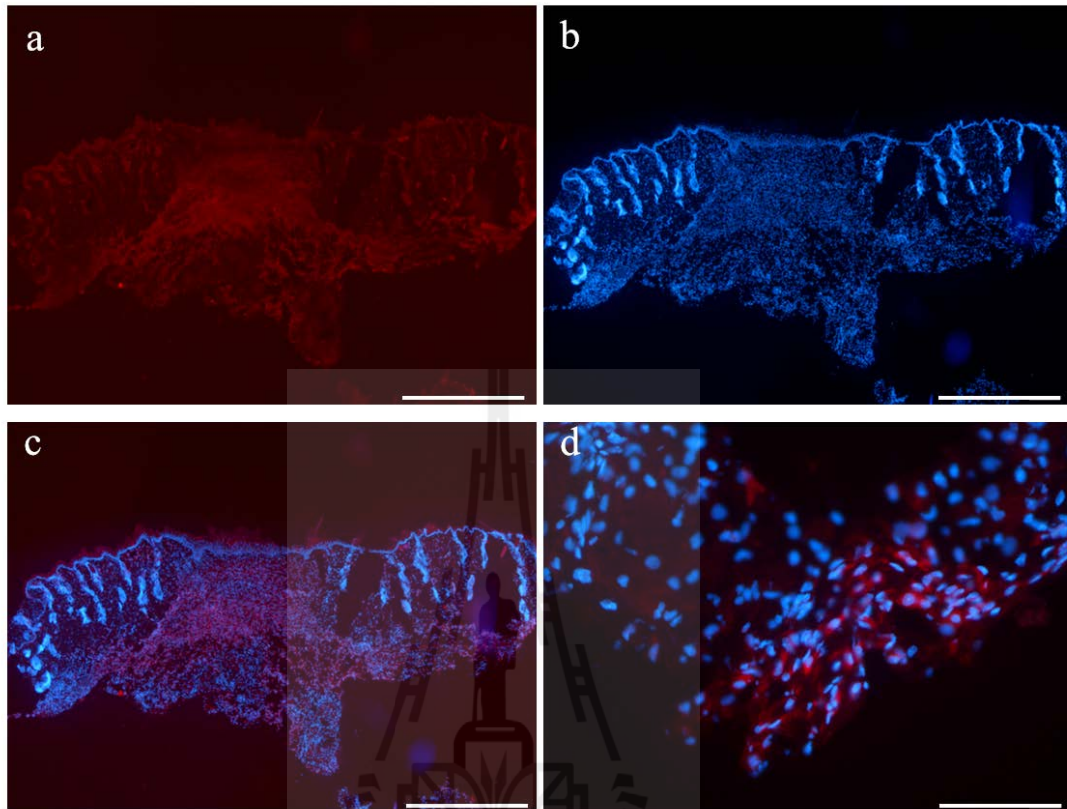


Figure 4.43 Immunofluorescence analysis of human CD34⁺ cells on wound tissue section treated with freshly isolated CD34⁺ cells at day 9 of wounding (red, a). Counterstaining of nuclei with DAPI (blue) on the same section (b). The overlay images of CD34⁺ cells with nuclei staining (c). Scale bar = 400 μm . High magnification image of human CD34-positive cells (d). Scale bar = 80 μm .

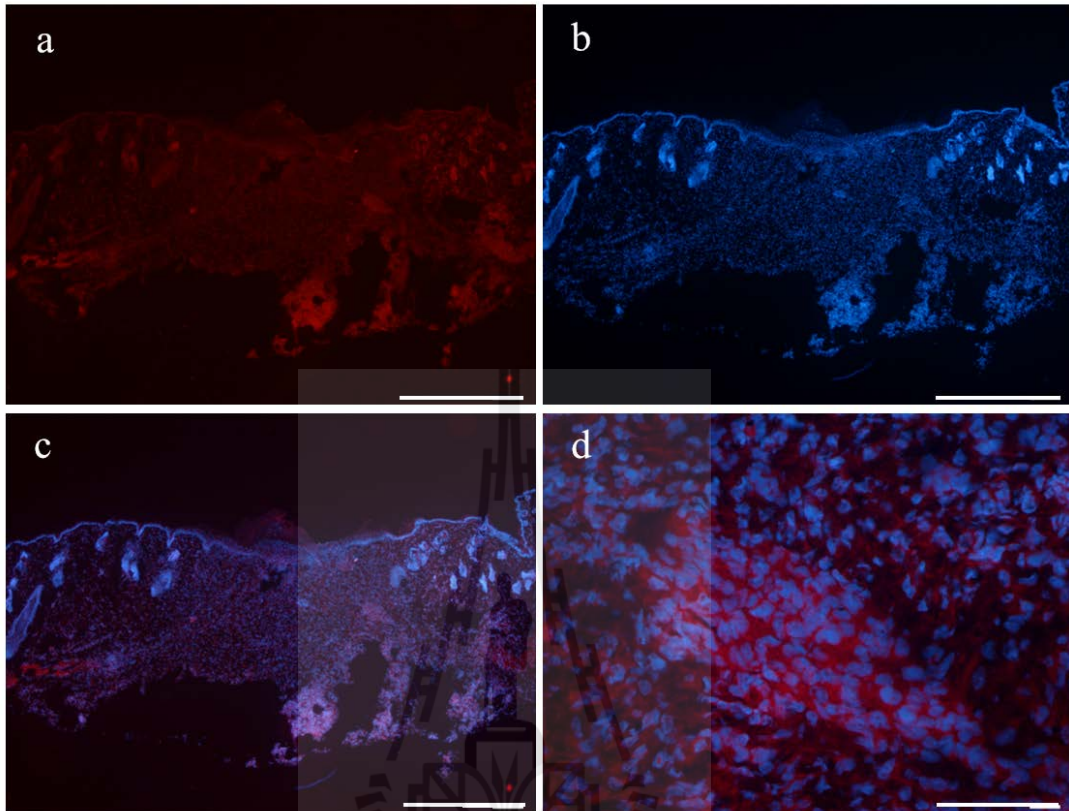


Figure 4.44 Immunofluorescence analysis of human CD34⁺ cells on wound tissue section treated with expanded CD34⁺ cells at day 9 of wounding (red, a). Counterstaining of nuclei with DAPI (blue) on the same section (b). The overlay images of CD34⁺ cells with nuclei staining (c). Scale bar = 400 μm . High magnification image of human CD34-positive cells (d). Scale bar = 80 μm .

CHAPTER V

DISCUSSION

5.1 Comparative *ex vivo* expansion capacity of CB-CD34⁺ cells in serum and serum-free medium

Hematopoietic stem cells (HSCs) can be obtained from several sources. The three main sources are bone marrow (BM), peripheral blood (PB) and umbilical cord blood (UCB). Among these, cord blood (CB) serves as the most powerful source for HSCs collection, especially, with non-invasive collection procedure. In addition, the CD34⁺ population containing HSCs isolated from CB exhibits superior advantages than those provided in BM and PB in many aspects, such as exhibiting lowest HLA antigens and containing highest potential of proliferation. These characteristics are crucial for achievement of hematopoietic stem cell transplantation (Gluckman, 1996). Although the proportion of CD34⁺ cells is enriched in the CB, the cell quantity available in single unit is insufficient for autologous transplantation. Based on this regard, expansion technology is needed in order to obtain high yield of CD34⁺CD38⁻ cells and maintain stemness of HSCs. In this work, the expansion culture conditions were successfully generated that yield significant increase of CD34⁺CD38⁻ and CD133⁺CD38⁻ cells in serum-free medium supplemented with cytokine cocktail. The CD34⁺CD38⁻ cells represent primitive HSC population, which is very crucial for blood cell transplantation applications. The CD133⁺CD38⁻ subpopulation appearing in

CD34⁺ enriched population is also serve as a source of quiescent stem cell which contains *in vivo* repopulating function (Boxall et al., 2009; Koutna et al., 2011). In addition, it has been investigated that CB-AC133⁺CD38⁻ is an improved marker that tracts and enriches for long-term culture-initiating cells and severe combined immunodeficiency (SCID)-repopulating cell (Ito et al., 2010). Therefore, successful expansion of both CD34⁺CD38⁻ and CD133⁺CD38⁻ cells is a keystone for not only the ability to overcome an insufficiency quantity of the cells but also the improvement of the stem cell transplantation. Interestingly, we observed the large amount of CD34⁺CD38⁻ cells (18.5 ± 0.4 folds) in 4F KSR medium after 7 days culture. More strikingly, in supportive of Wnt1 in the culture as 4FW KSR medium, higher significant increase of CD34⁺CD38⁻ cells was obtained (24.3 ± 2.1 folds) after 7 days culture. These investigations showed that Wnt1 is a stimulator for the expansion of HSCs cells. The folds expansion of CB-CD34⁺CD38⁻ cells proliferation in this study showed greater achievement than that reported in a previous study by Mishima and colleagues who obtained about 7 folds expansion by culture the cells in cytokine combination of SCF, TPO, Flt3L, IL-3, IL-6 and in the presence of osteoblast-differentiated MSC feeder cells (Mishima et al., 2010). However, expansion of HSCs without feeder cells is an easier procedure to handle, very convenient to perform in a large scale, has less cost, and no problems of hematopoietic cells attachment to the feeder cells. Moreover, the quantity of TPO used in our work was lower than that of Mishima et al. and was not needed to carry out the differentiation of MSC to osteoblast. Nevertheless, the scaffold may trap the expanded cells and reduce the actual outcome during the collection from the culture. Additionally, we found that the number of CD34⁺CD38⁻ cells in serum-free medium was higher than those in FBS

containing medium. Therefore, the utility of serum-free conditions (4F KSR and 4FW KSR) can reduce the risk of cross-contamination carried out by animal products and exhibit higher efficiency of CD34⁺CD38⁻ and CD133⁺CD38⁻ cells expansion than in serum containing media (4F cIMDM and 4FW cIMDM). Furthermore, our data of 4F KSR and 4FW KSR also indicated the lower increase of CD34⁻CD38⁺ progenitor cells as 20.1 ± 6.8 and 13.0 ± 3.7 folds, respectively, than those in 4F cIMDM and 4FW cIMDM as 62.8 ± 5.0 and 89.7 ± 12.2 folds, correspondingly. The CD34⁻CD38⁺ or co-expression of CD34 and CD38 are more committed progenitor cells which may result in less efficiency in transplantation, while the more primitive HSC function is found to be enriched in CD34⁺CD38⁻ population (Bhatia et al., 1997b). These findings suggest that 4F KSR and 4FW KSR are more appropriate culture conditions for HSPCs expansion and able to maintain CD34⁺ population than 4F cIMDM and 4FW cIMDM culture conditions. Altogether, by comparison of all 4 conditions in this work, the efficiency of culture conditions for CB- hematopoietic stem and progenitor cells (HSPCs) expansion can be arranged in order from high to low efficiency as 4FW KSR, 4F KSR, 4FW cIMDM, and 4F cIMDM, respectively.

An *ex vivo* expansion of CD34⁺ cells using various cytokine cocktails is an alternative approach to overcome the limitation and has been developed largely by many research groups. The combination of cytokine factors; SCF, Flt3L, TPO and IL-6 have been widely used for *ex vivo* expansion of CD34⁺ cells in medium containing serum (Gammaitoni et al., 2004; Piacibello et al., 2000). However, prolong culture resulted in an increasing of more committed progenitor cells which may dilute the number of true HSPCs and reduce the efficiency of engraftment. We also found the same phenomenon of high yield progenitor cells in CB-CD34⁺ cells cultured in 4F

cIMDM and 4FW cIMDM serum containing conditions even in a short period of time as 7 days. Therefore, serum should be eliminated from the stem cell culture. It has been reported the use of SCF, Flt3L, TPO and IL-6/sIL-6R for HSPC expansion in serum-free condition and the capacity to increase NOD/SCID-repopulating cells expansion (Ueda et al., 2000). In addition, Seet's team showed that the treatment with valproic acid in a serum-free condition for 7 days could enhance around 2-fold expansion of CD45⁺34⁺ progenitor cells (Seet et al., 2009). These studies, however, observed the population of more committed HSPCs rather than primitive HSPCs.

In fact, Wnt signals are activated through the canonical pathway for cell fate determination. Their roles in hematopoiesis have been identified as a growth factor for the development of hematopoietic stem cells. Wnt1 has been suggested its role in differentiation from human ESC to hematoendothelial cells (Woll et al., 2008). Previous studies have reported the significance of Wnt family signaling proteins in the expansion and self-renewal of HSPCs (Murdoch et al., 2003; Nikolova et al., 2007). However, there had not been any research on the use of Wnt1 in CB-HSCs expansion previously. Here, we demonstrated for the first time that Wnt1 effectively supported the CB-CD34⁺CD38⁻ and CD133⁺CD38⁻ cells expansion. This effect was more potent in serum-free medium than serum containing medium. In addition, Wnt1 supplementation in serum-free medium with Flt3L, SCF, TPO and IL-6 (4FW KSR) was also able to maintain the stemness property of expanded cells without affecting the differentiation capacity of hematopoietic progenitors. The 4FW KSR-expanded cells could give rise to all blood cell types in the presence of suitable growth factors for each blood cell lineage differentiation. In contrast, cells cultured in 4F KSR

without Wnt1, the expansion potential of HSCs was declined. Thus, this data confirms the stimulatory activity of Wnt1 on CB-HSCs proliferation.

Generally, Wnt signaling pathway is mediated in the regulation of stem cell fate and maintenance of mouse embryonic stem cells (ESCs) and human ESCs in undifferentiated state (Sato et al., 2004; Woll et al., 2008). Wnt3a, a canonical Wnt pathway activator, was found to promote short-term multilineage reconstitution of dormant c-kit(-) cells (Trowbridge et al., 2010). Activation of Wnt/ β -catenin signaling pathway can expand HSCs and plays a role in HSCs self-renewal. However, constitutive activation of β -catenin could abrogate HSCs differentiation and HSCs reconstitution *in vivo* (Reya et al., 2003). Therefore, Wnt1 may exert function as the up-regulator in CB-HSCs proliferation via the same pathway as Wnt3a or Wnt/ β -catenin signaling pathway. It has been reported that conditioned medium collected from 293T transfected with Wnt1, Wnt5a, or Wnt10b could enhance fetal liver AA4⁺Sca⁺kit⁺ cells (murine HSCs) expansion (Austin et al., 1997). The activation of Wnt pathway was also found in relation to Notch signaling, which is important in the early development of hematopoiesis (Duncan et al., 2005). Wnt-mediated maintenance of undifferentiated HSCs required the integration Notch signaling to inhibit differentiation. Thus, it would be suggested that Wnt1 may mediate the up-regulation of notch signaling pathway in expanded CB-HSCs and maintain stemness of the cells. Further process is required to clarify the role of Wnt1 protein in interaction with Notch signaling in the regulation of HSCs self-renewal.

In the present study, we also investigated whether enhancement of proliferation of CD34⁺ cells or HSPCs by 4F KSR and 4FW KSR would affect the pluripotency and self-renewal activity. In cellular level, we demonstrated that the expanded cells

have ability to produce clonogenic progenitor cells; CFU-GEMM, CFU-GM and BFU-E similar to freshly isolated CD34⁺ cells (Figure 4.9). Moreover, liquid culture differentiation assay indicated the capability of HSPCs in both 4F KSR and 4FW KSR to generate more mature blood cells (Figures 4.10-4.11). These findings support the achievement of repopulating capacity of expanded HSPCs.

These findings can be concluded that in the presence of the same cytokine cocktail, the serum-free medium is a better option than serum containing medium for HSPCs expansion, not only less animal product contamination but higher efficiency of the cells expansion also. In addition, Wnt1 can synergize SCF, Flt-3L, TPO, IL-6 in serum-free medium (4FW KSR) to stimulate CD34⁺CD38⁻ and CD133⁺CD38⁻ HSPCs proliferation. The advantages of the presence of both populations simultaneously are that they can synergize and enhance the capacity of blood cells reconstitution. Moreover, the utilization of human cytokines in the culture media is feasible, safe and not complicated or at risk by the use of animal product system. Furthermore, Wnt1 also enhances stemness preservation, maintains repopulating capacity and hematopoietic properties of HSPCs. Finally, Wnt1 can stimulate the survival and proliferation of HSPCs, demonstrating that Wnt1 comprises a novel class of hematopoietic cell regulator.

5.2 Multiple cocktails comparison for *ex vivo* expansion of CB-CD34⁺ cells in serum-free medium

Further investigation on *ex vivo* expansion in serum-free medium was performed on the next five cocktails (P0, P1, P2, P3 and P4) and compared with 4F

and 4FW. Overall, when cultured the cells in the medium, total nucleated number increased similarly to all cocktails on day 3 to day 5 of the cultures and this number continued to increase largely on day 7 with the highest expansion in P4 culture (15.4 ± 2.5 fold; Figure 4.12). However, the characterization of population number of $CD34^+CD38^-$ cells demonstrated that in P0 culture medium had the highest expansion on day 5 (10.0 ± 2.2 fold) while 4FW cocktail showed the highest number of $CD34^+CD38^-$ cells on day 7 ($24.3.0 \pm 2.1$ fold). Total $CD133^+CD38^-$ cells were found highest expansion in P0 culture medium on both days 5 and 7. Taken together, the efficiency of expansion ranging from high to low was 4FW, P4, P1, P0, P3, 4F and P2, respectively. These data suggest that addition of Wnt1 in a combination with Flt3L, SCF and/or TPO and IL-6 accelerates the proliferation of HSPCs. This study is the first time that reports the role of Wnt1 on the proliferative effect of HSPCs.

More specifically, the study extended to determine the pluripotency of expanded cells together with self-renewal capacity in terms of cellular and molecular levels. As previously described, the expanded cells from all culture conditions were performed on the liquid culture assay and colony forming assay. The results of all expanded cultures displayed the similar potential of differentiation into all mature hematopoietic lineages including progenitor cells; CFU-GEMM, CFU-GM and BFU-E (Figures 4.20-4.27). In molecular level, the data demonstrated that expanded HSPCs from all cultures in serum-free medium expressed key pluripotency and self-renewal genes of *Oct3/4* and *Nanog*. *Oct3/4*, a key pluripotency transcription factor of ES cells, was found to regulate *Sox2* expression in ES cells which then activated Oct-Sox enhancers to control expression of *Nonog* and even *Oct3/4* and *Sox2* itself (Masui et al., 2007). Thus, these results revealed mRNA expression of transcription factors

Oct3/4 and *Nanog* which mediate maintenance of pluripotency and self-renewal as ESCs (Chambers et al., 2003; Kashyap et al., 2009).

Interestingly, there was up-regulation of *Nanog* expression in the cells cultured in P1, P2 and P4, while the expression of *Oct3/4* was increased in those of P1 and P2 compared to freshly isolated CD34⁺ cells. Recent observation has shown that the maintenance of human ESCs in undifferentiated state is mediated by differential phosphorylation of several members of the canonical pathways involved in pluripotency and self-renewal such as Wnt and PI3K/AKT, human ESC-associated proteins such as SOX2, RIF1, SALL4, DPPA4, DNMT3B and 53 proteins which known as target genes of the pluripotency transcription factors SOX2, OCT4 and NANOG (Zoumaro-Djayoon et al., 2011). This observation suggests the evidence that Wnt pathway may be in part in mediating the regulation of OCT4/SOX2/NANOG trimeric complex to maintain the undifferentiated human ESC phenotype. Taken together, these data suggested that all cytokine cocktails, particularly P1, P2 and P4, could stabilize the expression of pluripotency and self-renewal genes which are crucial characteristic of stem cells.

HSCs transplantation has been used for the treatment of hematopoietic disorders, solid malignant tumors (McNiece et al., 2000; Shpall et al., 2002) and non-hematopoietic diseases as currently addressed in clinical trials in many countries around the world. Besides the property of expanded HSPCs in sustainment the stem cell pool in hematopoietic system of transplant patient, commitment to give rise to blood cells is also essential for immunological functions. After high-dose chemotherapy in cancer patients, neutropenia normally occurs. Myeloid lineages which play roles in the innate immune responses can protect against bacterial

infections in the initial phase of transplantation. The result in this study is consistent with previous observation that *ex vivo* expansion of CD34⁺ cells predominantly committed into myeloid progenitor cells with a negligible expansion into lymphoid lineage (Sangeetha et al., 2010). Thus, the natural myeloid/erythroid commitment by *ex vivo* culture may enhance engraftment efficiency and reduce mortality rate in clinical studies. Recently, Phase I clinical trial demonstrated that the utilization of the *ex vivo* expanded CB-CD34⁺ cells along with non-manipulating CB unit facilitated myeloid engraftment rate in patients. (Delaney et al., 2010). This data, therefore, highlights the importance of expanded CB unit for therapeutic purpose even though the real mechanism of supportive engraftment between non-manipulating and manipulate one has not been explored.

5.3 Wound healing in STZ-induced diabetic mice

Diabetes contains defects in immune-mediated wound healing, thus resulted in delayed wound repair and become a major problem in the clinic. The impaired wound healing in diabetes is caused by the changes in growth factor productions, cellular responses to mediators, extracellular matrix deposition, angiogenesis and wound contraction (Blakytyn and Jude, 2006). In this study, the use of expanded CD34⁺ cells for regenerative medicine related to diabetes was performed in streptozotocin (STZ)-induced diabetic mice to identify wound healing efficiency. In addition, the cytokines used for *ex vivo* expansion of CB-CD34⁺ cells were added to compare. ICR mice were succeeded to be diabetes by multi-low does injection of STZ which is contains the pancreatic β cell toxin that can induce rapid and irreversible necrosis of β cells (Lee et al., 2006). The effect mimics to the onset of human patients type 1 diabetes (Motyl

and McCabe, 2009). Over the 9 days of study period, all treated mice remained diabetes (high blood glucose level, 551.4 ± 53.0 mg/dl), suggesting that subcutaneously injection of the cells or cytokines nearby the wound area did not improve or maintain normoglycemia in STZ-diabetic mice within the short period of time. However, there were some clinical trials for the treatment of type 1 diabetes which performed by intravenous autologous HSC transplantation after high-dose cyclophosphamide and antithymocyte globulin (Couri et al., 2009; Snarski et al., 2011). Most patients were insulin independent with the mean follow up ranging from 7-30 months for all three clinical studies. Couri et al. reported the induction of insulin-free state as early as mean +2 days and contained the mean duration of symptom of hyperglycemia for 18.7 days after the infusion as observed in 23 patients (Couri et al., 2009).

To prevent the leak of cells or fluid out at the wound site, injection of fresh or expanded CD34⁺ cells or cytokines 4FW to the wound were performed by subcutaneous injection near the wound margin rather than injection into the wound directly. Theoretically, the new performing wound healing physiologically starts from the wound margin (Singer and Clark, 1999). Thus, the cells and cytokines performing with this application could be accounted for mediating in the starting process on wound healing. Wounds treated with cytokine 4FW did not enhance wound closure compared to the PBS treated wounds. Injection of fresh CD34⁺ cells into the wounds accelerated wound closure significantly as early as day 5 and continued to be observed until day 9, whereas, the injection of expanded CD34⁺ cells enhanced the wound closure at day 9 after the surgery significantly compared to the PBS treated control. These results are in accordance with previous reports on the improvement of

wound closure (Chan et al., 2007; Kim et al., 2010; Pedroso et al., 2011; Tark et al., 2010). The rate of wound closure in this study was found earlier than peripheral blood and bone marrow hematopoietic stem cells transplantation which observed on day 7 reported by Sivan-Loukianova et al. and Chan et al., respectively (Chan et al., 2007; Sivan-Loukianova et al., 2003). Moreover, Pedroso and colleague (2011) showed that 3D fibrin gel containing CB-CD34⁺ did not accelerate wound healing while the gel containing co-cultured of CB-CD34⁺ cells and CD34⁺-derived endothelial cells could improve wound healing as fast as 3 days post-injury. However, the acceleration of wound closure was not statistically different for the remaining time points (Pedroso et al., 2011). On the other hand, studies by transplantation with MSCs (Tark et al., 2010) and endothelial progenitor cells (Kim et al., 2010) showed that these cells could enhance wound closure as early as day 3 post-transplantation. The discrepancies between the rates of wound closure among those studies with the present work might be due to the species differences of mouse model.

Histological findings confirmed the improvement of wound healing in both fresh CD34⁺ cells and expanded CD34⁺ cells transplantation groups that exhibited lower epithelial gap between both sites of the wound margin than that of PBS treated group. In addition, the more densely compact collagen and regular arrangement of complete epidermis lining on the newly formed epidermal layer were found in fresh- and expanded CD34⁺ cells treated wounds at day 9 post-wounding. Inflammatory and neovascularization processes are important in wound healing (Broughton et al., 2006). Analysis of neovascularization inside the wound tissue was done by using endothelial CD31 marker. The data demonstrated that fresh-, expanded CD34⁺ cells-, and cytokine 4FW-treated wounds contained higher amount of CD68-positive

macrophages and CD31-positive capillaries than that of PBS-treated wounds after 5 days of wounding. On the other hand, the number of CD68-positive macrophages in those of treated groups at day 9 decreased lower than that of day 5 whereas these numbers in PBS control increased higher than that of day 5. Nevertheless, the CD31-positive capillaries on those of treated wounds continued to increase until day 9 and higher than that of PBS control. These findings suggest that fresh CD34⁺ cells, expanded CD34⁺ cells and cytokine 4FW promoted macrophages and capillaries recruitment and/or proliferation which might be contributed to re-epithelialization in the early process of wound healing (Singer and Clark, 1999). The number of macrophages that increased on day 9 on wounds treated with PBS control displayed the delayed wound healing process by recruitment of inflammatory cells to the wound area. While the wounds in treated groups contained a declining number of macrophages and an increase in capillaries on day 9 of wounding which suggested more advanced process in wound healing compared to PBS group. This data corresponds with previous report that injection of human peripheral blood CD34⁺ cells to wound of diabetic mice could accelerate revascularization and wound healing (Sivan-Loukianova et al., 2003). Although cytokine 4FW treated wounds displayed similar circumstance in the number of macrophages and capillaries contents to the fresh and expanded CD34⁺ cells, overall resulting in wound closure was not improved at the end of observation.

It has been proposed that stem cells have the effect on promoting wound healing (Stepanovic et al., 2003). There are two possibilities that stem cells may affect the wound healing. First, stem cells release growth factors, cytokines and mediators which stimulate the generation of neighboring tissues or cells (so called paracrine

effect) (Templin et al., 2009). Second, stem cells may either differentiate into regenerative cells in the wound site or stimulate tissue regeneration by collaborating with adjacent cells (Di Rocco et al., 2010; Heng et al., 2005). Conditioned medium of hematopoietic progenitor cell line or DKmix cells and DKmix cells have been shown to promote angiogenesis on murine wound model (Templin et al., 2009). In addition, conditioned media of human CB-derived endothelial progenitor cells has found to promote keratinocytes, fibroblasts and endothelial cells proliferations in paracrine manner in the same action performed by injection of endothelial progenitor cells on diabetic wound mice (Kim et al., 2010). These data demonstrate that the incorporated stem cells release cytokine that act in paracrine effect to enhance neovascularization and resulting in remodeling of extracellular matrix and recruitment of circulating stem cells. Cytokine 4FW used in this study could enhance microvessels and macrophages but did not result in wound closure acceleration similar to the use of fresh and expanded CB-CD34⁺ cells injections and previous reports using conditioned medium of stem cells (Kim et al., 2010; Templin et al., 2009). These results suggest that Wnt1 supplementation in SCF, Flt3L, IL-6 and TPO exert the paracrine effect on macrophages and endothelial cells recruitment and proliferation in early stage of wound healing process. However, the injection of cytokines alone may not be enough to induce more advanced wound healing process in the maturation and remodeling phase which may mediate in defective in keratinocytes and collagen matrix contractions. The amount of cytokines may also limit the efficiency.

SCF is produced by keratinocytes in the epidermis (Longley et al., 1993), and produced by endothelial cells (Weiss et al., 1995), fibroblasts (Longley et al., 1993) and mast cells (S. Zhang et al., 1998) in the dermis. SCF functions as the chemotactic

factor for mast cells that is one of the major effectors in the inflammatory process (Nilsson et al., 1994). SCF is also found in the dermis during the early phase of normal wound healing and declined thereafter (Huttunen et al., 2002). Additionally, SCF has been proposed to have anti-apoptotic role on keratinocytes regulated through transiently elevated transforming growth factor β -activated kinase 1 during wound healing (Lam et al., 2011). Expression of Flt3L was found in a variety of tissues including BM, fetal liver, thymus, spleen, gonads, placenta and brain. Flt3 expression is found on early B and T cell progenitors in BM and thymus and on peritoneal macrophages and monocytes within the hematopoietic compartments (Antonysamy and Thomson, 2000). Human skin keratinocytes and fibroblast express Flt3L (Morita et al., 1997). Furthermore, treatment with Flt3L in burn wound infection in mice resulted in enhancement of dendritic cells number and functions which in turn stimulate neutrophil recruitment and function in immune response to injection (Bohannon et al., 2008; 2010; Toliver-Kinsky et al., 2005). IL-6 is secreted mainly by epidermal keratinocytes, while macrophages, Langerhans cells and fibroblasts in dermis are the other sources in the skin (Ghazizadeh, 2007; Paquet and Pierard, 1996). Enhanced IL-6 expression in normal rat skin increased the epidermal proliferation and inflammation (Sawamura et al., 1998). However, conditioned medium of human ESC-derived endothelial precursor cells has been shown to enhance normal mice wound healing by distinctively secretory factors such as epidermal growth factor, basic fibroblast growth factor, granulocyte-macrophage colony-stimulating factor, IL-6, IL-8, platelet-derived growth factor-AA and vascular endothelial growth factor (Lee et al., 2011b). These data suggest that SCF, Flt3L and IL-6 might mediate significantly in the early phase of wound process. Many inflammatory cells type such as mast cells

and neutrophils may be recruited during the inflammatory process than usual that could prolong the outcome of wound healing. Thus, the improved wound healing might need more distinctively different cytokines to regulate and make the balance within the healing process.

The canonical Wnt signaling pathway (mediated by β -catenin) is thought to play a role in dermal fibroblast proliferation and motility and is elevated in fibroblasts during the proliferative phase of wound healing (Cheon et al., 2002). Moreover, the level of β -catenin level was found to enhance during the wound healing with the peak at 4 weeks following the insult and return to the baseline level by 12 weeks (Cheon et al., 2005). The canonical Wnt signaling also plays a role in epidermis but in a complicated way. The Wnt signal was found in elevated level in the wound and was suggested to mediate in maintenance and regeneration of hair follicle (Fathke et al., 2006). In addition, Wnt signaling has been shown to be the growth-inducer of stem cell compartments in skin which interfollicular progenitor cells expresses Wnt1 that can inhibit their growth and promote terminal differentiation (Slavik et al., 2007). Canonical Wnt signaling is found to relate with the development of some kind of skin tumors like malignant melanoma (Larue and Delmas, 2006) and pilomatrixoma (Clevers, 2006). Human adipose-derived stromal cells has been shown to produce cytokines in paracrine effect that induce the expression of Wnt1 in the de-epithelialized of skin mainly in the dermal fibroblasts (Kim et al., 2011). Moreover, the non-canonical Wnt pathway, in which Wnt4, Wnt5, Wnt11 and Wnt16 are found to involve in the signaling pathway of the skin (Kim et al., 2011). These data suggest that Wnt signaling including Wnt1 plays a role in the skin regeneration and wound healing. Thus, the injection of cytokine containing Wnt1 mediated in the canonical

Wnt signaling in this work may stimulate the regeneration of the skin to the fibroblast cells. However, other Wnt signals may be involved in the wound repair in the orchestrate manner for the improvement of wound healing. In addition, further analysis should be performed on fresh or expanded CD34⁺ cells in which cytokines or growth factors mediated in wound healing process are released and whether fibroblasts are affected by Wnt1.

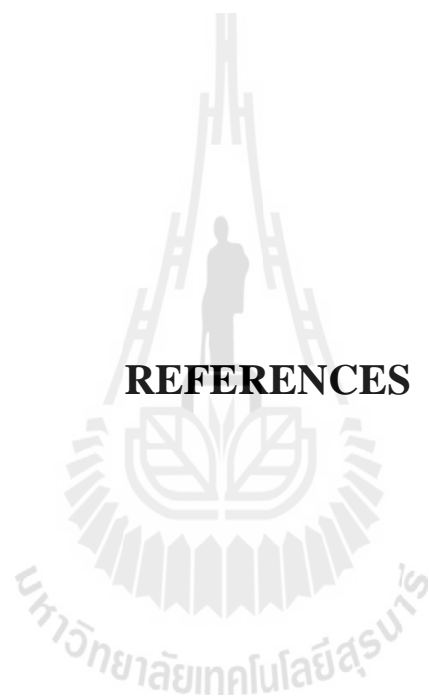
Wounds treated with fresh human CB-CD34⁺ cells or day 5-expanded CB-CD34⁺ cells contained the human CD34-positive cells at both inside the wound area and surrounding of tissue of the wound. This data suggests that these cells may cooperate in accelerate wound healing either by themselves in conjunction with other cells mediated in wound repair or paracrine factors that help to recruit stem cells, macrophages, endothelial cells, fibroblasts and other inflammatory cells to the wound site. Human CB-CD34⁺ cells may also differentiate into endothelial cells. However, the present work did not determine this differentiation. Thus, there would be interesting to identify further whether CB-CD34⁺ cells could transdifferentiate into endothelial cells in the wound area or not.

In conclusion, fresh and day 5-expanded CB-CD34⁺ cells accelerated wound healing in STZ-induced diabetic mice by improve macrophages and capillaries migration and proliferation. The implication of this work will be useful for the improvement of wound healing in diabetic patient in the future.

CHAPTER VI

CONCLUSION

This study demonstrated that *ex vivo* expansion by the use of cytokine cocktails in serum-free medium containing Wnt1 promoted proliferation of CB-CD34⁺ cells that also maintaining their self-renewal capacity at both cellular and molecular levels. Particularly, cocktail P0 and the combination of Wnt1 with Flt3L, SCF, IL-6 and TPO (4FW) exhibited the highest level of CD34⁺CD38⁻ cell expansion on day 5 and 7 of the culture, respectively (~10.0- and ~24.3- folds). Interestingly, these cocktails also enhanced the CD133⁺CD38⁻ population within the culture which mediated in the repopulating ability *in vivo*, especially, in that of P0. Study in STZ-induced diabetic mice has been shown that by injection of fresh human CB-CD34⁺ cells and day5-expanded human CB-CD34⁺ cells from 4FW in serum-free medium could accelerate wound healing. The improvement of wound repairing was mediated by the enhancement of CD68-positive macrophages and CD31-positive capillaries recruitment and proliferation. Cytokine 4FW contained the ability to increase CD68-positive macrophages and CD31-positive capillaries but not improved wound closure. Therefore, the implication of this work is therapeutic value in cord blood transplantation for hematologic and non-hematologic diseases, blood bank/stem cell bank applications and hematological studies in the future. The application of both fresh and expanded CD34⁺ cells from 4FW medium will also be useful for the treatment of wound healing in diabetic patient for the translational medicine purposes.



REFERENCES

REFERENCES

- Abe, T., Masuda, S., Ban, H., Hayashi, S., Ueda, Y., Inoue, M., Hasegawa, M., Nagao, Y., and Hanazono, Y. (2011). *Ex vivo* expansion of human HSCs with Sendai virus vector expressing HoxB4 assessed by sheep *in utero* transplantation. **Exp. Hematol.** 39: 47-54.
- Abu-Duhier, F.M., Goodeve, A.C., Wilson, G.A., Care, R.S., Peake, I.R., and Reilly, J.T. (2001). Genomic structure of human FLT3: implications for mutational analysis. **Br. J. Haematol.** 113: 1076-1077.
- Aekplakorn, W., Charialertsak, S., Kessomboon, P., Sangthong, R., Inthawong, R., Putwatana, P., Taneepanichskul, S., and Group, t.T.N.H.E.S.I.S. (2011). Prevalence and Management of Diabetes and Metabolic Risk Factors in Thai Adults. **Diabetes Care** 34: 1980-1985.
- Agnes, F., Shamon, B., Dina, C., Rosnet, O., Birnbaum, D., and Galibert, F. (1994). Genomic structure of the downstream part of the human FLT3 gene: exon/intron structure conservation among genes encoding receptor tyrosine kinases (RTK) of subclass III. **Gene** 145: 283-288.
- Alison, M.R., Poulson, R., Forbes, S., and Wright, N.A. (2002). An introduction to stem cells. **J. Pathol.** 197: 419-423.
- Antonchuk, J., Sauvageau, G., and Humphries, R.K. (2001). HOXB4 overexpression mediates very rapid stem cell regeneration and competitive hematopoietic repopulation. **Exp. Hematol.** 29: 1125-1134.

- Antonchuk, J., Sauvageau, G., and Humphries, R.K. (2002). HOXB4-induced expansion of adult hematopoietic stem cells *ex vivo*. **Cell** 109: 39-45.
- Antonysamy, M.A., and Thomson, A.W. (2000). Flt3 ligand (FL) and its influence on immune reactivity. **Cytokine** 12: 87-100.
- Ara, T., Tokoyoda, K., Sugiyama, T., Egawa, T., Kawabata, K., and Nagasawa, T. (2003). Long-term hematopoietic stem cells require stromal cell-derived factor-1 for colonizing bone marrow during ontogeny. **Immunity** 19: 257-267.
- Arai, F., Hirao, A., Ohmura, M., Sato, H., Matsuoka, S., Takubo, K., Ito, K., Koh, G.Y., and Suda, T. (2004). Tie2/angiopoietin-1 signaling regulates hematopoietic stem cell quiescence in the bone marrow niche. **Cell** 118: 149-161.
- Artavanis-Tsakonas, S., Rand, M.D., and Lake, R.J. (1999). Notch signaling: cell fate control and signal integration in development. **Science** 284: 770-776.
- Austin, T.W., Solar, G.P., Ziegler, F.C., Liem, L., and Matthews, W. (1997). A role for the Wnt gene family in hematopoiesis: expansion of multilineage progenitor cells. **Blood** 89: 3624-3635.
- Badillo, A.T., Redden, R.A., Zhang, L., Doolin, E.J., and Liechty, K.W. (2007). Treatment of diabetic wounds with fetal murine mesenchymal stromal cells enhances wound closure. **Cell Tissue Res.** 329: 301-311.
- Ballow, D., Meistrich, M.L., Matzuk, M., and Rajkovic, A. (2006). *Sohlh1* is essential for spermatogonial differentiation. **Dev. Biol.** 294: 161-167.

- Barcelos, L.S., Duplaa, C., Krankel, N., Graiani, G., Invernici, G., Katare, R., Siragusa, M., Meloni, M., Campesi, I., Monica, M., Simm, A., Campagnolo, P., Mangialardi, G., Stevanato, L., Alessandri, G., Emanuelli, C., and Madeddu, P. (2009). Human CD133⁺ progenitor cells promote the healing of diabetic ischemic ulcers by paracrine stimulation of angiogenesis and activation of Wnt signaling. **Circ. Res.** 104: 1095-1102.
- Barcena, A., Kapidzic, M., Muench, M.O., Gormley, M., Scott, M.A., Weier, J.F., Ferlatte, C., and Fisher, S.J. (2009). The human placenta is a hematopoietic organ during the embryonic and fetal periods of development. **Dev. Biol.** 327: 24-33.
- Bartley, T.D., Bogenberger, J., Hunt, P., Li, Y.S., Lu, H.S., Martin, F., Chang, M.S., Samal, B., Nichol, J.L., Swift, S., Johnson, M.J., Hsu, R.Y., Parker, V.P., Suggs, S., Skrine, J.D., Merewether, L.A., Clogston, C., Hsu, E., Hokom, M.M., Hornkohl, A., Choi, E., Pangelinan, M., Sun, Y., Mar, V., McNinch, J., Simonet, L., Jacobsen, F., Xie, C., Shutter, J., Chute, H., Basu, R., Selander, L., Trollinger, D., Sieu, L., Padilla, D., Trail, G., Elliott, G., Izumi, R., Covey, T., Crouse, J., Garcia, A., Xu, W., Del Castillo, J., Biron, J., Cole, S., Hu, M.C., Pacifici, R., Ponting, I., Saris, C., Wen, D., Yung, Y.P., Lin, H., and Rosselman, R.A. (1994). Identification and cloning of a megakaryocyte growth and development factor that is a ligand for the cytokine receptor Mpl. **Cell** 77: 1117-1124.
- Bashamboo, A., Taylor, A.H., Samuel, K., Panthier, J.J., Whetton, A.D., and Forrester, L.M. (2006). The survival of differentiating embryonic stem cells is dependent on the SCF-KIT pathway. **J. Cell Sci.** 119: 3039-3046.

- Basu, S., Ray, N.T., Atkinson, S.J., and Broxmeyer, H.E. (2007). Protein phosphatase 2A plays an important role in stromal cell-derived factor-1/CXC chemokine ligand 12-mediated migration and adhesion of CD34⁺ cells. **J. Immunol.** 179: 3075-3085.
- Baum, C.M., Weissman, I.L., Tsukamoto, A.S., Buckle, A.M., and Peault, B. (1992). Isolation of a candidate human hematopoietic stem-cell population. **Proc. Natl. Acad. Sci. USA.** 89: 2804-2808.
- Bersenev, A., Wu, C., Balcerek, J., and Tong, W. (2008). Lnk controls mouse hematopoietic stem cell self-renewal and quiescence through direct interactions with JAK2. **J. Clin. Invest.** 118: 2832-2844.
- Bertrand, F.E., Eckfeldt, C.E., Fink, J.R., Lysholm, A.S., Pribyl, J.A., Shah, N., and LeBien, T.W. (2000). Microenvironmental influences on human B-cell development. **Immunol. Rev.** 175: 175-186.
- Besmer, P. (1991). The kit ligand encoded at the murine Steel locus: a pleiotropic growth and differentiation factor. **Curr. Opin. Cell Biol.** 3: 939-946.
- Bhanot, P., Brink, M., Samos, C.H., Hsieh, J.C., Wang, Y., Macke, J.P., Andrew, D., Nathans, J., and Nusse, R. (1996). A new member of the frizzled family from *Drosophila* functions as a Wingless receptor. **Nature** 382: 225-230.
- Bhatia, M., Bonnet, D., Kapp, U., Wang, J.C., Murdoch, B., and Dick, J.E. (1997a). Quantitative analysis reveals expansion of human hematopoietic repopulating cells after short-term *ex vivo* culture. **J. Exp. Med.** 186: 619-624.
- Bhatia, M., Bonnet, D., Wu, D., Murdoch, B., Wrana, J., Gallacher, L., and Dick, J.E. (1999). Bone morphogenetic proteins regulate the developmental program of human hematopoietic stem cells. **J. Exp. Med.** 189: 1139-1148.

- Bhatia, M., Wang, J.C., Kapp, U., Bonnet, D., and Dick, J.E. (1997b). Purification of primitive human hematopoietic cells capable of repopulating immune-deficient mice. **Proc. Natl. Acad. Sci. USA.** 94: 5320-5325.
- Blackshaw, S., Harpavat, S., Trimarchi, J., Cai, L., Huang, H., Kuo, W.P., Weber, G., Lee, K., Fraioli, R.E., Cho, S.H., Yung, R., Asch, E., Ohno-Machado, L., Wong, W.H., and Cepko, C.L. (2004). Genomic analysis of mouse retinal development. **PLoS Biol.** 2: 1411-1431.
- Blakytyny, R., and Jude, E. (2006). The molecular biology of chronic wounds and delayed healing in diabetes. **Diabet. Med.** 23: 594-608.
- Blume-Jensen, P., Janknecht, R., and Hunter, T. (1998). The kit receptor promotes cell survival via activation of PI 3-kinase and subsequent Akt-mediated phosphorylation of Bad on Ser136. **Curr. Biol.** 8: 779-782.
- Bohannon, J., Cui, W., Cox, R., Przkora, R., Sherwood, E., and Toliver-Kinsky, T. (2008). Prophylactic treatment with fms-like tyrosine kinase-3 ligand after burn injury enhances global immune responses to infection. **J. Immunol.** 180: 3038-3048.
- Bohannon, J., Cui, W., Sherwood, E., and Toliver-Kinsky, T. (2010). Dendritic cell modification of neutrophil responses to infection after burn injury. **J. Immunol.** 185: 2847-2853.

- Boiron, J.M., Dazey, B., Cailliot, C., Launay, B., Attal, M., Mazurier, F., McNiece, I.K., Ivanovic, Z., Caraux, J., Marit, G., and Reiffers, J. (2006). Large-scale expansion and transplantation of CD34(+) hematopoietic cells: *in vitro* and *in vivo* confirmation of neutropenia abrogation related to the expansion process without impairment of the long-term engraftment capacity. **Transfusion** 46: 1934-1942.
- Boisset, J.C., van Cappellen, W., Andrieu-Soler, C., Galjart, N., Dzierzak, E., and Robin, C. (2010). *In vivo* imaging of haematopoietic cells emerging from the mouse aortic endothelium. **Nature** 464: 116-120.
- Boxall, S.A., Cook, G.P., Pearce, D., Bonnet, D., El-Sherbiny, Y.M., Blundell, M.P., Howe, S.J., Leek, J.P., Markham, A.F., and de Wynter, E.A. (2009). Haematopoietic repopulating activity in human cord blood CD133⁺ quiescent cells. **Bone Marrow Transplant.** 43: 627-635.
- Boyko, E.J., Ahroni, J.H., Smith, D.G., and Davignon, D. (1996). Increased mortality associated with diabetic foot ulcer. **Diabet. Med.** 13: 967-972.
- Bramono, D.S., Rider, D.A., Murali, S., Nurcombe, V., and Cool, S.M. (2010). The effect of human bone marrow stroma-derived heparan sulfate on the *ex vivo* expansion of human cord blood hematopoietic stem cells. **Pharm. Res.** 28: 1385-1394.
- Brawand, P., Fitzpatrick, D.R., Greenfield, B.W., Brasel, K., Maliszewski, C.R., and De Smedt, T. (2002). Murine plasmacytoid pre-dendritic cells generated from Flt3 ligand-supplemented bone marrow cultures are immature APCs. **J. Immunol.** 169: 6711-6719.

- Broudy, V.C. and Kaushansky, K. (1995). Thrombopoietin, the c-mpl ligand, is a major regulator of platelet production. **J. Leukoc. Biol.** 57: 719-725.
- Broudy, V.C., Lin, N.L., and Kaushansky, K. (1995). Thrombopoietin (c-mpl ligand) acts synergistically with erythropoietin, stem cell factor, and interleukin-11 to enhance murine megakaryocyte colony growth and increases megakaryocyte ploidy *in vitro*. **Blood** 85: 1719-1726.
- Broughton, G.I., Janis, J.E., and Attinger, C.E. (2006). Wound Healing: an overview. **Plast. Reconstr. Surg.** 117: 1e-S-32e-S.
- Bryder, D. and Jacobsen, S.E.W. (2000). Interleukin-3 supports expansion of long-term multilineage repopulating activity after multiple stem cell divisions *in vitro*. **Blood** 96: 1748-1755.
- Buske, C., Feuring-Buske, M., Abramovich, C., Spiekermann, K., Eaves, C.J., Coulombel, L., Sauvageau, G., Hogge, D.E., and Humphries, R.K. (2002). Deregulated expression of HOXB4 enhances the primitive growth activity of human hematopoietic cells. **Blood** 100: 862-868.
- Butler, J.M., Nolan, D.J., Vertes, E.L., Varnum-Finney, B., Kobayashi, H., Hooper, A.T., Seandel, M., Shido, K., White, I.A., Kobayashi, M., Witte, L., May, C., Shawber, C., Kimura, Y., Kitajewski, J., Rosenwaks, Z., Bernstein, I.D., and Rafii, S. (2010). Endothelial cells are essential for the self-renewal and repopulation of Notch-dependent hematopoietic stem cells. **Cell Stem Cell** 6: 251-264.

- Buza-Vidas, N., Antonchuk, J., Qian, H., Mansson, R., Luc, S., Zandi, S., Anderson, K., Takaki, S., Nygren, J.M., Jensen, C.T., and Jacobsen, S.E. (2006). Cytokines regulate postnatal hematopoietic stem cell expansion: opposing roles of thrombopoietin and LNK. **Genes Dev.** 20: 2018-2023.
- Caballero, S., Sengupta, N., Afzal, A., Chang, K.H., Li Calzi, S., Guberski, D.L., Kern, T.S., and Grant, M.B. (2007). Ischemic vascular damage can be repaired by healthy, but not diabetic, endothelial progenitor cells. **Diabetes** 56: 960-967.
- Calvi, L.M., Adams, G.B., Weibrecht, K.W., Weber, J.M., Olson, D.P., Knight, M.C., Martin, R.P., Schipani, E., Divieti, P., Bringhurst, F.R., Milner, L.A., Kronenberg, H.M., and Scadden, D.T. (2003). Osteoblastic cells regulate the haematopoietic stem cell niche. **Nature** 425: 841-846.
- Carver-Moore, K., Broxmeyer, H.E., Luoh, S.M., Cooper, S., Peng, J., Burstein, S.A., Moore, M.W., and de Sauvage, F.J. (1996). Low levels of erythroid and myeloid progenitors in thrombopoietin-and c-mpl-deficient mice. **Blood** 88: 803-808.
- Chalamalasetty, R.B., Dunty, W.C., Jr., Biris, K.K., Ajima, R., Iacovino, M., Beisaw, A., Feigenbaum, L., Chapman, D.L., Yoon, J.K., Kyba, M., and Yamaguchi, T.P. (2011). The Wnt3a/beta-catenin target gene Mesogenin1 controls the segmentation clock by activating a Notch signalling program. **Nat. Commun.** [On-line]. Available: <http://www.nature.com/ncomms/journal/v2/n7/abs/ncomms1381.html>.

- Chambers, I., Colby, D., Robertson, M., Nichols, J., Lee, S., Tweedie, S., and Smith, A. (2003). Functional expression cloning of Nanog, a pluripotency sustaining factor in embryonic stem cells. **Cell** 113: 643-655.
- Chamorro, M.N., Schwartz, D.R., Vonica, A., Brivanlou, A.H., Cho, K.R., and Varmus, H.E. (2005). FGF-20 and DKK1 are transcriptional targets of beta-catenin and FGF-20 is implicated in cancer and development. **EMBO. J.** 24: 73-84.
- Chan, R.K., Garfein, E., Gigante, P.R., Liu, P., Agha, R.A., Mulligan, R., and Orgill, D.P. (2007). Side population hematopoietic stem cells promote wound healing in diabetic mice. **Plast. Reconstr. Surg.** 120: 407-411; discussion 412-403.
- Chang, M.S., McNinch, J., Basu, R., Shutter, J., Hsu, R.Y., Perkins, C., Mar, V., Suggs, S., Welcher, A., Li, L., Lu, H., Bartley, T., Hunt, P., Martin, F., Samal, B., and Bogenberger, J. (1995). Cloning and characterization of the human megakaryocyte growth and development factor (MGDF) gene. **J. Biol. Chem.** 270: 511-514.
- Chanprasert, S., Geddis, A.E., Barroga, C., Fox, N.E., and Kaushansky, K. (2006). Thrombopoietin (TPO) induces c-myc expression through a PI3K- and MAPK-dependent pathway that is not mediated by Akt, PKC ζ or mTOR in TPO-dependent cell lines and primary megakaryocytes. **Cell Signal.** 18: 1212-1218.
- Chen, M.J., Yokomizo, T., Zeigler, B.M., Dzierzak, E., and Speck, N.A. (2009). Runx1 is required for the endothelial to haematopoietic cell transition but not thereafter. **Nature** 457: 887-891.

- Cheon, S., Poon, R., Yu, C., Khoury, M., Shenker, R., Fish, J., and Alman, B.A. (2005). Prolonged beta-catenin stabilization and tcf-dependent transcriptional activation in hyperplastic cutaneous wounds. **Lab. Invest.** 85: 416-425.
- Cheon, S.S., Cheah, A.Y., Turley, S., Nadesan, P., Poon, R., Clevers, H., and Alman, B.A. (2002). beta-Catenin stabilization dysregulates mesenchymal cell proliferation, motility, and invasiveness and causes aggressive fibromatosis and hyperplastic cutaneous wounds. **Proc. Natl. Acad. Sci. USA.** 99: 6973-6978.
- Chitteti, B.R., Cheng, Y.H., Poteat, B., Rodriguez-Rodriguez, S., Goebel, W.S., Carlesso, N., Kacena, M.A., and Srour, E.F. (2010). Impact of interactions of cellular components of the bone marrow microenvironment on hematopoietic stem and progenitor cell function. **Blood** 115: 3239-3248.
- Chou, F.S. and Mulloy, J.C. (2011). The thrombopoietin/MPL pathway in hematopoiesis and leukemogenesis. **J. Cell. Biochem.** 112: 1491-1498.
- Clements, W.K., Kim, A.D., Ong, K.G., Moore, J.C., Lawson, N.D., and Traver, D. (2011). A somitic Wnt16/Notch pathway specifies haematopoietic stem cells. **Nature** 474: 220-224.
- Clevers, H. (2006). Wnt/beta-catenin signaling in development and disease. **Cell** 127: 469-480.
- Conneally, E., Cashman, J., Petzer, A., and Eaves, C. (1997). Expansion *in vitro* of transplantable human cord blood stem cells demonstrated using a quantitative assay of their lympho-myeloid repopulating activity in nonobese diabetic-scid/scid mice. **Proc. Natl. Acad. Sci. USA.** 94: 9836-9841.

- Corbel, C., Salaun, J., Belo-Diabangouaya, P., and Dieterlen-Lievre, F. (2007). Hematopoietic potential of the pre-fusion allantois. **Dev. Biol.** 301: 478-488.
- Coskun, S. and Hirschi, K.K. (2010). Establishment and regulation of the HSC niche: roles of osteoblastic and vascular compartments. **Birth Defects Res. C Embryo Today** 90: 229-242.
- Couri, C.E., Oliveira, M.C., Stracieri, A.B., Moraes, D.A., Pieroni, F., Barros, G.M., Madeira, M.I., Malmegrim, K.C., Foss-Freitas, M.C., Simoes, B.P., Martinez, E.Z., Foss, M.C., Burt, R.K., and Voltarelli, J.C. (2009). C-peptide levels and insulin independence following autologous nonmyeloablative hematopoietic stem cell transplantation in newly diagnosed type 1 diabetes mellitus. **JAMA.** 301: 1573-1579.
- Cox, B., Kotlyar, M., Evangelou, A.I., Ignatchenko, V., Ignatchenko, A., Whiteley, K., Jurisica, I., Adamson, S.L., Rossant, J., and Kislinger, T. (2009). Comparative systems biology of human and mouse as a tool to guide the modeling of human placental pathology. **Mol. Syst. Biol.** 5: 279-293.
- Cross, J.C. (2005). How to make a placenta: Mechanisms of trophoblast cell differentiation in mice - A Review. **Placenta** 26: S3-S9.
- da Silva, C.L., Goncalves, R., dos Santos, F., Andrade, P.Z., Almeida-Porada, G., and Cabral, J.M. (2010). Dynamic cell-cell interactions between cord blood haematopoietic progenitors and the cellular niche are essential for the expansion of CD34(+), CD34(+)CD38(-) and early lymphoid CD7(+) cells. **J. Tissue Eng. Regen. Med.** 4: 149-158.

- Danaei, G., Finucane, M.M., Lu, Y., Singh, G.M., Cowan, M.J., Paciorek, C.J., Lin, J.K., Farzadfar, F., Khang, Y.H., Stevens, G.A., Rao, M., Ali, M.K., Riley, L.M., Robinson, C.A., and Ezzati, M. (2011). National, regional, and global trends in fasting plasma glucose and diabetes prevalence since 1980: systematic analysis of health examination surveys and epidemiological studies with 370 country-years and 2.7 million participants. **Lancet** 378: 31-40.
- de Barros, A.P., Takiya, C.M., Garzoni, L.R., Leal-Ferreira, M.L., Dutra, H.S., Chiarini, L.B., Meirelles, M.N., Borojevic, R., and Rossi, M.I. (2010). Osteoblasts and bone marrow mesenchymal stromal cells control hematopoietic stem cell migration and proliferation in 3D *in vitro* model. **PLoS One** 5: e9093-e9106.
- de Bruijn, M.F., Ma, X., Robin, C., Ottersbach, K., Sanchez, M.J., and Dzierzak, E. (2002). Hematopoietic stem cells localize to the endothelial cell layer in the midgestation mouse aorta. **Immunity** 16: 673-683.
- de Bruijn, M.F., Speck, N.A., Peeters, M.C., and Dzierzak, E. (2000). Definitive hematopoietic stem cells first develop within the major arterial regions of the mouse embryo. **EMBO. J.** 19: 2465-2474.
- De Felici, M., and Pesce, M. (1994). Growth factors in mouse primordial germ cell migration and proliferation. **Prog. Growth Factor Res.** 5: 135-143.
- De Paepe, M.E., Mao, Q., Ghanta, S., Hovanesian, V., and Padbury, J.F. (2011). Alveolar epithelial cell therapy with human cord blood-derived hematopoietic progenitor cells. **Am. J. Pathol.** 178: 1329-1339.

- de Sauvage, F.J., Hass, P.E., Spencer, S.D., Malloy, B.E., Gurney, A.L., Spencer, S.A., Darbonne, W.C., Henzel, W.J., Wong, S.C., Kuang, W.J., and et al. (1994). Stimulation of megakaryocytopoiesis and thrombopoiesis by the c-Mpl ligand. **Nature** 369: 533-538.
- Debili, N., Wendling, F., Cosman, D., Titeux, M., Florindo, C., Dusanter-Fourt, I., Schooley, K., Methia, N., Charon, M., Nador, R., Bettaieb, A., and Vainchenker, W. (1995). The Mpl receptor is expressed in the megakaryocytic lineage from late progenitors to platelets. **Blood** 85: 391-401.
- Delaney, C., Heimfeld, S., Brashem-Stein, C., Voorhies, H., Manger, R.L., and Bernstein, I.D. (2010). Notch-mediated expansion of human cord blood progenitor cells capable of rapid myeloid reconstitution. **Nat. Med.** 16: 232-236.
- Di Rocco, G., Gentile, A., Antonini, A., Ceradini, F., Wu, J.C., Capogrossi, M.C., and Toietta, G. (2011). Enhanced healing of diabetic wounds by topical administration of adipose tissue-derived stromal cells overexpressing stromal-derived factor-1: biodistribution and engraftment analysis by bioluminescent imaging. **Stem Cells Int.** [On-line]. Available: <http://www.hindawi.com/journals/sci/2011/304562/>.
- Dolence, J.J., Gwin, K., Frank, E., and Medina, K.L. (2011). Threshold levels of Flt3-ligand are required for the generation and survival of lymphoid progenitors and B-cell precursors. **Eur. J. Immunol.** 41: 324-334.

- Domashenko, A.D., Danet-Desnoyers, G., Aron, A., Carroll, M.P., and Emerson, S.G. (2010). TAT-mediated transduction of NF-Ya peptide induces the *ex vivo* proliferation and engraftment potential of human hematopoietic progenitor cells. **Blood** 116: 2676-2683.
- Dominici, M., Pritchard, C., Garlits, J.E., Hofmann, T.J., Persons, D.A., and Horwitz, E.M. (2004). Hematopoietic cells and osteoblasts are derived from a common marrow progenitor after bone marrow transplantation. **Proc. Natl. Acad. Sci. USA**. 101: 11761-11766.
- Doyonnas, R., Kershaw, D.B., Duhme, C., Merkens, H., Chelliah, S., Graf, T., and McNagny, K.M. (2001). Anuria, omphalocele, and perinatal lethality in mice lacking the CD34-related protein podocalyxin. **J. Exp. Med.** 194: 13-27.
- Drachman, J.G., and Kaushansky, K. (1997). Dissecting the thrombopoietin receptor: functional elements of the Mpl cytoplasmic domain. **Proc. Natl. Acad. Sci. USA**. 94: 2350-2355.
- Duailibi, M.T., Duailibi, S.E., Duailibi Neto, E.F., Negreiros, R.M., Jorge, W.A., Ferreira, L.M., Vacanti, J.P., and Yelick, P.C. (2011). Tooth tissue engineering: optimal dental stem cell harvest based on tooth development. **Artif. Organs**. 35:e129-e135.
- Duncan, A.W., Rattis, F.M., DiMascio, L.N., Congdon, K.L., Pazianos, G., Zhao, C., Yoon, K., Cook, J.M., Willert, K., Gaiano, N., and Reya, T. (2005). Integration of Notch and Wnt signaling in hematopoietic stem cell maintenance. **Nat. Immunol.** 6: 314-322.

- Durand, C., Robin, C., Bollerot, K., Baron, M.H., Ottersbach, K., and Dzierzak, E. (2007). Embryonic stromal clones reveal developmental regulators of definitive hematopoietic stem cells. **Proc. Natl. Acad. Sci. USA.** 104: 20838-20843.
- Ebihara, Y., Masuya, M., Larue, A.C., Fleming, P.A., Visconti, R.P., Minamiguchi, H., Drake, C.J., and Ogawa, M. (2006). Hematopoietic origins of fibroblasts: II. In vitro studies of fibroblasts, CFU-F, and fibrocytes. **Exp. Hematol.** 34: 219-229.
- Ehrlich, H.P. and Krummel, T.M. (1996). Regulation of wound healing from a connective tissue perspective. **Wound Repair Regen.** 4: 203-210.
- Eilken, H.M., Nishikawa, S., and Schroeder, T. (2009). Continuous single-cell imaging of blood generation from haemogenic endothelium. **Nature** 457: 896-900.
- Elkhafif, N., El Baz, H., Hammam, O., Hassan, S., Salah, F., Mansour, W., Mansy, S., Yehia, H., Zaki, A., and Magdy, R. (2011). CD133(+) human umbilical cord blood stem cells enhance angiogenesis in experimental chronic hepatic fibrosis. **APMIS.** 119: 66-75.
- Ema, H., Takano, H., Sudo, K., and Nakauchi, H. (2000). *In vitro* self-renewal division of hematopoietic stem cells. **J. Exp. Med.** 192: 1281-1288.
- Engstrom, M., Karlsson, R., and Jonsson, J.I. (2003). Inactivation of the forkhead transcription factor FoxO3 is essential for PKB-mediated survival of hematopoietic progenitor cells by kit ligand. **Exp. Hematol.** 31: 316-323.

- Erlandsson, A., Larsson, J., and Forsberg-Nilsson, K. (2004). Stem cell factor is a chemoattractant and a survival factor for CNS stem cells. **Exp. Cell. Res.** 301: 201-210.
- Fain, J.N. (2010). Release of inflammatory mediators by human adipose tissue is enhanced in obesity and primarily by the nonfat cells: a review. **Mediators Inflamm.** 2010: 513948.
- Fain, J.N., Madan, A.K., Hiler, M.L., Cheema, P., and Bahouth, S.W. (2004). Comparison of the release of adipokines by adipose tissue, adipose tissue matrix, and adipocytes from visceral and subcutaneous abdominal adipose tissues of obese humans. **Endocrinology** 145: 2273-2282.
- Fathke, C., Wilson, L., Shah, K., Kim, B., Hocking, A., Moon, R., and Isik, F. (2006). Wnt signaling induces epithelial differentiation during cutaneous wound healing. **BMC. Cell Biol.** 7: 4-12.
- Fewkes, N.M., Krauss, A.C., Guimond, M., Meadors, J.L., Dobre, S., and Mackall, C.L. (2010). Pharmacologic modulation of niche accessibility via tyrosine kinase inhibition enhances marrow and thymic engraftment after hematopoietic stem cell transplantation. **Blood** 115: 4120-4129.
- Fielding, C.A., McLoughlin, R.M., McLeod, L., Colmont, C.S., Najdovska, M., Grail, D., Ernst, M., Jones, S.A., Topley, N., and Jenkins, B.J. (2008). IL-6 regulates neutrophil trafficking during acute inflammation via STAT3. **J. Immunol.** 181: 2189-2195.

- Fleming, H.E., Janzen, V., Lo Celso, C., Guo, J., Leahy, K.M., Kronenberg, H.M., and Scadden, D.T. (2008). Wnt signaling in the niche enforces hematopoietic stem cell quiescence and is necessary to preserve self-renewal *in vivo*. **Cell Stem Cell** 2: 274-283.
- Foster, D.C., Sprecher, C.A., Grant, F.J., Kramer, J.M., Kuijper, J.L., Holly, R.D., Whitmore, T.E., Heipel, M.D., Bell, L.A., Ching, A.F., and et al. (1994). Human thrombopoietin: gene structure, cDNA sequence, expression, and chromosomal localization. **Proc. Natl. Acad. Sci. USA**. 91: 13023-13027.
- Fox, N., Priestley, G., Papayannopoulou, T., and Kaushansky, K. (2002). Thrombopoietin expands hematopoietic stem cells after transplantation. **J. Clin. Invest.** 110: 389-394.
- Fried, S.K., Bunkin, D.A., and Greenberg, A.S. (1998). Omental and subcutaneous adipose tissues of obese subjects release interleukin-6: depot difference and regulation by glucocorticoid. **J. Clin. Endocrinol. Metab.** 83: 847-850.
- Gallucci, R.M., Simeonova, P.P., Matheson, J.M., Kommineni, C., Guriel, J.L., Sugawara, T., and Luster, M.I. (2000). Impaired cutaneous wound healing in interleukin-6-deficient and immunosuppressed mice. **FASEB. J.** 14: 2525-2531.
- Gallucci, R.M., Sugawara, T., Yucesoy, B., Berryann, K., Simeonova, P.P., Matheson, J.M., and Luster, M.I. (2001). Interleukin-6 treatment augments cutaneous wound healing in immunosuppressed mice. **J. Interferon Cytokine Res.** 21: 603-609.

- Gammaitoni, L., Bruno, S., Sanavio, F., Gunetti, M., Kollet, O., Cavalloni, G., Falda, M., Fagioli, F., Lapidot, T., Aglietta, M., and Piacibello, W. (2003). *Ex vivo* expansion of human adult stem cells capable of primary and secondary hemopoietic reconstitution. **Exp. Hematol.** 31: 261-270.
- Gammaitoni, L., Weisel, K.C., Gunetti, M., Wu, K.D., Bruno, S., Pinelli, S., Bonati, A., Aglietta, M., Moore, M.A., and Piacibello, W. (2004). Elevated telomerase activity and minimal telomere loss in cord blood long-term cultures with extensive stem cell replication. **Blood** 103: 4440-4448.
- Gao, J., Graves, S., Koch, U., Liu, S., Jankovic, V., Buonamici, S., El Andaloussi, A., Nimer, S.D., Kee, B.L., Taichman, R., Radtke, F., and Aifantis, I. (2009). Hedgehog signaling is dispensable for adult hematopoietic stem cell function. **Cell Stem Cell** 4: 548-558.
- Geddis, A.E. (2010). Megakaryopoiesis. **Semin. Hematol.** 47: 212-219.
- Geddis, A.E., Fox, N.E., and Kaushansky, K. (2001). Phosphatidylinositol 3-kinase is necessary but not sufficient for thrombopoietin-induced proliferation in engineered Mpl-bearing cell lines as well as in primary megakaryocytic progenitors. **J. Biol. Chem.** 276: 34473-34479.
- Geissler, E.N., Liao, M., Brook, J.D., Martin, F.H., Zsebo, K.M., Housman, D.E., and Galli, S.J. (1991). Stem cell factor (SCF), a novel hematopoietic growth factor and ligand for c-kit tyrosine kinase receptor, maps on human chromosome 12 between 12q14.3 and 12qter. **Somat. Cell. Mol. Genet.** 17: 207-214.
- Gekas, C., Rhodes, K.E., Van Handel, B., Chhabra, A., Ueno, M., and Mikkola, H.K. (2010). Hematopoietic stem cell development in the placenta. **Int. J. Dev. Biol.** 54: 1089-1098.

- Georgiades, P., Ferguson-Smith, A.C., and Burton, G.J. (2002). Comparative developmental anatomy of the murine and human definitive placentae. **Placenta** 23: 3-19.
- Ghazizadeh, M. (2007). Essential role of IL-6 signaling pathway in keloid pathogenesis. **J. Nihon Med. Sch.** 74: 11-22.
- Gherghe, C.M., Duan, J., Gong, J., Rojas, M., Klauber-Demore, N., Majesky, M., and Deb, A. (2011). Wnt1 is a proangiogenic molecule, enhances human endothelial progenitor function, and increases blood flow to ischemic limbs in a HGF-dependent manner. **FASEB. J.** 25: 1836-1843.
- Gilliet, M., Boonstra, A., Paturel, C., Antonenko, S., Xu, X.L., Trinchieri, G., O'Garra, A., and Liu, Y.J. (2002). The development of murine plasmacytoid dendritic cell precursors is differentially regulated by FLT3-ligand and granulocyte/macrophage colony-stimulating factor. **J. Exp. Med.** 195: 953-958.
- Glejzer, A., Laudet, E., Leprince, P., Hennuy, B., Poulet, C., Shakhova, O., Sommer, L., Rogister, B., and Wislet-Gendebien, S. (2011). Wnt1 and BMP2: two factors recruiting multipotent neural crest progenitors isolated from adult bone marrow. **Cell. Mol. Life Sci.** 68: 2101-2114.
- Gluckman, E. (1996). The therapeutic potential of fetal and neonatal hematopoietic stem cells. **N. Engl. J. Med.** 335: 1839-1840.
- Goldman, D.C., Bailey, A.S., Pfaffle, D.L., Al Masri, A., Christian, J.L., and Fleming, W.H. (2009). BMP4 regulates the hematopoietic stem cell niche. **Blood** 114: 4393-4401.

- Gomei, Y., Nakamura, Y., Yoshihara, H., Hosokawa, K., Iwasaki, H., Suda, T., and Arai, F. (2010). Functional differences between two Tie2 ligands, angiopoietin-1 and -2, in regulation of adult bone marrow hematopoietic stem cells. **Exp. Hematol.** 38: 82-89.e81.
- Grellner, W. (2002). Time-dependent immunohistochemical detection of proinflammatory cytokines (IL-1beta, IL-6, TNF-alpha) in human skin wounds. **Forensic Sci. Int.** 130: 90-96.
- Grellner, W., Georg, T., and Wilske, J. (2000). Quantitative analysis of proinflammatory cytokines (IL-1beta, IL-6, TNF-alpha) in human skin wounds. **Forensic Sci. Int.** 113: 251-264.
- Guerif, F., Cadoret, V., Rahal-Perola, V., Lansac, J., Bernex, F., Panthier, J.J., Hochereau-de Reviers, M.T., and Royere, D. (2002). Apoptosis, onset and maintenance of spermatogenesis: evidence for the involvement of Kit in Kit-haplodeficient mice. **Biol. Reprod.** 67: 70-79.
- Guerriero, R., Parolini, I., Testa, U., Samoggia, P., Petrucci, E., Sargiacomo, M., Chelucci, C., Gabbianelli, M., and Peschle, C. (2006). Inhibition of TPO-induced MEK or mTOR activity induces opposite effects on the ploidy of human differentiating megakaryocytes. **J. Cell Sci.** 119: 744-752.
- Guo, Y., Hangoc, G., Bian, H., Pelus, L.M., and Broxmeyer, H.E. (2005). SDF-1/CXCL12 enhances survival and chemotaxis of murine embryonic stem cells and production of primitive and definitive hematopoietic progenitor cells. **Stem Cells** 23: 1324-1332.
- Gurney, A.L., Carver-Moore, K., de Sauvage, F.J., and Moore, M.W. (1994). Thrombocytopenia in c-mpl-deficient mice. **Science** 265: 1445-1447.

- Han, S., Dziedzic, N., Gadue, P., Keller, G.M., and Gouon-Evans, V. (2011). An endothelial cell niche induces hepatic specification through dual repression of wnt and notch signaling. **Stem Cells** 29: 217-228.
- Hannum, C., Culpepper, J., Campbell, D., McClanahan, T., Zurawski, S., Bazan, J.F., Kastelein, R., Hudak, S., Wagner, J., Mattson, J., and et al. (1994). Ligand for FLT3/FLK2 receptor tyrosine kinase regulates growth of haematopoietic stem cells and is encoded by variant RNAs. **Nature** 368: 643-648.
- Hao, Q.L., Shah, A.J., Thiemann, F.T., Smogorzewska, E.M., and Crooks, G.M. (1995). A functional comparison of CD34+CD38- cells in cord blood and bone marrow. **Blood** 86: 3745-3753.
- Hashizume, M., Hayakawa, N., and Mihara, M. (2008). IL-6 trans-signalling directly induces RANKL on fibroblast-like synovial cells and is involved in RANKL induction by TNF-alpha and IL-17. **Rheumatology (Oxford)** 47: 1635-1640.
- He, B., Reguart, N., You, L., Mazieres, J., Xu, Z., Lee, A.Y., Mikami, I., McCormick, F., and Jablons, D.M. (2005). Blockade of Wnt-1 signaling induces apoptosis in human colorectal cancer cells containing downstream mutations. **Oncogene** 24: 3054-3058.
- He, T.C., Sparks, A.B., Rago, C., Hermeking, H., Zawel, L., da Costa, L.T., Morin, P.J., Vogelstein, B., and Kinzler, K.W. (1998). Identification of c-MYC as a target of the APC pathway. **Science** 281: 1509-1512.
- He, B., You, L., Uematsu, K., Xu, Z., Lee, A.Y., Matsangou, M., McCormick, F., and Jablons, D.M. (2004). A monoclonal antibody against Wnt-1 induces apoptosis in human cancer cells. **Neoplasia** 6: 7-14.

- Heinrich, M.C., Dooley, D.C., Freed, A.C., Band, L., Hoatlin, M.E., Keeble, W.W., Peters, S.T., Silvey, K.V., Ey, F.S., Kabat, D., and et al. (1993). Constitutive expression of steel factor gene by human stromal cells. **Blood** 82: 771-783.
- Heinrich, P.C., Behrmann, I., Haan, S., Hermanns, H.M., Muller-Newen, G., and Schaper, F. (2003). Principles of interleukin (IL)-6-type cytokine signalling and its regulation. **Biochem. J.** 374: 1-20.
- Heissig, B., Hattori, K., Dias, S., Friedrich, M., Ferris, B., Hackett, N.R., Crystal, R.G., Besmer, P., Lyden, D., Moore, M.A., Werb, Z., and Rafii, S. (2002). Recruitment of stem and progenitor cells from the bone marrow niche requires MMP-9 mediated release of kit-ligand. **Cell** 109: 625-637.
- Heng, B.C., Liu, H., and Cao, T. (2005). Transplanted human embryonic stem cells as biological 'catalysts' for tissue repair and regeneration. **Med. Hypotheses** 64: 1085-1088.
- Heringer-Walther, S., Eckert, K., Schumacher, S.M., Uharek, L., Wulf-Goldenberg, A., Gembardt, F., Fichtner, I., Schultheiss, H.P., Rodgers, K., and Walther, T. (2009). Angiotensin-(1-7) stimulates hematopoietic progenitor cells *in vitro* and *in vivo*. **Haematologica** 94: 857-860.
- Hofmann, I., Stover, E.H., Cullen, D.E., Mao, J., Morgan, K.J., Lee, B.H., Kharas, M.G., Miller, P.G., Cornejo, M.G., Okabe, R., Armstrong, S.A., Ghilardi, N., Gould, S., de Sauvage, F.J., McMahon, A.P., and Gilliland, D.G. (2009). Hedgehog signaling is dispensable for adult murine hematopoietic stem cell function and hematopoiesis. **Cell Stem Cell** 4: 559-567.

- Hooper, A.T., Butler, J.M., Nolan, D.J., Kranz, A., Iida, K., Kobayashi, M., Kopp, H.G., Shido, K., Petit, I., Yanger, K., James, D., Witte, L., Zhu, Z., Wu, Y., Pytowski, B., Rosenwaks, Z., Mittal, V., Sato, T.N., and Rafii, S. (2009). Engraftment and reconstitution of hematopoiesis is dependent on VEGFR2-mediated regeneration of sinusoidal endothelial cells. **Cell Stem Cell** 4: 263-274.
- Horn, P., Bokermann, G., Cholewa, D., Bork, S., Walenda, T., Koch, C., Drescher, W., Hutschenreuther, G., Zenke, M., Ho, A.D., and Wagner, W. (2010). Impact of individual platelet lysates on isolation and growth of human mesenchymal stromal cells. **Cytotherapy** 12: 888-898.
- Hossle, J.P., Seger, R.A., and Steinhoff, D. (2002). Gene therapy of hematopoietic stem cells: strategies for improvement. **News Physiol. Sci.** 17: 87-92.
- Hou, T., Tieu, B.C., Ray, S., Recinos Iii, A., Cui, R., Tilton, R.G., and Brasier, A.R. (2008). Roles of IL-6-gp130 Signaling in Vascular Inflammation. **Curr. Cardiol. Rev.** 4: 179-192.
- Huang, C.L., Liu, D., Ishikawa, S., Nakashima, T., Nakashima, N., Yokomise, H., Kadota, K., and Ueno, M. (2008). Wnt1 overexpression promotes tumour progression in non-small cell lung cancer. **Eur. J. Cancer** 44: 2680-2688.
- Huang, E.J., Nocka, K.H., Buck, J., and Besmer, P. (1992). Differential expression and processing of two cell associated forms of the kit-ligand: KL-1 and KL-2. **Mol. Biol. Cell** 3: 349-362.
- Hubner, G., Brauchle, M., Smola, H., Madlener, M., Fassler, R., and Werner, S. (1996). Differential regulation of pro-inflammatory cytokines during wound healing in normal and glucocorticoid-treated mice. **Cytokine** 8: 548-556.

- Hung, C.N., Mar, K., Chang, H.C., Chiang, Y.L., Hu, H.Y., Lai, C.C., Chu, R.M., and Ma, C.M. (2011). A comparison between adipose tissue and dental pulp as sources of MSCs for tooth regeneration. **Biomaterials** 32: 6995-7005.
- Hurst, S.M., Wilkinson, T.S., McLoughlin, R.M., Jones, S., Horiuchi, S., Yamamoto, N., Rose-John, S., Fuller, G.M., Topley, N., and Jones, S.A. (2001). Il-6 and its soluble receptor orchestrate a temporal switch in the pattern of leukocyte recruitment seen during acute inflammation. **Immunity** 14: 705-714.
- Huttunen, M., Naukkarinen, A., Horsmanheimo, M., and Harvima, I.T. (2002). Transient production of stem cell factor in dermal cells but increasing expression of Kit receptor in mast cells during normal wound healing. **Arch. Dermatol. Res.** 294: 324-330.
- Huyhn, A., Dommergues, M., Izac, B., Croisille, L., Katz, A., Vainchenker, W., and Coulombel, L. (1995). Characterization of hematopoietic progenitors from human yolk sacs and embryos. **Blood** 86: 4474-4485.
- Ikeya, M., Lee, S.M., Johnson, J.E., McMahon, A.P., and Takada, S. (1997). Wnt signalling required for expansion of neural crest and CNS progenitors. **Nature** 389: 966-970.
- Imai, Y., Chou, T., Tobinai, K., Tanosaki, R., Morishima, Y., Ogura, M., Shimazaki, C., Taniwaki, M., Hiraoka, A., Tanimoto, M., Koike, T., Kogawa, K., Hirai, H., Yoshida, T., Tamura, K., Kishi, K., and Hotta, T. (2005). Isolation and transplantation of highly purified autologous peripheral CD34⁺ progenitor cells: purging efficacy, hematopoietic reconstitution in non-Hodgkin's lymphoma (NHL): results of Japanese phase II study. **Bone Marrow Transplant.** 35: 479-487.

- Ito, C.Y., Kirouac, D.C., Madlambayan, G.J., Yu, M., Rogers, I., and Zandstra, P.W. (2010). The AC133⁺CD38⁻, but not the rhodamine-low, phenotype tracks LTC-IC and SRC function in human cord blood *ex vivo* expansion cultures. **Blood** 115: 257-260.
- Ito, M., Kawa, Y., Ono, H., Okura, M., Baba, T., Kubota, Y., Nishikawa, S.I., and Mizoguchi, M. (1999). Removal of stem cell factor or addition of monoclonal anti-c-KIT antibody induces apoptosis in murine melanocyte precursors. **J. Invest. Dermatol.** 112: 796-801.
- Ivanovic, Z., Duchez, P., Chevaleyre, J., Vlaski, M., Lafarge, X., Dazey, B., Robert-Richard, E., Mazurier, F., and Boiron, J.M. (2011). Clinical-scale cultures of cord blood CD34⁺ cells to amplify committed progenitors and maintain stem cell activity. **Cell Transplant.** 20: 1453-1463.
- Iversen, M.M., Tell, G.S., Riise, T., Hanestad, B.R., Ostbye, T., Graue, M., and Midthjell, K. (2009). History of foot ulcer increases mortality among individuals with diabetes: ten-year follow-up of the Nord-Trondelag Health Study, Norway. **Diabetes Care** 32: 2193-2199.
- Iwama, A., Oguro, H., Negishi, M., Kato, Y., Morita, Y., Tsukui, H., Ema, H., Kamijo, T., Katoh-Fukui, Y., Koseki, H., van Lohuizen, M., and Nakauchi, H. (2004). Enhanced self-renewal of hematopoietic stem cells mediated by the polycomb gene product Bmi-1. **Immunity** 21: 843-851.
- Jacobson, L.O., Simmons, E.L., Marks, E.K., and Eldredge, J.H. (1951). Recovery from radiation injury. **Science** 113: 510-511.

- Jaffredo, T., Gautier, R., Eichmann, A., and Dieterlen-Lievre, F. (1998). Intraaortic hemopoietic cells are derived from endothelial cells during ontogeny. **Development** 125: 4575-4583.
- Jang, Y.K., Jung, D.H., Jung, M.H., Kim, D.H., Yoo, K.H., Sung, K.W., Koo, H.H., Oh, W., Yang, Y.S., and Yang, S.E. (2006). Mesenchymal stem cells feeder layer from human umbilical cord blood for *ex vivo* expanded growth and proliferation of hematopoietic progenitor cells. **Ann. Hematol.** 85: 212-225.
- Jazedje, T., Secco, M., Vieira, N.M., Zucconi, E., Gollop, T.R., Vainzof, M., and Zatz, M. (2009). Stem cells from umbilical cord blood do have myogenic potential, with and without differentiation induction in vitro. **J. Transl. Med.** 7: 6-14.
- Jones, S.A., Richards, P.J., Scheller, J., and Rose-John, S. (2005). IL-6 transsignaling: the in vivo consequences. **J. Interferon Cytokine Res.** 25: 241-253.
- Jung, Y., Song, J., Shiozawa, Y., Wang, J., Wang, Z., Williams, B., Havens, A., Schneider, A., Ge, C., Franceschi, R.T., McCauley, L.K., Krebsbach, P.H., and Taichman, R.S. (2008). Hematopoietic stem cells regulate mesenchymal stromal cell induction into osteoblasts thereby participating in the formation of the stem cell niche. **Stem Cells** 26: 2042-2051.
- Junrungsee, S., Kosachunhanun, N., Wongthanee, A., and Rerkasem, K. (2011). History of foot ulcers increases mortality among patients with diabetes in Northern Thailand. **Diabet. Med.** 28: 608-611.
- Kallianpur, A.R., Jordan, J.E., and Brandt, S.J. (1994). The SCL/TAL-1 gene is expressed in progenitors of both the hematopoietic and vascular systems during embryogenesis. **Blood** 83: 1200-1208.

- Karim, R.Z., Gerega, S.K., Yang, Y.H., Horvath, L., Spillane, A., Carmalt, H., Scolyer, R.A., and Lee, C.S. (2009). Proteins from the Wnt pathway are involved in the pathogenesis and progression of mammary phyllodes tumours. **J. Clin. Pathol.** 62: 1016-1020.
- Kashyap, V., Rezende, N.C., Scotland, K.B., Shaffer, S.M., Persson, J.L., Gudas, L.J., and Mongan, N.P. (2009). Regulation of stem cell pluripotency and differentiation involves a mutual regulatory circuit of the NANOG, OCT4, and SOX2 pluripotency transcription factors with polycomb repressive complexes and stem cell microRNAs. **Stem Cells Dev.** 18: 1093-1108.
- Katoh, M. (2002). WNT and FGF gene clusters (review). **Int. J. Oncol.** 21: 1269-1273.
- Katoh, M. (2003). Identification and characterization of human BCL9L gene and mouse Bcl9l gene *in silico*. **Int. J. Mol. Med.** 12: 643-649.
- Katoh, M. (2007). WNT signaling pathway and stem cell signaling network. **Clin. Cancer Res.** 13: 4042-4045.
- Khaodhjar, L., Ling, P.-R., Blackburn, G.L., and Bistrain, B.R. (2004). Serum levels of interleukin-6 and C-reactive protein correlate with body mass index across the broad range of obesity. **JPEN. J. Parenter. Enteral. Nutr.** 28: 410-415.
- Kharas, M.G., Okabe, R., Ganis, J.J., Gozo, M., Khandan, T., Paktinat, M., Gilliland, D.G., and Gritsman, K. (2010). Constitutively active AKT depletes hematopoietic stem cells and induces leukemia in mice. **Blood** 115: 1406-1415.

- Khurana, S., and Mukhopadhyay, A. (2008). *In vitro* transdifferentiation of adult hematopoietic stem cells: an alternative source of engraftable hepatocytes. **J. Hepatol.** 49: 998-1007.
- Kiel, M.J., Acar, M., Radice, G.L., and Morrison, S.J. (2009). Hematopoietic stem cells do not depend on N-cadherin to regulate their maintenance. **Cell Stem Cell** 4: 170-179.
- Kiel, M.J., Radice, G.L., and Morrison, S.J. (2007). Lack of evidence that hematopoietic stem cells depend on N-cadherin-mediated adhesion to osteoblasts for their maintenance. **Cell Stem Cell** 1: 204-217.
- Kiladjian, J.J., Elkassar, N., Hetet, C., Briere, J., Grandchamp, B., and Gardin, C. (1997). Study of the thrombopoietin receptor in essential thrombocythemia. **Leukemia** 11: 1821-1826.
- Kim, D.W., Lee, J.S., Yoon, E.S., Lee, B.I., Park, S.H., and Dhong, E.S. (2011). Influence of human adipose-derived stromal cells on Wnt signaling in organotypic skin culture. **J. Craniofac. Surg.** 22: 694-698.
- Kim, J.A., Kang, Y.J., Park, G., Kim, M., Park, Y.O., Kim, H., Leem, S.H., Chu, I.S., Lee, J.S., Jho, E.H., and Oh, I.H. (2009). Identification of a stroma-mediated Wnt/beta-catenin signal promoting self-renewal of hematopoietic stem cells in the stem cell niche. **Stem Cells** 27: 1318-1329.
- Kim, J.Y., Song, S.H., Kim, K.L., Ko, J.J., Im, J.E., Yie, S.W., Ahn, Y.K., Kim, D.K., and Suh, W. (2010). Human cord blood-derived endothelial progenitor cells and their conditioned media exhibit therapeutic equivalence for diabetic wound healing. **Cell Transplant.** 19: 1635-1644.

- Kim, Y.W., Koo, B.K., Jeong, H.W., Yoon, M.J., Song, R., Shin, J., Jeong, D.C., Kim, S.H., and Kong, Y.Y. (2008). Defective Notch activation in microenvironment leads to myeloproliferative disease. **Blood** 112: 4628-4638.
- Kimura, A. and Kishimoto, T. (2010). IL-6: regulator of Treg/Th17 balance. **Eur. J. Immunol.** 40: 1830-1835.
- Kinder, M., Wei, C., Shelat, S.G., Kundu, M., Zhao, L., Blair, I.A., and Pure, E. (2010). Hematopoietic stem cell function requires 12/15-lipoxygenase-dependent fatty acid metabolism. **Blood** 115: 5012-5022.
- Kirstetter, P., Anderson, K., Porse, B.T., Jacobsen, S.E., and Nerlov, C. (2006). Activation of the canonical Wnt pathway leads to loss of hematopoietic stem cell repopulation and multilineage differentiation block. **Nat. Immunol.** 7: 1048-1056.
- Ko, K.-H., Holmes, T., Palladinetti, P., Song, E., Nordon, R., O'Brien, T.A., and Dolnikov, A. (2011). GSK-3 β inhibition promotes engraftment of *ex vivo*-expanded hematopoietic stem cells and modulates gene expression. **Stem Cells** 29: 108-118.
- Kobayashi, H., Butler, J.M., O'Donnell, R., Kobayashi, M., Ding, B.S., Bonner, B., Chiu, V.K., Nolan, D.J., Shido, K., Benjamin, L., and Rafii, S. (2010). Angiocrine factors from Akt-activated endothelial cells balance self-renewal and differentiation of haematopoietic stem cells. **Nat. Cell. Biol.** 12: 1046-1056.

- Kohara, H., Omatsu, Y., Sugiyama, T., Noda, M., Fujii, N., and Nagasawa, T. (2007). Development of plasmacytoid dendritic cells in bone marrow stromal cell niches requires CXCL12-CXCR4 chemokine signaling. **Blood** 110: 4153-4160.
- Kondo, M., Wagers, A.J., Manz, M.G., Prohaska, S.S., Scherer, D.C., Beilhack, G.F., Shizuru, J.A., and Weissman, I.L. (2003). Biology of hematopoietic stem cells and progenitors: implications for clinical application. **Annu. Rev. Immunol.** 21: 759-806.
- Koutna, I., Peterkova, M., Simara, P., Stejskal, S., Tesarova, L., and Kozubek, M. (2011). Proliferation and differentiation potential of CD133⁺ and CD34⁺ populations from the bone marrow and mobilized peripheral blood. **Ann. Hematol.** 90: 127-137.
- Kramps, T., Peter, O., Brunner, E., Nellen, D., Froesch, B., Chatterjee, S., Murone, M., Zullig, S., and Basler, K. (2002). Wnt/wingless signaling requires BCL9/legless-mediated recruitment of pygopus to the nuclear beta-catenin-TCF complex. **Cell** 109: 47-60.
- Krause, D.S., Fackler, M.J., Civin, C.I., and May, W.S. (1996). CD34: structure, biology, and clinical utility. **Blood** 87: 1-13.
- Krosl, J., Austin, P., Beslu, N., Kroon, E., Humphries, R.K., and Sauvageau, G. (2003). *In vitro* expansion of hematopoietic stem cells by recombinant TAT-HOXB4 protein. **Nat. Med.** 9: 1428-1432.
- Labastie, M.C., Cortes, F., Romeo, P.H., Dulac, C., and Peault, B. (1998). Molecular identity of hematopoietic precursor cells emerging in the human embryo. **Blood** 92: 3624-3635.

- Lam, A.C., Li, K., Zhang, X.B., Li, C.K., Fok, T.F., Chang, A.M., James, A.E., Tsang, K.S., and Yuen, P.M. (2001). Preclinical *ex vivo* expansion of cord blood hematopoietic stem and progenitor cells: duration of culture; the media, serum supplements, and growth factors used; and engraftment in NOD/SCID mice. **Transfusion** 41: 1567-1576.
- Lam, C.R., Tan, M.J., Tan, S.H., Tang, M.B., Cheung, P.C., and Tan, N.S. (2011). TAK1 regulates SCF expression to modulate PKBalpha activity that protects keratinocytes from ROS-induced apoptosis. **Cell Death Differ.** 18: 1120-1129.
- Larue, L. and Delmas, V. (2006). The WNT/Beta-catenin pathway in melanoma. **Front. Biosci.** 11: 733-742.
- Lee, K.B., Choi, J., Cho, S.B., Chung, J.Y., Moon, E.S., Kim, N.S., and Han, H.J. (2011a). Topical embryonic stem cells enhance wound healing in diabetic rats. **J. Orthop. Res.** 29: 1554-1562.
- Lee, M.J., Kim, J., Lee, K.I., Shin, J.M., Chae, J.I., and Chung, H.M. (2011b). Enhancement of wound healing by secretory factors of endothelial precursor cells derived from human embryonic stem cells. **Cytotherapy** 13: 165-178.
- Lee, M.Y., Lim, H.W., Lee, S.H., and Han, H.J. (2009). Smad, PI3K/Akt, and Wnt-dependent signaling pathways are involved in BMP-4-induced ESC self-renewal. **Stem Cells** 27: 1858-1868.

- Lee, T.N., Alborn, W.E., Knierman, M.D., and Konrad, R.J. (2006). The diabetogenic antibiotic streptozotocin modifies the tryptic digest pattern for peptides of the enzyme O-GlcNAc-selective N-acetyl-beta-d-glucosaminidase that contain amino acid residues essential for enzymatic activity. **Biochem. Pharmacol.** 72: 710-718.
- Li, B., Bailey, A.S., Jiang, S., Liu, B., Goldman, D.C., and Fleming, W.H. (2010). Endothelial cells mediate the regeneration of hematopoietic stem cells. **Stem Cell Res.** 4: 17-24.
- Lin, G.L. and Hankenson, K.D. (2011). Integration of BMP, Wnt, and Notch signaling pathways in osteoblast differentiation. **J. Cell. Biochem.** 112: 3491-3501.
- Lin, Z.Q., Kondo, T., Ishida, Y., Takayasu, T., and Mukaida, N. (2003). Essential involvement of IL-6 in the skin wound-healing process as evidenced by delayed wound healing in IL-6-deficient mice. **J. Leukoc. Biol.** 73: 713-721.
- Liu, Z.J., Italiano, J., Jr., Ferrer-Marin, F., Gutti, R., Bailey, M., Poterjoy, B., Rimsza, L., and Sola-Visner, M. (2011). Developmental differences in megakaryocytopoiesis are associated with up-regulated TPO signaling through mTOR and elevated GATA-1 levels in neonatal megakaryocytes. **Blood** 117: 4106-4117.
- Livnah, O., Stura, E.A., Middleton, S.A., Johnson, D.L., Jolliffe, L.K., and Wilson, I.A. (1999). Crystallographic evidence for preformed dimers of erythropoietin receptor before ligand activation. **Science** 283: 987-990.

- Lo Celso, C., Fleming, H.E., Wu, J.W., Zhao, C.X., Miake-Lye, S., Fujisaki, J., Cote, D., Rowe, D.W., Lin, C.P., and Scadden, D.T. (2009). Live-animal tracking of individual haematopoietic stem/progenitor cells in their niche. **Nature** 457: 92-96.
- Lo Muzio, L. (2001). A possible role for the WNT-1 pathway in oral carcinogenesis. **Crit. Rev. Oral. Biol. Med.** 12: 152-165.
- Longley, B.J., Jr., Morganroth, G.S., Tyrrell, L., Ding, T.G., Anderson, D.M., Williams, D.E., and Halaban, R. (1993). Altered metabolism of mast-cell growth factor (c-kit ligand) in cutaneous mastocytosis. **N. Engl. J. Med.** 328: 1302-1307.
- Lorenz, E., Uphoff, D., Reid, T.R., and Shelton, E. (1951). Modification of irradiation injury in mice and guinea pigs by bone marrow injections. **J. Natl. Cancer Inst.** 12: 197-201.
- Luis, T.C., Weerkamp, F., Naber, B.A., Baert, M.R., de Haas, E.F., Nikolic, T., Heuvelmans, S., De Krijger, R.R., van Dongen, J.J., and Staal, F.J. (2009). Wnt3a deficiency irreversibly impairs hematopoietic stem cell self-renewal and leads to defects in progenitor cell differentiation. **Blood** 113: 546-554.
- Lyman, S.D. (1995). Biology of flt3 ligand and receptor. **Int. J. Hematol.** 62: 63-73.
- Lyman, S.D. and Jacobsen, S.E. (1998). c-kit ligand and Flt3 ligand: stem/progenitor cell factors with overlapping yet distinct activities. **Blood** 91: 1101-1134.
- Ma, Y.D., Park, C., Zhao, H., Oduro, K.A., Jr., Tu, X., Long, F., Allen, P.M., Teitelbaum, S.L., and Choi, K. (2009). Defects in osteoblast function but no changes in long-term repopulating potential of hematopoietic stem cells in a mouse chronic inflammatory arthritis model. **Blood** 114: 4402-4410.

- Madani, R., Karastergiou, K., Ogston, N.C., Miheisi, N., Bhome, R., Haloob, N., Tan, G.D., Karpe, F., Malone-Lee, J., Hashemi, M., Jahangiri, M., and Mohamed-Ali, V. (2009). RANTES release by human adipose tissue *in vivo* and evidence for depot-specific differences. **Am. J. Physiol. Endocrinol. Metab.** 296: E1262-1268.
- Maggio, M., Guralnik, J.M., Longo, D.L., and Ferrucci, L. (2006). Interleukin-6 in aging and chronic disease: a magnificent pathway. **J. Gerontol. A. Biol. Sci. Med. Sci.** 61: 575-584.
- Maharlooei, M.K., Bagheri, M., Solhjoui, Z., Jahromi, B.M., Akrami, M., Rohani, L., Monabati, A., Noorafshan, A., and Omrani, G.R. (2011). Adipose tissue derived mesenchymal stem cell (AD-MSC) promotes skin wound healing in diabetic rats. **Diabetes Res. Clin. Pract.** 93: 228-234.
- Maillard, I., Koch, U., Dumortier, A., Shestova, O., Xu, L., Sai, H., Pross, S.E., Aster, J.C., Bhandoola, A., Radtke, F., and Pear, W.S. (2008). Canonical notch signaling is dispensable for the maintenance of adult hematopoietic stem cells. **Cell Stem Cell** 2: 356-366.
- Majeti, R., Park, C.Y., and Weissman, I.L. (2007). Identification of a hierarchy of multipotent hematopoietic progenitors in human cord blood. **Cell Stem Cell** 1: 635-645.
- Mancini, S.J., Mantei, N., Dumortier, A., Suter, U., MacDonald, H.R., and Radtke, F. (2005). Jagged1-dependent Notch signaling is dispensable for hematopoietic stem cell self-renewal and differentiation. **Blood** 105: 2340-2342.

- Manova, K., Huang, E.J., Angeles, M., De Leon, V., Sanchez, S., Pronovost, S.M., Besmer, P., and Bachvarova, R.F. (1993). The expression pattern of the c-kit ligand in gonads of mice supports a role for the c-kit receptor in oocyte growth and in proliferation of spermatogonia. **Dev. Biol.** 157: 85-99.
- Manz, M.G., Traver, D., Akashi, K., Merad, M., Miyamoto, T., Engleman, E.G., and Weissman, I.L. (2001a). Dendritic cell development from common myeloid progenitors. **Ann. NY. Acad. Sci.** 938: 167-173; discussion 173-164.
- Manz, M.G., Traver, D., Miyamoto, T., Weissman, I.L., and Akashi, K. (2001b). Dendritic cell potentials of early lymphoid and myeloid progenitors. **Blood** 97: 3333-3341.
- Massa, S., Balciunaite, G., Ceredig, R., and Rolink, A.G. (2006). Critical role for c-kit (CD117) in T cell lineage commitment and early thymocyte development in vitro. **Eur. J. Immunol.** 36: 526-532.
- Masui, S., Nakatake, Y., Toyooka, Y., Shimosato, D., Yagi, R., Takahashi, K., Okochi, H., Okuda, A., Matoba, R., Sharov, A.A., Ko, M.S., and Niwa, H. (2007). Pluripotency governed by Sox2 via regulation of Oct3/4 expression in mouse embryonic stem cells. **Nat. Cell Biol.** 9: 625-635.
- Matsumoto, T., Ingham, S.M., Mifune, Y., Osawa, A., Logar, A., Usas, A., Kuroda, R., Kurosaka, M., Fu, F.H., and Huard, J. (2011). Isolation and Characterization of Human Anterior Cruciate Ligament-Derived Vascular Stem Cells. **Stem Cells Dev.** [On-line]. Available: <http://www.liebertonline.com/doi/abs/10.1089/scd.2010.05028>.

- Mayani, H., Dragowska, W., and Lansdorp, P.M. (1993). Characterization of functionally distinct subpopulations of CD34⁺ cord blood cells in serum-free long-term cultures supplemented with hematopoietic cytokines. **Blood** 82: 2664-2672.
- Mayani, H. and Lansdorp, P.M. (1998). Biology of human umbilical cord blood-derived hematopoietic stem/progenitor cells. **Stem Cells** 16: 153-165.
- McKenna, H.J., Stocking, K.L., Miller, R.E., Brasel, K., De Smedt, T., Maraskovsky, E., Maliszewski, C.R., Lynch, D.H., Smith, J., Pulendran, B., Roux, E.R., Teepe, M., Lyman, S.D., and Peschon, J.J. (2000). Mice lacking flt3 ligand have deficient hematopoiesis affecting hematopoietic progenitor cells, dendritic cells, and natural killer cells. **Blood** 95: 3489-3497.
- McMahon, A.P., Joyner, A.L., Bradley, A., and McMahon, J.A. (1992). The midbrain-hindbrain phenotype of Wnt-1/Wnt-1- mice results from stepwise deletion of engrailed-expressing cells by 9.5 days postcoitum. **Cell** 69: 581-595.
- McNiece, I., Jones, R., Bearman, S.I., Cagnoni, P., Nieto, Y., Franklin, W., Ryder, J., Steele, A., Stoltz, J., Russell, P., McDermitt, J., Hogan, C., Murphy, J., and Shpall, E.J. (2000). *Ex vivo* expanded peripheral blood progenitor cells provide rapid neutrophil recovery after high-dose chemotherapy in patients with breast cancer. **Blood** 96: 3001-3007.
- Medvinsky, A. and Dzierzak, E. (1996). Definitive hematopoiesis is autonomously initiated by the AGM region. **Cell** 86: 897-906.

- Mehrotra, M., Rosol, M., Ogawa, M., and Larue, A.C. (2010). Amelioration of a mouse model of osteogenesis imperfecta with hematopoietic stem cell transplantation: microcomputed tomography studies. **Exp. Hematol.** 38: 593-602.
- Merchant, A., Joseph, G., Wang, Q., Brennan, S., and Matsui, W. (2010). Gli1 regulates the proliferation and differentiation of HSCs and myeloid progenitors. **Blood** 115: 2391-2396.
- Mikami, I., You, L., He, B., Xu, Z., Batra, S., Lee, A.Y., Mazieres, J., Reguart, N., Uematsu, K., Koizumi, K., and Jablons, D.M. (2005). Efficacy of Wnt-1 monoclonal antibody in sarcoma cells. **BMC. Cancer** 5: 53.
- Mikkola, H.K. and Orkin, S.H. (2006). The journey of developing hematopoietic stem cells. **Development** 133: 3733-3744.
- Miller, J.R., Hocking, A.M., Brown, J.D., and Moon, R.T. (1999). Mechanism and function of signal transduction by the Wnt/beta-catenin and Wnt/Ca²⁺ pathways. **Oncogene** 18: 7860-7872.
- Minamiguchi, H., Ishikawa, F., Fleming, P.A., Yang, S., Drake, C.J., Wingard, J.R., and Ogawa, M. (2008). Transplanted human cord blood cells generate amylase-producing pancreatic acinar cells in engrafted mice. **Pancreas** 36: e30-35.
- Mishima, S., Nagai, A., Abdullah, S., Matsuda, C., Taketani, T., Kumakura, S., Shibata, H., Ishikura, H., Kim, S.U., and Masuda, J. (2010). Effective ex vivo expansion of hematopoietic stem cells using osteoblast-differentiated mesenchymal stem cells is CXCL12 dependent. **Eur. J. Haematol.** 84: 538-546.

- Miyake, N., Brun, A.C., Magnusson, M., Miyake, K., Scadden, D.T., and Karlsson, S. (2006). HOXB4-induced self-renewal of hematopoietic stem cells is significantly enhanced by p21 deficiency. **Stem Cells** 24: 653-661.
- Mohamed-Ali, V., Goodrick, S., Rawesh, A., Katz, D.R., Miles, J.M., Yudkin, J.S., Klein, S., and Coppel, S.W. (1997). Subcutaneous adipose tissue releases interleukin-6, but not tumor necrosis factor- α , in vivo. **J. Clin. Endocrinol. Metab.** 82: 4196-4200.
- Moore, M.A., and Metcalf, D. (1970). Ontogeny of the haemopoietic system: yolk sac origin of *in vivo* and *in vitro* colony forming cells in the developing mouse embryo. **Br. J. Haematol.** 18: 279-296.
- Morita, E., Tanaka, T., Shinoda, S., Kameyoshi, Y., Yamamoto, S., Lee, D.G., and Sugiyama, M. (1997). Expression of multiple forms of fetal liver kinase-2 (flk-2/flt-3) ligand in cultured human keratinocytes. **Arch. Dermatol. Res.** 289: 177-179.
- Motyl, K., and McCabe, L.R. (2009). Streptozotocin, type I diabetes severity and bone. **Biol. Proced. Online** 11: 296-315.
- Muller, A.M., Medvinsky, A., Strouboulis, J., Grosveld, F., and Dzierzak, E. (1994). Development of hematopoietic stem cell activity in the mouse embryo. **Immunity** 1: 291-301.
- Murdoch, B., Chadwick, K., Martin, M., Shojaei, F., Shah, K.V., Gallacher, L., Moon, R.T., and Bhatia, M. (2003). Wnt-5A augments repopulating capacity and primitive hematopoietic development of human blood stem cells in vivo. **Proc. Natl. Acad. Sci. USA.** 100: 3422-3427.

- Murray, P.D.F. (1932). The Development *in vitro* of the Blood of the Early Chick Embryo. **Proc. R. Soc. Lond. B.** 111: 497-521.
- Nagasawa, T. (2006). Microenvironmental niches in the bone marrow required for B-cell development. **Nat. Rev. Immunol.** 6: 107-116.
- Nagasawa, T., Omatsu, Y., and Sugiyama, T. (2011). Control of hematopoietic stem cells by the bone marrow stromal niche: the role of reticular cells. **Trends Immunol.** 32: 315-320.
- Naik, S.H., Proietto, A.I., Wilson, N.S., Dakic, A., Schnorrer, P., Fuchsberger, M., Lahoud, M.H., O'Keeffe, M., Shao, Q.X., Chen, W.F., Villadangos, J.A., Shortman, K., and Wu, L. (2005). Cutting edge: generation of splenic CD8⁺ and CD8⁻ dendritic cell equivalents in Fms-like tyrosine kinase 3 ligand bone marrow cultures. **J. Immunol.** 174: 6592-6597.
- Nakamura, Y., Arai, F., Iwasaki, H., Hosokawa, K., Kobayashi, I., Gomei, Y., Matsumoto, Y., Yoshihara, H., and Suda, T. (2010). Isolation and characterization of endosteal niche cell populations that regulate hematopoietic stem cells. **Blood** 116: 1422-1432.
- Nakao, T., Geddis, A.E., Fox, N.E., and Kaushansky, K. (2008). PI3K/Akt/FOXO3a pathway contributes to thrombopoietin-induced proliferation of primary megakaryocytes *in vitro* and *in vivo* via modulation of p27(Kip1). **Cell Cycle** 7: 257-266.
- Namikawa, R., Muench, M.O., de Vries, J.E., and Roncarolo, M.G. (1996). The FLK2/FLT3 ligand synergizes with interleukin-7 in promoting stromal-cell-independent expansion and differentiation of human fetal pro-B cells *in vitro*. **Blood** 87: 1881-1890.

- Naoe, T. and Kiyoi, H. (2004). Normal and oncogenic FLT3. **Cell. Mol. Life Sci.** 61: 2932-2938.
- Nie, Y., Han, Y.C., and Zou, Y.R. (2008). CXCR4 is required for the quiescence of primitive hematopoietic cells. **J. Exp. Med.** 205: 777-783.
- Nikolova, T., Wu, M., Brumbarov, K., Alt, R., Opitz, H., Boheler, K.R., Cross, M., and Wobus, A.M. (2007). WNT-conditioned media differentially affect the proliferation and differentiation of cord blood-derived CD133⁺ cells *in vitro*. **Differentiation** 75: 100-111.
- Nilsson, G., Butterfield, J.H., Nilsson, K., and Siegbahn, A. (1994). Stem cell factor is a chemotactic factor for human mast cells. **J. Immunol.** 153: 3717-3723.
- Nilsson, S.K., Simmons, P.J., and Bertoncello, I. (2006). Hemopoietic stem cell engraftment. **Exp. Hematol.** 34: 123-129.
- Nishikawa, S.I., Nishikawa, S., Kawamoto, H., Yoshida, H., Kizumoto, M., Kataoka, H., and Katsura, Y. (1998). *In vitro* generation of lymphohematopoietic cells from endothelial cells purified from murine embryos. **Immunity** 8: 761-769.
- Nishio, Y., Koda, M., Kamada, T., Someya, Y., Yoshinaga, K., Okada, S., Harada, H., Okawa, A., Moriya, H., and Yamazaki, M. (2006). The use of hemopoietic stem cells derived from human umbilical cord blood to promote restoration of spinal cord tissue and recovery of hindlimb function in adult rats. **J. Neurosurg. Spine.** 5: 424-433.
- Noda, M., Omatsu, Y., Sugiyama, T., Oishi, S., Fujii, N., and Nagasawa, T. (2011). CXCL12-CXCR4 chemokine signaling is essential for NK-cell development in adult mice. **Blood** 117: 451-458.

- Notta, F., Doulatov, S., Laurenti, E., Poeppl, A., Jurisica, I., and Dick, J.E. (2011). Isolation of single human hematopoietic stem cells capable of long-term multilineage engraftment. **Science** 333: 218-221.
- Oberlin, E., El Hafny, B., Petit-Cocault, L., and Souyri, M. (2010). Definitive human and mouse hematopoiesis originates from the embryonic endothelium: a new class of HSCs based on VE-cadherin expression. **Int. J. Dev. Biol.** 54: 1165-1173.
- Ogami, K. (1996). Gene expression and transcriptional regulation of thrombopoietin. **Stem Cells** 14(Suppl 1): 148-153.
- Oh, I.-H. (2010). Microenvironmental targeting of Wnt/ β -catenin signals for hematopoietic stem cell regulation. **Expert Opin. Biol. Ther.** 10: 1315-1329.
- Ohishi, K., Varnum-Finney, B., and Bernstein, I.D. (2002). Delta-1 enhances marrow and thymus repopulating ability of human CD34(+)CD38(-) cord blood cells. **J. Clin. Invest.** 110: 1165-1174.
- Ohta, H., Sekulovic, S., Bakovic, S., Eaves, C.J., Pineault, N., Gasparetto, M., Smith, C., Sauvageau, G., and Humphries, R.K. (2007). Near-maximal expansions of hematopoietic stem cells in culture using NUP98-HOX fusions. **Exp. Hematol.** 35: 817-830.
- Omatsu, Y., Sugiyama, T., Kohara, H., Kondoh, G., Fujii, N., Kohno, K., and Nagasawa, T. (2010). The essential functions of adipo-osteogenic progenitors as the hematopoietic stem and progenitor cell niche. **Immunity** 33: 387-399.

- Otto, A., Schmidt, C., Luke, G., Allen, S., Valasek, P., Muntoni, F., Lawrence-Watt, D., and Patel, K. (2008). Canonical Wnt signalling induces satellite-cell proliferation during adult skeletal muscle regeneration. **J. Cell. Sci.** 121: 2939-2950.
- Papayannopoulou, T., Brice, M., Broudy, V.C., and Zsebo, K.M. (1991). Isolation of c-kit receptor-expressing cells from bone marrow, peripheral blood, and fetal liver: functional properties and composite antigenic profile. **Blood** 78: 1403-1412.
- Paquet, P. and Pierard, G.E. (1996). Interleukin-6 and the skin. **Int. Arch. Allergy. Immunol.** 109: 308-317.
- Pedroso, D.C.S., Tellechea, A., Moura, L., Fidalgo-Carvalho, I., Duarte, J., Carvalho, E., and Ferreira, L. (2011). Improved survival, vascular differentiation and wound healing potential of stem cells co-cultured with endothelial cells. **PLoS One** 6: e16114-e16125.
- Pennica, D., Swanson, T.A., Welsh, J.W., Roy, M.A., Lawrence, D.A., Lee, J., Brush, J., Taneyhill, L.A., Deuel, B., Lew, M., Watanabe, C., Cohen, R.L., Melhem, M.F., Finley, G.G., Quirke, P., Goddard, A.D., Hillan, K.J., Gurney, A.L., Botstein, D., and Levine, A.J. (1998). WISP genes are members of the connective tissue growth factor family that are up-regulated in wnt-1-transformed cells and aberrantly expressed in human colon tumors. **Proc. Natl. Acad. Sci. USA.** 95: 14717-14722.
- Pereira, C., Clarke, E., and Damen, J. (2007). Hematopoietic colony-forming cell assays. **Methods Mol. Biol.** 407: 177-208.

- Pessina, A., Bonomi, A., Sisto, F., Baglio, C., Cavicchini, L., Ciusani, E., Cocce, V., and Gribaldo, L. (2010). CD45⁺/CD133⁺ positive cells expanded from umbilical cord blood expressing PDX-1 and markers of pluripotency. **Cell Biol. Int.** 34: 783-790.
- Peter, I.S. and Davidson, E.H. (2011). A gene regulatory network controlling the embryonic specification of endoderm. **Nature** 474: 635-639.
- Piacibello, W., Gammaitoni, L., Bruno, S., Gunetti, M., Fagioli, F., Cavalloni, G., and Aglietta, M. (2000). Negative influence of IL3 on the expansion of human cord blood *in vivo* long-term repopulating stem cells. **J. Hematother. Stem Cell Res.** 9: 945-956.
- Piao, C.S., Li, B., Zhang, L.J., and Zhao, L.R. (2012). Stem cell factor and granulocyte colony-stimulating factor promote neuronal lineage commitment of neural stem cells. **Differentiation** 83: 17-25.
- Pinson, K.I., Brennan, J., Monkley, S., Avery, B.J., and Skarnes, W.C. (2000). An LDL-receptor-related protein mediates Wnt signalling in mice. **Nature** 407: 535-538.
- Pozzobon, M., Bollini, S., Iop, L., De Gaspari, P., Chiavegato, A., Rossi, C.A., Giuliani, S., Fascetti Leon, F., Elvassore, N., Sartore, S., and De Coppi, P. (2010). Human bone marrow-derived CD133(+) cells delivered to a collagen patch on cryoinjured rat heart promote angiogenesis and arteriogenesis. **Cell Transplant.** 19: 1247-1260.

- Pradhan, L., Nabzdyk, C., Andersen, N.D., LoGerfo, F.W., and Veves, A. (2009). Inflammation and neuropeptides: the connection in diabetic wound healing. **Expert Rev. Mol. Med.** [On-line]. Available: http://journals.cambridge.org/abstract_S1462399409000945
- Pranke, P., Hendrikx, J., Debnath, G., Alespeiti, G., Rubinstein, P., Nardi, N., and Visser, J. (2005). Immunophenotype of hematopoietic stem cells from placental/umbilical cord blood after culture. **Braz. J. Med. Biol. Res.** 38: 1775-1789.
- Price, M.A. (2006). CKI, there's more than one: casein kinase I family members in Wnt and Hedgehog signaling. **Genes Dev.** 20: 399-410.
- Qian, H., Buza-Vidas, N., Hyland, C.D., Jensen, C.T., Antonchuk, J., Mansson, R., Thoren, L.A., Ekblom, M., Alexander, W.S., and Jacobsen, S.E. (2007). Critical role of thrombopoietin in maintaining adult quiescent hematopoietic stem cells. **Cell Stem Cell** 1: 671-684.
- Qiu, L., Meagher, R., Welhausen, S., Heye, M., Brown, R., and Herzig, R.H. (1999). *Ex vivo* expansion of CD34⁺ umbilical cord blood cells in a defined serum-free medium (QBSF-60) with early effect cytokines. **J. Hematother. Stem Cell Res.** 8: 609-618.
- Ranganathan, P., Weaver, K.L., and Capobianco, A.J. (2011). Notch signalling in solid tumours: a little bit of everything but not all the time. **Nat. Rev. Cancer** 11: 338-351.

- Raslova, H., Baccini, V., Loussaief, L., Comba, B., Larghero, J., Debili, N., and Vainchenker, W. (2006). Mammalian target of rapamycin (mTOR) regulates both proliferation of megakaryocyte progenitors and late stages of megakaryocyte differentiation. **Blood** 107: 2303-2310.
- Ray, P., Krishnamoorthy, N., and Ray, A. (2008). Emerging functions of c-kit and its ligand stem cell factor in dendritic cells: regulators of T cell differentiation. **Cell Cycle** 7: 2826-2832.
- Reali, C., Scintu, F., Pillai, R., Cabras, S., Argiolu, F., Ristaldi, M.S., Sanna, M.A., Badiali, M., and Sogos, V. (2006). Differentiation of human adult CD34⁺ stem cells into cells with a neural phenotype: role of astrocytes. **Exp. Neurol.** 197: 399-406.
- Reya, T., Duncan, A.W., Ailles, L., Domen, J., Scherer, D.C., Willert, K., Hintz, L., Nusse, R., and Weissman, I.L. (2003). A role for Wnt signalling in self-renewal of haematopoietic stem cells. **Nature** 423: 409-414.
- Rhodes, K.E., Gekas, C., Wang, Y., Lux, C.T., Francis, C.S., Chan, D.N., Conway, S., Orkin, S.H., Yoder, M.C., and Mikkola, H.K. (2008). The emergence of hematopoietic stem cells is initiated in the placental vasculature in the absence of circulation. **Cell Stem Cell** 2: 252-263.
- Rincon, M., Anguita, J., Nakamura, T., Fikrig, E., and Flavell, R.A. (1997). Interleukin (IL)-6 directs the differentiation of IL-4-producing CD4⁺ T cells. **J. Exp. Med.** 185: 461-469.

- Robin, C., Bollerot, K., Mendes, S., Haak, E., Crisan, M., Cerisoli, F., Lauw, I., Kaimakis, P., Jorna, R., Vermeulen, M., Kayser, M., van der Linden, R., Imanirad, P., Verstegen, M., Nawaz-Yousaf, H., Papazian, N., Steegers, E., Cupedo, T., and Dzierzak, E. (2009). Human placenta is a potent hematopoietic niche containing hematopoietic stem and progenitor cells throughout development. **Cell Stem Cell** 5: 385-395.
- Rodewald, H.R., Kretzschmar, K., Swat, W., and Takeda, S. (1995). Intrathymically expressed c-kit ligand (stem cell factor) is a major factor driving expansion of very immature thymocytes in vivo. **Immunity** 3: 313-319.
- Rongvaux, A., Willinger, T., Takizawa, H., Rathinam, C., Auerbach, W., Murphy, A.J., Valenzuela, D.M., Yancopoulos, G.D., Eynon, E.E., Stevens, S., Manz, M.G., and Flavell, R.A. (2011). Human thrombopoietin knockin mice efficiently support human hematopoiesis in vivo. **Proc. Natl. Acad. Sci. USA**. 108: 2378-2383.
- Rosner, M., Mikula, M., Preitschopf, A., Feichtinger, M., Schipany, K., and Hengstschlager, M. (2011). Neurogenic differentiation of amniotic fluid stem cells. **Amino Acids** [On-line]. Available: <http://www.springerlink.com/content/c6l32508k223wt43/>.
- Rossant, J. and Cross, J.C. (2001). Placental development: lessons from mouse mutants. **Nat Rev Genet** 2: 538-548.
- Rowlinson, J.M. and Gering, M. (2010). Hey2 acts upstream of Notch in hematopoietic stem cell specification in zebrafish embryos. **Blood** 116: 2046-2056.

- Rusten, L.S., Lyman, S.D., Veiby, O.P., and Jacobsen, S.E. (1996). The FLT3 ligand is a direct and potent stimulator of the growth of primitive and committed human CD34⁺ bone marrow progenitor cells *in vitro*. **Blood** 87: 1317-1325.
- Sacchetti, B., Funari, A., Michienzi, S., Di Cesare, S., Piersanti, S., Saggio, I., Tagliafico, E., Ferrari, S., Robey, P.G., Riminucci, M., and Bianco, P. (2007). Self-renewing osteoprogenitors in bone marrow sinusoids can organize a hematopoietic microenvironment. **Cell** 131: 324-336.
- Salm, S., Burger, P.E., and Wilson, E.L. (2011). TGF- β and stem cell factor regulate cell proliferation in the proximal stem cell niche. **Prostate** [On-line]. Available: <http://onlinelibrary.wiley.com/doi/10.1002/pros.21505/abstract>.
- Salter, A.B., Meadows, S.K., Muramoto, G.G., Himburg, H., Doan, P., Daher, P., Russell, L., Chen, B., Chao, N.J., and Chute, J.P. (2009). Endothelial progenitor cell infusion induces hematopoietic stem cell reconstitution *in vivo*. **Blood** 113: 2104-2107.
- Sambrook, J. (2001). Molecular cloning : a laboratory manual / Joseph Sambrook, David W. Russell. Cold Spring Harbor, N.Y. **Cold Spring Harbor Laboratory** 5: 4-13.
- Sangeetha, V.M., Kale, V.P., and Limaye, L.S. (2010). Expansion of cord blood CD34 cells in presence of zVADfmk and zLLYfmk improved their *in vitro* functionality and *in vivo* engraftment in NOD/SCID mouse. **PLoS One** 5: e12221-e12233.

- Santaguida, M., Schepers, K., King, B., Sabnis, A.J., Forsberg, E.C., Attema, J.L., Braun, B.S., and Passegué, E. (2009). JunB protects against myeloid malignancies by limiting hematopoietic stem cell proliferation and differentiation without affecting self-renewal. **Cancer Cell** 15: 341-352.
- Sasaki, T., Mizuochi, C., Horio, Y., Nakao, K., Akashi, K., and Sugiyama, D. (2010). Regulation of hematopoietic cell clusters in the placental niche through SCF/Kit signaling in embryonic mouse. **Development** 137: 3941-3952.
- Sassetti, C., Tangemann, K., Singer, M.S., Kershaw, D.B., and Rosen, S.D. (1998). Identification of podocalyxin-like protein as a high endothelial venule ligand for L-selectin: parallels to CD34. **J. Exp. Med.** 187: 1965-1975.
- Sassetti, C., Van Zante, A., and Rosen, S.D. (2000). Identification of endoglycan, a member of the CD34/podocalyxin family of sialomucins. **J. Biol. Chem.** 275: 9001-9010.
- Sato, N., Meijer, L., Skaltsounis, L., Greengard, P., and Brivanlou, A.H. (2004). Maintenance of pluripotency in human and mouse embryonic stem cells through activation of Wnt signaling by a pharmacological GSK-3-specific inhibitor. **Nat. Med.** 10: 55-63.
- Sawamura, D., Meng, X., Ina, S., Sato, M., Tamai, K., Hanada, K., and Hashimoto, I. (1998). Induction of keratinocyte proliferation and lymphocytic infiltration by *in vivo* introduction of the IL-6 gene into keratinocytes and possibility of keratinocyte gene therapy for inflammatory skin diseases using IL-6 mutant genes. **J. Immunol.** 161: 5633-5639.

- Schallmoser, K., Bartmann, C., Rohde, E., Reinisch, A., Kashofer, K., Stadelmeyer, E., Drexler, C., Lanzer, G., Linkesch, W., and Strunk, D. (2007). Human platelet lysate can replace fetal bovine serum for clinical-scale expansion of functional mesenchymal stromal cells. **Transfusion** 47: 1436-1446.
- Scheinecker, C., Strobl, H., Fritsch, G., Csmarits, B., Krieger, O., Majdic, O., and Knapp, W. (1995). Granulomonocyte-associated lysosomal protein expression during *in vitro* expansion and differentiation of CD34⁺ hematopoietic progenitor cells. **Blood** 86: 4115-4123.
- Scheller, J., Chalaris, A., Schmidt-Arras, D., and Rose-John, S. (2011). The pro- and anti-inflammatory properties of the cytokine interleukin-6. **Biochim. Biophys. Acta.** 1813: 878-888.
- Scheller, M., Huelsken, J., Rosenbauer, F., Taketo, M.M., Birchmeier, W., Tenen, D.G., and Leutz, A. (2006). Hematopoietic stem cell and multilineage defects generated by constitutive beta-catenin activation. **Nat. Immunol.** 7: 1037-1047.
- Schiedlmeier, B., Klump, H., Will, E., Arman-Kalcek, G., Li, Z., Wang, Z., Rimek, A., Friel, J., Baum, C., and Ostertag, W. (2003). High-level ectopic HOXB4 expression confers a profound *in vivo* competitive growth advantage on human cord blood CD34⁺ cells, but impairs lymphomyeloid differentiation. **Blood** 101: 1759-1768.
- Schofield, R. (1978). The relationship between the spleen colony-forming cell and the haemopoietic stem cell. **Blood Cells** 4: 7-25.

- Seet, L.-F., Teng, E., Lai, Y.-S., Laning, J., Kraus, M., Wnendt, S., Merchav, S., and Chan, S.L. (2009). Valproic acid enhances the engraftability of human umbilical cord blood hematopoietic stem cells expanded under serum-free conditions. **Eur. J. Haematol.** 82: 124-132.
- Seita, J. and Weissman, I.L. (2010). Hematopoietic stem cell: self-renewal versus differentiation. **Wiley Interdiscip. Rev. Syst. Biol. Med.** 2: 640-653.
- Sellamuthu, S., Manikandan, R., Thiagarajan, R., Babu, G., Dinesh, D., Prabhu, D., and Arulvasu, C. (2011). In vitro trans-differentiation of human umbilical cord derived hematopoietic stem cells into hepatocyte like cells using combination of growth factors for cell based therapy. **Cytotechnology** 63: 259-268.
- Sera, Y., LaRue, A.C., Moussa, O., Mehrotra, M., Duncan, J.D., Williams, C.R., Nishimoto, E., Schulte, B.A., Watson, P.M., Watson, D.K., and Ogawa, M. (2009). Hematopoietic stem cell origin of adipocytes. **Exp. Hematol.** 37: 1108-1120, 1120 e1101-1104.
- Shah, A.J., Smogorzewska, E.M., Hannum, C., and Crooks, G.M. (1996). Flt3 ligand induces proliferation of quiescent human bone marrow CD34⁺CD38⁻ cells and maintains progenitor cells *in vitro*. **Blood** 87: 3563-3570.
- Shpall, E.J., Quinones, R., Giller, R., Zeng, C., Baron, A.E., Jones, R.B., Bearman, S.I., Nieto, Y., Freed, B., Madinger, N., Hogan, C.J., Slat-Vasquez, V., Russell, P., Blunk, B., Schissel, D., Hild, E., Malcolm, J., Ward, W., and McNiece, I.K. (2002). Transplantation of *ex vivo* expanded cord blood. **Biol. Blood Marrow. Transplant.** 8: 368-376.
- Siminovitch, L., McCulloch, E.A., and Till, J.E. (1963). The distribution of colony-forming cells among spleen colonies. **J. Cell. Physiol.** 62: 327-336.

- Singer, A.J. and Clark, R.A. (1999). Cutaneous wound healing. **N. Engl. J. Med.** 341: 738-746.
- Singh, P., Hoggatt, J., Hu, P., Speth, J.M., Fukuda, S., Breyer, R.M., and Pelus, L.M. (2012). Blockade of prostaglandin E2 signaling through EP1 and EP3 receptors attenuates Flt3L-dependent dendritic cell development from hematopoietic progenitor cells. **Blood** 119: 1671-1682.
- Singh, T. and Newman, A.B. (2011). Inflammatory markers in population studies of aging. **Ageing. Res. Rev.** 10: 319-329.
- Sivan-Loukianova, E., Awad, O.A., Stepanovic, V., Bickenbach, J., and Schatteman, G.C. (2003). CD34⁺ blood cells accelerate vascularization and healing of diabetic mouse skin wounds. **J. Vasc. Res.** 40: 368-377.
- Slavik, M.A., Allen-Hoffmann, B.L., Liu, B.Y., and Alexander, C.M. (2007). Wnt signaling induces differentiation of progenitor cells in organotypic keratinocyte cultures. **BMC. Dev. Biol.** 7: 9.
- Smola, H., Thiekotter, G., and Fusenig, N.E. (1993). Mutual induction of growth factor gene expression by epidermal-dermal cell interaction. **J. Cell. Biol.** 122: 417-429.
- Snarski, E., Milczarczyk, A., Torosian, T., Paluszewska, M., Urbanowska, E., Krol, M., Boguradzki, P., Jedynasty, K., Franek, E., and Wiktor-Jedrzejczak, W. (2011). Independence of exogenous insulin following immunoablation and stem cell reconstitution in newly diagnosed diabetes type I. **Bone Marrow Transplant.** 46: 562-566.

- Sohma, Y., Akahori, H., Seki, N., Hori, T., Ogami, K., Kato, T., Shimada, Y., Kawamura, K., and Miyazaki, H. (1994). Molecular cloning and chromosomal localization of the human thrombopoietin gene. **FEBS. Lett.** 353: 57-61.
- Sriwijitkamol, A., Mounngern, Y., and Vannaseang, S. (2011). Assessment and prevalences of diabetic complications in 722 Thai type 2 diabetes patients. **J. Med. Assoc. Thai.** 94 Suppl 1: S168-174.
- Staudt, N.D., Aicher, W.K., Kalbacher, H., Stevanovic, S., Carmona, A.K., Bogyo, M., and Klein, G. (2010). Cathepsin X is secreted by human osteoblasts, digests CXCL-12 and impairs adhesion of hematopoietic stem and progenitor cells to osteoblasts. **Haematologica** 95: 1452-1460.
- Stepanovic, V., Awad, O., Jiao, C., Dunnwald, M., and Schatteman, G.C. (2003). Leprdb diabetic mouse bone marrow cells inhibit skin wound vascularization but promote wound healing. **Circ. Res.** 92: 1247-1253.
- Stier, S., Cheng, T., Dombkowski, D., Carlesso, N., and Scadden, D.T. (2002). Notch1 activation increases hematopoietic stem cell self-renewal *in vivo* and favors lymphoid over myeloid lineage outcome. **Blood** 99: 2369-2378.
- Stier, S., Ko, Y., Forkert, R., Lutz, C., Neuhaus, T., Grunewald, E., Cheng, T., Dombkowski, D., Calvi, L.M., Rittling, S.R., and Scadden, D.T. (2005). Osteopontin is a hematopoietic stem cell niche component that negatively regulates stem cell pool size. **J. Exp. Med.** 201: 1781-1791.
- Stirewalt, D.L. and Radich, J.P. (2003). The role of FLT3 in haematopoietic malignancies. **Nat. Rev. Cancer** 3: 650-665.

- Sugiyama, T., Kohara, H., Noda, M., and Nagasawa, T. (2006). Maintenance of the hematopoietic stem cell pool by CXCL12-CXCR4 chemokine signaling in bone marrow stromal cell niches. **Immunity** 25: 977-988.
- Sun, L., Lee, J., and Fine, H.A. (2004). Neuronally expressed stem cell factor induces neural stem cell migration to areas of brain injury. **J. Clin. Invest.** 113: 1364-1374.
- Sungaran, R., Markovic, B., and Chong, B.H. (1997). Localization and regulation of thrombopoietin mRNA expression in human kidney, liver, bone marrow, and spleen using *in situ* hybridization. **Blood** 89: 101-107.
- Taghizadeh, R.R., Cetrulo, K.J., and Cetrulo, C.L. (2011). Wharton's Jelly stem cells: Future clinical applications. **Placenta** [On-line]. Available: <http://www.sciencedirect.com/science/article/pii/S0143400411002189>
- Taichman, R.S. (2005). Blood and bone: two tissues whose fates are intertwined to create the hematopoietic stem-cell niche. **Blood** 105: 2631-2639.
- Takahashi, S. (2011). Downstream molecular pathways of FLT3 in the pathogenesis of acute myeloid leukemia: biology and therapeutic implications. **J. Hematol. Oncol.** 4: 13-23.
- Tark, K.C., Hong, J.W., Kim, Y.S., Hahn, S.B., Lee, W.J., and Lew, D.H. (2010). Effects of human cord blood mesenchymal stem cells on cutaneous wound healing in leprdb mice. **Ann. Plast. Surg.** 65: 565-572.
- Tavian, M., Coulombel, L., Luton, D., Clemente, H.S., Dieterlen-Lievre, F., and Peault, B. (1996). Aorta-associated CD34+ hematopoietic cells in the early human embryo. **Blood** 87: 67-72.

- Tavian, M., Robin, C., Coulombel, L., and Peault, B. (2001). The human embryo, but not its yolk sac, generates lympho-myeloid stem cells: mapping multipotent hematopoietic cell fate in intraembryonic mesoderm. **Immunity** 15: 487-495.
- Taylor, E., Taoudi, S., and Medvinsky, A. (2010). Hematopoietic stem cell activity in the aorta-gonad-mesonephros region enhances after mid-day 11 of mouse development. **Int. J. Dev. Biol.** 54: 1055-1060.
- Templin, C., Grote, K., Schledzewski, K., Ghadri, J.R., Schnabel, S., Napp, L.C., Schieffer, B., Kurzen, H., Goerdt, S., Landmesser, U., Koenen, W., and Faulhaber, J. (2009). *Ex vivo* expanded haematopoietic progenitor cells improve dermal wound healing by paracrine mechanisms. **Exp. Dermatol.** 18: 445-453.
- Teo, A.K. and Vallier, L. (2010). Emerging use of stem cells in regenerative medicine. **Biochem. J.** 428: 11-23.
- Tesch, G.H. and Allen, T.J. (2007). Rodent models of streptozotocin-induced diabetic nephropathy. **Nephrology (Carlton)** 12: 261-266.
- Tetsu, O. and McCormick, F. (1999). Beta-catenin regulates expression of cyclin D1 in colon carcinoma cells. **Nature** 398: 422-426.
- Till, J.E. and McCulloch, C.E. (1961). A direct measurement of the radiation sensitivity of normal mouse bone marrow cells. **Radiat. Res.** 14: 213-222.
- Toliver-Kinsky, T.E., Cui, W., Murphey, E.D., Lin, C., and Sherwood, E.R. (2005). Enhancement of dendritic cell production by fms-like tyrosine kinase-3 ligand increases the resistance of mice to a burn wound infection. **J. Immunol.** 174: 404-410.

- Tolwinski, N.S., Wehrli, M., Rives, A., Erdeniz, N., DiNardo, S., and Wieschaus, E. (2003). Wg/Wnt signal can be transmitted through arrow/LRP5,6 and Axin independently of Zw3/Gsk3beta activity. **Dev. Cell** 4: 407-418.
- Tortolani, P.J., Johnston, J.A., Bacon, C.M., McVicar, D.W., Shimosaka, A., Linnekin, D., Longo, D.L., and O'Shea, J.J. (1995). Thrombopoietin induces tyrosine phosphorylation and activation of the Janus kinase, JAK2. **Blood** 85: 3444-3451.
- Traver, D., Akashi, K., Manz, M., Merad, M., Miyamoto, T., Engleman, E.G., and Weissman, I.L. (2000). Development of CD8alpha-positive dendritic cells from a common myeloid progenitor. **Science** 290: 2152-2154.
- Trowbridge, J.J., Guezguez, B., Moon, R.T., and Bhatia, M. (2010). Wnt3a activates dormant c-Kit(-) bone marrow-derived cells with short-term multilineage hematopoietic reconstitution capacity. **Stem Cells** 28: 1379-1389.
- Trowbridge, J.J., Scott, M.P., and Bhatia, M. (2006a). Hedgehog modulates cell cycle regulators in stem cells to control hematopoietic regeneration. **Proc. Natl. Acad. Sci. USA**. 103: 14134-14139.
- Trowbridge, J.J., Xenocostas, A., Moon, R.T., and Bhatia, M. (2006b). Glycogen synthase kinase-3 is an *in vivo* regulator of hematopoietic stem cell repopulation. **Nat. Med.** 12: 89-98.
- Tsagias, N., Koliakos, I., Lappa, M., Karagiannis, V., and Koliakos, G.G. (2011). Placenta perfusion has hematopoietic and mesenchymal progenitor stem cell potential. **Transfusion** 51: 976-985.

- Tzeng, Y.S., Li, H., Kang, Y.L., Chen, W.C., Cheng, W.C., and Lai, D.M. (2011). Loss of Cxcl12/Sdf-1 in adult mice decreases the quiescent state of hematopoietic stem/progenitor cells and alters the pattern of hematopoietic regeneration after myelosuppression. **Blood** 117: 429-439.
- Ueda, T., Tsuji, K., Yoshino, H., Ebihara, Y., Yagasaki, H., Hisakawa, H., Mitsui, T., Manabe, A., Tanaka, R., Kobayashi, K., Ito, M., Yasukawa, K., and Nakahata, T. (2000). Expansion of human NOD/SCID-repopulating cells by stem cell factor, Flk2/Flt3 ligand, thrombopoietin, IL-6, and soluble IL-6 receptor. **J. Clin. Invest.** 105: 1013-1021.
- Um, S., Choi, J.R., Lee, J.H., Zhang, Q., and Seo, B. (2011). Effect of leptin on differentiation of human dental stem cells. **Oral Dis.** 17: 662-669.
- Urdzikova, L., Likavcanova-Masinova, K., Vanecek, V., Ruzicka, J., Sedy, J., Sykova, E., and Jendelova, P. (2011). Flt3 ligand synergizes with granulocyte-colony-stimulating factor in bone marrow mobilization to improve functional outcome after spinal cord injury in the rat. **Cytotherapy** 13: 1090-1104.
- Varnum-Finney, B., Brashem-Stein, C., and Bernstein, I.D. (2003). Combined effects of Notch signaling and cytokines induce a multiple log increase in precursors with lymphoid and myeloid reconstituting ability. **Blood** 101: 1784-1789.
- Varnum-Finney, B., Halasz, L.M., Sun, M., Gridley, T., Radtke, F., and Bernstein, I.D. (2011). Notch2 governs the rate of generation of mouse long- and short-term repopulating stem cells. **J. Clin. Invest.** 121: 1207-1216.

- Varnum-Finney, B., Xu, L., Brashem-Stein, C., Nourigat, C., Flowers, D., Bakkour, S., Pear, W.S., and Bernstein, I.D. (2000). Pluripotent, cytokine-dependent, hematopoietic stem cells are immortalized by constitutive Notch1 signaling. **Nat Med** 6: 1278-1281.
- Vigon, I., Mornon, J.P., Cocault, L., Mitjavila, M.T., Tambourin, P., Gisselbrecht, S., and Souyri, M. (1992). Molecular cloning and characterization of MPL, the human homolog of the v- mpl oncogene: Identification of a member of the hematopoietic growth factor receptor superfamily. **Proc. Natl. Acad. Sci. USA.** 89: 5640-5644.
- Visnjic, D., Kalajzic, Z., Rowe, D.W., Katavic, V., Lorenzo, J., and Aguila, H.L. (2004). Hematopoiesis is severely altered in mice with an induced osteoblast deficiency. **Blood** 103: 3258-3264.
- Walenda, T., Bokermann, G., Ventura Ferreira, M.S., Piroth, D.M., Hieronymus, T., Neuss, S., Zenke, M., Ho, A.D., Muller, A.M., and Wagner, W. (2011). Synergistic effects of growth factors and mesenchymal stromal cells for expansion of hematopoietic stem and progenitor cells. **Exp. Hematol.** 39: 617-628.
- Wang, J.C., Doedens, M., and Dick, J.E. (1997). Primitive human hematopoietic cells are enriched in cord blood compared with adult bone marrow or mobilized peripheral blood as measured by the quantitative *in vivo* SCID-repopulating cell assay. **Blood** 89: 3919-3924.
- Wang, Y., Kellner, J., Liu, L., and Zhou, D. (2011). Inhibition of p38 mitogen-activated protein kinase promotes *ex vivo* hematopoietic stem cell expansion. **Stem Cells Dev.** 20: 1143-1152.

- Wang, Y.Y., Yang, Y., Chen, Q., Yu, J., Hou, Y., Han, L., He, J., Jiao, D., and Yu, H. (2008). Simultaneous knockdown of p18INK4C, p27Kip1 and MAD1 via RNA interference results in the expansion of long-term culture-initiating cells of murine bone marrow cells *in vitro*. **Acta. Biochim. Biophys. Sin. (Shanghai)** 40: 711-720.
- Watts, K., Zhang, X., Beard, B., Chiu, S.Y., Trobridge, G.D., Humphries, R.K., and Kiem, H.-P. (2011). Differential effects of HOXB4 and NUP98-HOXA10hd on hematopoietic repopulating cells in a nonhuman primate model. **Human Gene Therapy** 22: 1475-1482.
- Watts, K.L., Delaney, C., Humphries, R.K., Bernstein, I.D., and Kiem, H.-P. (2010). Combination of HOXB4 and delta-1 ligand improves expansion of cord blood cells. **Blood** 116: 5859-5866.
- Weber, J.M., Forsythe, S.R., Christianson, C.A., Frisch, B.J., Gigliotti, B.J., Jordan, C.T., Milner, L.A., Guzman, M.L., and Calvi, L.M. (2006). Parathyroid hormone stimulates expression of the Notch ligand Jagged1 in osteoblastic cells. **Bone** 39: 485-493.
- Wehrle-Haller, B. (2003). The role of Kit-ligand in melanocyte development and epidermal homeostasis. **Pigment Cell Res.** 16: 287-296.
- Wehrle-Haller, B. and Weston, J.A. (1995). Soluble and cell-bound forms of steel factor activity play distinct roles in melanocyte precursor dispersal and survival on the lateral neural crest migration pathway. **Development** 121: 731-742.

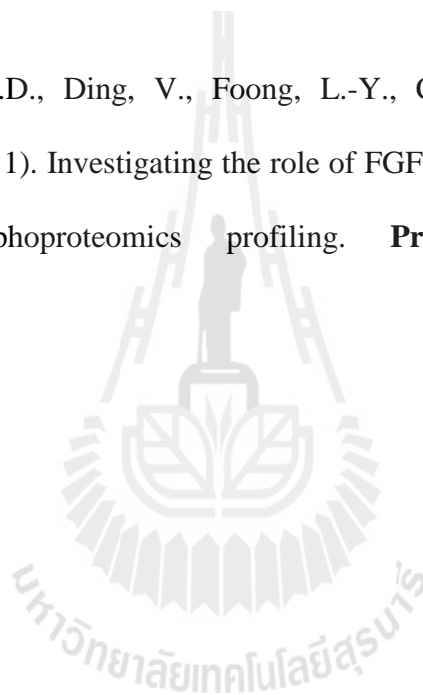
- Weinhold, B., Bader, A., Poli, V., and Ruther, U. (1997). Interleukin-6 is necessary, but not sufficient, for induction of the human C-reactive protein gene *in vivo*. **Biochem. J.** 325(Pt 3): 617-621.
- Weinhold, B. and Ruther, U. (1997). Interleukin-6-dependent and -independent regulation of the human C-reactive protein gene. **Biochem. J.** 327(Pt 2): 425-429.
- Weisberg, S.P., McCann, D., Desai, M., Rosenbaum, M., Leibel, R.L., and Ferrante, A.W., Jr. (2003). Obesity is associated with macrophage accumulation in adipose tissue. **J. Clin. Invest.** 112: 1796-1808.
- Weiss, R.R., Whitaker-Menezes, D., Longley, J., Bender, J., and Murphy, G.F. (1995). Human dermal endothelial cells express membrane-associated mast cell growth factor. **J. Invest. Dermatol.** 104: 101-106.
- Wendling, F., Maraskovsky, E., Debili, N., Florindo, C., Teepe, M., Titeux, M., Methia, N., Breton-Gorius, J., Cosman, D., and Vainchenker, W. (1994). cMpl ligand is a humoral regulator of megakaryocytopoiesis. **Nature** 369: 571-574.
- Witthuhn, B.A., Quelle, F.W., Silvennoinen, O., Yi, T., Tang, B., Miura, O., and Ihle, J.N. (1993). JAK2 associates with the erythropoietin receptor and is tyrosine phosphorylated and activated following stimulation with erythropoietin. **Cell** 74: 227-236.
- Woll, P.S., Morris, J.K., Painschab, M.S., Marcus, R.K., Kohn, A.D., Biechele, T.L., Moon, R.T., and Kaufman, D.S. (2008). Wnt signaling promotes hematoendothelial cell development from human embryonic stem cells. **Blood** 111: 122-131.

- Wong, H.C., Bourdelas, A., Krauss, A., Lee, H.J., Shao, Y., Wu, D., Mlodzik, M., Shi, D.L., and Zheng, J. (2003). Direct binding of the PDZ domain of Dishevelled to a conserved internal sequence in the C-terminal region of Frizzled. **Mol. Cell.** 12: 1251-1260.
- Wu, C.H. and Nusse, R. (2002). Ligand receptor interactions in the Wnt signaling pathway in *Drosophila*. **J. Biol. Chem.** 277: 41762-41769.
- Xia, Y.P., Zhao, Y., Marcus, J., Jimenez, P.A., Ruben, S.M., Moore, P.A., Khan, F., and Mustoe, T.A. (1999). Effects of keratinocyte growth factor-2 (KGF-2) on wound healing in an ischaemia-impaired rabbit ear model and on scar formation. **J. Pathol.** 188: 431-438.
- Xie, C.G., Wang, J.F., Xiang, Y., Qiu, L.Y., Jia, B.B., Wang, L.J., Wang, G.Z., and Huang, G.P. (2006). Cocultivation of umbilical cord blood CD34⁺ cells with retro-transduced hMSCs leads to effective amplification of long-term culture-initiating cells. **World J. Gastroenterol.** 12: 393-402.
- Xie, Y., Yin, T., Wiegraebe, W., He, X.C., Miller, D., Stark, D., Perko, K., Alexander, R., Schwartz, J., Grindley, J.C., Park, J., Haug, J.S., Wunderlich, J.P., Li, H., Zhang, S., Johnson, T., Feldman, R.A., and Li, L. (2009). Detection of functional haematopoietic stem cell niche using real-time imaging. **Nature** 457: 97-101.
- Yan, W., Suominen, J., and Toppari, J. (2000). Stem cell factor protects germ cells from apoptosis in vitro. **J. Cell Sci.** 113(Pt 1): 161-168.

- Yang, M., Li, K., Ng, P.C., Chuen, C.K., Lau, T.K., Cheng, Y.S., Liu, Y.S., Li, C.K., Yuen, P.M., James, A.E., Lee, S.M., and Fok, T.F. (2007). Promoting effects of serotonin on hematopoiesis: *ex vivo* expansion of cord blood CD34⁺ stem/progenitor cells, proliferation of bone marrow stromal cells, and antiapoptosis. **Stem Cells** 25: 1800-1806.
- Yao, S., Chen, S., Clark, J., Hao, E., Beattie, G.M., Hayek, A., and Ding, S. (2006). Long-term self-renewal and directed differentiation of human embryonic stem cells in chemically defined conditions. **Proc. Natl. Acad. Sci. USA.** 103: 6907-6912.
- Yoshihara, H., Arai, F., Hosokawa, K., Hagiwara, T., Takubo, K., Nakamura, Y., Gomei, Y., Iwasaki, H., Matsuoka, S., Miyamoto, K., Miyazaki, H., Takahashi, T., and Suda, T. (2007a). Thrombopoietin/MPL signaling regulates hematopoietic stem cell quiescence and interaction with the osteoblastic niche. **Cell Stem Cell** 1: 685-697.
- Yoshihara, H., Arai, F., Hosokawa, K., Hagiwara, T., Takubo, K., Nakamura, Y., Gomei, Y., Iwasaki, H., Matsuoka, S., Miyamoto, K., Miyazaki, H., Takahashi, T., and Suda, T. (2007b). Thrombopoietin/MPL signaling regulates hematopoietic stem cell quiescence and interaction with the osteoblastic niche. **Cell Stem Cell** 1: 685-697.
- Zeigler, B.M., Sugiyama, D., Chen, M., Guo, Y., Downs, K.M., and Speck, N.A. (2006). The allantois and chorion, when isolated before circulation or chorio-allantoic fusion, have hematopoietic potential. **Development** 133: 4183-4192.

- Zhang, C.C., Kaba, M., Ge, G., Xie, K., Tong, W., Hug, C., and Lodish, H.F. (2006a). Angiopoietin-like proteins stimulate *ex vivo* expansion of hematopoietic stem cells. **Nat. Med.** 12: 240-245.
- Zhang, C.C., Kaba, M., Iizuka, S., Huynh, H., and Lodish, H.F. (2008). Angiopoietin-like 5 and IGFBP2 stimulate *ex vivo* expansion of human cord blood hematopoietic stem cells as assayed by NOD/SCID transplantation. **Blood** 111: 3415-3423.
- Zhang, J., Niu, C., Ye, L., Huang, H., He, X., Tong, W.G., Ross, J., Haug, J., Johnson, T., Feng, J.Q., Harris, S., Wiedemann, L.M., Mishina, Y., and Li, L. (2003). Identification of the haematopoietic stem cell niche and control of the niche size. **Nature** 425: 836-841.
- Zhang, S., Anderson, D.F., Bradding, P., Coward, W.R., Baddeley, S.M., MacLeod, J.D., McGill, J.I., Church, M.K., Holgate, S.T., and Roche, W.R. (1998). Human mast cells express stem cell factor. **J. Pathol.** 186: 59-66.
- Zhang, X.B., Beard, B.C., Beebe, K., Storer, B., Humphries, R.K., and Kiem, H.P. (2006b). Differential effects of HOXB4 on nonhuman primate short- and long-term repopulating cells. **PLoS Med.** 3: e173-e184.
- Zhao, C., Chen, A., Jamieson, C.H., Fereshteh, M., Abrahamsson, A., Blum, J., Kwon, H.Y., Kim, J., Chute, J.P., Rizzieri, D., Munchhof, M., VanArsdale, T., Beachy, P.A., and Reya, T. (2009). Hedgehog signalling is essential for maintenance of cancer stem cells in myeloid leukaemia. **Nature** 458: 776-779.
- Zhao, L.R., Singhal, S., Duan, W.M., Mehta, J., and Kessler, J.A. (2007). Brain repair by hematopoietic growth factors in a rat model of stroke. **Stroke** 38: 2584-2591.

- Zhu, J., Garrett, R., Jung, Y., Zhang, Y., Kim, N., Wang, J., Joe, G.J., Hexner, E., Choi, Y., Taichman, R.S., and Emerson, S.G. (2007). Osteoblasts support B-lymphocyte commitment and differentiation from hematopoietic stem cells. **Blood** 109: 3706-3712.
- Zhu, S., Patel, K.V., Bandinelli, S., Ferrucci, L., and Guralnik, J.M. (2009). Predictors of Interleukin-6 Elevation in Older Adults. **J. Am. Geriatr. Soc.** 57: 1672-1677.
- Zoumaro-Djayoon, A.D., Ding, V., Foong, L.-Y., Choo, A., Heck, A.J.R., and Muñoz, J. (2011). Investigating the role of FGF-2 in stem cell maintenance by global phosphoproteomics profiling. **Proteomics** 11: 3962-3971.



APPENDICES



APPENDIX A

SOLUTION PREPARATION

1. Reagent for CD34⁺ cells isolation

1.1 PBS

Mix the reagent as follow:

| | | |
|----------------------------------|------|---|
| NaCl | 8.00 | g |
| Na ₂ HPO ₄ | 1.44 | g |
| KCl | 0.20 | g |
| KH ₂ PO ₄ | 0.24 | g |

Add sterile Ultra-pure water to bring a volume up to 1000 ml. Adjust the pH of the solution to 7.4. Sterilize by autoclaved at 121°C for 15 minutes and store at room temperature

1.2 Washing buffer (PBS pH 7.4, 0.1% BSA, 2 mM EDTA)

To prepare 1000 ml solution, mix the stock solution as follow:

- 5 ml of 20% BSA (20.0 g/100 ml, filter sterile)
- 100 ml of 20 mM EDTA (0.74g/100 ml, filter sterile)

Add sterile PBS to bring a volume up to 100 ml. Store the solution at 4°C.

2. Reagent for cell culture

2.1 cIMDM

Mix the reagent as follow:

| | | |
|---|--------|----|
| - IMDM | 1.77 | g |
| - FBS | 10.0 | ml |
| - 55 mM β -mercaptoethanol | 0.09 | ml |
| - NaHCO ₃ | 0.3024 | g |
| - 1000 U/ml Penicillin/1000 μ g/ml Streptomycin | 2.00 | ml |
| - 2 mg/ml Amphotericin B | 0.20 | ml |

Add sterile ultra-pure water to bring a volume up to 100 ml and adjust pH to

7.4. Sterilize by filter sterile.

2.2 KSR medium

Mix the reagent as follow:

| | | |
|---|--------|----|
| - IMDM | 1.77 | g |
| - Knocked out serum | 10.0 | ml |
| - 55 mM β -mercaptoethanol | 0.09 | ml |
| - NaHCO ₃ | 0.3024 | g |
| - 1000 U/ml Penicillin/1000 μ g/ml Streptomycin | 2.00 | ml |
| - 2 mg/ml Amphotericin B | 0.20 | ml |

Add sterile ultra-pure water to bring a volume up to 100 ml and adjust pH to

7.4. Sterilize by filter sterile.

2.3 α -MEM

Mix the reagent as follow:

| | | |
|---|-------|----|
| - α -MEM | 10.1 | g |
| - FBS | 100.0 | ml |
| - NaHCO ₃ | 2.2 | g |
| - 1000 U/ml Penicillin/1000 μ g/ml Streptomycin | 10.0 | ml |
| - 2 mg/ml Amphotericin B | 1.0 | ml |

Add sterile ultra-pure water to bring a volume up to 1000 ml and adjust pH to

7.4. Sterilize by filter sterile.

2.4 IMDM + 2% FBS

Mix the reagent as follow:

| | | |
|---|--------|----|
| - IMDM | 1.77 | g |
| - FBS | 2.0 | ml |
| - 55 mM β -mercaptoethanol | 0.09 | ml |
| - NaHCO ₃ | 0.3024 | g |
| - 1000 U/ml Penicillin/1000 μ g/ml Streptomycin | 2.00 | ml |
| - 2 mg/ml Amphotericin B | 0.20 | ml |

Add sterile ultra-pure water to bring a volume up to 100 ml and adjust pH to

7.4. Sterilize by filter sterile.

2.5 Trypsin/EDTA

Mix the reagent as follow:

| | | |
|-----------|------|---|
| - Trypsin | 0.25 | g |
|-----------|------|---|

- EDTA 0.04 g

Add sterile PBS to bring a volume up to 100 ml.

3. Reagent for immunofluorescent staining

3.1 4% Paraformaldehyde

Dissolve 4 g. of paraformaldehyde in 90 ml. of H₂O to dissolve and adjust the pH to pH 7.4. Then, add 10 ml. 10x PBS (for a final concentration of 4 g. in 100 ml. of 1x PBS). Filter sterilize through a 0.22 µm filter. Store at 4°C.

4. Reagent for agarose gel electrophoresis

4.1 5x TBE buffer

Mix the reagent as follow:

| | |
|-----------------------|---------|
| - Tris base | 53.0 g |
| - Boric acid | 27.5 g |
| - 0.5 M EDTA (pH 8.0) | 20.0 ml |

Add the ultra-pure water to 1,000 ml

4.2 6x DNA loading dye

Mix 0.025 g bromophenol blue, 0.025 g xylene cyanol and 3 ml of 100% glycerol in distilled water to a 10 ml final volume and store at 4°C.

5. Reagent for wound healing assay

5.1 0.1 M Citrate buffer pH 4.5

To prepare 100 ml solution, mix the stock solution as follow:

- 26.7 ml of 0.1 M Citric acid (19.21 g/1 liter)
- 23.3 ml of 0.2 M Dibasic sodium phosphate (35.6 g/1 liter)

Adjust the final pH to pH 4.5 and filter sterilize through a 0.22 μm filter.



APPENDIX B

STATISTICAL DESCRIPTION

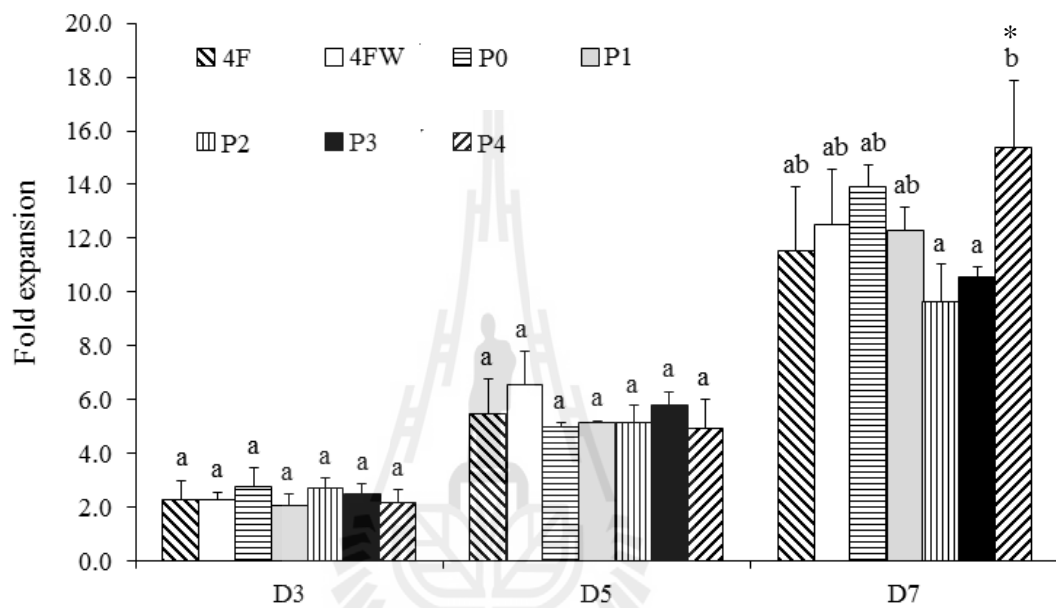


Figure B.1 Statistical description of Figure 4.12:

a is statistically different from b on the same day of culture.

ab is not statistically different from a and b on the same day of culture.

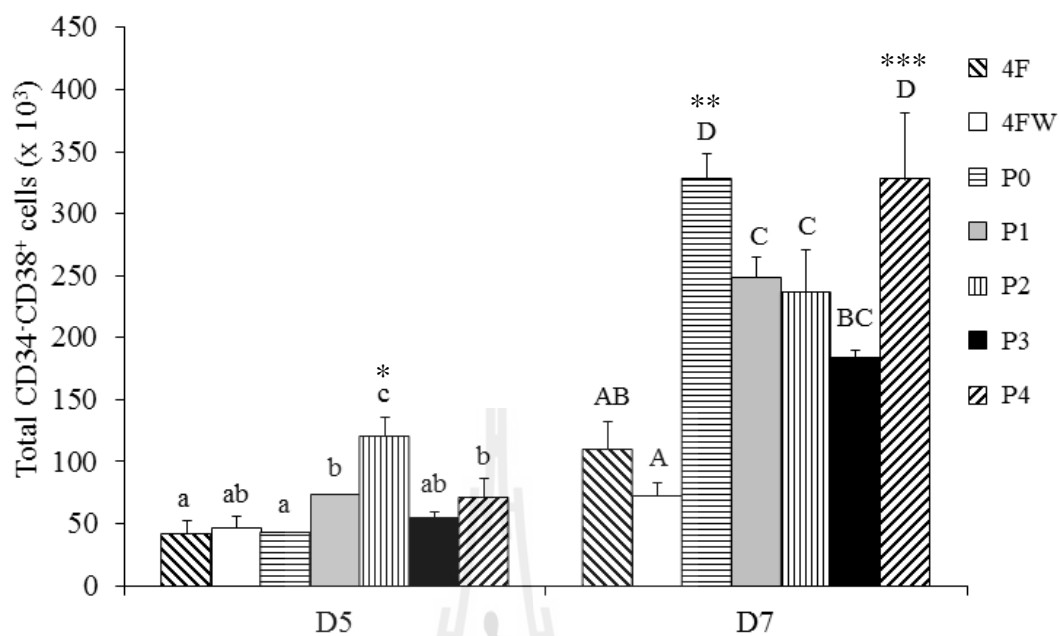


Figure B.2 Statistical description of Figure 4.15:

a is statistically different from b and c.

b is statistically different from c.

ab is not statistically different from a and b.

ab is statistically different from c.

A and AB are statistically different from C and D.

AB is not statistically different from A and BC.

BC is statistically different from D.

C is statistically different from D.

CURRICULUM VITAE

Name Miss Kamonnaree Chotinantakul

Date of Birth October 7, 1979

Place of Birth Phrae, Thailand

Education

| | |
|--------------|--|
| 2006-present | Ph.D candidate Suranaree University of Technology, Thailand |
| 2002-2004 | M.Sc. (Microbiology) Faculty of Medicine, Siriraj Hospital, Mahidol University, Thailand |
| 1998-2001 | B.Sc. (Medical Technology) (1 st Class Honors) Faculty of Associated Medical Science, Chiangmai University, Thailand |

Award

International Society for Stem Cell Research (ISSCR) travel award in ISSCR 7th Annual Meeting, Barcelona, Spain 2009.

Scholarship

SUT outstanding academic performance scholarships